LABILITY AND SOLUBILITY

OF URANIUM AND THORIUM IN SOIL

HAYAM AHMED

MChem (hons.), MSc.

Thesis submitted to the University of Nottingham
for the degree of Doctor of Philosophy

August 2014

ABSTRACT

The approach used in this study tested the application of an isotope dilution technique (ID) as a means of measuring the *labile* U(VI) and Th pools in soils. Uranium and Th lability and solubility were investigated for two sets of soils. The first set (Field soils) consisted of thirty seven soil samples representing five contrasting local ecosystems; the second dataset (BGSc) included 40 soils sub-sampled from the British Geological Survey (BGS) archive. Field soil pore water samples were taken from soil columns held at close to field capacity to measure U and Th solubility and speciation; the effects of time, temperature and reducing conditions on Th and U speciation were investigated. Soils were extracted with four single extractants: CH_3COONH_4, EDTA, 0.43 M HNO_3 and TMAH to determine their ability to solubilize labile U and Th.

Solubility of Th and U varied with soil characteristics, influenced by pH, DOC, DIC and phosphate concentrations. The K_d values for Th and U varied by 4 and 3 orders of magnitude respectively over the range of soils studied. The formation of soluble uranyl carbonate complexes give rise to a strong positive correlation between U and DIC concentrations in soil solutions. This was particularly clear under anaerobic conditions and also at high temperatures which encouraged microbial activity and high CO_2 partial pressures.

Isotopically exchangeable $^{238}U(VI)$ (the 'E-value', U_E) in the soils studied varied from 2.7 to 39.1% of the total soil U content. On average, over all groups of soils, CH_3COONH_4, EDTA and TMAH underestimated E-value by factors of 13.7, 9.5 and 1.6, respectively, while extraction with 0.43 M HNO_3 overestimated E-value by only a factor of 1.04. Thus, on average across a range of soils, dilute nitric acid gave the best estimate of E-value compared to other extractants. Generally, E-values for U(VI) did not correspond consistently with any single chemical extraction procedure although the degree of correspondence was soil-dependent. Using U_E and Th_{TMAH} as input parameters in the geochemical speciation model WHAM-VII improved the prediction of U and Th solubility compared to using the total metal content or the pools extractable by (other) single extraction methods.

Finally, preliminary experiments confirmed the validity of ID for measuring labile soil Th without disturbance of soil-solution equilibrium.

To……

My mother, who is the dearest to my heart

My father, who lives in my heart forever….

My children, who are the best thing in my life

ACKNOWLEDGEMENTS

First and foremost I would like to say thank you to my supervisors. Thank you to George Shaw and Scott Young for their supervision and support throughout my PhD study with patience, motivation, and enthusiasm. This thesis would not have been possible without the help and guidance of my supervisors.

I thank the Egyptian Government for financial support over the course of my PhD. I would also like to thank all my colleagues in the Environmental Science department, University of Nottingham for support and sharing over the course of my PhD. A special thank to Darren Hepworth, John Corrie, and Emma Hooley for their technical and administrative support. Thank you to Simon Chinery and Louise Ander from BGS for providing isotopes and soils.

Last but not least, I would like to thank my family: my father, my mother, my brothers and sisters for their constant love and support, and for being proud of me all the time. Thank you to my husband for his support, encouragement, understanding and looking after our children during the last 6 months. Finally, I thank my children, Zahraa, Mohamed and Ahmed, for all their love and support.

TABLE OF CONTENTS

TABLE OF FIGURES

TABLE OF TABLES

ABBREVIATION LIST

Th	Thorium
U	Uranium
Ar	Arable soils
AW	Acidic woodland soils
AM	Acidic moorland soils
Ca	Calcareous soils
Ba	Biosolid-amended arable soils
BGSc	British Geological Survey collection
DOC	Dissolved organic carbon
DIC	Dissolved inorganic carbon
HA	Humic acid
FA	Fulvic acid
HPLC	High pressure liquid chromatography
ICP-MS	Inductively coupled plasma - mass spectrometry
LOD	Limit of detection
LOQ	Limit of quantification
ppb	Parts per billion
MQ water	Milli-Q purified water
MW	Molecular weight
SD	Standard deviation
SE	Standard error
RSD	Residual standard deviation
RMSD	Rroot mean square difference
SEC	Size exclusion chromatography
SOC	Soil organic carbon
SIC	Soil inorganic carbon
LOI	Loss on ignition

SEP	Sequential extraction procedure
WHAM	Windermere Humic Aqueous Model
CPS	counts-per-second
ID	Isotopic Dilution technique
Gm	Geometric mean
GSD	Geometric standard deviation
Am	Arithmetic mean
SD	standard deviation
min	Minimum
max	Maximum
K_d	Solid-liquid distribution coefficient

1 INTRODUCTION

Radioactivity from natural sources is the main contribution to human radiation exposure (Barisic et al., 1992; Kiss et al., 1988); therefore more attention has recently been given to the mobility, speciation and fractionation of natural radionuclides, including U and Th. To estimate the potential risk posed by U and Th to humans and to predict their transfer in ecosystems and agriculture, information on the geochemical speciation and dynamics of U and Th in soils is required (Duff et al., 2002). Furthermore, the geochemical factors affecting U and Th availability and solid-solution partitioning must be determined. It is recognized that the mobility and plant uptake of potentially toxic elements is related to the available metal pool rather than the total metal concentration. Therefore, increasing interest has been given to quantifying metal solubility, bioavailability and lability and the development of new techniques to speciate and fractionate U and Th in soils and sediments (Kohler et al., 2003; Um et al., 2010; Duquène et al., 2010; Guo et al., 2010; Bond et al., 2008). In general, modelling of trace metal solubility and speciation is now becoming increasingly common in environmental research and risk assessment.

In this chapter, a general introduction to the analytical methods used to measure U and Th fractionation is presented as a base for the later chapters which deal with the effect of soil properties on the lability and solubility of U and Th. The overall objectives and the structure of the thesis are also presented in this chapter.

1.1 Fractionation of U and Th in soils

Soil acid digestion is generally used to determine the total U and Th contents in soils because mineral acids such as HF, $HClO_4$ and HNO_3 mobilize all forms of metals including inert forms strongly incorporated into primary minerals and silicates. In addition to the use of mineral acids, a range of methods has been developed to determine the lability and fractionation of Th and U in soil using selective fractionation procedures based on single or sequential extractions (Schultz et al., 1998; Gooddy et al., 1995; Takeda et al., 2006b; Guo et al., 2007, 2010). Other methods to determine metal partitioning include dynamic (non-equilibrium) based extraction methods (e.g. column leaching experiments) (Shiowatana et al., 2001;

Fedotov et al., 2002; Kurosaki et al., 2002; Jimoh et al., 2004), the diffusive gradient in thin film technique (DGT) (Zhang et al., 2001; Vandenhove et al., 2007b; Duquène et al., 2010), isotopic dilution (Payne et al., 2004; Payne and Waite, 1991; Kohler et al., 2003; Bond et al., 2008) and fractionation based on particle size using Asymmetrical Flow Field-Flow Fractionation (AsFlFFF) (Ranville et al., 2007; Reszat and Hendry, 2007) or size exclusion chromatography (SEC) (Jackson et al., 2005; Casartelli and Miekeley, 2003; Wu et al., 2004). In addition, mechanistic geochemical models such as WHAM-VII (Tipping et al., 2011; Stockdale and Bryan, 2012, 2013) and NICA-Donnan (Bonten et al., 2008) can also be used to predict metal speciation and fractionation in soil solution and solid phases.

1.1.1 Single chemical extraction methods

Single extraction procedures have been widely used to assess the labile fractions of metals that are related to plant uptake and which can be used in risk assessment calculations (Degryse et al., 2009; Singh, 2007). The ideal chemical extractant should release both the immediately available metal fraction and the fraction of the reserve which replenishes the immediately available fraction over time (Levesque and Mathur, 1988; Singh, 2007). However, in reality, there is no single extraction procedure which can estimate the fraction of an element available for uptake by plants in most soils and under all soil conditions. Therefore, a wide range of protocols has been used by different investigators (Levesque and Mathur, 1988; Ure 1996; Lebourg et al., 1996; Ure and Davidson, 2002; Takeda et al., 2006; Vandenhove et al., 2007; Rao et al., 2008; Singh, 2007). Single extractants can be classified into a) dilute mineral and organic acids (e.g. HNO_3, HCl, CH_3COOH), b) alkaline reagents (e.g. $NaHCO_3$, tetra-methyl ammonium hydroxide (TMAH)), c) chelating agents (e.g. EDTA and DTPA) and d) salt solutions (e.g. $CaCl_2$, KNO_3, CH_3COONH_4) which can be used at varying concentrations and with a range of extraction times, temperatures and soil:solution ratios (Novozamsky et al., 1993; Goody et al., 1995; Ure, 1996; Young et al., 2000; Meers et al., 2007; Anjos et al., 2012). Various studies have compared U and Th concentrations measured by single extractions to plant uptake of U and Th. For example, $NaHCO_3$ (0.5 M) and CH_3COONH_4 (1.0 M) were used by Sheppard and Evenden (1992) to estimate the available U in ^{238}U-spiked soils; the extraction efficiency of $NaHCO_3$ was greater than that of CH_3COONH_4 but the

extracted U was not correlated with soil-to-plant transfer of U. Shahandeh and Hossner (2002a) used citric acid, HEDTA and DTPA to solubilize U in contaminated soils. More recently, Vandenhove et al. (2007b) investigated the influence of soil properties on U uptake by ryegrass from 18 $^{238}U(VI)$ spiked soils. The authors did not find a significant correlation between the soil-to-plant transfer factor for U and the U concentrations either in soil solution or extracted by 1 M CH_3COONH_4 (pH 5 and 7). Vandenhove et al. (2007c) compared U concentrations in soil pore water, two single extractants (0.4 M $MgCl_2$ and 0.11 M CH_3COOH) and DGT-measured U concentrations with U uptake by ryegrass from 6 soils with different U contamination levels and different soil properties. In this case plant uptake was highly correlated with soil pore water U concentration and DGT-measured U concentration (r = 0.9), while extracted U concentration was less strongly correlated (r = 0.7) with plant uptake. Takeda et al. (2006b) used dilute acid (1.0, 0.1, 0.01 M HNO_3), a chelating agent (0.05 M EDTA), a neutral salt solution (1 M NH_4OAc, 1 M NH_4NO_3, 0.01 M $CaCl_2$) and pure water to extract U and Th from 16 agricultural soils and correlate the extracted concentrations with plant uptake. It was found that the extracted Th and U concentrations were not correlated with plant uptake. On the other hand, the amount of U and Th extracted by 0.43 M HNO_3, 0.01 M $CaCl_2$ or 0.1 M $Ba(NO_3)_2$, representing the reactive metal fraction in equilibrium with soil solution, was used to calculate the solid-solution partition coefficient in two acid sandy (humus-iron podzol) soil profiles (Gooddy et al., 1995). In a recent study, Guo et al. (2010) evaluated Th bioavailability in soil samples collected from rare earth industrial areas in China using single extraction methods (0.1 M $CaCl_2$, 1 M NH_4NO_3, 0.11 M HOAc and different concentrations of EDTA). They found that a mixture of 0.02 M EDTA + 0.5 M NH_4OAc (pH 4.6) was suitable for determining Th bioavailability in soils based on a significant correlation with Th uptake by wheat plants.

Uranium exists in soils in two oxidation states; U(VI) which dominates under oxidising conditions and U(IV) which dominates under reducing conditions. Both uranium oxidation states are different with respect to solubility, mobility and speciation; U(VI) exists as the uranyl cation (UO_2^{2+}) and associated complexes with organic and inorganic ligands and is relatively soluble, while U(IV) forms relatively insoluble solid phases such as uraninite (Langmuir, 1997; Grypos et al., 2007). Single

extraction procedures using dilute (bi) carbonates can completely remove U(VI) from contaminated soils and sediments without interfering with U(IV) quantitation. Payne et al. (1998) and Kohler et al. (2004) reported that desorption of U(VI) from most mineral phases is expected to be complete under extraction with dilute (bi) carbonates. Sodium bicarbonate (0.5 M) was used by Mason et al. (1997) who found that the amount of U released by $NaHCO_3$ from contaminated soils from the Fernald Environmental Management Project (FEMP) in laboratory column studies was equal to 75-90% of total U, corresponding approximately to the percentage of uranium in the oxidized state U(VI). Moreover, the authors showed that the addition of sodium peroxide oxidized U(IV) to U(VI) and thus increased the extractable U amount. The efficiency of surfactants and bicarbonate (among other extractants) for the release of U(VI) adsorbed onto Oak Ridge soils under laboratory conditions was investigated by Gadelle et al. (2001). Desorption efficiency with bicarbonate was lower than with surfactants due to the buffering capacity of the acidic soils, but if the pH of the extracting solution was kept high enough to stabilize the dissolved uranyl carbonate complexes, bicarbonate extracted U as efficiently as surfactants (Gadelle et al., 2001). Bond et al. (2008) used formate buffer (0.5 M; pH 3.5) to estimate the amount of U(VI) that was adsorbed on mineral surfaces in contaminated sediment or U(VI) present in mineral phases that could be dissolved by dilute acids as U(VI) co-precipitated within poorly crystalline oxides or carbonates. Formate buffer (pH 3.5) was more efficient at releasing U(VI) co-precipitated with carbonate mineral phase than acetate buffer (pH 4.7) as any U(VI) released is not likely to be re-adsorbed at pH 3.5 (Payne et al., 1998; Bond et al., 2008).

Degryse et al. (2009) suggested that EDTA in appropriate concentrations, ranging from approximately 50 to 100 mmol per kg soil, may represent the best estimator of the labile pool of several metals compared with other single extractants. In fact, this appears to be metal-specific and depends on the stability of the specific metal-EDTA complex. For example, the stability constant ($\log_{10}$ value) for a 1:1 EDTA-UO_2^{2+} complex is only 7.4 which is extremely low compared with the Ca-EDTA complex ($\log_{10}K$ = 10.7). Furthermore, the presence of the EDTA-UO_2^{2+} complex is limited above pH 6.5 due to formation of U-hydroxyl and carbonate species (Francis et al., 2000). Thus, extraction with EDTA is expected to underestimate the labile U pool in

soil. In addition, dilute nitric acid, at a range of concentrations, has been suggested as an extractant of the labile metal pool, particularly in acidic soils (Tipping et al., 2003; Almas et al., 2007; Degryse et al., 2009) and has been successfully used as an input variable to mechanistic geochemical models to predict metal solubility in soils (Tipping et al., 2003). However, dilute nitric acid may overestimate the labile pool of metals such as Zn, Ca and Pb in calcareous soils due to the mobilization of the non-labile metal pool by dissolving carbonate binding phases (Degryse et al., 2009; Marzouk et al., 2013). In contrast to this observation, HNO_3 may underestimate the labile pool of U and Th in calcareous soils due to the large buffering capacity of soil carbonate. The mode of operation of the HNO_3 extraction protocol is entirely due to changes in pH value and so, because soils differ in the suspension pH values produced depending on their buffer capacities and initial pH values, the method is intrinsically flawed for calcareous soils. On the other hand, solubilization of thorium by HNO_3 may be limited by the flocculation of humic and fulvic acids at extremely low pH values if the main stable form of Th in solution, in the absence of synthetic chelating agents, is organically-complexed Th.

1.1.2 Sequential extraction procedures (SEP)

In contrast to single chemical extraction procedures, sequential extraction procedures (SEPs) can provide detailed information on the different chemical forms of metals expected to be present in soil, rather than just distinguishing between labile and non-labile metal fractions. In SEPs a soil or sediment is subjected to a series of chemical extractants with a gradual increase in extraction power. Many SEPs used in recent years are modified from that originally developed by Tessier et al. (1979) and Ure et al. (1993) (BCR method). They vary in the number of fractions extracted, the type and order of chemical extractants used (Table 1.1). The use of SEPs for natural radionuclides is limited and usually uses Tessier method or the Schultz modification of the Tessier method (Schultz et al. 1998) rather than the BCR method (Table 1.1) (Bunzl et al., 1995; Blanco et al., 2005; Strok and Smodis, 2010). Blanco et al. (2005) applied and compared two SEPs, the Tessier method and the Schultz modification of the Tessier method, to the fractionation of ^{238}U, ^{230}Th and ^{226}Ra in soil samples. The two methods yield different results and the Schultz modification better suits the objectives of this type of sequential method in terms of reproducibility and recovery.

More recently, Strok and Smodis (2010) compared the Schultz modification of the Tessier method and a revised BCR method (Table 1.1) for the fractionation of ^{238}U, ^{230}Th and ^{226}Ra in soil samples and found that the results obtained by the two methods were not fully comparable and were method and metal dependent. The authors concluded that the extracted fractions obtained using each method are operationally-defined and should not be used interchangeably in the same study.

Despite the detailed information obtained from SEPs on metal fractionation, SEP methods have been widely criticised, mainly for the lack of complete selectivity of reagents in each step of the procedure (Gleyzes et al., 2002; Young et al., 2005; Singh, 2007, Laing, 2010a; Rao et al., 2008). For example, it has been suggested that, the metal fraction extracted in the second step of the Tessier method (carbonate fraction; NaOAc/HOAc) would be specifically adsorbed on surfaces, particularly on Fe oxide surfaces (Gleyzes et al., 2002). Moreover, re-adsorption and redistribution of metals have been noticed when there is incomplete dissolution of some phases and change in pH from the previous step (Bermond, 2001; Gleyzes et al., 2002). Labile metal (measured by isotopic dilution (ID)) and plant uptake is unlikely to correspond to any single or combined SEP fractions (Ahnstrom and Parker, 2000; Punshon et al., 2003; Atkinson et al., 2011). For example, Punshon et al. (2003) did not find a relationship between plant uptake of U and U measured in single or combined fractions from a sequential extraction procedure. It was concluded that care should be taken when drawing conclusions regarding bioavailability based on sequential extraction results (Laing, 2010a).

To try to avoid the limitations of sequential extraction procedures, such as re-adsorption and redistribution of metals during fractionation, dynamic leaching approaches have recently been developed (Laing, 2010a; Tongtavee et al., 2005b; Shiowatana et al., 2001). Such approaches not only provide fractional distribution data for assessing the potential availability and mobility of metals but also provide elution profiles which can be used for investigation of elemental associations and to explore the degree of anthropogenic contamination in relation to naturally-occurring metal (Buanuam et al., 2005).

Table 1.1: Selected sequential extraction procedures used for the fractionation of U and Th in soils and sediments

	Sequential extraction steps				
	F1	**F2**	**F3**	**F4**	**F5**
Tessier et al. (1979)	*Exchangeable* 1 M $MgCl_2$ pH 7	*Carbonates* 1.0 M NaOAc/HOAc, pH 5	*Oxides Fe/Mn* 0.04 M $NH_2OH.HCl$ in 25% HOAc	*Organic matter* H_2O_2/NH_4OAc	*Residual* $HF/HClO_4$
Schultz et al. (1998) *(modification of Tessier procedure)*	*Exchangeable* 0.4 M $MgCl_2$ pH 5	*Organic matter* 5-6% NaOCl pH 7.5	*Carbonates* 1.0 M NaOAc in 25% HOAc	*Oxides Fe/Mn* 0.04 M $NH_2OH.HCl$ pH 2 (HNO_3)	*Residual* $HNO_3/HCl/HF/HClO_4$
Martinez-Aguirre and Perianez, (2001)	*Carbonates* 1.0 M NaOAc/HOAc, pH 5	*Organic matter* 0.1 M Na-pyrophosphate pH 9 (NaOH)	*Amorphous oxyhydroxides* Tamm's acid oxalate	*Crystalline oxides* Coffins reagent (Na-citrate+citric acid)	
Guo et al. (2007)	*Exchangeable* 1 M $MgCl_2$ pH 7	*Carbonates* 1.0 M NaOAc/HOAc, pH 5	*Organic matter* 0.1 M Na-pyrophosphate pH 9.8 (NaOH)	*Amorphous oxyhydroxides* Tamm's acid oxalate	*Crystalline oxides* Coffins reagent (Na-citrate + citric acid)
Strok and Smodis, (2010) *(revised BCR method)*	*Carbonates* 0.11 M HOAc	*Oxides Fe/Mn* 0.5 M $NH_2OH.HCl$/ 0.05 M HNO_3	*Organic matter* 8.8 M H_20_2/1M NH_4OAc	*Residual* Na_2O_2 fusion and HNO_3/ $HCI/HF/H_2SO_4$	
Kaplan and Serkiz, (2001)	Aqueous Saturation with surface water	*Exchangeable* 0.44 M HOAc + 0.1 M $Ca(NO_3)_2$	*Organic matter* 0.1 M Na-pyrophosphate	*Amorphous oxides* 0.175 M Ammonium oxalate/0.1 M oxalic acid	*Crystalline oxides* Na-dithionite in Na-citrate + citric acid

OAc (acetate)

1.1.3 Isotopic dilution technique (ID)

Various studies have reported that the isotope dilution technique is the most appropriate method to quantify the 'chemically reactive' or 'labile' metal pool in soils (Smolders et al., 1999; Tongtavee et al., 2005a; Degryse et al., 2009). Buekers et al. (2008) reported that isotopically exchangeable metal concentrations (E-values) were superior to total soil metal concentrations when used to predict metal solubility in geochemical speciation models. Essentially, the isotopically exchangeable metal represents the soil metal fraction which forms a dynamic equilibrium between the solid and solution phases in a soil suspension. The isotopically exchangeable $^{238}U(VI)$ in soil is determined by suspending a soil sample in a dilute electrolyte, typically $CaCl_2$ or $Ca(NO_3)_2$, for a specific *pre-equilibrium* time, then adding a small amount of a rare isotope (eg. ^{233}U or ^{236}U) to the soil suspension. After a given equilibration time, the U(VI) isotope ratio ($^{233}U/^{238}U$) is determined in the soil supernatant, which allows the quantification of the fraction of $^{238}U(VI)$ in dynamic equilibrium between solid and liquid phases in the soil into which the tracer has been added.

Uranium in solution may be associated with colloids including organic matter, amorphous iron hydroxide and clay particles (Singhal, 2005; Bouby et al., 2011; Yuheng et al., 2013; Yang et al., 2013). Elements (e.g. Cu, Zn) associated with colloids may be isotopically non-exchangeable, which leads to significant overestimation of the E-value (Lombi et al., 2003; Ma et al., 2006). To minimize the possible interference of non-isotopically exchangeable metal associated with colloids <0.2 µm in the determination of E-value, a resin purification step was applied in this study (Section 2.6.4).

A few studies have used the isotopic dilution technique to measure the 'labile' or 'accessible' $^{238}U(VI)$ in contaminated soils and sediments and to investigate the reversibility of U binding onto synthetic solid phase (e.g. modified bauxite refinery residue (MBRR); Clark et al., 2011). In addition, isotopic dilution was used in a few studies to verify the use of single chemical extraction methods to estimate the 'labile' or 'accessible' U(VI) pool in contaminated soils and sediments. Payne and Waite (1991) measured the 'accessible' U in rock samples from two ore deposits in Australia using isotope exchange; in this study crushed rock materials were equilibrated with

synthetic ground water then spiked with $^{236}U(VI)$. Approximately 20 – 25% of the total U content was determined to be isotopically exchangeable within a time scale of days. The authors found that only a small amount of U(VI) was dissolved in a NH_4Cl extract, thus they concluded that most of the isotopically exchangeable U(VI) was specifically adsorbed to the mineral surfaces rather than associated via ion exchange. Measurement of isotopically exchangeable $^{238}U(VI)$, using $^{236}U(VI)$ as the spike isotope, was also applied by Del Nero et al. (1999) to study the sorption/desorption processes of U in clayey and Fe-oxyhydroxide rich samples from the oxidizing weathered zones around the natural Bangombe Nuclear Reactor in Gabon. Payne et al. (2001) estimated the 'accessible' U using chemical extraction with Tamm's acid oxalate (TAO) and the results were then verified using isotope exchange; samples from the Koongarra uranium deposit, Northern Australia, were suspended in 0.1 M $NaNO_3$ and equilibrated for 24 hr then spiked with $^{236}U(VI)$ and equilibrated for a further 48 hr. Isotope exchange confirmed the validity of Tamm's acid oxalate (TAO) as an extractant of labile U. Similarly, Kohler et al. (2003) studied the U(VI) distribution coefficient (K_d) in contaminated sediments and used different methods for estimating the adsorbed U(VI). A significant correlation ($r = 0.998$) was found between the uranium E-value (using $^{233}U(VI)$ as the spike isotope) and a bicarbonate (1.44×10^{-2} M $NaHCO_3$ and 2.8×10^{-3} M Na_2CO_3, pH 9.45) extractable U fraction, with a slope of 0.96 ± 0.01. The results supported the use of the bicarbonate extraction method for estimating the quantity of labile U(VI) in contaminated sediments that do not contain U(IV). Payne et al. (2004) reported that the isotope exchange technique can be used to quantify U derived from different sources. Isotopic exchange and single extraction techniques combined with spectroscopic measurements were used by Bond et al. (2007) to estimate U(VI) release kinetics and the contributions of desorption and dissolution to U(VI) release from vadose zone sediments from a depth-sequence. According to Bond et al. (2007) the tracer $^{233}U(VI)$ probably exchanges first with the adsorbed U(VI) on mineral surfaces exposed to the bulk solution. After initially rapid isotopic exchange, slower exchange occurs with U(VI) being adsorbed in micropores, due to the limitation of mass transfer, and with U(VI) associated with precipitated or co-precipitated mineral phases, depending on kinetic constraints (Bond et al., 2007). The authors found that there was a good agreement between isotopically exchangeable U(VI) and bicarbonate-extracted U for the samples in the sediment profile with low

U(VI) contamination (U(VI) release was primarily due to U(VI) desorption), whilst there was a lack of agreement between isotopic exchange results and bicarbonate extraction for the highly contaminated sediments at shallow depths. Both desorption and dissolution contribute to U(VI) release in (bi)carbonate extraction. In a study by Kohler et al. (2003) sediments were contaminated in the range of 3 to 8 mg kg^{-1} U while Bond et al. (2007) contaminated sediments in the range of 3 to 106 mg kg^{-1} U. More recently, the distribution and concentration of U in contaminated sediments sampled near radioactive waste storage tanks at Hanford, Washington (USA) were estimated by Um et al. (2010) using single extraction methods (8 N HNO_3 and bicarbonate as in Kohler et al. (2003)) and isotope exchange (^{233}U(VI) as spike isotope). U desorption K_d values calculated using isotope exchange were lower than those computed from bicarbonate and acid extractions. However, the K_d values calculated using the three methods were likely to reside within the range of measurement uncertainty. Clark et al. (2011) used isotope exchange between ^{238}U and ^{232}U, and ^{232}Th and ^{229}Th to study the reversibility of U and Th binding onto modified bauxite refinery residue (MBRR). The labile U comprised 80-90% of the total U adsorbed in MBRR suggesting that U adsorption is mostly reversible, while Th was very strongly bound to MBRR and irreversibly bound over a pH range 3-8. However, the isotope exchange data supported the use of some single extractants, such as the bicarbonate extraction method, to estimate the 'labile' U(VI). However, measuring the 'labile' U(VI) by isotopic exchange is preferable to single extraction measurements as no assumptions are required about the nature of the extracted phases (Payne et al., 2001).

1.1.4 Fractionation using size exclusion chromatography (SEC)

Size exclusion chromatography has been widely used to measure the molecular size distributions of natural organic matter (Perminova et al., 2003; Asakawa et al., 2008, 2011). Recently, SEC interfaced with a multi-element measurement method such as ICP-MS has been applied to the study of the fractionation of trace elements bound to particles and molecules of different sizes, particularly for the analysis and distribution of trace elements associated with dissolved organic matter in ground water, soil extracts and solutions (Jackson et al., 2005; Schmitt et al., 2001; Casartelli and Miekeley, 2003; Bednar et al., 2007; Sadi et al., 2002; Wu et al., 2004; Takeda et al.,

2009; Kozai et al., 2013). Size exclusion chromatography is applicable to the separation of dissolved macromolecules over a molecular size range of ca. 200 - 1000, 000 Da, depending on the gel phase used in the column (Jackson et al., 2005). The samples are injected into a column tightly packed with a porous polymer gel material (stationary phase) with pores of different sizes. Molecules and colloids which are larger than the pores of the gel elute first in the excluded volume, while small molecules are able to move into and through the pore network of the gel phase which leads to a longer retention time. Molecules therefore elute at different times as a function of their molecular size, hence the relative molecular weights of different fractions, together with any adsorbed or complexed elements, can be differentiated (Jackson et al., 2005; Pelekani et al., 1999; Laing et al., 2010b). Ideally, the analyte should not interact with the column gel phase during separation, such that the fractionation is based solely on size. However, this is rarely true in practice as hydrophobic adsorption and charge repulsion and attraction affect the retention time of molecules in the column and hence their apparent molecular size (Pelekani et al., 1999; Jackson et al., 2005). For these reasons Collins, (2004) concluded that molecular separation using SEC is actually a combination of size-based fractionation, ion exchange and ion exclusion effects. It is recognized that the mobile phase composition, pH and ionic strength can greatly affect the SEC size fractionation by affecting the surface charge characteristics of the gel phase, the organic matter charge and structure and hence the interaction between the analyte and the gel phase (Gloor et al., 1981; Swift and Posner, 1971; Pelekani et al., 1999). Miles and Brezonik, (1983) investigated the effect of the mobile phase composition on the molecular weight distribution of aquatic humic substances and found that at low ionic strength significant ionic interactions occurred, while at high ionic strength (>0.2) ionic effects were suppressed. In addition, the chemical properties of humic substances (e.g aromatic structure and functional group composition) affect the intensity of the interaction between the humic substances and the gel phase (Pelekani et al., 1999; Asakawa et al., 2011). For example, in the case of humic substance with a high proportion of aromatic components the specific hydrophobic adsorption to the gel phase would prevent the size exclusion separation of humic substances (Egeberg and Alberts, 2003; Asakawa et al., 2011).

In order to minimize the interactions between the humic substances and SEC gel phase (non-size exclusion effects), many different buffer solutions have been used as mobile phases, such as TRIS (tris(hydroxymethyl)aminomethane; pH 8.07), phosphate buffer (pH 7.0), CAPS (3-(cyclohexyloamino)-1-propanesulfonic acid) buffer (pH 10.4 with NaOH) or sodium tetraborate (Schmitt et al., 2001; Perminova, 1999). Sodium phosphate buffer (pH 7.0)/acetonitrile (3:1, v/v) was found to be applicable for different HAs, and displayed high reproducibility and recovery (87.0 – 94.5%) (Asakawa et al., 2008). In addition to the reported problem of the incomplete recovery of dissolved humic substances during SEC separation, a further problem arises from the possible dissociation of organic-metal complexes through interaction with both the gel and mobile phases (Schmitt et al., 2001; Jackson et al., 2005; Asakawa et al., 2008, 2011). It was concluded that only organic-metal complexes whose dissociation rate is insignificant during the separation process are applicable to SEC analysis (Collins, 2004). The affinity of free metal ions, arising from dissociation of labile complexes, for the column gel phase produces diffuse and unreliable elution patterns (Jackson et al., 2005). Jackson et al. (2005) studied the fractionation of Ni and U in four contaminated sediment water extracts using SEC. The Ni recovery was low (1.6-18.3% of total Ni, except for one sample with 28% recovery), because SEC was not efficient at eluting the free metal cation or labile complexes, while U recovery (22-75% of total U) was greater than Ni. Casartelli and Miekely (2003) applied SEC to verify the possible association of Th and light rare-earth elements (LREEs) with natural organic matter in soil water and showed that complexation by high molecular mass organic matter (humic substances) dominates over low molecular mass organic and/or inorganic complexes, suggesting that association with labile organic acids or inorganic ligands is of minor importance in the soils studied.

1.1.5 Geochemical speciation model WHAM-VII

Recently, geochemical ‘assemblage’ models have been developed and used to describe soil solution chemistry in a variety of soils (Tipping, 1994; Lofts et al., 2001; Weng et al., 2001, 2002; Gustafsson, 2001). The assemblage models consider the soil as a set of independent reactive surfaces and comprise several advanced models to describe ion sorption to different soil surfaces including organic matter (solid and dissolved), oxyhydroxides and clay. Commonly used models are WHAM (the

Windermere Humic Aqueous Model; Tipping, 1998; Lofts and Tipping, 1998), ECOSAT (Weng et al., 2001), ORCHESTRA (Meeussen, 2003) and Visual Minteq (Gustafsson, 2001). These geochemical models were designed to describe the chemistry and speciation of oxic aqueous environments, then extended to describe soil solution speciation and the solid-solution partitioning. Recently, WHAM has been used to investigate the fractionation and solubility of a range of metals in whole soil (Tipping et al., 2003; Marzouk et al., 2013; Almas et al., 2007; Buekers et al., 2008) but not, to date, to predict the solubility and fractionation of Th and U in whole soils.
WHAM is a mechanistically based equilibrium model which is internally consistent with regards to mass and charge balance. It partitions the free energy of metal-geocolloid interactions into 'chemical bonding' and 'electrostatic' components (Tipping, 1994, 1998). WHAM has been parameterized from an extensive set of experimental data (Tipping, 2002) and uses intrinsic chemical constants developed for isolated pure surfaces to simulate whole soils (humic acids, fulvic acids, metal oxides and clay surfaces) (Tipping, 1994, 1998; Lofts and Tipping, 1998). According to WHAM, the different phases are in chemical equilibrium with the solution phase and the interaction between the phases does not affect the ion binding properties (Lofts and Tipping, 1998).

The current version of WHAM-VII is a combination of three submodels: Humic Ion-Binding Model VII (Tipping et al., 2011), used to describe metal ion binding to humic substances (HA and FA; solid (particulate phase) and dissolved (colloidal phase)), Surface Complexation Model (SCM), describes metal ion binding to oxides of Fe, Al, Mn and Si (Lofts and Tipping, 1998), and a simple cation exchange model, based on Donnan expressions, (Tipping, 1994) used to describe nonspecific binding of metal ions to aluminosilicate clays. In addition, an inorganic speciation model is included in WHAM(VII) and considers the cation complex formation with inorganic ligands in soil solution. An electrostatic model was included in humic ion-binding model VII and SCM to describe the electrostatic interactions; the electrostatic interactions of a given phase are assumed to be uninfluenced by those of any other phase (Lofts and Tipping, 1998).

Humic Ion-Binding Model VII is the most important component of the overall model. It treats HAs and FAs as rigid hydrophobic spheres of uniform size with binding sites, of different binding strength, positioned on their surfaces. Two types of discrete binding sites are distinguished and can be identified as carboxylic (strong acid) and phenolic (weak acid) acid groups. Each binding site type includes four different groups present in equal amounts and characterised by intrinsic equilibrium constants (pKa; where in this situation the humic substances have zero surface charge). The model takes account of competition for binding sites between metal cations and with protons and the increased range of binding strengths resulting from the formation of bidentate and tridentate binding sites. In addition, a small number of very strong binding sites have been taken into account using an additional parameter (ΔLK_2) (Tipping, 1998; Tipping et al., 2011).

WHAM-VII is simpler than WHAM-VI in its postulated multidentate metal binding sites (Tipping et al., 2011) although Model VII incorporates more metals than Model VI. It differs from Model VI with regards to metal cation binding; the arrangement of multidentate sites has been modified (multidentate sites containing more than one type of phenolic acid groups are omitted from Model VII) and some parameters eliminated. In addition, the number of datasets used to calibrate Model VII is approximately double that used for Model VI, which results in better description of metal binding at high pH. However, even though Model VII represents an improvement on Model VI, its predictions do not differ greatly (Tipping et al., 2011).

A problem with geochemical models such as WHAM is that they require a large number of input variables, some of which may be difficult to measure. A prime example is the 'reactive metal fraction' which is used as a predictor of metal concentration and speciation in the soil solution; a reliable estimate of the reactive metal fraction is therefore critical to successful prediction of metal soil-solution partitioning and the concentration of active adsorption phases (organic matter content, clay content and mineral oxides) (Buekers et al., 2008). Inevitably, assumptions are required to quantify model variables such as the 'active organic matter fraction' and the 'reactive surface area' of Fe oxides (Degryse et al., 2009). These limitations may influence the predictive ability of WHAM and should be taken into account if

geochemical models such as WHAM are to become accepted in practical applications like soil remediation and risk assessment.

1.2 Aims, objectives and thesis structure

The primary aim of this work was to develop and test isotopic dilution as a means of determining isotopically exchangeable (labile) $^{238}U(VI)$ in a wide range of contrasting soils and to:

i) assess the soil factors controlling U lability in soils;
ii) evaluate chemical extraction approaches for the characterization of reactive thorium in soils;
iii) investigate the dominant soil properties controlling U and Th solubilities in soils and rank them according to their contribution to try to reduce the uncertainty linked with soil K_d values used in risk assessment models;
iv) evaluate the effectiveness of the geochemical model WHAM-VII to predict solid-solution partitioning and solubilities of U and Th in soils.

The thesis is arranged in the following sequence

Chapter 2 presents the optimisation of ICP-MS for Th and U analysis at low concentrations to demonstrate that ICP-MS is suitable for measuring trace Th and U concentrations in environmental samples. This chapter also describes the general materials and methods used for measuring soil characteristics and soil pore water extraction by Rhizon soil moisture samplers. The development of an isotope dilution (ID) technique to measure labile $^{238}U(VI)$ in soils (E-value) and the presence of non-labile $^{238}U(VI)$ in suspended colloidal particles (SCP-U) is also presented.

Chapter 3 investigates the vertical distribution and mobility of uranium and thorium in soils at adjacent but contrasting arable and woodland sites based on the same parent material. The effect of long-term application of phosphate fertilizer on U and Th concentrations in the arable soil was determined by the exploration of U/Th ratios as a means of determining U enrichment and comparison with U/Th ratios in the woodland soil and the deeper arable soils. In addition, the chemical fractionation of U and Th in both arable and woodland soils was investigated using a sequential extraction procedure.

Chapter 4 investigates the lability of U and Th in two sets of soils: Field soils consisted of a collection of thirty seven soil samples representing five contrasting local ecosystems and BGSc soils included 40 soils sub-sampled from the British Geological Survey (BGS) archive. Preliminary experiments were conducted to study the effect of trace-isotope equilibration time and the effect of spike isotope concentration and pH on measured ^{238}U(VI) E-values. The lability of U(VI) was measured using isotope dilution with or without a chelex resin purification step and using four different single extraction approaches. The soil factors influencing ^{238}U(VI) E-values were assessed. The U labile fraction, measured using different methods, was investigated as a function of soil properties and flaws in the E-value protocol and chemical extraction methods were identified. Four single extraction methods were evaluated for the characterization of labile Th in the two sets of soils. In addition, an empirical model was used and assessed for its ability to describe and predict U (isotopically exchangeable fraction) and Th (chemically extracted fraction) lability using soil properties.

In Chapter 5, a simple continuous leaching approach for U and Th fractionation was developed. Two contrasting soils; Biosolid-amended Arable soil and Acidic Moorland topsoil were used in this chapter. Soil was placed in a small column and leached continuously with dilute nitric acid at a steady flow rate for 27 hr; during this time 115 fractions were collected to study the fractionation of U and Th in soils. Release patterns of U and Th were compared with some major and trace elements to investigate metal associations through similarities in release patterns and correlation analysis. In addition, the concentrations of Th and U released during continuous leaching were compared with concentrations obtained using batch extraction techniques and/or isotopic dilution (E-values).

Chapter 6 describes the dynamics of Th and U in soils and investigates the dominant soil properties controlling U and Th solubilities in the two sets of soils described in Chapter 4. Pore water from Field soils was extracted with *Rhizon* Soil Moisture Samplers and Rhizon-extracted soil pore water U (U_{pw}) was compared with U concentrations in 0.01 M $Ca(NO_3)_2$ extracts ($U_{Ext)}$ to determine whether U_{Ext} can be

used as a surrogate for pore water U concentration. An empirical model was assessed for its ability to predict and describe U and Th free ion activities using a limited number of soil properties. In addition, an empirical model was used to predict U and Th $\log_{10}K_d$ values, calculated based on total metal contents (K_d), reactive metal concentrations instead of total metal (K_d^{lab}), or free metal ion activities in soil solution rather than total concentrations in solution ($^{*}K_d^{lab}$), as a function of the soil variables thought most likely to affect Th and U solubilities in soils.

In Chapter 7, the effectiveness of the mechanistic geochemical model WHAM-VII in predicting solid-solution partitioning and solubilities of U and Th in the two sets of soils described in Chapter 4 was evaluated. The WHAM model requires an estimate of the reactive metal concentration across all adsorbed phases to be used as a predictor of metal soil solution partitioning. Therefore, reactive metal concentration measured by different approaches (Chapter 4) was used as an input variable in WHAM to predict U and Th concentrations in soil solution. A biosolid-amended arable soil was saturated with MilliQ water and incubated for 47 days at a range of temperatures (5, 10, 16, 25, and 30 ^{o}C) and the soil solution was extracted using *Rhizon* soil moisture samplers (see Section 2.3.1 for details) at 1, 5, 11, 19, 28, 40, and 47 days to study the effect of soil temperature and reducing conditions on U and Th solubilities and complexation in soil solution. In addition, the speciation of U and Th in soil pore water and their distribution in dissolved organic matter (DOM) size fractions were investigated using SEC-ICP-MS.

Finally, general conclusions are presented in Chapter 8 alongside results of preliminary experiments for testing the ID technique for measuring ^{232}Th lability using ^{230}Th isotope tracer and optimising the composition of soil suspending solution to allow accurate determination of ^{232}Th E-value (lability) and finally some suggestions for future work.

2 MATERIALS AND METHODS

This chapter presents the general materials and methods used for soil characterization including measurement of soil pH, organic matter content, mineral oxide content, clay content, phosphate and major and trace metal concentrations. Soil pore water extraction by Rhizon soil moisture samplers is also described. Optimisation of ICP-MS for Th and U analysis at low concentrations is presented to demonstrate that ICP-MS is suitable for measuring trace Th and U concentrations in environmental samples. An isotope dilution technique (ID) is developed to measure labile ^{238}U in soils (E-value) and the presence of non-labile ^{238}U in suspended colloidal particles (SCP-U) is investigated.

2.1 Optimisation of ICP-MS for Th and U analyses at low concentrations

2.1.1 Thorium and uranium calibration

Thorium and uranium have traditionally been measured by radiometric techniques such as alpha spectroscopy, gamma spectroscopy and neutron activation analysis. However, these techniques are time consuming and are not suitable for accurate determination of Th concentrations at the levels typically found in environmental samples, such as natural waters. It has been reported that ICP-MS (inductively coupled plasma mass spectrometry) offers a low detection limit for Th and has several advantages over the traditional radiometric techniques especially for radionuclides with half life ($t_{1/2}$) values > 10^4 years which have high mass:activity ratios (Schramel et al., 1997; Holmes and Pilvio, 2000; Holmes, 2001).

Optimisation of ICP-MS for ^{232}Th analyses at low concentrations

Uncertainty in measured Th concentrations is highly dependent on the calibration method used. It has been reported that the calibration itself is the major source of uncertainty for both ‘external calibration’ and ‘standard addition’ approaches. Other factors, such as dilutions, weighing or instrument repeatability, make only minor contributions to uncertainty. When external calibration is used, the matrix of the calibration standards should be matched as closely as possible to that of the sample to minimise matrix interferences.

2.1.2 Experimental

In this section, experiments are described to establish a suitable technique for Th and U calibration and to examine the factors limiting both accuracy and precision of analysis.

2.1.2.1 Thorium and uranium calibration in 2% HNO3

In this experiment external Th and U calibrations were performed using six calibration concentrations. A logarithmic series of standards was established using a sequence of 1-in-10 dilutions of the original stock (1 ml 1000 ppm stock + 9 ml of 2% 'Trace Analysis Grade' nitric acid (Fisher Scientific)). The following Th and U concentrations were thus obtained: 0.0001, 0.001, 0.01, 0.1, 1.0, and 10 µg L^{-1}.

Iridium and bismuth as internal standards

In ICP-MS an internal standard must be used to correct the analyte signal for any drift in instrumental sensitivity (cps ppb^{-1}) over the course of the analysis. Iridium and bismuth have atomic masses close to U and Th. Because of this, and their low abundance in naturally occurring samples, all standards and blanks were spiked with Ir and Bi as internal standards at a concentration of c. 20 µg L^{-1}. Calibration blanks (2% nitric acid) were measured first, followed by a sequence of calibration standards, starting with the lowest concentration (0.0001 µg L^{-1}).

2.1.2.2 Thorium and uranium calibration curves in 3.5% HNO3

In this experiment, external Th and U calibrations were performed using eight calibration concentrations. A logarithmic series of standards was prepared, as described previously, but in 3.5% ultra-pure *Optima* grade nitric acid (Fisher Scientific; Man. Seastar Chemicals, Canada) to try to reduce 'carry-over' of either Th or U from one analysis to the next. Calibration standards included Th and U concentrations of 0.00001, 0.0001, 0.001, 0.01, 0.1, 1.0, 10, and 100 µg L^{-1}. Ten replicates of a blank solution (3.5% HNO_3) were run before and after standards in order to identify and quantify any carry-over of U or Th from analyses of individual standards to the following standard. Blanks and standards were uniformly spiked with Ir as an internal standard (0.24 µg L^{-1}).

2.1.2.3 Instrumental settings on the ICP-MS

Analyses were undertaken on a Thermo-Scientific XSeries^{II} ICP-MS. The instrument was run in 'standard mode' (evacuated hexapole) and with a high resolution 'Xs' skimmer cone to maximise sensitivity in the absence of any anticipated polyatomic interferences. Sample delivery was via a Cetac ASX-520 series auto-sampler. Analytes included ^{193}Ir, ^{206,207,208}Pb, ^{209}Bi, ^{232}Th and ^{238}U. The Pb isotopes were included in an attempt to generate sufficient data for an 'internal cross calibration factor' to improve the conversion of 'analogue' detector signals to equivalent 'pulse counting' data. Instrumental settings are shown in Appendix 2.1.

2.1.2.4 Thorium and uranium analysis in soil solution

Soil samples were collected from an arable field within the University of Nottingham farm, Leicestershire, UK ($52^0$49'48''N-$1^0$14'23''W). The soil belongs to the Wick series (a sandy loam) developed in a layer of fluvio-glacial sand and gravel (c. 80 - 100 cm thick) overlying Triassic Keuper Marl. Soil samples were taken as triplicate auger borings from the soil surface, in 10 cm depth intervals, to 80 cm in the arable field. All soil samples were air-dried, sieved to < 2 mm and 1.0 g samples equilibrated with 10 ml MilliQ water in polycarbonate centrifuge tubes for 24 hours with reciprocal shaking. Suspensions were then centrifuged at 2200 g for 15 min and the supernatant filtered to < 0.22 μm using Millipore syringe filters. Concentrations of Th and U in the soil solutions were then measured by ICP-MS using a calibration line in the range 0.01 – 1.0 μg L^{-1}.

2.1.3 Results

2.1.3.1 Thorium and uranium calibration in 2% HNO3

Four of the calibration standard concentrations (0.001, 0.01, 0.1, and 1.0 μg L^{-1}; ◊) formed a straight calibration line for both U and Th, whereas the lowest and highest concentrations (0.0001 (□), and 10 (Δ) μg L^{-1}) were displaced from the calibration line (Figure 2.1). This may be due to contamination in the lowest concentration and an imperfect conversion from analogue to pulse-counting data when the detector tripped to analogue signal at higher concentrations. The data, therefore, suggest that calibration between 0.001 – 1.0 μg L^{-1} should provide a reliable linear response.

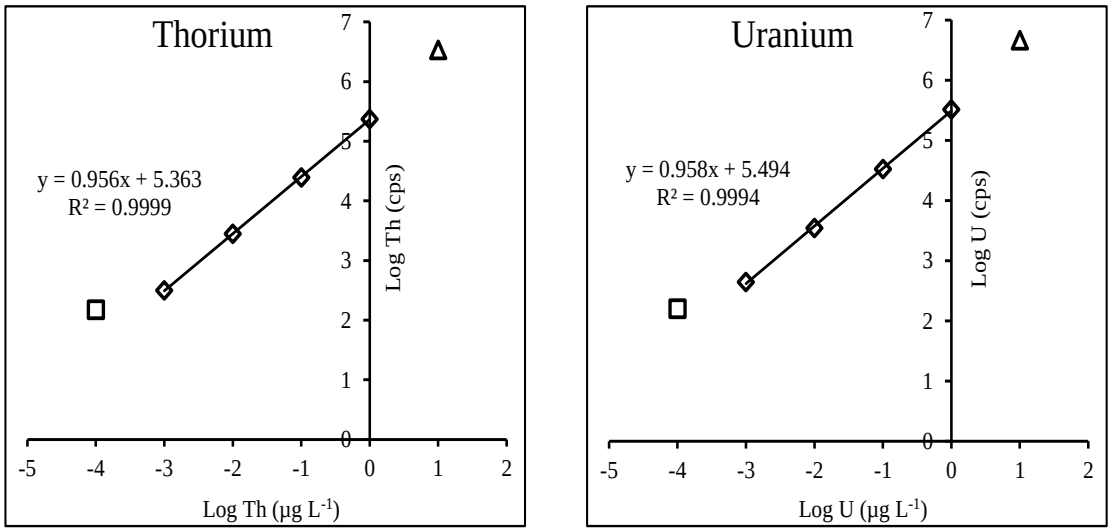

Figure 2.1: Thorium and uranium calibration curves in 2% HNO3. Data are segregated into 'low' (□), 'reliable' (◊) and 'high' (Δ) concentration ranges.

2.1.3.2 Thorium and uranium calibration curve in 3.5% HNO_3

Thorium adheres to the internal components of analytical instruments such as ICP-MS, as well as the sample vessel walls and sample delivery tubing associated with auto-samplers etc. (Bailey, 1993; Holmes, 2001; Holmes and Pilvio, 2000). Therefore, loss of Th can occur from solutions at low concentrations. Contamination is also likely when desorption of sorbed Th occurs into samples with low concentrations after running sample solutions with high concentrations through the instrument (so-called 'carry-over' from one sample to the next – see section 2.1.2.2). Nitric acid (2%) is commonly used as the matrix solution for many ICP-MS analyses, whereas in Th analysis the nitric acid concentration should be greater to (try to) reduce or prevent Th adhering to internal ICP-MS components. The 3.5% HNO_3 was used for Th and U analysis in this experiment. Figures 2.2 and 2.3 show Th and U calibration curves in 3.5% HNO_3 with eight calibration points at 0.00001, 0.0001, 0.001, 0.01, 0.1, 1.0, 10, and 100 µg L^{-1}.

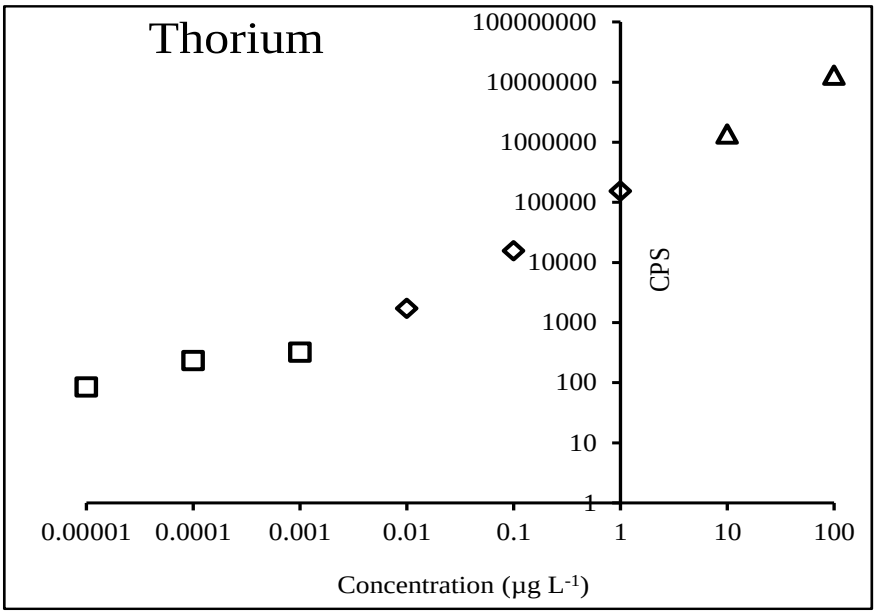

Figure 2.2: Thorium calibration curve in 3.5% HNO_3 with eight calibration points (log_{10} scale). Data are segregated into 'low' (□), 'reliable' (◊) and 'high' (Δ) concentration ranges; detector response (counts per second, cps) is corrected for internal standard drift.

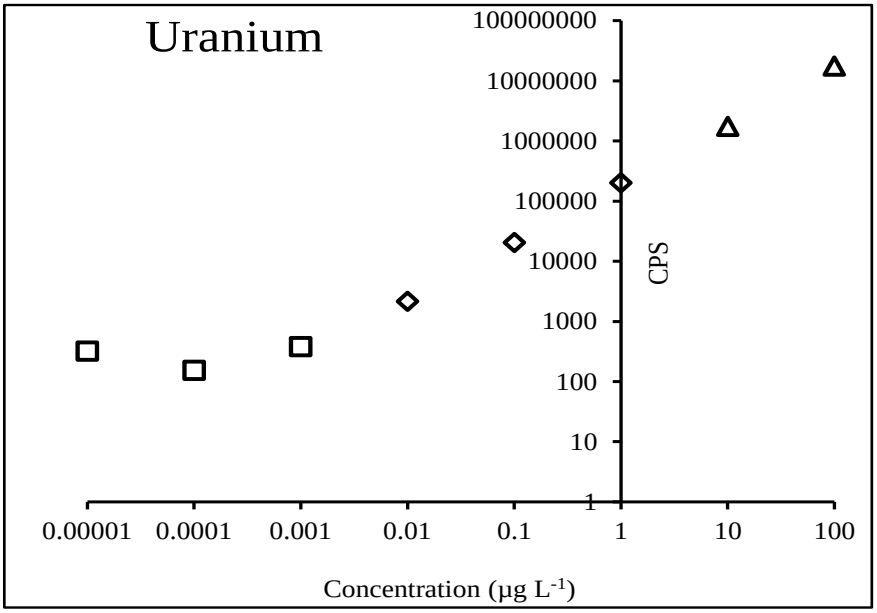

Figure 2.3: Uranium calibration curve in 3.5% HNO3 with eight calibration points (log10 scale). Data are segregated into 'low' (□), 'reliable' (◊) and 'high' (Δ) concentration ranges; detector response (counts per second, cps) is corrected for internal standard drift.

Apparent high sensitivity at low concentrations of Th (0.00001 - 0.001 µg L^{-1})

At very low Th concentrations (0.00001 - 0.001 µg L^{-1}) the ICP-MS sensitivity was apparently very high and sharply increased with decreasing Th concentration in the range 0.00001 - 0.001 µg L^{-1} as shown in Table 2.1. In contrast to Th, sensitivity of the ICP-MS to U at low concentrations was very low and decreased with decreasing U concentration in the range 0.001 - 0.00001 µg L^{-1} as shown in Table 2.1.

Table 2.1: Thorium and uranium sensitivity for different concentration ranges.

Concentration (ppb)	^{232}Th Sensitivity (CPS/ppb)	^{238}U Sensitivity (CPS/ppb)
0.00001	3.00E+06	-1.00E+07
0.0001	2.00E+06	-2.00E+06
0.001	214434	60379
0.01	160663	186690
0.1	156117	202084
1	154380	201652
10	136453	174622
100	130501	175914

Both elements displayed reasonably constant sensitivities (c. 158000 and 190000 cps ppb^{-1}) within the concentration range 0.01 – 1.0 µg L^{-1} and at higher concentrations (detector analogue signals) the sensitivity apparently declined due to an imperfect cross calibration factor.

'Memory' effect of thorium in ICP-MS analysis

Measuring blanks after the standards (the last standard to be analysed in the sequence was 100 µg L^{-1}) resulted in a large 'memory' effect (Table 2.2) which was attributed to the natural tendency of Th to adhere to the internal components of the ICP-MS and auto-sampler delivery tubing. However, blanks were not analysed directly after the standards: four washout samples (3.5% HNO_3) were run first (Table 2.2). Thorium and U cps in the first washout sample run directly after the standards were very high (4133 and 18438, respectively) and decreased to 582 and 1507, respectively, in the fourth washout sample run directly before blanks were analysed (Table 2.2). Figures

2.4 and 2.5 show the raw 'count-per-second' (CPS) data for a sequence of 10 blank solutions before and after a 100 µg L^{-1} standard analysis for Th and U, respectively, and show the high degree of 'carry-over' in the case of Th compared to U. Thus, 'carry-over' may cause a problem when higher concentration samples are analysed prior to lower concentration samples. Potential solutions to this problem may be to increase the wash-out time to remove any adhering Th, or to increase the nitric acid concentration. Alternatively, a complexing reagent may be required to clean tubing between samples.

Table 2.2: ICP-MS signal (counts-per-second) for the 100 ppb Th and U calibration standard and for 4 washout samples analysed immediately after the 100 ppb standard. Also shown are analyses of a series of 10 blanks run before and after the calibration standard.

Sample	Before standards analysis		After standards analysis	
	^{232}Th (CPS)	^{238}U (CPS)	^{232}Th (CPS)	^{238}U (CPS)
Standard (100 ppb)	-	-	15,538,693	20,680,866
Washout 1	-	-	4,133	18,438
Washout 2	-	-	1,877	6,290
Washout 3	-	-	400	1,231
Washout 4	-	-	582	1,507
Blank 1	66	512	244	666
Blank 2	61	471	237	675
Blank 3	70	465	256	668
Blank 4	99	506	188	616
Blank 5	55	432	134	506
Blank 6	57	452	124	523
Blank 7	60	454	152	533
Blank 8	55	422	99	474
Blank 9	54	426	92	476
Blank 10	58	423	93	471

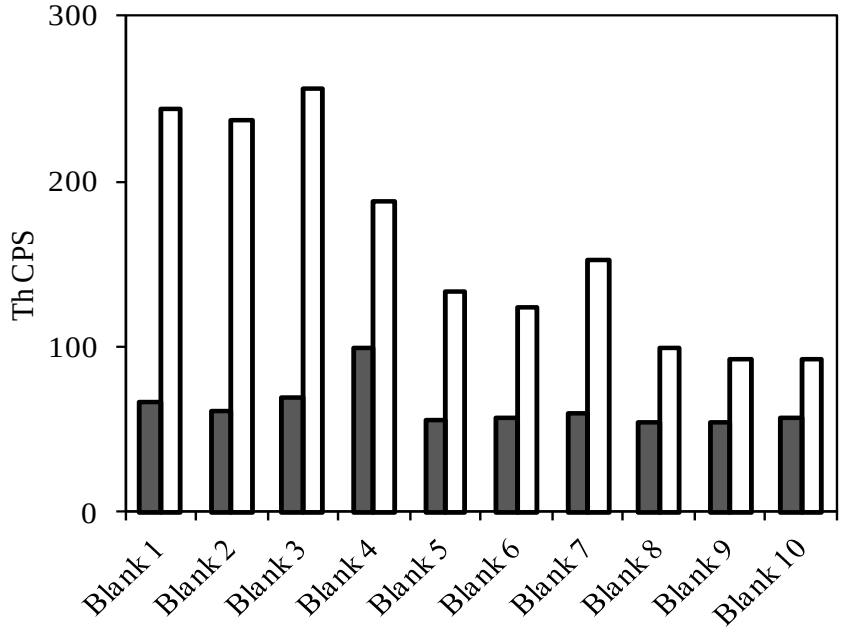

Figure 2.4: Uncorrected counts-per-second data for thorium before and after analysis of standards. Blanks raw CPS before standards analysis ( ), blanks raw CPS after standards analysis ( ).

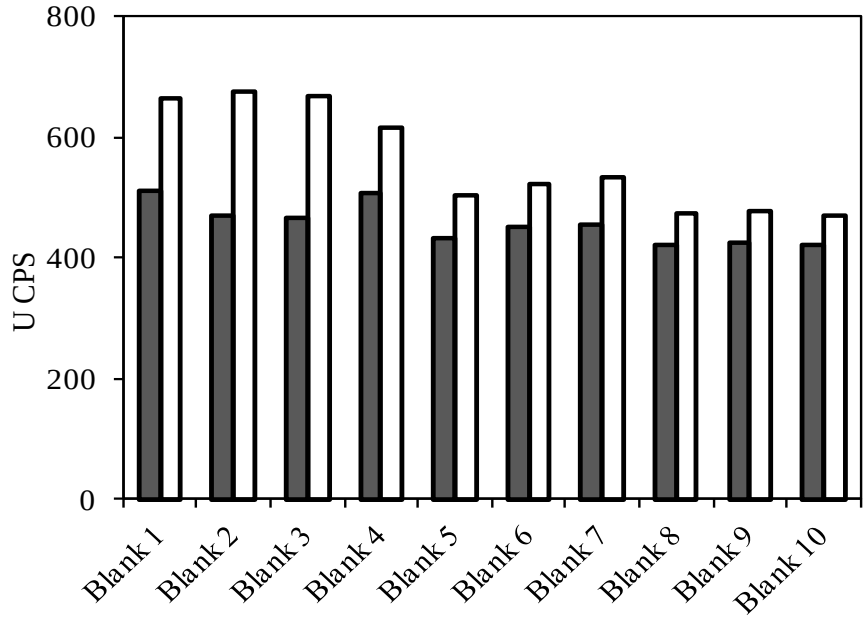

Figure 2.5: Uncorrected counts-per-second data for uranium before and after standards analysis. Blanks raw CPS before standards analysis ( ), blanks raw CPS after standards analysis ( ).

It can be concluded that, due to the high sensitivity of the ICP-MS at very low Th concentrations (0.00001 - 0.001 µg L^{-1}) and the joint effects of 'carry-over' and detector shift to analogue mode at high concentrations (10 and 100 µg L^{-1}), Th and U

calibration curves are probably best confined to a range of 0.01 - 1.0 µg L^{-1} as shown in Figure 2.6.

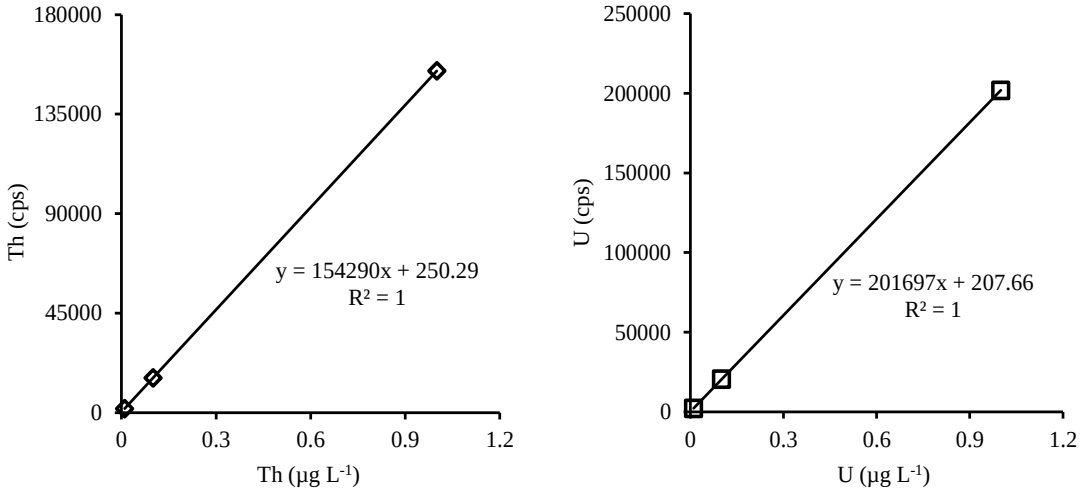

Figure 2.6: Thorium and uranium calibration curves in 3.5% HNO_3 at three calibration concentrations (0.01, 0.1, and 1.0 µg L^{-1}).

2.1.3.3 Thorium and uranium detection limits

For the Th and U calibration lines established in the range 0.01 – 1.0 µg L^{-1} in 3.5 % nitric acid solution, the limit of detection and limit of quantification were calculated according to the following relationships:

Limit of Detection (LOD) = 3.0 × Standard deviation of 10 blank solutions

Limit of Quantification (LOQ) = 10 × Standard deviation of 10 blank solutions

The LOD and LOQ values for Th were 0.27 ng L^{-1} and 0.9 ng L^{-1}, respectively, using the ten blanks run before the standards were analysed. This compared to 1.09 ng L^{-1} and 3.6 ng L^{-1} using blanks run after the instrument had been exposed to a standard solution of 100 µg L^{-1}, as shown in Table 2.3. It appears that the 'carry-over' of Th in ICP-MS may cause poor detection limits due to slow washout of previous samples or standards. This may be avoided by increasing the wash-out time but it is clear that the memory effect from such high concentrations is substantial and persistent. Nevertheless, the detection limits achieved are excellent compared to values reported in the literature. Marin et al. (1994) and Holmes (2001) reported a Th detection limit between 15 and 30 ng L^{-1}. In addition, the Th detection limit was found to be 5 ng L^{-1}

using the blanks prior to analysis of standards and 50 ng L^{-1} using the blanks run after standards (Holmes and Pilvio, 2000). The LOD and LOQ for U were obtained under the same experimental conditions for Th and found to be 0.67 and 2.2 ng L^{-1} respectively.

Table 2.3: Thorium and uranium limits of detection and limits of quantification (µg L^{-1}) for calibration in the range 0.01 – 1.0 µg L^{-1}; ten blank solutions were run either before or after a calibration block ending with a 100 µg L^{-1} standard solution.

Element	Before standards analysis		After standards analysis	
	LOD	LOQ	LOD	LOQ
^{232}Th	0.0003	0.0009	0.0011	0.0036
^{238}U	0.0007	0.0022	0.0011	0.0038

2.1.3.4 Thorium and uranium analysis in soil solution

In soil solution samples Th and U were determined quantitatively by external calibration. Concentrations of Th and U were found to be in the range 0.1 – 1.0 µg L^{-1} which falls within the linear calibration range (0.01 - 1.0 µg L^{-1} Th and U) with no likelihood of the detector tripping to analogue and minimal 'carry-over' problems.

Table 2.4: Thorium and uranium concentrations in soil solutions extracted from different depth samples taken from Wick series soil.

Depth	^{232}Th	^{238}U
(cm)	(µg L^{-1})	
5	0.13	0.18
15	0.26	0.25
25	0.22	0.26
35	0.40	0.33
45	0.48	0.22
55	0.48	0.19
65	0.45	0.22
75	1.13	0.26

2.2 Soil characterisation procedures

2.2.1 Soil pH

Soil pH was measured using a combined glass electrode (Ag/AgCl; PHE 1004) with a Hanna pH meter (Model 209). Air dried soil (< 2 mm) was shaken with MilliQ water with a soil: solution ratio of 1:2.5 on an end-over-end shaker for 30 min. The electrode was calibrated using buffers at pH 4.01 and pH 7 before the soil suspension pH measurement: pH was recorded when the reading was stable. For some applications soil pH was measured in 0.01M $Ca(NO_3)_2$ soil suspensions used for isotopic dilution measurements with a soil: solution ratio of 1:10.

2.2.2 Loss on ignition

Organic matter content was estimated by loss on ignition (LOI). Approximately 5 g of air dried soil (<2 mm) was ignited in a muffle furnace at 550 ^{o}C for 8 hr (Heiri et al., 2001). The LOI (%) was then determined gravimetrically.

2.2.3 Soil mechanical analysis

Air dried soil (0.5 g; < 2 mm) was suspended in 25 ml of 30% H_2O_2 overnight to oxidise the soil organic matter. The soil suspension was then heated in a water bath to 60 ^{o}C for 1.5 hr and then the temperature ramped up to 90 ^{o}C for 2 hr. The solution was decanted and the soil washed twice with deionised water. A dispersing agent ('Calgon', 25 ml of 0.057 M of sodium hexametaphosphate in 0.66 M of sodium carbonate) was added to the soil and suspensions were homogenised in an ultrasonic bath. Soil particle size was analysed using a Beckham Coulter LS 230 particle size analyser in the department of Geography, the University of Nottingham.

2.2.4 Soil total carbon, nitrogen and sulphur content

Analysis of total carbon, nitrogen and sulphur was undertaken using a CNS analyser (Flash EA1112; CE Instruments). Approximately 15 - 20 mg of dry finely ground soil was weighed into tin capsules and 5 mg of vanadium pentoxide was then added to each capsule. Capsules were carefully crimped to avoid spillage. A blank (capsule containing only vanadium pentoxide) and certified soil reference standards were used

for calibration. Peat and sandy certified soil standards were provided by Elemental Microanalysis; product codes B2176 and B2180.

2.2.5 Dissolved organic and inorganic carbon determination in soil solution

Concentrations of DOC and DIC in soil solution were determined using a Shimadzu total organic carbon analyser (TOC-VCPH). Soil solution samples were quantified against standards of potassium hydrogen phthalate (1000 mg L^{-1} total carbon) and Na_2CO_3-$NaHCO_3$ (1000 mg L^{-1} inorganic carbon; IC), diluted to appropriate concentrations using MilliQ water. The fulvic acid (FA) concentration in soil solution was estimated by assuming that dissolved organic matter (DOM) contains 50% C and 65% of this organic matter consists of active fulvic acid (Cheng et al., 2005; Buekers et al., 2008), while carbonate was measured as DIC. Soil inorganic carbon (SIC) was measured as total inorganic carbon in air dried finely ground soils (50 – 100 mg samples) with pH >5 using a Shimadzu SSM-5000a solid sample combustion unit. Soil organic carbon (SOC) was calculated as the difference between soil total carbon (STC; Section 2.2.4) and soil inorganic carbon (SIC). The active particulate humic acid (HA) concentration was estimated by assuming that solid organic matter (SOM) contains 58% SOC and 50% of this organic matter consists of active humic acid (Weng et al., 2002; Buekers et al., 2008) and the ratio of Active HA to FA was taken to be 84:16 (Tipping et al., 1995a and 2003).

2.2.6 Anions in soil solution

The concentrations of anions (SO_4^{2-}, NO_3^-, Cl^-, F^-, and PO_4^{3-}) were measured by ion chromatography (Dionex IC, DX500). The separation column used was an IonPac AS14A (4x250mm) ion exchange column with a pre-guard column AG14A (4x50mm). The mobile phase was 3.5 mM Na_2CO_3/1.0 mM $NaHCO_3$ at a flow rate of 1.4 ml min^{-1}.

2.2.7 Acid digestion for elemental analysis

Samples (approximately 200 mg) of finely ground soil were digested in PFA vials within a 48-place Teflon-coated graphite block digester (Model A3, Analysco Ltd, Chipping Norton, UK) with 2 ml HNO_3 (70%, TAG) and 1 ml $HClO_4$ (70%, AR) at

80 ^{o}C for 8 hr then at 100 ^{o}C for 2 hr. A volume of 2.5 ml HF (40%, AR) was then added to the digestion vessels and the samples heated to 120 ^{o}C for 8 hr. After that a further 2.5 ml HNO_3 and 2.5 ml MilliQ water were added to the dry residue and heated for 30 min at 50 ^{o}C, acids were Analytical Reagent (AR) or Trace Analysis Grade (TAG) from Fisher Scientific, UK. The digested soil samples were diluted to 50 ml with MilliQ water (5% HNO_3) and the total U and Th concentrations were measured by ICP-MS (Section 2.5.1).

2.2.8 Dithionite-citrate-bicarbonate (DCB) extraction for oxide determination

Iron and manganese oxides were determined by extracting the soil (0.25 g; dry ground soil) with 20 ml of a solution containing 0.07 M sodium dithionite, 0.3 M trisodium citrate and 1 M sodium hydrogen carbonate (method adapted from Anschutz et al. 1998). Dithionite was used to reduce Fe (III) to Fe (II), sodium citrate used to buffer pH, complex Fe (II) ions and prevent decomposition of dithionite to hydrogen sulphite. Sodium bicarbonate was used to increase pH. Soil samples were shaken in a water bath for 24 hr at 20 ^{o}C, with loosened lids, then centrifuged at 2200 g for 15 min and filtered using 0.22 µm Millipore syringe filters. Solutions were then diluted 1-in-10 with 2% TAG HNO_3 before measuring Fe and Mn concentrations by ICP-MS (Section 2.5.1).

2.2.9 Available and total phosphate

Available phosphate was extracted with 0.5 M sodium bicarbonate solution (Olsen et al., 1954) and assayed colorimetrically by measuring absorbance (1 cm cell at 880 nm) in a CE 1011 spectrophotometer (Cecil instrument). Total soil phosphate was determined in the acid soil digests.

2.3 Soil solution extraction

2.3.1 Soil pore water extraction by Rhizon soil moisture samplers

Fresh moist soils (< 4 mm) were used for soil pore water extraction. Soil samples (500-880 g) were packed into 15 cm high wide neck plastic columns in triplicate and saturated with MilliQ water before soil pore water extraction. The soil solution was extracted using Rhizon soil moisture samplers (MOM model, Rhizosphere Research

Products, Eijkelkamp, The Netherlands). The Rhizon samplers filter the solution through a series of submicron filters. All samplers were previously cleaned by forcing 50 ml of MilliQ water through the probe, and then dried before use. A sampler was inserted obliquely into each column as the soils were being packed and incubated for 7 days at 16 ^{o}C. The soil solutions were collected daily using suction from a syringe connected to the sampler Luer lock. In the first two days after saturating the soil the collection period lasted for 1-3 hr in order to extract at least 8 ml solution: with increasing incubation time the time required to collect soil solution increased, dependent on soil type (for example, soils with high organic matter content require sampling times up to 15 hr after 4 days of saturating the soil). The soil solution collected in the syringe (around 8 ml) was transferred to a universal tube and stored at 4 °C prior to analysis. The extracted pore solution was divided into two aliquots: the first aliquot was acidified with 3.5% HNO_3 (Optima grade HNO_3) and used to measure the total dissolved Th and U and some major and trace elements by ICP-MS (Section 2.5.1), while the second aliquot was used to measure dissolved organic carbon (DOC), dissolved inorganic carbon (DIC) and anions.

2.3.2 Soil solution extraction by dilute electrolyte

For dry soils with limited collected amount, approximately 1 g soil (< 2 mm) was suspended in 0.01 M $Ca(NO_3)_2$ solution (10 ml) and equilibrated on an end-over-end shaker for 3 days as the pre-equilibrium time used for measuring E-values (mg kg^{-1}) (Section 2.6). The soil suspensions were then centrifuged at 2200 g for 15 min and the supernatant filtered using 0.22 µm Millipore syringe filters. The extracted solution was divided into two portions: one of them was acidified with 3.5% HNO_3 (Optima grade HNO_3) and used to measure the total dissolved Th and U and some major and trace elements by ICP-MS (Section 2.5.1), while the second portion was used to measure dissolved organic carbon (DOC), dissolved inorganic carbon (DIC) and anions.

2.4 Single and sequential extraction procedures

2.4.1 Single extraction of Th and U

Triplicate samples of soils (c. 2.0 g < 2 mm sieved) were suspended in one of four extractants: 20 ml of 1% TMAH (Watts, 2002), 10 ml 0.05 M Na_2-EDTA (Quevauviller et al., 1996), 20 ml of 0.43 M HNO_3 (Tipping et al., 2003) or 20 mL of 1 M NH_4COOCH_3 (Sheppard and Evenden, 1992). Soil suspensions were then shaken on an end-over-end shaker, in polypropylene centrifuge tubes, for 4 hr, 2 hr, 2 hr and 2 hr, respectively, before being centrifuged at 2200 g for 15 min and the supernatant filtered using 0.22 µm Millipore syringe filters. For some soils, 0.43 M HNO_3 soil suspensions were shaken on an end-over-end shaker for different times (2, 4, 6, 16, 24, 48, 72, 96, 120 hr) to study the effect of equilibration time on 0.43 M HNO_3 extracted U and Th. The nitric acid and EDTA filtrates were diluted 10× with MilliQ water, the TMAH extract was diluted 10× with 1% TMAH, while ammonium acetate extracted solution was diluted 2× with MilliQ water and acidified with HNO_3 to produce 3.5% acid prior to U and Th analysis by ICP-MS (Section 2.5.1).

Table 2.5: Summary of the four single extraction methods.

Extractants	Concentration	Equilibration time (hr)	Soil: solution ratio (g:ml)
TMAH	1%	4	1:10
Na_2-EDTA	0.05 M	2	1:5
HNO_3	0.43 M	2	1:10
NH_4COOCH_3	1 M	2	1:10

2.4.2 Sequential extraction procedure (SEP)

A sequential chemical extraction procedure was carried out following the method described by Li and Thornton (2001), modified from that of Tessier et al. (1979). The extraction was carried out progressively, on an initial soil weight of 1.0 g, following the sequence listed below.

- Fraction 1 – 'Exchangeable': 1.0 g soil was extracted for 20 min with 8 ml 0.5 M $MgCl_2$, with continuous agitation at room temperature.

- Fraction 2 – ‘Carbonate-bound’ and ‘specifically adsorbed’: the soil residue from step 1 was extracted with 8 ml 1 M NaOAc (sodium acetate) (adjusted to pH 5.0 with HOAc) for 5 hr with continuous agitation.
- Fraction 3 – ‘Bound to Fe/Mn oxides’: residual soil from step 2 was extracted with 20 ml 0.04 M $NH_2OH.HCl$ in 25% (v/v) HOAc at 96 ^oC in a water bath for 6 hr with occasional agitation.
- Fraction 4 – ‘Bound to organic matter and sulphides’: the residue from step 3 was extracted with 3 ml 0.02 M HNO_3 and 5 ml 30% H_2O_2 (adjusted to pH 2 with HNO_3); samples were heated to 85 ^oC in a water bath and maintained for 2 hr with occasional agitation; 3 ml of H_2O_2 were then added and the mixture was heated again for 3 hr at 85 ^oC with intermittent agitation; after cooling, 5 ml 3.2 M NH_4OAc in 20% HNO_3 (v/v) were added and the tubes were agitated for 30 min.

After each successive extraction, the supernatant solution was separated by centrifugation at 2200 g for 15 minutes and the supernatant filtered (0.22 µm, Millipore syringe filters) then diluted and acidified to 2% HNO_3 prior to Th and U analysis by ICP-MS operating in standard mode with a high resolution ‘Xs’ skimmer cone. Detection limits were 0.27 and 0.67 ng L^{-1} for Th and U, respectively.

2.5 Chemical analysis

2.5.1 ICP-MS settings for Th, U and multi-element analysis

Analyses of Th and U were undertaken on a Thermo-Scientific $XSeries^{II}$ ICP-MS, the instrument was run in ‘standard mode’ (evacuated hexapole) and with a high resolution ‘Xs’ skimmer cone (Section 2.1.2.3). External Th and U calibration standards in the range from 0.1 to 1 µg L^{-1} in 3.5% ultra-pure *Optima* grade nitric acid were used to quantify Th and U concentrations (Section 2.1.3.2).

Major and trace cation analyses were undertaken by ICP-MS with a ‘hexapole collision cell’ (7% hydrogen in helium) to reduce polyatomic interferences. Sc (100 µg L^{-1}), Ge (50 µg L^{-1}), Rh (20 µg L^{-1}) and Ir (10 µg L^{-1}) in 2% HNO_3 were used as internal standards. Two sets of external multi-element calibration standards were used for trace elements (0 – 100 µg L^{-1}) and major elements (0 - 30 µg L^{-1}). Sample

processing was undertaken using Plasmalab software using internal cross calibration between pulse-counting and analogue detector modes where required.

Some U determinations were composed of mixed analogue and pulse-counted measurements, so internal cross-calibration was used and U was also measured (by ICP-MS) in 'collision cell with kinetic energy discrimination' mode (CCT-KED). Both sets of results were compared as shown in Figure 2.7.

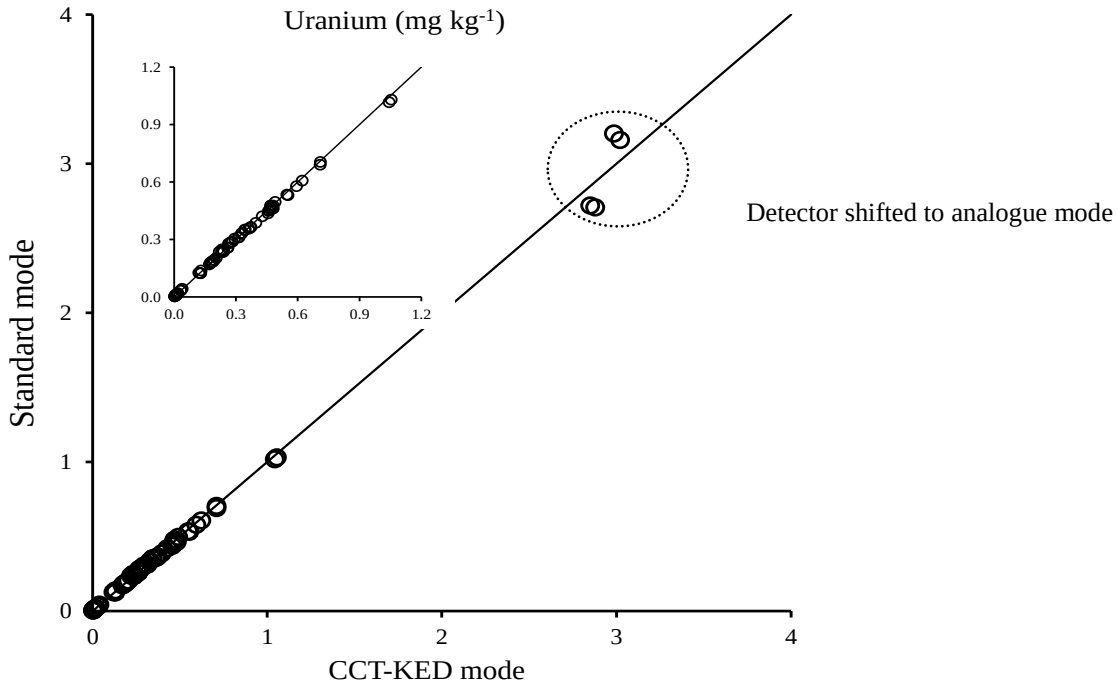

Figure 2.7: Uranium concentrations (mg kg-1) measured by ICP-MS in standard and collision cell modes. The solid line represents 1:1 line.

2.5.2 Use of size exclusion chromatography to speciate U and Th

Soil pore water fractionation based on molecular size and determination of complexes of Th and U with dissolved organic matter (DOM) in soil pore water was carried out by high performance liquid chromatography (HPLC; Dionex ICS-3000 chromatography system) and HPLC-SEC (size exclusion column) coupled to ICP-MS. The size exclusion column (SEC; GE Healthcare, Superose 12 10/300 GL) comprises a stationary phase of cross-linked agarose matrix with a separation range from 1 to 300 KDa. A guard column (Hamilton, Peek PRP-X100) was used upstream of the SEC column to prevent blockage. The mobile phase (1 ml min^{-1}) was 0.1 mol L^{-1} Tris(hydroxymethyl)aminomethane (TRIS buffer) with pH adjusted to 8.2 using

50% TAG HNO_3. Soil pore water samples of 100 µl were injected with an autosampler, controlled by Chromeleon® software. Samples were introduced directly from the SEC column to the nebuliser of the ICP-MS for Th and U analysis in standard mode (Section 2.5.1).

2.6 Measuring isotopically exchangeable ^{238}U

2.6.1 Preliminary test of ^{233}U isotope dilution methodology

Testing the validity of the method with Amberlite IR – 120 resin

To test the overall experimental, analytical and data processing protocols E-values were measured on an indifferent resin exchange system in which all the (added) ^{238}U present was in a labile form. For this purpose a two-step experiment was carried out. First, samples of Amberlite IR-120 (20 mg) were equilibrated with 10 ml 0.01 M $Ca(NO_3)_2$ containing aliquots of ^{238}U, for 24 hr, in an end-over-end shaker. The ^{238}U concentration added was gauged from the results obtained from a trial adsorption isotherm experiment with 5 mg kg^{-1} ^{238}U. Secondly, the resin suspensions were spiked with different volumes (0.25, 0.5, 0.75, 1.0, 1.25 ml) of ^{233}U spike solution (8.52 µg L^{-1}) and returned to the shaker for a further 24 hr to allow isotopic equilibration between ^{238}U and ^{233}U. At the end of the equilibration period, the suspensions were centrifuged at 2200 g for 15 min, filtered and acidified (with 3.5% HNO_3) prior to assay of the ^{233}U: ^{238}U ratio by ICP-MS.

Effect of isotopic equilibration time

The spike equilibration time (4 days) was adopted following the results of a preliminary experiment in which four soils - acidic woodland (AW), acidic moorland (AM), biosolid-amended arable (Ba) and calcareous-arable soils (Ca) - were spiked with ^{233}U and equilibrated for 1 - 5 days during which (apparent) E-values were measured daily. A period of four days was chosen as a compromise between allowing sufficient time for isotopic equilibration and avoiding the development of anaerobic conditions in the soil suspensions.

Effect of tracer concentration and pH on E-value

To study the effect of varying spike concentrations and pH on ^{238}U E-value, four soils - acidic moorland (AM), arable (Ar), biosolid-amended arable (Ba) and calcareous-arable soils (Ca) - were spiked with four concentrations of isotope solution representing 5, 10, 20 and 30 % of the measured E-values; the concentrations of ^{233}U spike added to the soil suspensions to measure E-values were first estimated based on TMAH extraction. Variable concentrations of the spike solution were added to the soil suspension after suspending the soils in 0.01 M $Ca(NO_3)_2$ and equilibrating for 3 days. After equilibration of the spiked soil suspensions for a further 4 days the suspensions were centrifuged at 2200 g for 15 min, filtered and acidified (3.5% HNO_3) prior to assay of ^{233}U: ^{238}U ratio by ICP-MS. The pH values of spiked soil suspensions were measured prior to isolation of the supernatant phase.

2.6.2 Measuring isotopically exchangeable ^{238}U in soils

Experimental procedure

To measure the concentration of labile U, subsamples of soil (c. 1.0 g; < 2 mm) were first pre-equilibrated with 20 ml of 0.01 M $Ca(NO_3)_2$ for 3 days by end-over-end shaking in polypropylene centrifuge tubes. The soil suspensions were then spiked with ^{233}U tracer ($^{233}UO_2^{2+}$). As the ^{233}U tracer was kept in a 2% nitric acid matrix, the addition of acidified spike solution may decrease the soil suspension pH and overestimate the labile U pool. Therefore, the volume of ^{233}U spike solution was as small as possible to minimize the mobilization of non-labile ^{238}U from the soil. Moreover, ^{233}U is an artificial isotope with no natural isotopic abundance, so very small amounts of the spike isotope were enough to allow accurate determination of the U isotope ratio or concentration of ^{233}U. The available ^{238}U in each soil was initially estimated by tetra methyl ammonium hydroxide (TMAH) extraction (Section 2.4.1). The ^{238}U solid - liquid distribution coefficient (K_d) was measured for each soil as ^{238}U extracted by TMAH to dissolved U measured in 0.01 M $Ca(NO_3)_2$ soil suspension. The ^{233}U K_d value was considered to be the same as that of ^{238}U; sufficient ^{233}U was added to the soil suspension to achieve 10 × ^{233}U limit of quantification (LOQ; cps) as minimum. The aim was to determine a tracer concentration which could be accurately measured by ICP-MS, without affecting the apparent E-value. The amount of ^{233}U

spike added ranged from 5 - 15% of the amount of ^{238}U extracted from each soil with TMAH.

After spiking, the suspensions were equilibrated for a further 4 days to attain isotopic equilibrium, centrifuged at 2200 g for 15 min and the supernatant solution filtered using 0.2 µm Millipore syringe filters. Subsamples of the filtrates were acidified to give 3.5% HNO_3 prior to assay of (i) the isotopic ratio (^{233}U : ^{238}U) and (ii) the concentrations of both isotopes. Isotopic ratios were measured by ICP-MS in standard mode with a high resolution 'Xs' skimmer cone using up to 15 integrations, each isotope with a very short dwell time of 2.5 ms, quadrupole minimum and maximum settle times of 1 ms, safe resting mass of 205 amu and 100 × 15 sweeps, to minimise the effects of plasma noise.

2.6.3 Calculation of E-values

Mass discrimination or mass bias is a source of error when analysing isotope ratios using quadrupole ICP-MS. To account for differences in detection sensitivity between the two U isotopes a mixed solution of ^{233}U and ^{238}U (0.1 µg L^{-1}) was used to determine the mass bias correction factor (K-Factor; Equation 2.1), IR and CR are the isotopic ratio and the measured count (cps) ratio in the mixed solution.

$$\mathrm{K-Factor} = \frac{\mathrm{IR}}{\mathrm{CR}} \qquad (2.1)$$

Although it is expected that the value of mass bias should be small for two isotopes with similar and high atomic masses, the low U concentrations in environmental samples makes it important to correct for mass bias.

It is possible to determine the E-value for ^{238}U from isotopic ratios alone (corrected CR values) or from isotopic concentrations determined using calibration standards. Because the spike isotope used (^{233}U) is essentially absent from natural systems and ^{238}U has a natural abundance of 99.28%, the ^{238}U E-value ($^{238}U_E$, mg kg^{-1}) can be calculated from equation 2.2,

$$^{238}U_E = 1.021 \times \left[\frac{^{233}C_{spike} \times V_{spike}}{W_{soil}}\right]\left(\frac{CPS_{238}}{CPS_{233}}\right) \qquad (2.2)$$

where 1.021 is the ratio of isotopic masses, $^{233}C_{spike}$ is the gravimetric concentration of the ^{233}U spike solution used (mg L^{-1}), V_{spike} is the volume (L) of spike used for each sample, W_{soil} is the weight of soil (kg) and CPS represents the measured count rate (counts per second) in the filtered supernatant solution at the mass indicated, corrected for mass discrimination effects using the K-factor (equation 2.1). Equation (2.2) is considerably simpler than expressions normally used to quantify stable isotope dilution (Marzouk et al., 2013) because the soil is considered to have only ^{238}U present and the spike was 100% ^{233}U.

E-values were also calculated from equation 2.3, following conventional calibration of the ICP-MS with standard solutions of both isotopes. External ^{233}U and ^{238}U calibration standards in the range from 0.025 to 0.1 µg L^{-1} and 0.1 to 1 µg L^{-1}, respectively, in 3.5% ultra-pure *Optima* grade nitric acid were used, Rh (20 µg L^{-1}) and Ir (10 µg L^{-1}) in 2 % TAG HNO_3 were used as internal standards as described in section 2.5.1.

$$^{238}U_E = {}^{238}U_{conc}\left[K_d + \frac{V_{total}}{W_{soil}}\right] \qquad (2.3)$$

Where $^{238}U_{conc}$ is the measured concentration of ^{238}U in the supernatant solution of an equilibrated spiked soil suspension, K_d is the ^{233}U spike distribution coefficient (L kg^{-1}) determined and V_{total} is the volume (L) of liquid in the soil suspension. Detection limits were 0.026 and 0.7 ng L^{-1} for ^{233}U and ^{238}U.

2.6.4 Measuring isotopically exchangeable ^{238}U in soil with a resin purification procedure

The problem of non-labile elements in suspended colloidal particles (SCP; < 0.2 µm) in soil suspensions has been demonstrated during measurement of isotopically exchangeable Zn, Cd and Cu (Lombi et al., 2003) and Ni (Nolan et al., 2009). Hamon & McLaughlin (2002) proposed a resin extraction method to overcome this problem but this is as yet untested for U. Thus, un-acidified subsamples of the spiked filtrates (10 ml) were shaken for 2 hr with 100 mg analytical grade Chelex-100 resin (Bio-Rad Laboratories, UK) previously converted from the Na to the Ca form to minimize pH changes in the soil extract (Lombi & Gerzabek, 1998). The resin was then rinsed twice with MilliQ water to remove any surface-adsorbed sub-micron colloidal particulates.

The resin-adsorbed U (UO_2^{2+}) was then eluted in 10 ml of 0.5 M HNO_3 (Lombi et al., 2003) and the ratio of ^{233}U and ^{238}U determined as described above. It is assumed that the resin phase reflects the isotopic ratio in the true solution phase and has not absorbed particulate material. The E-values obtained by assay of the equilibrated electrolyte and resin phases are denoted as E_{soln} and E_{resin}, respectively. Both estimates of E-value (E_{soln} and E_{resin}) were then compared to determine the presence of non-labile SCP-^{238}U.

2.7 Geochemical modelling of Th and U solubility

The WHAM geochemical model (Version VII; Lofts and Tipping, 2011) was used to predict Th and U speciation and concentration in the soil pore water (n = 37) extracted from soil columns or in the solution phase of soil suspensions used to determine E-values (0.01 M $Ca(NO_3)_2$, 1g: 10ml) (n = 40). The input variables included soil pH, temperature, the atmospheric partial pressure of CO_2 ($PCO_2 = 3.83 \times 10^{-4}$ atm), total suspended particulate matter SPM (g L^{-1}), total reactive Th and U concentrations (mol L^{-1}), adsorption phases (clay content, mineral oxides, HA and FA; g L^{-1}), colloidal phases in soil suspension (FA; g L^{-1}), dissolved Na, Mg, K, Ca, Al, Mn, Fe (III), Co, Ni, Cu, Zn, Cd and Pb as dissolved species (mol L^{-1}), anions (PO_4^{3-}, NO_3^-, SO_4^{2-}, Cl^-; mol L^{-1}). The model outputs include the predicted total Th and U concentrations in soil solution (mol L^{-1}) and the proportion of Th and U fractions associated with each soil particulate and colloidal phase. Details of WHAM (VII) settings and variables, along with results, are described in Chapter 7.

2.8 Statistical analysis

Minitab (version 16.2.2) was used for various statistical analyses including Pearson correlation coefficients, T-tests, Analysis of variance (ANOVA) and step-wise regression; the default level of confidence used in all these analyses was 95% ($P < 0.05$). The 'Solver' add-in in Microsoft Excel was used to optimize parameters in empirical models; the residual standard deviation (RSD) was used to assess the goodness of fit of the empirical models to experimental data.

3 FACTORS AFFECTING URANIUM AND THORIUM FRACTIONATION AND PROFILE DISTRIBUTION IN CONTRASTING ARABLE AND WOODLAND SOILS

3.1 INTRODUCTION

Since the 1960s, human exposure to natural radionuclides has increased by two or three orders of magnitude (Baxter, 1991). However, recently more attention has been given to the magnitude and distribution of natural radionuclides (e.g. U and Th) in soils, as radiation from natural sources is the main contribution to human exposure (Barisic et al., 1992; Kiss et al., 1988). Natural radioactivity in soils is largely a product of the mineral composition of the soil parent material and is primarily associated with uranium, thorium and their decay series. However, additional inputs of U into the environment have occurred in the past half century from sources that include mining, the nuclear industry, military use and application of fertilizers to arable soils (del Carmen Rivas, 2005; Tunney et al., 2009). A simple hazard ranking of potential contaminants in phosphate fertilizers was performed by Sauerbeck (1993) who examined the range of contaminant concentrations in phosphate rocks and compared it to average element concentrations in the Earth's crust; the conclusion was that As, Cd, Cr, F, Sr, Th, U and Zn are most likely to accumulate in P-fertilized soils. Research to date has confirmed this for Cd, F and U (Stacey et al., 2010 and references therein). A considerable amount is already known about the chemistry and soil-to-plant transfer of Cd, while much less information is available for fertilizer-derived F and U. In agricultural ecosystems the uranium concentration in soil has undoubtedly increased due to the long term-application of phosphate fertilizer (Nanzyo et al., 1993; Rothbaum et al., 1979; Takeda et al., 2005 and 2006a; Yamaguchi et al., 2009). However, there is disagreement concerning the mobility and bioavailability of U in soils. Some studies suggest that U accumulation from long-term application of P fertilizer to field plots is confined only to surface soil layers with insignificant uptake by plants or leaching to surface waters (Rothbaum et al., 1979; Taylor, 2007). In contrast, Spalding and Sackett (1972) attributed the apparent increase in U concentrations measured in North American rivers to phosphate fertilizers applied to agricultural soils.

Measuring total elemental concentrations in soil is useful to assess the extent of contamination but provides only limited information on mobility and bioavailability. To assess the likely bioavailability and mobility of radionuclides it is often useful to have knowledge of soil chemical characteristics and the chemical forms of radionuclides present, as well as the source of radioactivity. The most reactive forms of natural radionuclides are adsorbed onto soil geocolloidal components (organic matter, clays, carbonates, Fe/Mn oxides) enabling participation in biogeochemical processes (Navas et al., 2005). Quantification of these phases can utilize experimental protocols and classification schemes widely applied to trace metals. The latter typically include fractions such as 'exchangeable' (mainly on alumino-silicate clays), 'specifically adsorbed' (to Fe and Mn oxides, humus etc), 'co-precipitated' (within carbonates, sulphides, phosphates and silicates) and 'residual' (eg primary mineral forms) (Li and Thornton, 2001). Each operational fraction may occur in a variety of structural forms. Thus, sequential extraction procedures (SEPs) are commonly used to fractionate metals in soils (Tessier et al., 1979; Lake et al., 1984; Ure et al., 1993). Of the many SEPs available, the Tessier protocol, and its variants, has been the most widely applied for heavy metals and for radionuclides (Bunker et al., 2000; Blanco et al., 2004).

The aims of this chapter were:

(i) to investigate the vertical distribution and mobility of uranium and thorium in soils at adjacent but contrasting arable and woodland sites based on the same parent material;

(ii) to assess the effect of long-term application of phosphate fertilizer on U and Th concentrations in the arable soil;

(iii) to determine the distribution and chemical fractionation of U and Th within arable and woodland soil profiles.

3.2 MATERIALS AND METHODS

3.2.1 Study area and soil samples

The study area is shown in Plate 1. Soil samples were collected from an arable field within the University of Nottingham farm, Leicestershire, UK ($52^0$49'48''N-$1^0$14'23''W) and from an adjacent mature woodland strip. The soil belongs to the Wick series (a sandy loam) based on fluvio-glacial sand and gravel (c. 80 - 100 cm) overlying Triassic Keuper Marl. Soil samples were taken as triplicate auger borings from the soil surface, in 10 cm depth intervals, to 90 cm in the arable field and to 70 cm depth in the woodland: a total of 27 and 21 soil samples were taken from the arable and woodland sites, respectively. All soil samples were air-dried and sieved (< 2 mm) prior to chemical analysis.

The arable soil is thought to have received repeated phosphate fertilizer applications for over 100 years whereas the mature woodland strip is believed to have been established at least prior to 1940 and so is unlikely to be enriched with phosphate fertilizer, apart from inputs from roosting birds. Thus the woodland site provides a reasonable reference against which the effect of arable management on U and Th fractionation and distribution through the soil profile, and the effect of long-term application of phosphate fertilizer, can be assessed. Unfortunately there are no accurate records of the history of fertilizer application to the arable soil. Ploughing in light textured arable soils in the UK is typically to a depth of approximately 23 cm. It is normally undertaken once annually, in autumn or early spring. It has the effect of inverting rather than mixing the topsoil and does not, in itself, transfer a significant proportion of nutrients held in the solid phase down into the subsoil, as seen in ^{15}N labelled studies (Bhogal et al., 1997; Recous et al., 1988).

Plate 3.1: The boundary between adjacent arable and deciduous woodland sites on the University of Nottingham Farm at Sutton Bonington, Leicestershire, UK ($52^0$49'46''N-$1^0$14'21''W).

3.2.2 Soil characterization

Soil samples were air-dried and sieved (< 2 mm) prior to chemical analysis. Soil organic matter content (SOM) was estimated from loss on ignition (% LOI) (Section 2.2.2). Soil pH values were measured in deionised water suspensions (1 : 2.5 soil : solution ratio) after shaking for 30 minutes (Section 2.2.1). Subsamples of the <2 mm sieved soils were ground in an agate planetary ball mill (Model PM400; Retch GmbH & Co., Germany) before acid digestion of 200 mg of finely ground soil (Section 2.2.6). Determination of total uranium and thorium content and multi-element analysis was measured by ICP-MS (Model X-Series^{II}, Thermo-Fisher Scientific, Bremen, Germany) operating in collision cell mode (7% hydrogen in helium) to reduce polyatomic interferences. Internal standards included Rh (10 µg L^{-1}) and Ir (10 µg L^{-1}) in 2 % TAG HNO_3. External Th and U calibration standards (Claritas-PPT grade CLMS-2, SPEX Certiprep, Stanmore, UK) were used in the concentration range 1 - 10 µg L^{-1}. External multi-element calibration standards (Claritas-PPT grade CLMS-2, SPEX Certiprep, Stanmore, UK) included Ca and Al were also used. Available phosphate was determined using extraction by Olsen's method and colorimetric assay (Rowell, 1994); total soil phosphate was determined colorimetrically on the acid soil digests. Reactive iron hydrous oxide was solubilized using the dithionite extraction

method of Kostka and Luther (1994) (Section 2.2.7) and assayed by ICP-MS operating in 'collision cell mode with kinetic energy discrimination (CCT-KED)' (Section 2.5.1).

A sequential chemical extraction was carried out following the method described by Li and Thornton (2001), developed from that of Tessier et al. (1979). The full details of sequential extraction procedure are described in Chapter 2 (Section 2.4.2).

3.3 RESULTS AND DISCUSSION

3.3.1 General soil characteristics

Tables 3.1a and 3.1b show measured soil properties in the arable and woodland soil profiles, respectively; values represent the average of three auger borings at each site. The soil pH decreased slightly with depth in the woodland soil, from pH 4.9 at the surface to 4.5 at 70 cm. In the arable soil, pH values were near neutral (6.75) at the soil surface and increased gradually through the soil profile to a maximum value (7.22) at 90 cm (Tables 3.1a and 3.1b) suggesting prolonged movement of agricultural lime. Both soils exhibited a decreasing trend with depth in organic matter content (%LOI); this was more pronounced in the woodland soil which had a much higher organic matter content than the arable soil in the top 20 – 30 cm. The Fe oxide content increased slightly with soil depth in the arable soil (from 8.0 to 9.9 g kg^{-1}) but decreased slightly down the woodland soil profile from 10.7 to 9.4 g kg^{-1}.

Table 3.1a: Values of soil pH, organic matter (%LOI) and Fe oxide content, available phosphate-P, Ca and Al concentrations in the arable soil profile at 10 cm depth intervals. Values are averages of three replicate auger borings.

Depth (cm)	pH	LOI (%)	Fe_2O_3 (g kg^{-1})	P-available (mg kg^{-1})	Ca (mg kg^{-1})	Al (mg kg^{-1})
0-10	6.75	4.26	8.00	65.9	2463	20700
10-20	6.79	4.09	8.26	67.1	2543	20276
20-30	6.69	3.59	8.29	71.1	2124	20886
30-40	6.85	3.18	8.90	69.9	2169	21007
40-50	6.95	2.15	9.11	40.2	1595	22161
50-60	7.00	1.68	9.40	22.9	1440	22722
60-70	7.05	1.68	9.50	18.2	1496	23581
70-80	7.19	1.32	9.50	14.8	1544	25495
80-90	7.22	0.82	9.88	11.7	2149	34484

Table 3.1b: Values of soil pH, organic matter (%LOI) and Fe oxide content, available phosphate-P, Ca and Al concentrations in the woodland soil profile at 10 cm depth intervals. Values are averages of three replicate auger borings.

Depth (cm)	pH	LOI (%)	Fe_2O_3 (g kg^{-1})	P-available (mg kg^{-1})	Ca (mg kg^{-1})	Al (mg kg^{-1})
0-10	4.92	11.15	10.66	16.1	2242	20897
10-20	4.65	8.64	10.59	15.8	1530	21992
20-30	4.61	4.65	10.43	13.4	1058	22209
30-40	4.56	3.27	10.31	14.9	916	22684
40-50	4.54	2.12	10.01	13.8	908	24005
50-60	4.51	2.73	9.52	13.9	1303	25616
60-70	4.50	2.73	9.40	13.9	2666	25702

Table 3.2a: Correlation matrix for the elemental analysis of the arable soil profile.

	Ca	Al	Mn	Fe	Sr	U	Th	P-total
Al	-0.14							
	0.720							
Mn	0.02	**0.97**						
	0.962	*0.000*						
Fe	-0.30	**0.98**	**0.93**					
	0.435	*0.000*	*0.000*					
Sr	**0.93**	-0.30	-0.16	-0.46				
	0.000	*0.439*	*0.682*	*0.218*				
U	**0.94**	-0.18	-0.04	-0.34	**0.87**			
	0.001	*0.647*	*0.914*	*0.378*	*0.002*			
Th	-0.37	**0.93**	**0.86**	**0.95**	-0.56	-0.37		
	0.323	*0.000*	*0.003*	*0.000*	*0.118*	*0.326*		
P-total	**0.78**	**-0.68**	-0.54	**-0.79**	**0.89**	**0.86**	**-0.86**	
	0.014	*0.046*	*0.136*	*0.012*	*0.001*	*0.020*	*0.003*	
P-available	**0.72**	**-0.72**	-0.59	**-0.82**	**0.85**	**0.77**	**-0.89**	1.00
	0.029	*0.029*	*0.098*	*0.007*	*0.004*	*0.037*	*0.001*	*0.000*

Italic and bold figures represent *P* and significant values, respectively**.**

Table 3.2b: Correlation matrix for the elemental analysis of the woodland profile.

	Ca	Al	Mn	Fe	Sr	U	Th	P-total
Al	-0.53							
	0.275							
Mn	-0.12	**0.90**						
	0.827	*0.015*						
Fe	-0.14	**0.87**	**0.93**					
	0.785	*0.026*	*0.007*					
Sr	-0.45	**0.99**	**0.93**	**0.88**				
	0.369	*0.000*	*0.007*	*0.022*				
U	-0.61	**0.91**	0.77	0.76	**0.86**			
	0.199	*0.013*	*0.074*	*0.083*	*0.028*			
Th	-0.67	**0.97**	0.80	0.80	**0.94**	**0.96**		
	0.143	*0.001*	*0.057*	*0.058*	*0.006*	*0.002*		
P-total	**0.91**	-0.79	-0.47	-0.41	-0.73	**-0.83**	**-0.87**	
	0.011	*0.064*	*0.351*	*0.426*	*0.102*	*0.042*	*0.025*	
P-available	0.76	-0.65	-0.40	-0.29	-0.62	-0.72	-0.75	**0.85**
	0.079	*0.160*	*0.427*	*0.578*	*0.194*	*0.109*	*0.086*	*0.033*

Italic and bold figures represent *P* and significant values, respectively.

3.3.2 Uranium, phosphate and thorium in arable and woodland soils

The total soil P concentration in the surface layers of the arable soil profile was greater than in the woodland soil down to a point of convergence at a depth of 50 cm (Figure 3.1a). This provides strong evidence for residual fertilizer P accumulation in the arable soil. By contrast, the woodland profile showed only minor surface accumulation of P, possibly due to leaf litter cycling to the soil surface and import by birds or aerial deposition. Phosphate is strongly sorbed by variable charge geo-colloids, especially Fe oxides, or precipitated as poorly soluble Ca-phosphates, and often accumulates in the surface horizon in agricultural and non-agricultural soils (Takeda et al., 2004). A correlation matrix of woodland soil properties (Table 3.2b) showed that U and Th were highly correlated (r = 0.96) and both were highly correlated with Al (r = 0.91 and 0.97, respectively) suggesting an association with clay or Al hydrous oxides. For the arable soil, however, U and Th were not significantly correlated (Table 3.2a) and, whereas Th was correlated with Al (r = 0.93), U was not (r = -0.18) but was much more strongly associated with soil P content (r = 0.86; Figure 3.2a) and Ca concentration (r = 0.94; Figure 3.2b).

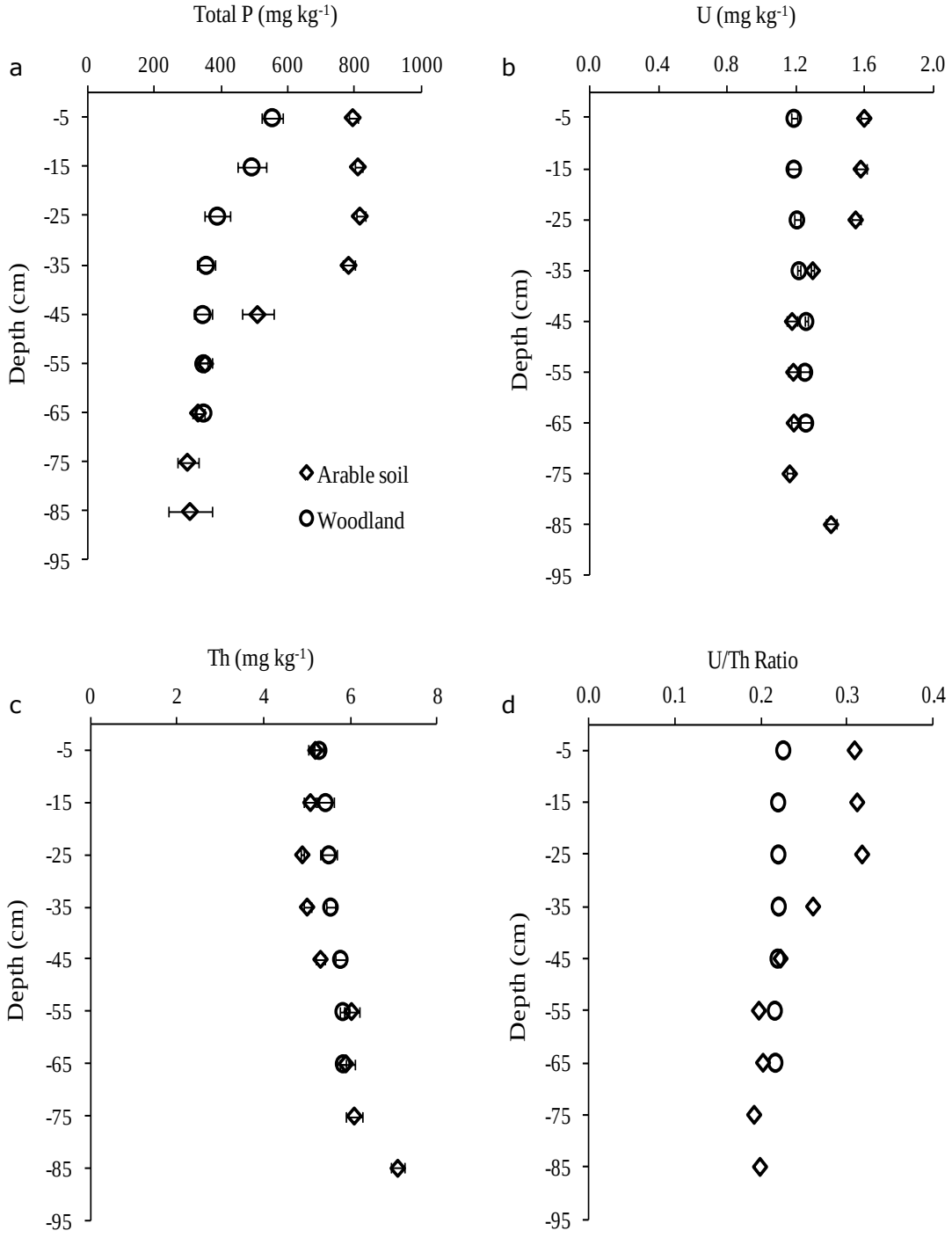

Figure 3.1: Soil profile distribution of total P (a), U (b) and Th (c) concentrations and the U/Th concentration ratio (d) in the arable (◊) and woodland (○) soils; horizontal bars are the standard errors of three auger borings.

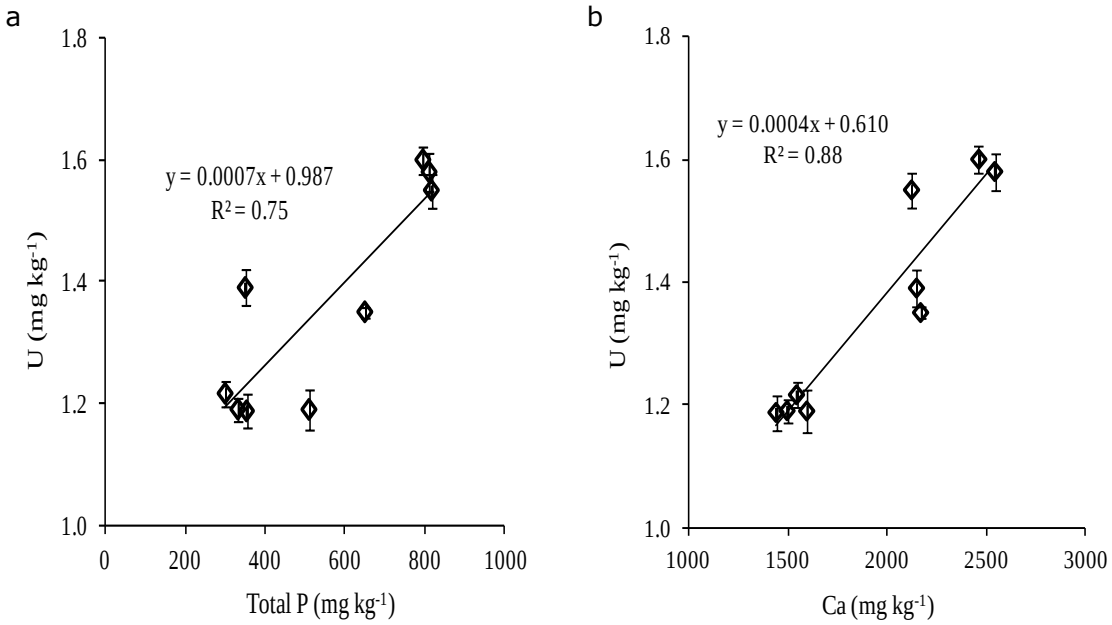

Figure 3.2: Relationship between U concentration and (a) total phosphate-P concentration and (b) total Ca concentration in the arable soil. Data are average values of three auger borings ± standard errors.

The trend in U concentration within the arable soil profile was broadly similar to that of P (Figure 3.1a and b), with clear evidence of surface enrichment. By contrast, the U concentration in the woodland soil was uniform throughout the soil profile, ranging from 1.19 mg kg^{-1} at the surface to 1.26 mg kg^{-1} at 85 cm depth. The comparison of the two soil profiles strongly suggests that the U content in the arable soil surface (0-40 cm) has been increased by phosphate fertilizers, or possibly liming materials, while the woodland soil U concentration simply reflects the soil parent material and the limited effects of weathering and pedogenesis. The Th distribution was very similar in both arable and woodland soils (Figure 3.1c). The increase in Th concentration with soil depth was too large to be explained as simple 'dilution' of mineral constituents with soil humus in the surface layers. Movement of Th bound to soluble humus acids (fulvic acid) is possible but this might be expected to produce a greater distinction between the woodland and arable profiles. The trend may have arisen from colloidal movement or simply mixing within the profile between the underlying Keuper Marl clay and the overlying fluvio-glacial sand and gravel. Navas et al. (2005) studied the depth distribution of the naturally occurring radionuclides ^{238}U and ^{232}Th in a soil toposequence along a mountain slope in the central Spanish Pyrenees. Uranium was depleted in all upper soil layers and enriched in deeper layers, while Th exhibited a uniform depth distribution in all soil profiles.

The concentration ratio of U to Th has also been suggested as a reliable indicator of U enrichment in soils arising specifically from the application of phosphate fertilizer (Yoshida et al., 1998; Takeda et al., 2004 and 2006a). This is because the U concentration in phosphate fertilizers is 10–200 times greater than in soils whereas the Th content is lower than found in most soils (Tsumura and Yamasaki, 1993). Thus the gravimetric ratio of U/Th (Figure 3.1d) strongly suggests the application of a U-enriched material to the arable soil surface. The trend in U/Th ratio down the profile merged with that of the woodland soil at 45 cm with a background value of 0.22. Similarly, Figure 3.3 shows the U/Th ratio as a function of total P concentration in the arable soil profile (r value = 0.96) which seems to verify the source of the excess U.

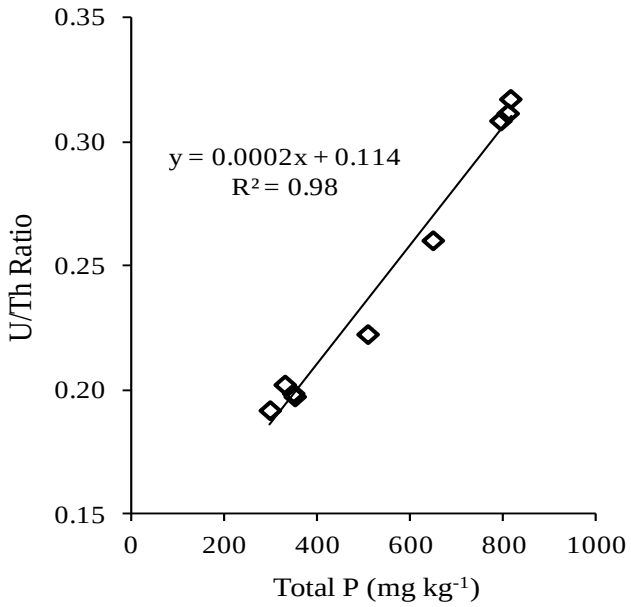

Figure 3.3: Relationship between total phosphate-P concentration and U/Th concentration ratio in the arable soil.

Calculating the background ratio of U/Th in the arable soil as 0.20 (Figure 3.1d), it is possible to estimate the excess U retained within the profile of the arable soil using the following relationship:

$$\Delta U = \sum_{i=1}^{n} [U_{soil} - (Th_{soil} \times 0.2)] \times d \times 10{,}000 \times D$$

Where ΔU (g ha^{-1}) is the excess U added to the soil, U_{soil} and Th_{soil} are the gravimetric concentrations (mg kg^{-1}) in each depth interval (d, m); the constant 10,000 is m^2 ha^{-1} and D is the soil bulk density, estimated as 1.2 t m^{-3}. Values of ΔU (g ha^{-1}) for each

layer (i) are summed down to the layer at 45 cm depth in which 'background' U/Th occurs (n).

Table 3.3 shows the excess U throughout the arable soil profile (0-90 cm); the total amount applied was estimated to be 2.5 kg ha^{-1}. The average excess concentration in the top 30 cm was 0.56 mg kg^{-1}; 80% of the excess U was in the top 30 cm of the soil profile (Table 3.3). The degree of U accumulation and distribution in surface soils must be influenced by factors such as application rate, quality of P fertilizers and the affinity of the soil for U. Rothbaum et al. (1979) reported that most of the superphosphate fertilizer U applied to the clay loam soil at Rothamsted Experimental Station (UK) was retained, like P, in the surface 23 cm of the arable soils or was adsorbed by the organic surface layers of soils under permanent grassland. However, no evidence of U enrichment due to fertilizer applications was found in the subsoils (23-46 cm). Rothbaum et al. (1979) applied superphosphate to three experimental plots at Rothamsted between 1889 and 1976 at the rate of 33 kg P ha^{-1} y^{-1} and 15 g U ha^{-1} y^{-1}. A fourth plot located at Papatoetoe, New Zealand, received superphosphate at the rate of 37 kg P ha^{-1} y^{-1} and 16 g U ha^{-1} y^{-1} between 1889 to 1975/76. Two acid soils from Park Grass, Rothamsted, and Papatoetoe, New Zealand, showed annual U increases of 0.008 and 0.014 mg kg^{-1} (0.7 and 1.2 mg kg^{-1} over the period of fertilizer application), whereas two neutral to alkaline soils from Barfield, Rothamsted, showed U increase in soils from 0.003 and 0.004 mg kg^{-1} y^{-1} (0.26 and 0.35 mg kg^{-1} over the period of fertilizer application). The excess concentration in the current study was less than that reported by Yamasaki et al. (2001), Takeda et al. (2005 and 2006a), Taylor (2007) and Yamaguchi et al. (2009) in different agricultural soils with long term application of phosphate fertilizers. Takeda et al. (2006a) reported that continuous application of superphosphate for 61 years produced an excess concentration of U in andosols (0-20 cm) of 2.0 mg kg^{-1}.

Table 3.3: Estimating the amount of U accumulated in arable soil due to long-term application of phosphate fertilizers.

Depth	Th	U	Excess U	Excess U amount	Excess U amount
(cm)		(mg/kg)		(g/ha)	(%)
0-10	5.19	1.60	0.562	674	26.6
10-20	5.08	1.58	0.564	677	53.2
20-30	4.89	1.55	0.572	686	80.2
30-40	5.00	1.30	0.300	360	94.4
40-50	5.31	1.18	0.118	142	100.0
50-60	6.02	1.19	-0.014	-16.8	99.3
60-70	5.90	1.19	0.010	12.0	99.8
70-80	6.09	1.22	0.002	2.4	99.9
80-90	7.09	1.41	-0.008	-9.6	99.5
Sum				2527	

3.3.3 Fractionation of U in the soils

The 'non-residual' fractions (F1 – F4) of U, measured by sequential extraction, are shown as a function of soil depth in Figure 3.4. Most U in the arable and woodland soils was in the residual phase: the non-residual fraction ranged from 13 to 25% of total U in the arable soil and from 13 to 15% in the woodland soil. In the arable soil the excess U accumulated in the surface layers (0 – 50 cm) clearly remained considerably more reactive than the native U; the proportion of excess U (% reactivity of the fertilizer-derived U) that is reactive in the top 30 cm of the arable soil ranged from 29 to 42 % of the fertilizer-derived U. Below 50 cm the % reactive U was fairly constant (mean = 14%) and remarkably similar to the woodland soil profile (mean = 15%) throughout its depth. Throughout the arable soil profile the reactive U was fairly evenly distributed between F1 – F4 and the excess U in the surface layers (0 – 50 cm) showed a similar distribution (between fractions) to the native reactive U. By contrast, in the woodland profile exchangeable U (F1) was much smaller than the other three fractions but increased with depth with a concurrent decrease in F4 (humus-bound U). It should be acknowledged that the existence of 'carbonate-bound' U (nominally Fraction 2) in the acidic woodland soil is highly unlikely and so U in F2 can probably

be regarded as originating from specifically adsorbed forms held on humus- and Fe/Mn oxides.

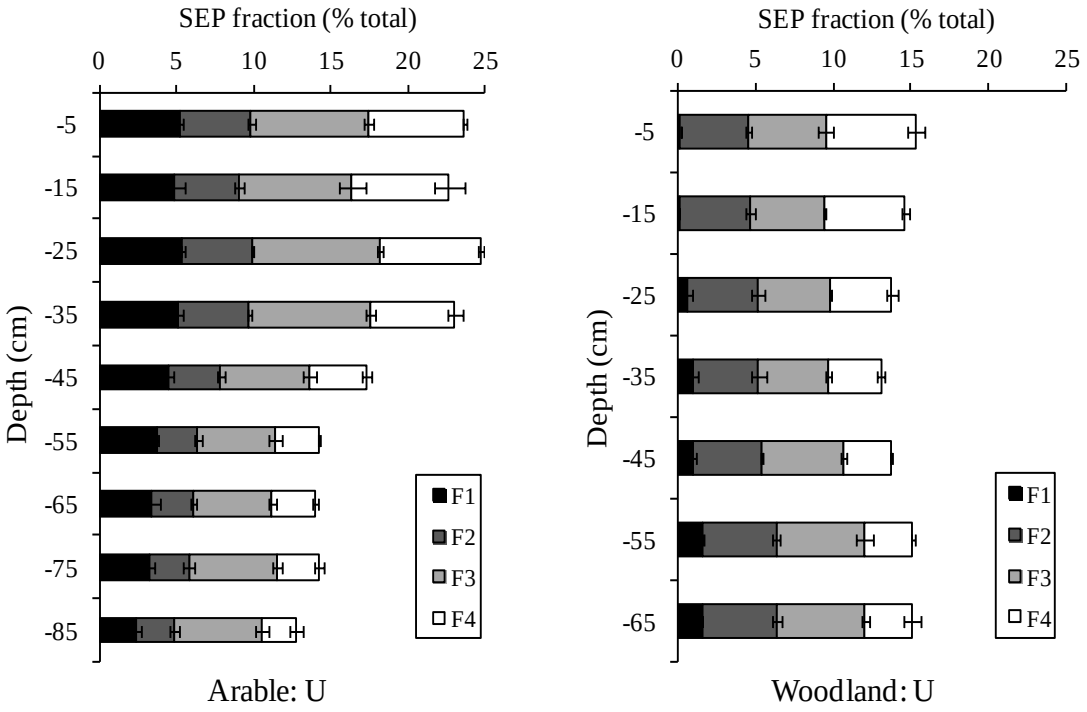

Figure 3.4: Fractionation of U in arable and woodland soil profiles. Data are average values of three auger borings ± standard errors.

Several previous studies reported an affinity between U and organic matter in soils or sediments in some highly contaminated areas (Dhoum and Evans, 1998; Sowder et al., 2003; Blanco et al., 2005). A strong positive correlation was found between U sorption (solid liquid distribution coefficient, K_d) and soil organic matter when Vandenhove et al. (2007a) added U(VI) into different types of soils with a range of organic matter content (2.97 - 15.3 % OM) indicating that U binds to the soil organic matter. Kaplan and Serkiz (2001) found that U was associated primarily with the residual fraction (91%) in wetland uncontaminated sediment, while in contaminated sediments U was distributed between exchangeable and organically bound fractions. In a humus rich andisol, organic matter and non-crystalline clay minerals played an important role for the accumulation of fertilizer-derived U (Takeda et al., 2006a). Yamaguchi et al. (2009) reported that soil organic matter provided an important pool of U in upland field and pasture soils, whereas U from phosphate fertilizer was adsorbed on poorly crystalline Fe/Al minerals in paddy soils. In the current study

reactive U was associated with the arable topsoil and, as shown in Figure 3.5, there was a very significant correlation between soil phosphate content and reactive soil U ($r = 0.99$, $P < 0.001$), which reflects the origin of reactive uranium in the arable soil.

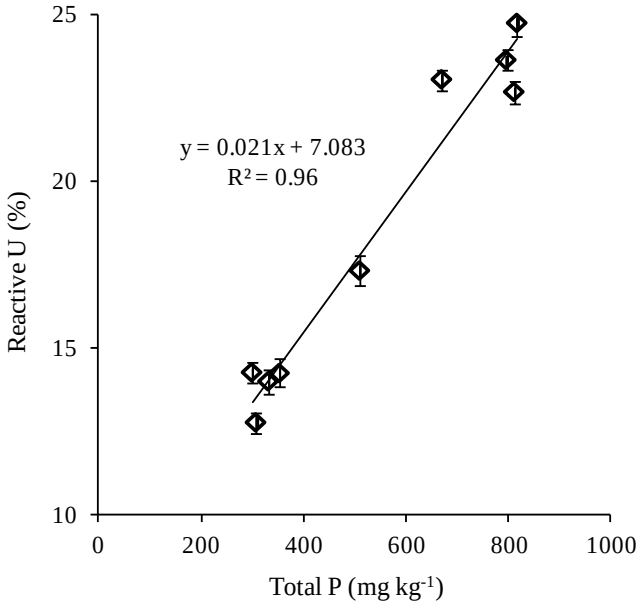

Figure 3.5: Reactive U (%) as a function of total P in arable soil profile. Reactive U % is the summation of the four non-residual U fractions. Data are average values of three auger borings ± standard errors.

3.3.4 Distribution of fertilizer-derived U in soil phases

Figure 3.6 shows U distribution among different arable soil phases compared to that in the woodland soil. In the arable soil U was distributed more evenly across the fractions of the non-residual phase with the following order: F3 (bound to Fe-Mn oxides) > F4 (bound to organic matter and sulphide) > F1 (exchangeable) > F2 (bound to carbonate and specifically adsorbed). Each non-residual phase and the total non-residual fraction (reactive U) of the arable soil were significantly correlated with the U/Th ratio in the arable soil profile ($r > 0.9$, $P \leq 0.002$). However, the U contents in the fractions F1, F3 and F4 in the arable soil were higher than those of the woodland; the differences in U content were remarkable, especially in F1 and F3 (Figure 3.6). The exchangeable fraction (F1) represents the form in which metals are most available for plant uptake. The second step extracts metals bound to carbonate and specifically adsorbed phases, this fraction can become easily available and mobile under conditions of lower soil pH, while metals bound to oxide and organic/sulphide

fractions are stable and more strongly held within the soil constituents than the first two fractions. By comparing U partitioning in the arable and woodland soils (Figure 3.6), it appears that humus and (Fe, Al) oxides play an important role for the accumulation of the fertilizer-derived U in the arable topsoil. In general, low solubility of U in soil causes accumulation of U in the soil surface (Rothbaum et al., 1979; Takeda et al., 2006a; Taylor, 2007; Yamaguchi et al., 2009).

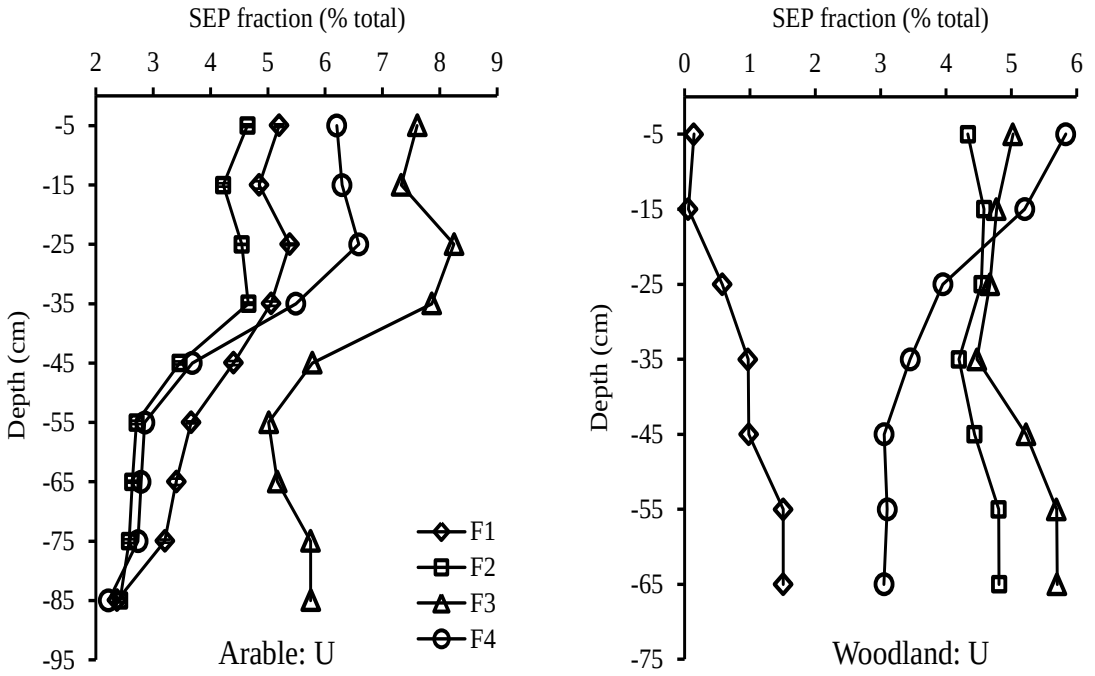

Figure 3.6: Distribution of U among different arable soil phases compared to that in woodland profile.

3.3.5 Fractionation of Th in the soils

The partitioning of Th in the arable and woodland soils was broadly similar (Figure 3.7): almost all the soil Th was in the residual fraction (97 and 95% of the total Th in arable and woodland soils, respectively). This reflects the fact that thorium is usually held within the most resistant phases of soils and sediments and is non-labile under most conditions (Braun et al., 1998; Blanco et al., 2005; Testa et al., 1999). The distribution of Th and U in a sediment receiving discharge from fertilizer plants into the Odiel River (Spain) indicated that, whereas U was mainly (>70%) associated with reactive fractions, Th was found mainly in the residual fraction (Martínez-Aguirre and Periáñez, 2001). It is well established that the ‘mobility’ or ‘reactivity’ of U is much greater than that of Th in soils (Sheppard, 1980).

Most of the reactive Th appeared to be bound to humus (F4) and it is likely that Th solubilized in F2 in the woodland soil was also actually humus-bound Th. Organic matter appeared to control the adsorption of reactive Th even at depths in the soil profile where organic matter content was particularly low (0.8%). Only in highly contaminated soils was Th found to be substantially present in the non-residual fraction. Thus, Kaplan and Knox (2003) found that >80% of Th in contaminated wetland sediments was associated with humus and enhanced mobility of Th at the study site was thought to result from Th-DOC complexes. Guo et al. (2008) investigated the effects of soil organic matter on the distribution and mobility of Th fractions in soil contaminated by the rare earth industry. They showed that increasing the soil organic matter (as humic acid) from 4.5 to 40.7 g kg^{-1} lowered the exchangeable Th and Th bound to carbonate fractions. Humic acids are thought to complex free Th ions but they also encourage adsorption to oxides by forming ternary surface complexes ≡SO–O–HA–Th (Chen and Wang, 2007).

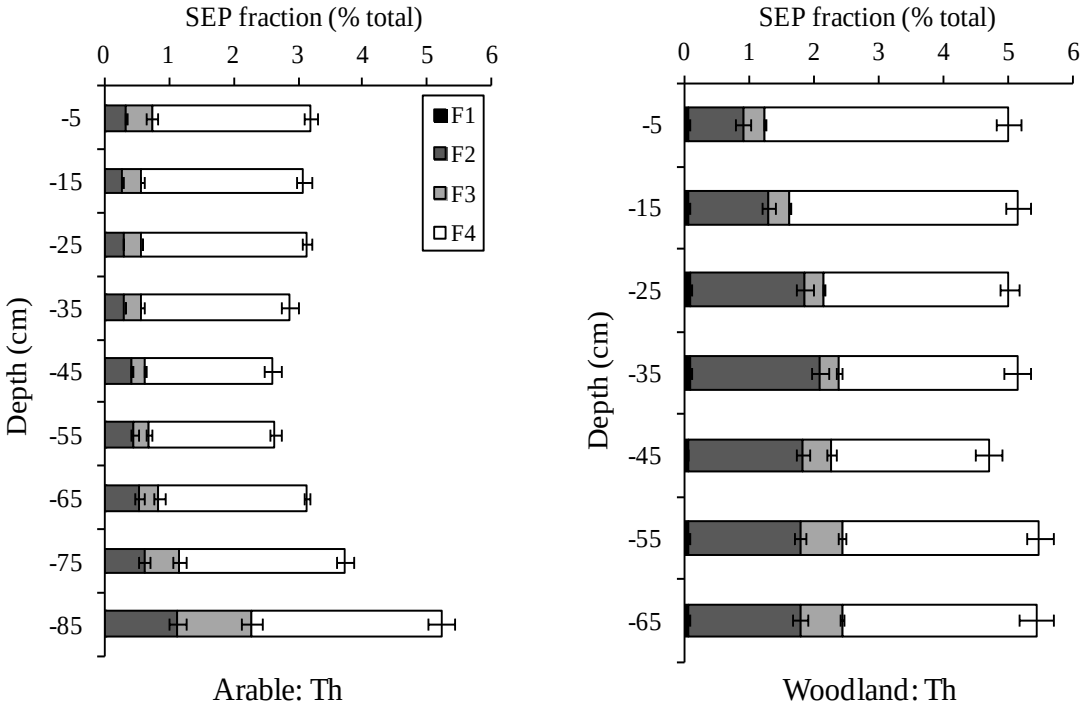

Figure 3.7: Fractionation of Th in arable and woodland soil profiles. Data are average values of three auger borings ± standard errors.

3.4 CONCLUSIONS

The work in this chapter investigated the vertical distribution and fractionation of uranium and thorium in soils under contrasting arable and woodland sites based on the same parent material. The effect of long-term application of phosphate fertilizer on U and Th concentrations in the arable soil was also assessed. There was clear evidence of U enrichment in the surface layers of the arable soil (0 – 40 cm) due to long-term application of phosphate fertilizers, shown by the distribution of U concentrations in the soil profile, the U/Th ratio, a comparison with an adjacent woodland soil and a strong correlation between 'excess U' and phosphate. The 'excess' U in arable soil, associated with long term P fertilizer application, was approximately 2.5 kg ha^{-1} with 80% in the top 30 cm of the soil profile.

A sequential extraction technique was used to investigate the soil constituents that contribute to retention of U in soil. Fertilizer-derived U was adsorbed, bound to organic matter and Fe-Mn oxides in the arable top soil. The 'excess' U accumulated in the arable topsoil was also considerably more reactive than the co-existing native U. Thus the reactive fraction of the excess U ranged from 29 to 42 % compared with 14 to 15 % reactivity of the native U.

There was a significant relationship between soil phosphate content and U reactivity which probably reflects the origin of the reactive uranium. Thorium in both soils and U in woodland soil showed a consistent reactivity down the soil profile; the proportion of reactive or non-residual U was almost five times that of Th. Uranium by comparison was much more reactive than Th and was distributed more evenly across the 4 reactive fractions; most of the small amount of reactive Th present appeared to be bound to humus (F4).

4 CHARACTERIZING URANIUM IN SOILS: COMPLEMENTARY INSIGHTS FROM ISOTOPIC EXCHANGE AND SINGLE EXTRACTIONS

4.1 INTRODUCTION

Uranium contamination from activities such as ore mining and processing, exploitation of hydrocarbons (coal, oil and shale gas) and production of phosphate fertilizers is likely to increase in future and thus presents a potential risk to human health (UNSCEAR, 1988; IAEA, 2003). In the last fifty years, it was observed that levels of environmental radioactivity could be greater in the vicinity of coal-fired power stations than nuclear generators, due to the relatively high concentration of U and Th present in coal (Bellis et al., 2001). Total metal concentrations in soils exhibit little relation to the mobility and toxicity of metals because speciation and distribution in the soil solid and solution phases exerts a key control on their potential availability to plants and organisms (Nolan et al., 2003; Degryse et al., 2011). It is recognised that U(IV) and U(VI) can exist in non-labile or 'unavailable' states in soils, fixed within primary mineral matrices and occluded within secondary mineral phases such as carbonates and phosphates (Langmuir, 1978; Singh et al., 2010).

The assessment of trace element availability in soils has a long developmental history which has focussed on chemical extraction procedures (Rauret, 1998; Meers et al., 2007; Singh, 2007; Rao et al., 2008). In this context, the ideal extractant provides an estimate of the 'labile' metal content of the soil which may constitute the plant-available reservoir of soil metal and may control metal solubility. However, in reality, there is no single extraction procedure which can estimate the fraction of an element available for uptake by plants in most soils and under all soil conditions. Many different extractants have been used by different investigators (Levesque and Mathur, 1988; Ure 1996; Lebourg et al., 1996; Ure and Davidson, 2002; Takeda et al., 2006b; Vandenhove et al., 2007b; Rao et al., 2008; Singh, 2007). Although they are widely used to fractionate soil metals, extraction methods are prone to a high degree of operational dependence (Tessier and Campbell, 1988; Payne et al., 2001 and 2004; Clark et al., 2011), lack of specificity (Singh, 2007) and possible re-adsorption during extraction (Rendell et al., 1980). By contrast, determination of an isotopically

exchangeable fraction in the presence of a dilute electrolyte (the E-value) may provide an unambiguous assessment of chemical reactivity (Nakhone and Young, 1993; Smolders et al., 1999; Young et al., 2000; Tongtavee et al., 2005; Young et al., 2006; Gabler et al., 2007; Degryse et al., 2011). The isotopic exchange technique discriminates between labile (isotopically exchangeable) and non-labile (fixed) U pools in soils. The labile $^{238}U(VI)$ pool in soil may be determined by adding to a soil suspension a small amount of an isotope which is not naturally present (eg. ^{233}U) but in the same chemical form (U^{VI}). After a given equilibration time, the U(VI) isotope ratio ($^{233}U/^{238}U$) is determined in the soil supernatant, which allows the quantification of the $^{238}U(VI)$ pool in soil into which the tracer has been diluted. Buekers et al. (2008) reported that E-values were superior to total soil metal concentrations when used to predict metal solubility in soil geochemical models. The E-value has also been shown to represent a reasonable approximation to the plant-available reservoir of some metals (Oliver et al., 2006; Young et al., 2007 and references therein). Moreover, the isotopic exchange method can be used without disturbance of the soil solid-solution equilibrium, and is robust to changes in electrolyte composition and solid : liquid ratio.

In this chapter preliminary experiments were conducted to develop a procedure for measuring the E-value of soil U(VI). Following this, a more in-depth study was conducted that compared soil E-values with quantities of U extracted by different single extraction methods. Isotopic exchange was used in this chapter to determine the labile fractions of $^{238}U(VI)$ in 77 soils and to compare the results with single extraction data.

At present, the use of isotopic dilution to determine labile uranium pools in soil is a relatively under-exploited technique (Section 1.1.3). The objectives of this study were therefore to:

(i) develop and test isotopic dilution with ^{233}U (as UO_2^{2+}) as a means of determining isotopically exchangeable (labile) $^{238}UO_2^{2+}$ in uncontaminated soils;

(ii) assess the soil factors controlling U lability in soils with contrasting properties;

(iii) test for the presence of sub-micron colloids containing non-labile U in dilute soil electrolyte suspensions;

(iv) compare U(VI) E-values with a range of common soil extractants to determine their ability to solubilize labile uranium;

(v) evaluation of chemical extraction approaches for the characterization of reactive Th.

4.2 MATERIALS AND METHODS

4.2.1 Study area and soil samples

Two sets of soils were used in this study. Thirty seven soil samples (Field soils, a mix of topsoils and subsoils) were collected in central England, representing five contrasting ecosystems which cover a wide range of different soil characteristics: arable (Ar, n = 3), acidic woodland (AW, n = 3), acidic moorland (AM, n = 11), calcareous soils (Ca, n = 3) from arable, woodland and grassland sites and biosolid-amended arable soils (Ba, n = 17) from a sewage processing farm.

Arable and acidic woodland soils locations are shown in Plate 3.1 (Section 3.2.1). Samples were collected from an arable field within the University of Nottingham farm, Leicestershire, UK (52°49'48''N-1°14'23''W) and from an adjacent mature woodland strip (Section 3.2.1). Three arable soil samples were collected from three different depth intervals (0-14, 14-28, and 24-36 cm) and three soils from the acidic woodland site at the following depths: 0-12, 12-24, and 24-36 cm.

Acidic moorland soils were sampled from Sherwood Forest and Budby Common (53°12'40''N-1°04'22''W) at three different sites and different soil depths below the surface (Figure 4.1). Five soil samples were collected from under heather (*Calluna vulgaris*) (Plates 4.1 and 4.2) at different soil depths: 2-8 cm, 8-12 cm, 12-14 cm, 20-30 cm, and 30-40 cm. Three soil samples were collected from under Silver Birch (*Betula pendula*) at different soil depths 0-8 cm, 10-20 cm, and 20-35 cm. Finally, three soil samples were collected from under Scots Pine (*Pinus sylvestris*) at different soil depths below the surface: 11-15 cm, 15-35 cm, and 35-45 cm, with the shallowest

of these being taken directly beneath a layer of forest litter overlying the mineral soil. Sherwood Forest is encompassed within a larger area, with the main sites being Sherwood Forest Country Park and Budby South Forest. The whole site lies on a dry, nutrient-poor soil overlying the Sherwood Sandstone. Woodland is dominated by mature native trees including Sessile Oak (*Quercus petraea*) and Silver Birch (*Betula pendula*).

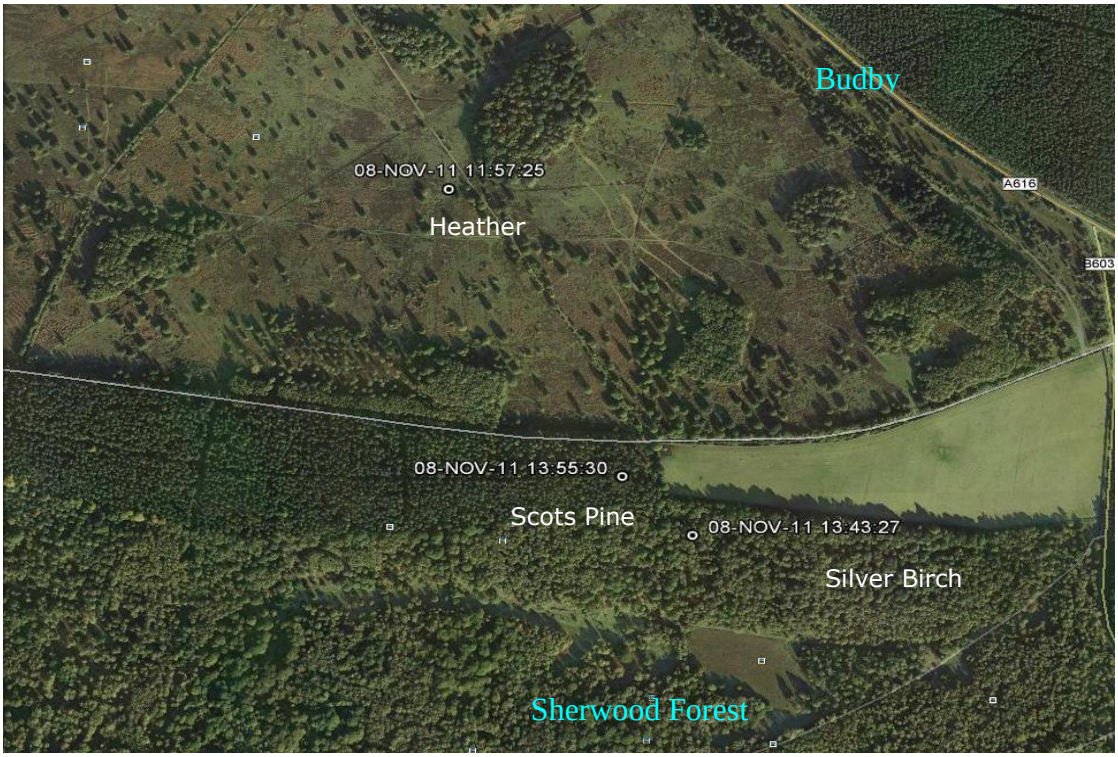

Figure 4.1: A labelled aerial view of Sherwood Forest and Budby Common shows the three sampling sites.

Plate 4.1: Budby Common, showing heather tussocks interspersed with grass sward.

Plate 4.2: Soil pit excavated under heather, 2–40 cm below the surface (Budby Common).

Calcareous soils were sampled from the Stoke Rochford Estate, Lincolnshire, from the Elmton soil series, described as shallow, well drained, brashy calcareous fine loamy soils developed over Jurassic limestone. Arable (52°51'25''N-0°38'55''W), grassland and woodland topsoils (Plate 4.3) were collected from a valley with permanent grassland (52°50'53"N-0°40'26"W) and adjacent mature woodland (52°50'56"N-0°40'22"W); these are Lithomorphic Rendzina soils over limestone and thus have no associated subsoil.

Plate 4.3: Example of mixed ecosystem sites on similar parent material: arable, woodland and grassland sites located on calcareous deposits in Lincolnshire, UK.

Biosolid-amended arable soils were sampled at a sewage treatment facility ('sewage farm'), run by Severn Trent Water at Stoke Bardolph near Nottingham, England (52°57'36''N-1°02'37''W). The farm is approximately 700 ha in area with approximately 60 fields. The site is managed within the guidelines governing 'dedicated sites' set out by the 1989 Sludge Regulations (HMSO, 1989) and until recently was utilised for dairying and production of livestock feed. Current cropping is mainly fodder maize which is ensiled and the resulting silage is used as feedstock for a large bio-reactor complex. Sewage sludge has been applied to parts of this land for approximately 100 years. An intensive geochemical survey of the farm has been conducted at five yearly intervals. This involves collecting soil from 0-25 and 25-50

cm horizons and determining a wide range of metals and metalloids (Heaven and Delve, 1997). The geochemical survey of the farm does not include Th and U, therefore the current study investigated Th and U concentrations and availability in the surface layer of different fields at Stoke Bardolph. Seventeen soil samples were collected from six fields at different locations (Figure 4.2): four samples from Field 6 (6A, 6B, 6C, and 6D), two from Field 7 (7A, and 7B), six samples from Field 8 (8A, 8B, 8C, 8D, 8E, and 8T), two samples from Field 9 (9A, and 9B), two samples from Field 10 (10A, and 10B) and one sample from Field 11 (11A).

The first set of soils covers a wide range of soil characteristics, but it includes only three calcareous soils with the same parent material. Therefore a second set of 40 soils was sub-sampled from the British Geological Survey (BGS) archive, (Keyworth, Nottingham, UK.) to cover a wider range of soil pH (calcareous soils - 22 soils had pH (H_2O) values >7) and soil characteristics. This set of soils was designated as 'British Geological Survey collection' (BGSc).

Figure 4.2: Aerial view of sewage farm shows the sampling point locations.

4.2.2 Soil characterization

Soil samples (200 g) were air-dried and sieved to < 2 mm. Soil pH values were measured in 0.01 M $Ca(NO_3)_2$ soil suspension (1 : 10 soil : solution ratio). Inorganic carbon expressed as $\%CaCO_3$ and organic carbon was calculated as the difference between total carbon and inorganic carbon. Subsamples of the < 2 mm sieved soils were ground in an agate ball-mill and total U and Th concentrations were measured at the University of Nottingham (UoN) for both soil sets (Section 2.5.1); for the second soil set (BGSc), the University of Nottingham total U measurements were compared to those measured at BGS. Available phosphate was determined using extraction by Olsen's method and a colorimetric assay (Rowell, 1994). Reactive iron, aluminium and manganese hydrous oxides were solubilized using the dithionite extraction method (Section 2.2.7).

4.2.3 Measuring E-values (E_{soln}) and E-resin (E_{resin})

A recovery experiment was carried out to investigate whether $^{238}U(VI)$ added to and equilibrated with resin (Amberlite IR-120) can be recovered by the isotopic dilution technique and to test the validity of the technique with a $^{233}U(VI)$ tracer (Section 2.6.1). The effect of varying soil-spike equilibration time prior to isotopic analysis was also investigated as a source of discrepancies in the results of isotope exchange experiments. The effect of varying spike levels on E-value and soil pH was also investigated (for details see Section 2.6.1). The E-value for $^{238}U(VI)$ was determined from isotopic ratios alone or from isotopic calibration standards (Section 2.6.3). The E-values obtained by assay of the equilibrated electrolyte (Section 2.6.2) and resin phases (Section 2.6.4) are denoted as E_{soln} and E_{resin} respectively. Both estimates of E-value (E_{soln} and E_{resin}) were then compared to determine the presence of non-labile $^{238}U(VI)$ in suspended colloidal particles (SCP-^{238}U) (Section 2.6.4).

4.2.4 Chemical extraction of soil uranium

Chemically reactive soil U and Th were extracted with different single extraction methods (for details see Section 2.4.1). To study the effect of equilibration time on nitric acid extraction, six soils - calcareous (Ca; arable, woodland and grassland), acidic woodland (AW), acidic moorland (AM) and biosolid-amended arable (Ba) soils

- were suspended in 0.43 M nitric acid (1 : 10 soil : solution) (Tipping et al., 2003) and equilibrated for 2 – 120 hr during which U and Th concentrations were measured at 2, 4, 6, 16, 24, 48, 72, 96, and 120 hr. The pH values of soil suspensions were measured prior to isolation of the supernatant phase.

4.2.5 Describing ^{238}U lability as a function of soil properties

An empirical model was established and assessed for its ability to describe and predict ^{238}U(VI) lability as a function of measured soil characteristics. A simple linear multi-regression model allows the inclusion of a large number of soil variables. Correlation between ^{238}U(VI) lability and measured soil properties (pH, total U (U_{total}; mg kg^{-1}), % SOM, % clay, available phosphate (P_{avail}; mg kg^{-1}) and Fe, Mn, Al oxide contents (mg kg^{-1})) was tested and the significance of each variable was determined using the step-wise regression function in Minitab vs 16.22. Variables that were significant ($P < 0.05$) in predicting ^{238}U(VI) lability were included in the regression model (Equation 4.1). The Solver function in Microsoft Excel was used to optimize constants in the empirical model.

$$\%E\text{-}value = k_0 + k_1\,(pH) + k_2\,(U_{total}) + k_3\,(\%SOM) + k_4\,(FeOx) + k_5\,(MnOx) + k_6\,(AlOx) + k_7\,(P_{avail}) + k_8\,(\%Clay) + k_9\,(\%CaCO_3) \quad (4.1)$$

4.3 RESULTS AND DISCUSSION

4.3.1 Soil characteristics

Figure 4.3 summarizes selected soil characteristics (pH, %SOM, FeOx, %Clay and total U) which may affect U lability within the broad groups of soils, while Table 4.1 lists details of soil properties, including available-P, Al and Mn oxide content. Within the soils collected for this study pH covered a wide range (pH 3.05 – 7.24), with 13 very acidic soils (pH <4.0) and 14 soils with pH >7.0. Soil organic matter (%SOM) ranged from 1.4 – 30%, with the exception of two soils from the BGSc set with 40% and 50% organic matter. Iron oxide content (FeOx) varied from 3.6 to 40 g kg^{-1}, with three soils higher than this range (45, 48, 65 g kg^{-1}); Al and Mn oxide contents (AlOx and MnOx) (0.5 – 8.9 and 0.04 – 7.2 g kg^{-1}, respectively) were significantly lower than FeOx. The wide range of %SOM and FeOx is likely to affect U lability. Phosphate status varied widely from very low concentrations in the BGSc soils to extremely large available-P concentrations in the Ba soils (Table 4.1). Clay content ranged from 3% in sandy soils to a maximum of 32%. Other soil properties also collectively covered a very broad range.

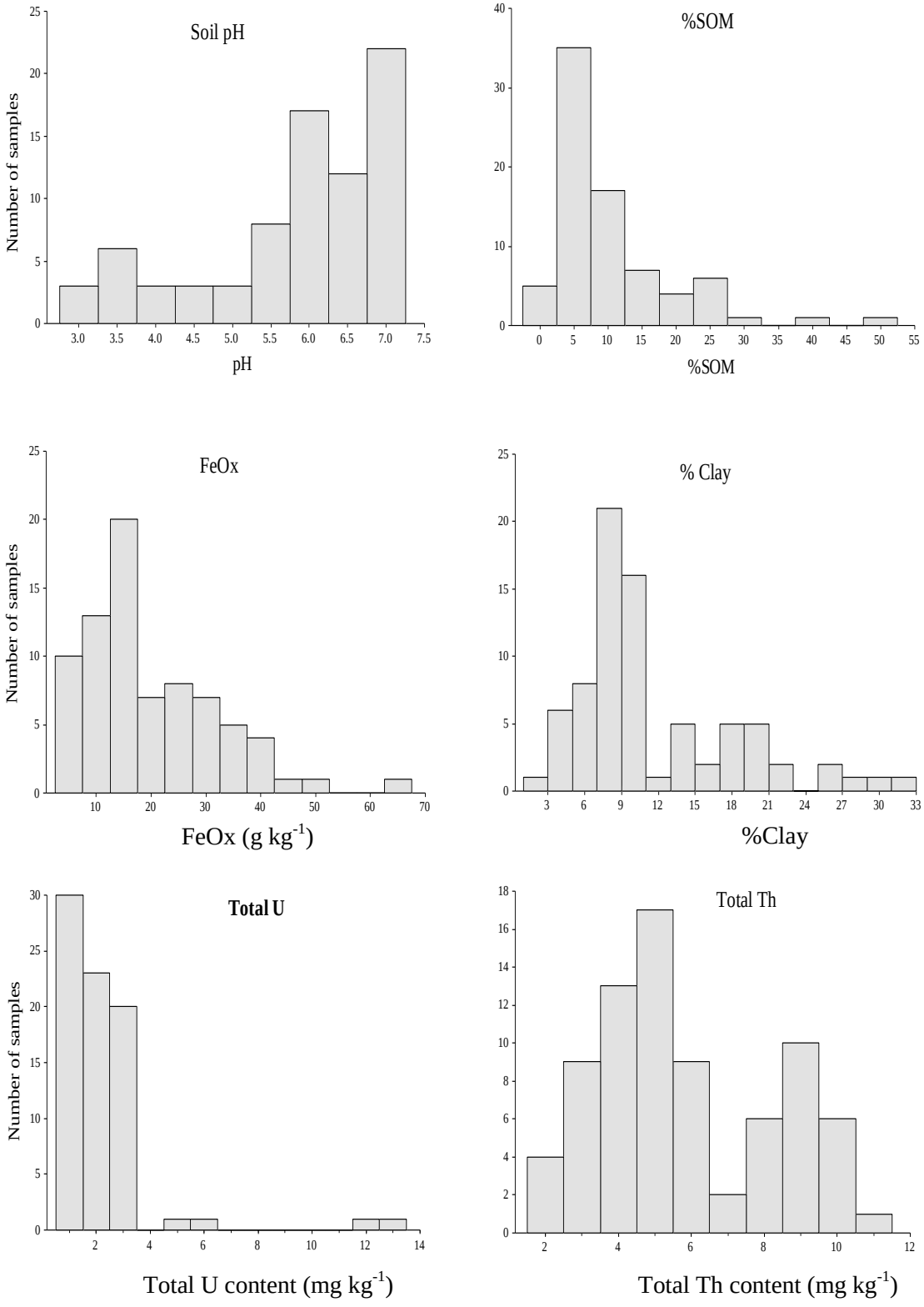

Figure 4.3: Histograms of soil characteristics; pH, %SOM, FeOx (g kg^{-1}) and %clay and total U and Th concentrations (mg kg^{-1}).

Table 4.1: Summary of soil properties and total U and Th concentrations of the studied soil samples (n = 77). The first set of soils (a; n = 37) and BGSc soils (b; n = 40).

Soil	Depth	pH	SOM	Avail-P	FeOx	AlOx	MnOx	Clay	Total U	Total Th
(a)	**Cm**		**%**	**(mg kg^{-1})**	**(g kg^{-1})**	**(g kg^{-1})**	**(g kg^{-1})**	**%**	**(mg kg^{-1})**	**(mg kg^{-1})**
Ar		**6.20**	**2.81**	**95.61**	**8.6**	**1.00**	**0.28**	**4.70**	**1.33**	**4.83**
Ar-1	0-14	6.27	3.58	100.23	8.3	0.96	0.28	6.11	1.39	5.01
Ar-2	14-28	6.19	2.89	91.30	8.3	1.01	0.29	4.15	1.26	4.67
Ar-3	24-36	6.15	1.97	95.29	9.4	1.03	0.28	3.84	1.35	4.81
AW		**3.96**	**4.70**	**18.50**	**10.4**	**1.77**	**0.11**	**5.12**	**1.19**	**4.91**
AW-1	0-12	4.40	9.30	19.95	10.6	1.80	0.11	4.14	1.14	4.73
AW-2	12-24	3.72	3.24	22.92	10.4	1.83	0.06	5.42	1.24	4.87
AW-3	24-36	3.78	1.57	12.61	10.1	1.68	0.14	5.81	1.18	5.13
AM		**3.53**	**6.68**	**41.21**	**7.5**	**1.35**	**0.15**	**9.29**	**0.98**	**3.36**
AM-H-1	2-8	3.32	9.51	18.11	6.7	0.90	0.04	8.91	0.96	3.29
AM-H-2	8-12	3.56	3.20	21.20	7.9	0.83	0.04	9.54	0.98	3.58
AM-H-3	12-14	3.57	4.97	16.17	8.1	1.18	0.05	9.34	0.96	3.43
AM-H-4	20-30	3.80	1.31	33.88	7.8	1.23	0.13	9.72	1.04	3.67
AM-H-5	30-40	4.32	1.68	30.33	10.37	2.87	0.31	9.75	1.19	4.63
AM-B-1	0-8	3.05	18.02	59.38	6.07	0.95	0.23	8.08	0.85	2.66
AM-B-2	10-20	3.17	7.50	38.48	6.60	0.93	0.09	9.14	0.89	2.94
AM-B-3	20-35	3.51	1.42	39.14	8.14	0.88	0.11	9.71	1.07	3.47
AM-P-1	11-15	3.08	24.29	77.65	6.77	1.49	0.14	8.41	0.95	2.84
AM-P-2	15-35	3.64	1.08	67.84	7.19	1.50	0.19	9.75	0.93	3.19
AM-P-3	35-45	3.86	0.53	51.12	7.28	2.11	0.35	9.80	0.93	3.22
Ca	Topsoil	**7.09**	**6.98**	**44.97**	**15.42**	**1.60**	**0.40**	**3.74**	**1.07**	**3.95**
Ca-Ar		7.12	4.61	46.32	15.71	1.56	0.40	3.68	1.25	3.85
Ca-W		7.12	6.96	51.91	12.70	1.54	0.38	3.77	1.01	4.37
Ca-G		7.03	9.38	36.67	17.87	1.70	0.42	3.76	0.96	3.61
Ba	Topsoil	**6.15**	**14.33**	**325.13**	**15.24**	**3.68**	**0.74**	**8.39**	**2.61**	**5.07**
Field-6		**6.07**	**9.59**	**234.76**	**14.58**	**2.92**	**0.39**	**8.91**	**2.27**	**5.60**
6A		6.01	8.28	252.14	6.01	2.82	0.49	8.86	2.28	5.16
6B		6.36	9.00	267.24	6.36	3.06	0.48	8.92	2.36	6.37
6C		6.00	7.31	191.45	6.00	2.91	0.29	9.04	1.97	4.51
6D		5.91	13.78	228.20	5.91	2.88	0.31	8.82	2.46	6.36
Field-7		**6.32**	**3.82**	**129.11**	**20.22**	**2.41**	**1.12**	**9.35**	**2.27**	**5.37**
7A		6.28	3.30	135.66	6.28	2.56	1.36	9.34	2.32	4.57
7B		6.37	4.35	122.57	6.37	2.26	0.87	9.36	2.23	6.17
Field-8		**6.05**	**23.13**	**522.69**	**14.04**	**4.94**	**0.84**	**7.53**	**3.05**	**4.68**
8A		6.14	22.55	483.24	6.14	4.73	0.81	7.55	2.96	4.04
8B		5.85	21.09	860.37	5.85	5.72	0.89	7.62	3.02	5.42
8C		5.93	16.98	437.67	5.93	4.10	0.79	8.03	2.44	3.93
8D		5.97	26.06	504.25	5.97	5.38	1.02	7.45	3.29	5.14
8E		6.07	27.69	517.48	6.07	5.30	0.72	7.07	3.15	3.90
8T		6.33	24.40	333.10	6.33	4.39	0.84	7.48	3.40	5.63
Field-9		**6.26**	**18.85**	**350.40**	**12.92**	**4.30**	**0.75**	**7.86**	**2.89**	**4.83**
9A		6.19	21.85	356.49	12.70	4.56	0.72	7.66	3.07	5.43
9B		6.32	15.86	344.31	13.14	4.05	0.78	8.05	2.71	4.22
Field-10		**6.11**	**3.83**	**126.77**	**16.90**	**2.20**	**0.85**	**9.42**	**1.98**	**4.62**
10A		6.14	4.11	106.30	18.10	2.20	0.91	9.39	2.19	5.73
10B		6.09	3.54	147.24	15.71	2.20	0.78	9.46	1.76	3.51
Field-11		**6.58**	**13.49**	**239.55**	**16.53**	**3.39**	**0.55**	**8.47**	**2.82**	**6.12**

Arable soil (Ar), Acidic Woodland (AW), Acidic Moorland (AM), Calcareous arable, woodland and grassland (Ca-Ar, W, G) and Biosolid-amended arable soils (Ba).

Soil (b)	pH	SOM %	Avail-P (mg kg^{-1})	FeOx (g kg^{-1})	AlOx (g kg^{-1})	MnOx (g kg^{-1})	Clay %	Total U (mg kg^{-1})	Total Th (mg kg^{-1})
BGSc	**6.36**	**9.32**	**41.46**	**26.30**	**2.80**	**1.42**	**15.11**	**2.83**	**7.11**
BGSc_1	6.95	7.02	17.75	25.20	2.50	1.36	6.06	2.58	8.80
BGSc_2	7.01	3.49	43.09	37.79	2.72	2.05	7.49	2.49	7.95
BGSc_3	7.10	3.36	45.49	30.03	2.66	1.77	10.48	2.54	7.56
BGSc_4	4.62	18.26	27.32	5.79	3.01	0.23	7.87	2.23	6.25
BGSc_5	5.91	7.80	16.45	36.71	5.46	7.24	18.54	3.29	9.82
BGSc_6	5.60	8.36	8.66	34.69	6.20	1.08	14.49	2.60	8.11
BGSc_7	6.75	12.05	27.31	28.84	4.67	1.63	16.67	11.52	9.40
BGSc_8	5.12	11.17	17.26	27.30	4.10	2.21	17.27	4.80	8.77
BGSc_9	6.94	8.21	24.39	28.12	2.52	5.45	19.60	2.14	4.82
BGSc_10	6.85	3.32	66.31	24.11	2.29	1.84	13.82	2.40	8.56
BGSc_11	6.65	2.71	34.70	22.19	3.13	1.82	11.54	2.07	7.37
BGSc_12	6.91	4.73	37.03	22.69	1.74	1.58	6.82	2.21	8.61
BGSc_13	6.44	8.26	54.44	28.80	1.89	0.34	7.32	1.49	6.30
BGSc_14	5.44	4.92	20.74	35.48	2.66	0.61	14.65	2.50	11.13
BGSc_15	7.05	5.02	28.53	29.37	2.88	1.30	31.99	3.14	9.38
BGSc_16	6.69	5.51	55.47	25.68	2.18	0.89	26.57	2.42	8.90
BGSc_17	6.95	5.99	17.89	40.15	3.06	0.68	28.21	2.69	10.39
BGSc_18	7.08	5.66	51.09	14.51	1.42	0.66	17.01	1.11	4.96
BGSc_19	7.05	7.11	66.65	3.61	0.77	0.35	20.72	1.13	4.08
BGSc_20	7.12	38.73	52.73	4.17	0.68	0.17	16.89	0.70	2.05
BGSc_21	6.74	7.56	148.70	24.24	1.77	0.92	22.58	2.12	8.96
BGSc_22	6.21	5.64	52.48	29.88	2.20	0.87	18.76	2.49	8.89
BGSc_23	6.04	16.56	28.98	20.06	2.07	0.41	9.85	3.40	7.05
BGSc_24	7.10	12.80	71.44	17.68	1.17	0.63	19.72	3.19	9.77
BGSc_25	5.48	13.10	35.83	40.65	1.77	0.30	5.76	1.53	5.12
BGSc_26	5.37	23.91	12.06	15.22	0.97	0.34	2.95	1.48	2.03
BGSc_27	5.23	49.73	16.64	24.77	3.87	0.28	9.47	12.62	2.49
BGSc_28	6.91	4.00	94.38	47.59	2.77	1.19	8.71	2.43	8.08
BGSc_29	7.24	1.42	28.91	12.69	1.30	0.42	5.23	1.05	4.01
BGSc_30	7.05	2.86	64.18	12.50	0.94	0.56	5.54	1.22	4.78
BGSc_31	7.11	2.14	64.90	9.52	1.08	0.39	7.90	0.97	2.64
BGSc_32	6.68	17.15	36.09	23.00	1.32	0.41	7.71	1.78	6.35
BGSc_33	6.88	9.62	57.50	3.95	0.48	0.08	17.67	1.05	2.27
BGSc_34	7.19	3.93	57.36	14.02	1.65	0.66	13.92	1.02	3.52
BGSc_35	5.56	4.04	32.52	45.14	5.76	1.55	20.96	3.11	10.13
BGSc_36	5.57	4.96	44.19	35.87	3.46	0.86	13.38	2.44	8.25
BGSc_37	5.30	6.46	9.60	65.33	8.88	6.77	22.22	3.24	8.26
BGSc_38	5.41	3.65	36.76	29.04	4.00	1.84	30.32	3.31	9.57
BGSc_39	5.91	6.45	36.50	36.74	3.82	3.93	26.78	5.64	9.27
BGSc_40	5.19	5.09	15.97	38.87	6.14	0.94	20.81	3.16	9.69

Soils sub-sampled from the British Geological Survey (BGS) archive.

Comparing the total U concentrations of BGSc soils digested and measured at both BGS and UoN confirmed the overall reproducibility of the digestion method and the analysis undertaken at both institutions; the average ratio (BGS/UoN) was 1.005 with SD = 0.006. Total U ranged from 0.7 to 5.6 mg kg^{-1}, with the exception of two soils from BGSc with 11.5 and 12.6 mg kg^{-1} U (Fig. 4.3). Total Th varied from 2.0 – 11.1 mg kg^{-1}.

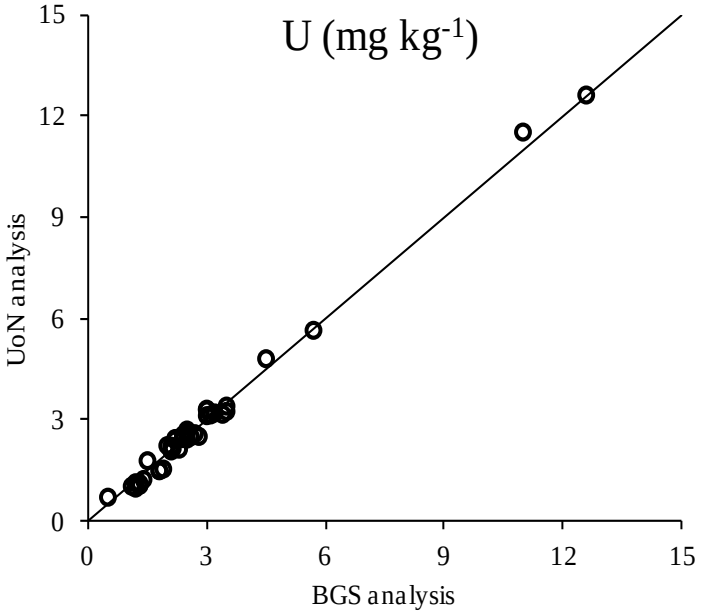

Figure 4.4: Comparing U concentrations (mg kg^{-1}) measured at the British Geological Survey (BGS) and the University of Nottingham (UoN), (n = 40). The solid line represents the 1:1 line.

Bellis et al. (2001) used the U/Th ratio as a potential indicator of the source and relative elevation of U concentration and suggested that the U/Th ratio could be a more robust indicator of contamination than the actual U concentration, given the problems of sample variability and standardisation. In the current study the U/Th ratio varied from 0.23 to 5.10 (Figure 4.5) compared with the average crustal ratio of 0.3 (Bellis et al., 2001). Excluding the two BGSc soils with the highest U/Th ratios (1.23 and 5.10), the U/Th ratio ranged from 0.23 to 1.10 for all soils investigated. The biosolid-amended soils (Ba) showed some indication of U enrichment, with U/Th ratios varying from 0.37 to 1.10 as shown in Figure 4.5.

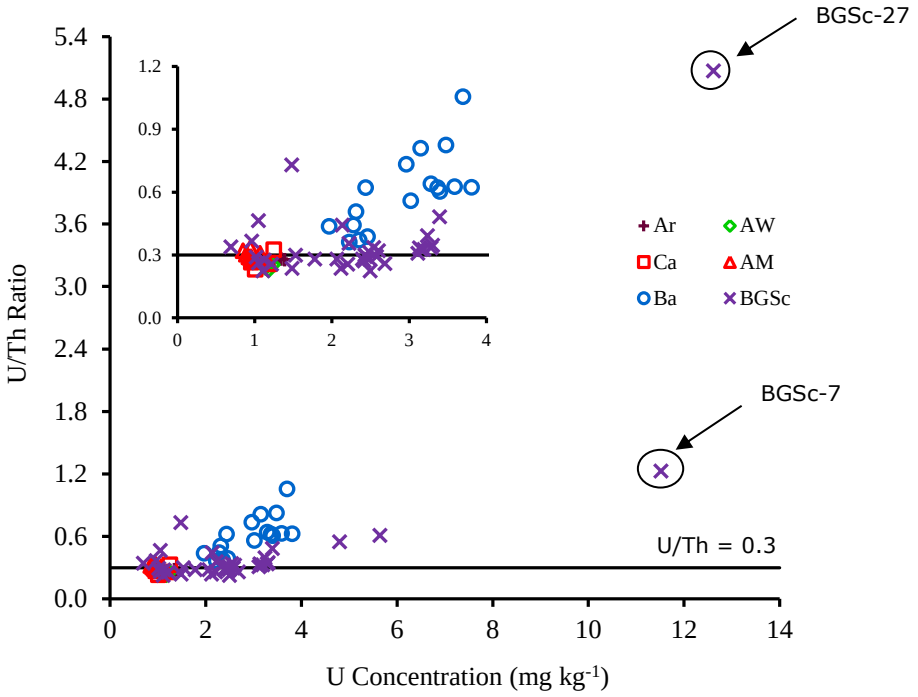

Figure 4.5: The U/Th concentration ratio as a function of total soil U concentration (mg kg^{-1}) for all soils in this study.

Correlations between soil characteristics and total U and Th concentrations in the soil samples studied are shown in Table 4.2. Weak correlations were observed between soil pH and FeOx and between soil pH and MnOx. Total U concentration was weakly correlated with pH, %SOM and available-P and significantly correlated with FeOx, AlOx, MnOx and %Clay. Significant positive correlations were observed between total concentration of Th and each of FeOx, AlOx, MnOx and %Clay. This may be due to the binding of U and Th on these solid phases. Duquene et al. (2006) reported that Uranium can be associated with numerous minerals and phases in soils such as oxides, hydroxides, sulfates, phosphates, carbonates, and clay minerals. Excluding the two soils with high U concentrations (11.5 and 12.6 mg kg^{-1} U) gives a significant correlation ($r = 0.61$, $P < 0.001$) between Th and U concentrations.

Table 4.2: Correlation matrix between measured soil characteristics and total U and Th concentrations in the soil samples studied (n = 73); four soils with outlying values have been excluded from the correlation matrix (BGSc-7; U_{total} = 11.5 mg kg^{-1}, BGSc-20; %SOM = 39%, BGSc-27; U_{total} = 12.6 mg kg^{-1} and %SOM = 50%, BGSc-37; FeOx = 65 g kg^{-1}). P values are in brackets and the significant correlations are in bold italic type.

Soil properties	**pH**	**% SOM %**	**Avail-P (mg kg^{-1})**	**FeOx (g kg^{-1})**	**AlOx (g kg^{-1})**	**MnOx (g kg^{-1})**	**Clay %**	**Total U (mg kg^{-1})**
% SOM	-0.07 (>0.05)							
Avail-P	0.06 (>0.05)	**0.68** ***(<0.001)***						
FeOx	**0.33** ***(<0.01)***	-0.21 (>0.05)	-0.23 (>0.05)					
AlOx	0.04 (>0.05)	**0.37** ***(<0.01)***	**0.53** ***(<0.001)***	**0.48** ***(<0.001)***				
MnOx	**0.26** ***(<0.05)***	-0.10 (>0.05)	-0.08 (>0.05)	**0.53** ***(<0.001)***	**0.42** ***(<0.001)***			
Clay	0.21 (>0.05)	**-0.28** ***(<0.05)***	**-0.27** ***(<0.05)***	**0.48** ***(<0.001)***	**0.25** ***(<0.05)***	**0.41** ***(<0.001)***		
Total U	**0.24** ***(<0.05)***	**0.28** ***(<0.05)***	**0.36** ***(<0.05)***	**0.52** ***(<0.001)***	**0.70** ***(<0.001)***	**0.49** ***(<0.001)***	**0.41** ***(<0.001)***	
Total Th	**0.30** ***(<0.05)***	**-0.23** ***(<0.05)***	-0.21 (>0.05)	**0.80** ***(<0.001)***	**0.46** ***(<0.001)***	**0.46** ***(<0.001)***	**0.62** ***(<0.001)***	**0.61** ***(<0.001)***

4.3.2 Preliminary investigation: Testing the isotopic exchangeability of 238U(VI) adsorbed on Amberlite IR-120 resin

Figure 4.6 shows, as a function of ^{233}U spike concentration, the ratio of (i) the E-value for ^{238}U in Amberlite IR-120 resin suspensions to the total ^{238}U added and (ii) the proportion of the spike isotope (^{233}U) adsorbed in the resin to the proportion of the ^{238}U present. Both variables should have a value of 1.0 if there is complete isotopic equilibrium and the adsorbed ^{238}U is entirely labile and not bound irreversibly to the resin. There was no significant effect of ^{233}U concentration and both variables were close to 1.0, confirming the validity of the isotopic dilution protocol, analysis and calculation under the conditions employed.

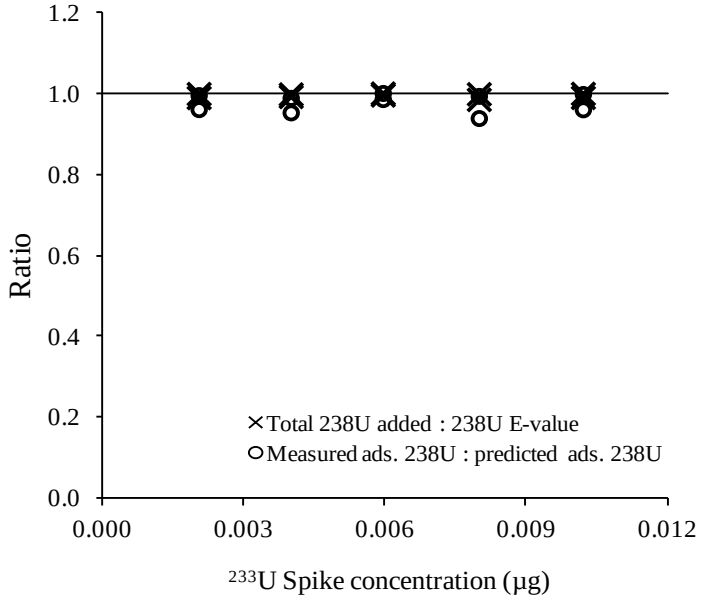

Figure 4.6: The ratio of total (added) ^{238}U to the measured ^{238}U E-value (×) and the ratio of measured resin-adsorbed ^{238}U to predicted adsorbed ^{238}U (○) from the ^{233}U spike distribution coefficient; both variables are shown as a function of ^{233}U concentration (µg).

4.3.3 Preliminary investigation: Effect of tracer-isotope (^{233}U) equilibration time on ^{238}U E-value

Ideally, the measured E-value in soils should be independent of variables such as solid : solution ratio, electrolyte composition of the suspension and the pre-equilibration time. However, there is inevitably some variation with isotope equilibration time (Young et al., 2006) because of slow mixing of the tracer-isotope with the non-labile U pool in the soil. As a result E-values are expected to increase with isotopic contact time, albeit at a progressively slower rate. Most published results for trace metal E-values suggest that a reasonably discrete labile pool is distinguished after 2-3 days equilibration (Young et al., 2000 and 2006). Oliver et al. (2006) reported that E-value procedures involve less than 1 week equilibration with the tracer, while Hamon et al. (2008) suggested an isotopic mixing time of 1-3 days as being enough for isotopic equilibration to be achieved. Currently, there are no equivalent studies of U isotope dynamics in soils. Payne et al. (2001) used 48 hr as the isotope (^{236}U) equilibration time to estimate the amount of accessible U in the Koongarra U deposit in northern Australia. Kohler et al. (2003) compared U extracted with a bicarbonate solution (2 weeks) and the isotopically exchangeable U in contaminated sediments measured after 1 week and 10 months: extracted U was very well correlated (with slopes of 1.22 and 0.996 for 1 week and 10 months of isotopic exchange, respectively) with the isotopically labile pool at both times.

Bond et al., (2007) measured the labile U(VI) pool in contaminated vadose zone sediments using the isotope exchange technique with ^{233}U(VI) tracer. The contaminated sediments were equilibrated first with artificial ground water then spiked with ^{233}U tracer. The ^{233}U(VI) tracer activity in a sediment suspension decreased rapidly during the first 48 hr, and then began to decrease at a slower rate that appeared to continue after 1350 hr of isotopic exchange. Um et al. (2010) split contaminated sediment into two size fractions (fine and coarse); samples were contacted with synthetic groundwater for 1 day, then spiked with ^{233}U and the labile ^{238}U was measured over a period of 30 days. The coarse sample showed no change in labile U concentration with time. The labile ^{238}U concentration in the fine sample increased at a relatively fast rate during the first 7 days, and then slowly increased with time to reach a steady state at 21 days.

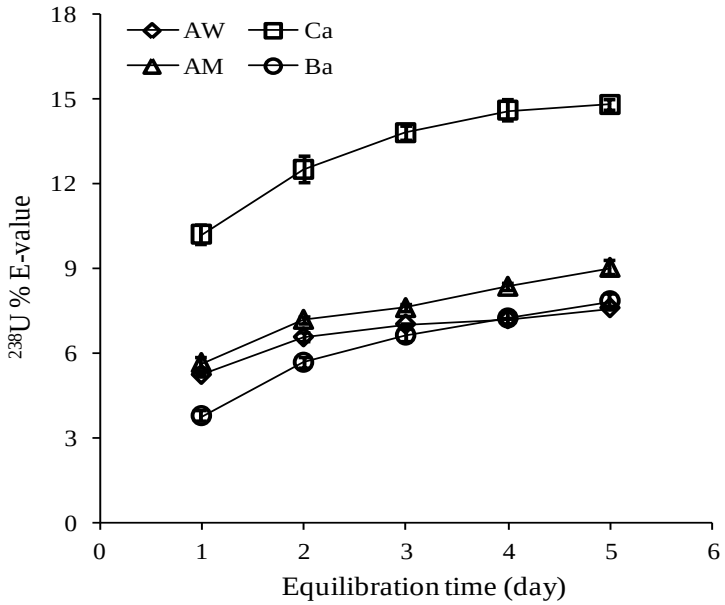

Figure 4.7: The E-value (%) as a function of equilibration time for four soils: Acidic Woodland (AW; ◊, pH 3.4, %LOI 3.2, U_{tot} 1.18 mg kg^{-1}), Calcareous (Ca; □, pH 7.2, %LOI 7.92, U_{tot} 1.25 mg kg^{-1}), Acidic Moorland (AM; Δ, pH 3.6, %LOI 15.9, U_{tot} 1.02 mg kg^{-1}) and Biosolid-amended soils (Ba; ○, pH 6.14, %LOI 19.7, U_{tot} 2.44 mg kg^{-1}). The error bars denote standard errors of three replicates.

Figure 4.7 shows the results of a preliminary experiment in which isotopic equilibration was determined over a period of 5 days for four soils with different characteristics. In all soils the U E-values were a minor proportion of the soil U content (3.8 – 14.8% of total soil U) but were highest in the calcareous soil. In all soils, the ^{238}U E-value increased between 1 and 5 days equilibration with the ^{233}U spike to a greater degree than normally seen for heavy metals such as Cd and Zn in soils (Young et al., 2000). It is not possible to determine unequivocally whether a gradual increase in E-value is due to progressive access of the spike isotope (^{233}U) to less labile pools (of ^{238}U) or whether there is a change in disposition of ^{238}U over the period studied, such as solubilisation due to Fe oxide reduction or $CaCO_3$ dissolution. In the case of the three acid soils there was virtually no change in ^{238}U solubility but an increase in ^{233}U adsorption; in the calcareous soil both processes were apparent. Because the results in Figure 4.7 indicate little practical change in E value after four days of contact with the spike-isotope (0.39, 0.20, 0.67 and 0.61% increase in E-value in acidic woodland, calcareous, acidic moorland and biosolid-amended arable soils, respectively), four days was adopted as the standard time for isotopic equilibration under aerobic conditions.

4.3.4 Effect of spike concentration and pH on ^{238}U E-value

It is difficult to generalize and use the same spike amount for different soils as the amount of spike required to make robust estimates of E-value depends on the soil properties controlling the partitioning of the tracer such as pH and soil organic matter content (Hamon et al., 2008). The amount of tracer isotope added to the soil must be sufficiently high to allow accurate determination of the isotope ratio or concentration in the solution extracted from the soil, but at the same time it must also be sufficiently low to minimize perturbation of the system's dynamic equilibrium. If a large amount of the spike isotope has been added, changes in the speciation of the element under investigation may take place; moreover, some of the isotope may undergo precipitation reactions and cease to participate in isotopic exchange reactions which, in turn, leads to an overestimation of the E-value. The acidity of the spike solution may affect the soil suspension pH and, hence, the measured metal lability. Gabler et al. (2007) and Sterckeman et al. (2009) reported that the effect of the spike solution pH on E-value can vary according to the soil composition, the soil buffering capacity and metal speciation. It has been recommended to use spike solutions with pH >4 (Sterckeman et al., 2009).

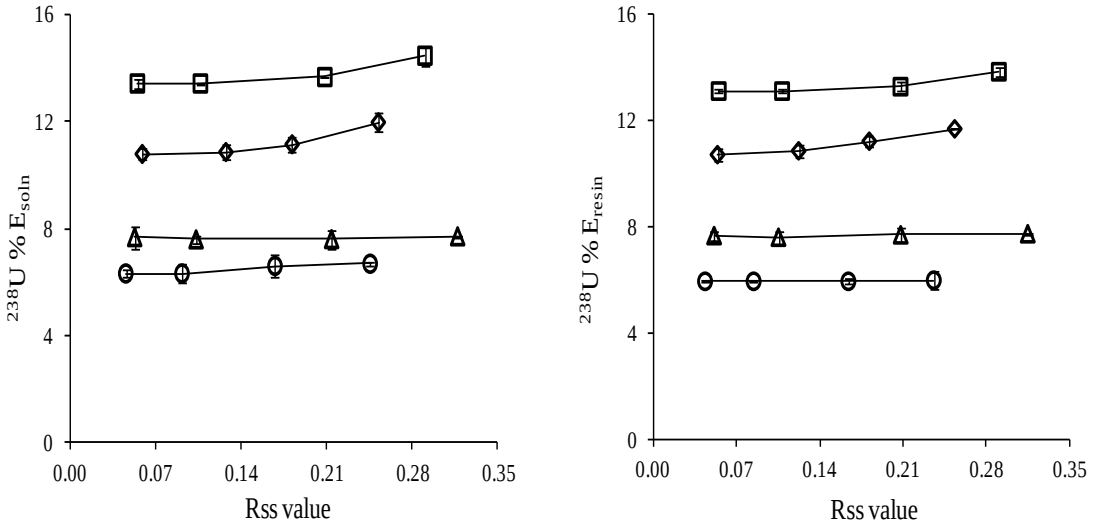

Figure 4.8: E-values as a proportion (%) of the total soil ^{238}U, measured in the solution (E_{soln}) or resin (E_{resin}) phases, as a function of the measured Rss value (isotopic ratio of the spike isotope ^{233}U to the native isotope in solution ^{238}U) in Arable (Ar; ◊), Calcareous (Ca; □), Acidic Moorland (AM; Δ) and Biosolid-amended (Ba; ○) soils. The error bars denote standard errors of % E-values for three replicates.

Figure 4.8 shows the effect of increasing the ^{233}U(VI) spike concentration on the assessment of ^{238}U E-value in four soils (Ar; arable, Ca; calcareous, AM; acidic moorland and Ba; biosolid-amended soils) with different characteristics from isotope ratios measured either in the solution (E_{soln}) or Chelex-100 resin phases (E_{resin}). The ^{238}U(VI) %E-values are presented as a function of the measured isotopic ratio in solution of the spike isotope (^{233}U(VI)) relative to that of ^{238}U(VI) isotope (Rss); Rss value increases with increased spike. There was a good agreement in %E-value at different spike concentrations across a range of soil properties. As shown in Figure 4.8, E-values appeared to be consistent across a range of spike concentrations. In Ca and AM soils the measured E-value increased slightly but not significantly with increasing Rss ($P = 0.07$ and 0.67 for Ca and AM soils, respectively), while in Ar and Ba soils, there was a significant effect of spike concentration on measured E-value ($P = 0.018$ and 0.038 for Ar and Ba soils, respectively). The change in E-value with Rss was not consistent in Ba soil and may be ascribed to the colloidal interferences from suspended humic acid or colloidal phosphate complexes in the soil suspension. This explanation appears credible because when a Chelex-100 resin purification step was used to eliminate submicron colloidal particles (SCP) interferences, the spike level no longer had a significant effect on E-value (E_{resin}) ($P = 0.17$). Increasing the amount of ^{233}U(VI) spike resulted in an increase in the Ar soil E-value (1.19% increase in the E-value at the highest spike level relative to the lowest one). Although pH values measured in the four soil suspensions at the minimum and maximum spike loadings were not significantly different ($P = 0.84$), the increase in arable soil E-value was consistent with the decrease in spiked soil suspension pH ($r = -0.96$ $p = 0.036$). Gabler et al. (2007) ascribed the decrease in soil suspension pH after the addition of the acidified spike solution to the soil sample buffering capacity and the amount of the spike added. However, the ^{233}U spike amount and volume added to the Ar soil were similar and slightly less than that added (from the same stock solution) to the Ba and Ca soils respectively; the decrease in pH value was more pronounced in the Ar soil (0.7 pH units comparing to 0.1 pH units in Ca, AM and Ba soils; Table 4.3). Therefore, the decrease in the Ar soil suspension pH might be attributed to the soil buffering capacity. With increasing the spike level, ^{233}U concentrations in spiked soil suspensions increased in the four soils with the same ratio. The concentration of ^{238}U(VI) was nearly constant in Ca, AM and Ba soils, but increased in the Ar soil

(from 13.1 to 19.7 ng l^{-1}) with increasing the spike level and the coincident decrease in soil suspension pH. The Ar soil E-value appeared to be less pH dependent than ^{238}U(VI) solution concentrations.

Table 4.3: Effect of different amounts of the spike solution on the soil suspension pH; pH was measured in the spiked soil suspension after equilibration time and prior to isolation of the supernatant phase.

Soil samples	pH in the spiked soil suspension			
	5% spike	10% spike	20% spike	30% spike
Ar	5.76	5.66	5.37	5.07
Ca	7.04	6.97	7.00	6.95
AM	3.13	3.11	3.06	3.05
Ba	5.95	5.93	5.89	5.84

The current results demonstrated that even a small amount of the spike isotope ^{233}U added to the soil suspension, equivalent to just 5% of the E-value, produced low uncertainty in the E-value (≤ uncertainty at high spike amounts) determination and allowed accurate detection of isotope ratios and concentrations. The effect of varying spike levels on ^{238}U E-value has not been investigated before. In the literature only a single concentration of U spike has been used. For example, Kohler et al. (2003) spiked contaminated sediments (10 g suspended in 200 ml artificial ground water) with 6 - 9 ×10^{-9} mol l^{-1} ^{233}U (0.5 - 0.75 Bq mL^{-1}) as uranyl nitrate, while Payne et al. (2001) spiked the Koongarra uranium deposit samples suspension with (10^{7} mol l^{-1}) ^{236}U. Previous U isotopic exchange studies have been performed on contaminated samples and the spike *activity* was measured rather than concentration or isotope ratio; therefore relatively high levels of U tracer isotopes were applied.

4.3.5 Non-isotopically exchangeable uranium in suspended colloidal particles (SCP-^{238}U): a comparison of E_{soln} and E_{resin}

Values of E_{soln} and E_{resin} were compared to determine whether submicron colloidal particles (SCP; < 0.2 µm) containing non-labile ^{238}U(VI) were present in the solution phase of soil suspensions and whether non-labile SCP-^{238}U(VI) was affected by soil properties. In theory, after washing, the Chelex-100 resin used in the purification step to determine E_{resin} (Section 2.6.4) contains only $^{238}UO_2^{2+}$ and $^{233}UO_2^{2+}$ from soluble ionic forms whereas submicron suspended colloidal particulate (SCP) forms are excluded. Thus, if non-labile SCP-^{238}U(VI) is present in the filtered (< 0.2 µm) solution from the equilibrated soil suspension used to determine E-values the value of E_{soln} should exceed that of E_{resin} ($E_{resin} < E_{soln}$). The two estimates of ^{238}U lability ($\%E_{soln}$ and $\%E_{resin}$) were significantly correlated (r = 0.996, P = 0.000) as shown in Figure 4.9, E_{soln} was, on average, only 2.2% higher than $E_{resin.}$ However, a paired T-test showed that the two ^{238}U lability estimates were significantly different (P < 0.001).

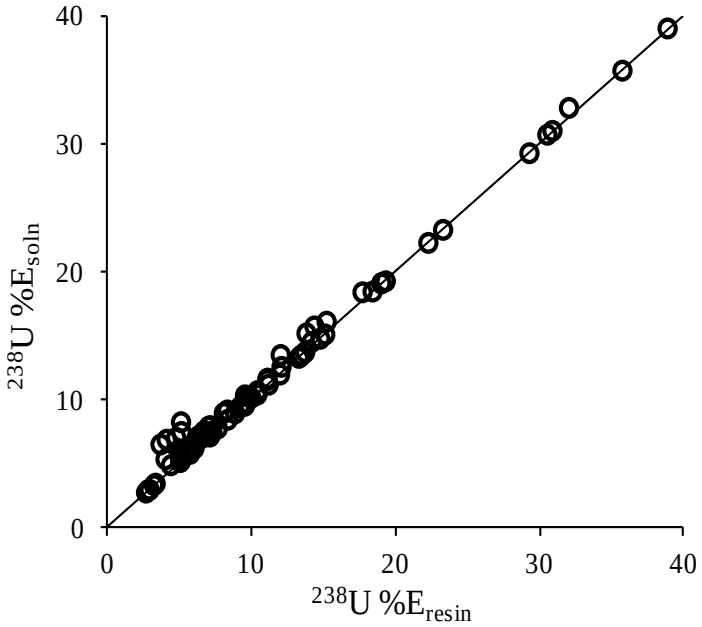

Figure 4.9: Comparison of the isotopically exchangeable ^{238}U pool measured as E_{soln} and E_{resin} for all soils (n=77). The solid line represents the 1:1 relation. The average standard errors for measurement of $\%E_{soln}$ and $\%E_{resin}$ were 0.22% and 0.29% respectively.

The ratio of $\%E_{soln}$: $\%E_{resin}$ as a function of $\%E_{resin}$ and soil pH is shown in Figure 4.10. The E_{soln} : E_{resin} ratio was larger and more variable at low $^{238}U(VI)$ lability (low $\%E_{resin}$; Figure 4.10). This trend is as expected because as the lability increases E_{soln} values will gradually approach those of E_{resin}. The largest difference between E_{soln} and E_{resin} was found in the biosolid-amended (Ba) soils from a sewage processing farm; E_{soln} was, on average, 20.3% higher than E_{resin}. For all other soils (Ar, AW, Ca, AM and BGSc), E_{soln} was on average only 1.55% higher than E_{resin}. At low soil pH, the E_{soln}:E_{resin} ratio approached a value of 1.0 (Figure 4.10); the smallest differences between E_{soln} and E_{resin} (in the range 0 - 1.5%) were observed in the AW (pH ≤3.78), AM (pH ≤4.32) and BGSc (pH<6.5) soils, which had the lowest pH values.

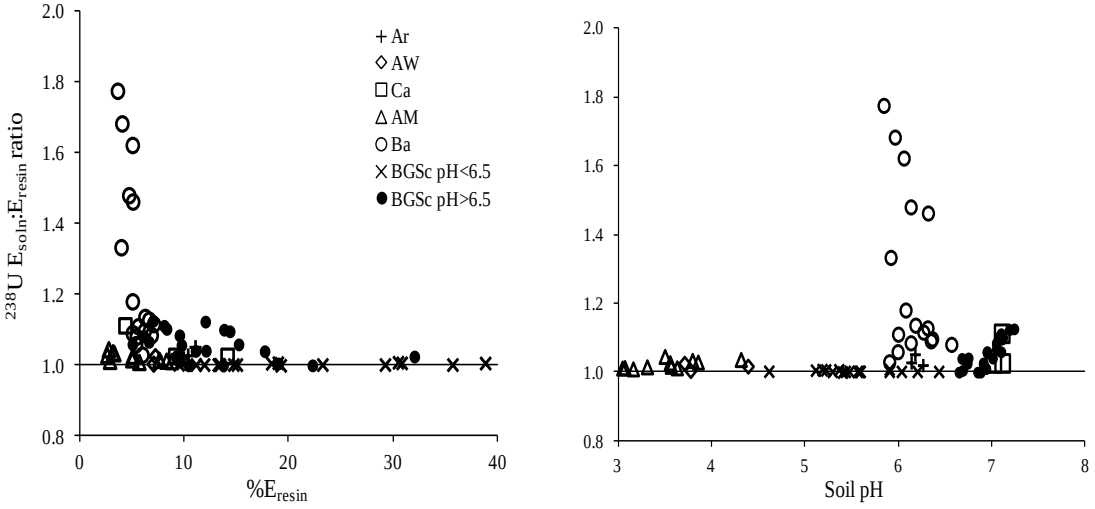

Figure 4.10: The ratio of E_{soln} : E_{resin} as a function of $\%E_{resin}$ (a) and soil pH (b) in Arable (Ar; +), Acidic Woodland (AW; ◊), Calcareous (Ca; □), Acidic Moorland (AM; Δ), Biosolid-amended (Ba; ○), BGSc pH<6.5 (×) and BGSc pH>6.5 (●) soils, (n = 77).

In the Ba soils, the presence of non-labile SCP-^{238}U was significantly related to P and DOC in the filtered soil solution (Table 4.4). These results tentatively suggest that 'nano-particulate' SCP-^{238}U might be associated with phosphate and organic colloids. Poorly soluble uranyl phosphates, like sodium meta-autunite, may form negatively charged stable colloids at neutral-alkaline conditions that can enhance U transport in contaminated sediment (Zheng et al., 2006; Singh et al., 2010). For the remaining soils (Ar, AW, Ca, AM and BGSc), with increasing soil pH the values of E_{soln} exceeded those of E_{resin} (Figure 4.10) and the ratio of E_{soln}:E_{resin} was significantly positively

correlated with pH and DIC (Table 4.4). This agrees with the observation that SCP-bound metals such as Zn and Cu are more mobile at high pH (Kaplan et al., 1996; Oste et al., 2001; Lombi et al., 2003; Marzouk et al., 2013) and could indicate the presence of U within carbonate colloids. Nevertheless, the overall results suggest that measuring E_{soln} will lead to only a small overestimation of the true E-value, even in soils with high pH and carbonate contents. In soils with exceptionally high phosphate and well humified organic matter contents, there appears to be a greater presence of non-labile SCP-U.

Table 4.4: Correlation coefficients (r) between E_{soln}:E_{resin} ratio and selected properties of the filtered (< 0.2 µm) soil solutions (n = 17 for Ba soils and n = 60 for all other soils); P-values are in brackets.

Soil variable	E_{soln} : E_{resin} ratio	
	Biosolid-amended soils (Ba)	All other soils (Ar, AW, Ca, AM, BGSc)
P	**0.87 (0.000)**	0.19 (0.146)
pH	-0.41 (0.099)	**0.57 (0.000)**
DOC	**0.54 (0.025)**	**-0.29 (0.026)**
DIC	-0.72 (0.001)	**0.48 (0.003)**
SOM	**0.78 (0.000)**	-0.08 (0.527)

4.3.6 The effect of soil properties on ^{238}U(VI) lability (E-value)

The E-value for $^{238}UO_2^{2+}$ ranged from 2.7 to 39.1 % of the total soil ^{238}U content in the soil samples studied (n = 77). The average (± std. dev.) E-value in each soil category in the first soil set (Figure 4.11) followed the order: AM (5.1±0.09%) < Ba (6.7±0.13%) < AW (8±0.16%) < Ca (9.6±0.23%) < Ar (10.8±0.3%). For the BGSc soils (n = 40) %E-values ranged from 5.3 to 39.1% (mean = 16.1±8.2%) but there was no information about the land use and so the soil set was divided into two subsets according to the soil pH measured in 0.01 M $Ca(NO_3)_2$ soil suspension: pH<6.5 (4.62 – 6.44; n = 17) and pH>6.5 (6.65 – 7.24; n = 23). The %E-values in these two subsets were 19.5±8.5% (pH<6.5) and 13.6±7.1% (pH > 6.5) respectively (Figure 4.11).

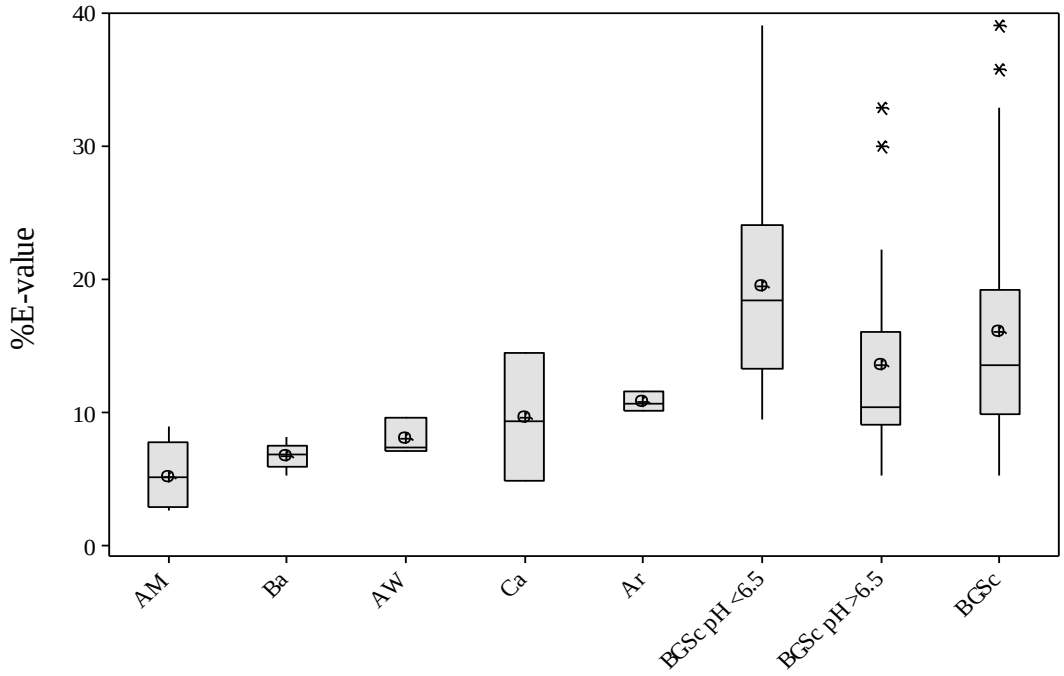

Figure 4.11: Box and whisker plot showing $^{238}U(VI)$ %E-value for AM (n= 11), Ba (n = 17), AW (n=3), Ca (n=3), Ar (n=3) and BGSc (n=40) soils. The box and whisker plot shows median (horizontal lines) and mean (open cross symbols) values for the soils. The box confines the upper boundaries of the first and third quartiles, the upper and lower whiskers extend to the highest and lowest data point respectively within 1.5 box heights (of the box); outliers beyond the whiskers are also shown as asterisk symbols.

Figure 4.11 shows a wider range of U lability in the calcareous (Ca) soil than in other ecosystems (AM, Ba, AW, Ar); although the three Ca surface soils had the same parent material the land use and/or soil characteristics appear to affect the U lability. There was a greater proportion of labile U in acid moorland (AM) and acid woodland (AW) topsoils than in subsoils producing a significant correlation for %E-value with SOM in both soils ($r = 0.81$, $P < 0.001$). Unlike AM and AW soils, the variation in U lability with soil depth in the arable soil (Ar) was small, ranging from 10.2% at the soil surface (0 - 14 cm) to 10.7% at 30 cm depth; this was probably a consequence of the long-term application of phosphate fertilizers and accumulation in the surface layers of the arable soil (see Chapter 3 for details). Although the biosolid-amended soils (Ba) showed some indication of U enrichment (Section 4.3.1), they exhibited lower UO_2^{2+} lability and a very restricted range of %E-values. This may be attributed to their extremely high phosphate concentrations and relatively constant pH resulting from an on-site liming policy to increase and maintain a limited range of soil pH values, around pH 6.5.

Table 4.5: Correlation coefficients (r values) between %E-value or E-value (mg kg^{-1}) and selected soil properties (n = 77). Significant values are shown in bold italic where P-value is <0.05.

	Soil variable								
	pH	%SOM	Avail-P	FeOx	AlOx	MnOx	%Clay	Total U	$\%CaCO_3$
%E-value	0.19	***0.25***	***-0.33***	***0.65***	**0.28**	***0.31***	***0.31***	***0.53***	0.02
	>0.05	***<0.05***	***<0.01***	***<0.001***	**<0.05**	***<0.01***	***<0.01***	***<0.001***	>0.05
E-value	0.024	***0.47***	-0.13	***0.36***	***0.32***	0.20	0.20	***0.82***	-0.14
(mg kg^{-1})	>0.05	***<0.001***	>0.05	***<0.01***	***<0.01***	>0.05	>0.05	***<0.001***	>0.05

Total soil metal concentration and FeOx content were found to be highly significantly correlated with %U lability as shown in Table 4.5, while MnOx, AlOx, %clay and %SOM were relatively weakly correlated with %U lability. Available-P was the only measured soil variable which was negatively correlated with %U lability. Many studies have reported the importance of hydrous iron oxides for the adsorption of U (Hsi and Langmuir, 1985; Waite et al., 1994; Duff and Amrhein, 1996; Payne et al., 1996; Lenhart and Honeyman, 1999). Sowder et al. (2003) and Vandenhove et al. (2007a) reported that positively charged U-species are surface-adsorbed on the oxides' negatively charged surfaces; it has also been suggested that U-species become incorporated into the amorphous or poorly crystalline iron oxides over the dissolution/precipitation cycles of soil oxide coatings. In addition, UO_2^{2+}-phosphate interactions are important in controlling UO_2^{2+} mobility in both natural and polluted environments (Cheng et al., 2004; Phillips et al. 2007; Singh et al., 2010). Vandenhove et al. (2007a) studied the effect of soil properties on the soil solution U concentration for ^{238}U spiked soils and ascribed the decrease in soil solution U concentration and availability in the presence of phosphates to precipitation reactions; formation of uranyl phosphate precipitates as autunite-group $\{(X^m)_{2/m}[(UO_2)(PO_4)]_2 \cdot xH_2O\}$ which is important because of its low solubility, slow dissolution kinetics and a wide range of cation substitution (e.g. Na, Mg, Cu, Ba) (Del Nero et al., 1999; Koch-Steindl and Pröhl, 2001; Zheng et al., 2006) or enhanced U sorption by the formation of ternary surface complexes involving both UO_2^{2+} and PO_4^{3-} (Payne et al., 1996). At low pH, U adsorption to iron oxides is not sufficient to retard U mobility and transport. Moreover, carbonate effects are less significant than at high pH, but U and phosphates can precipitate (Langmuir, 1997) forming a wide

range of uranyl phosphate solids which are less soluble than schoepite, especially at low pH (Singh et al., 2010). This may explain the observed negative correlation between %E-value and available-P concentration in the current study. As clay minerals and organic matter provide exchange sites, they are expected to increase sorption of the uranyl cation UO_2^{2+} and other positively charged U species (Vandenhove et al., 2007a). It might be expected that such fractions contribute mainly to the labile U pool.

The effect of soil pH on ^{238}U(VI) lability (E-value)

In the current dataset, no significant correlation was found between soil pH and U lability (Table 4.5). Figure 4.12 shows the relationship between %U lability and soil pH for the two soil datasets. There are two contradictory trends in lability with soil pH: whereas U labilities in Ar, AW, Ca, AM and Ba soils were positively correlated with pH ($r = 0.38$, $P < 0.01$), U labilities in the BGSc soils were negatively correlated with pH ($r = -0.423$, $P < 0.01$). The two BGSc soils with the highest values of %U lability (39.1 and 36%) and low pH values (5.3 and 5.23) also had the highest values for %SOM (50%) and FeOx (65 g kg^{-1}), respectively. By contrast, in the very acidic moorland and woodland soils (AM and AW), although the change in pH with soil depth was not clear, %U lability decreased substantially with soil depth producing a correlation with SOM. Therefore it appears that soil pH may not have been the most important characteristic for U lability and co-variance with other soil properties such as adsorption phases may control and explain the variance in U lability.

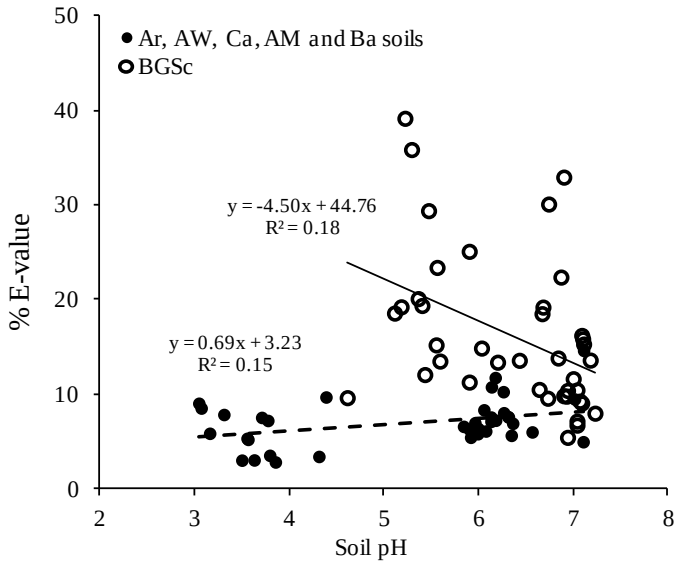

Figure 4.12: Relationship between ^{238}U(VI) %E-value (% of total U content) and soil pH for Ar, AW, Ca, AM, Ba (●; n = 37) and BGSc (○; n = 40) soils.

The effect of soil total U content on ^{238}U(VI) lability (E-value)

The trend in metal lability with total soil metal content depends on whether the soil metal is (i) associated with primary or secondary minerals or (ii) bound to the soil surface adsorption sites, which may give rise to contradictory trends in lability with total metal content. If soil metal content is bound to the surface adsorption sites, a positive correlation between %E-value and metal content would be expected. In contrast, if total U content is bound to primary or secondary minerals, a negative correlation between total U content and %E-value would be expected. This means that even if the E-value is completely randomly distributed, some degree of negative correlation between %E-value and total metal content would be produced. In the current study, the range of total U concentration was quite small (0.7 – 12.6 mg kg^{-1}) with only two samples above 5.6 mg kg^{-1}: 11.5 and 12.6 mg kg^{-1}. A weak positive correlation was found between %E-value and total U concentration in the soils studied (Figure 4.13a, Table 4.5); this is likely to be the result of U enrichment in some soils, producing labile UO_2^{2+} bound to adsorption sites. To examine the trend for soils apparently enriched with U, data for soils with a U/Th ratio ≥ 0.4 were examined separately: the ^{238}U(VI) %E-value as a function of total soil U content for these soils is shown in Figure 4.13b and shows a strongly positive correlation ($r = 0.85$, $P < 0.001$).

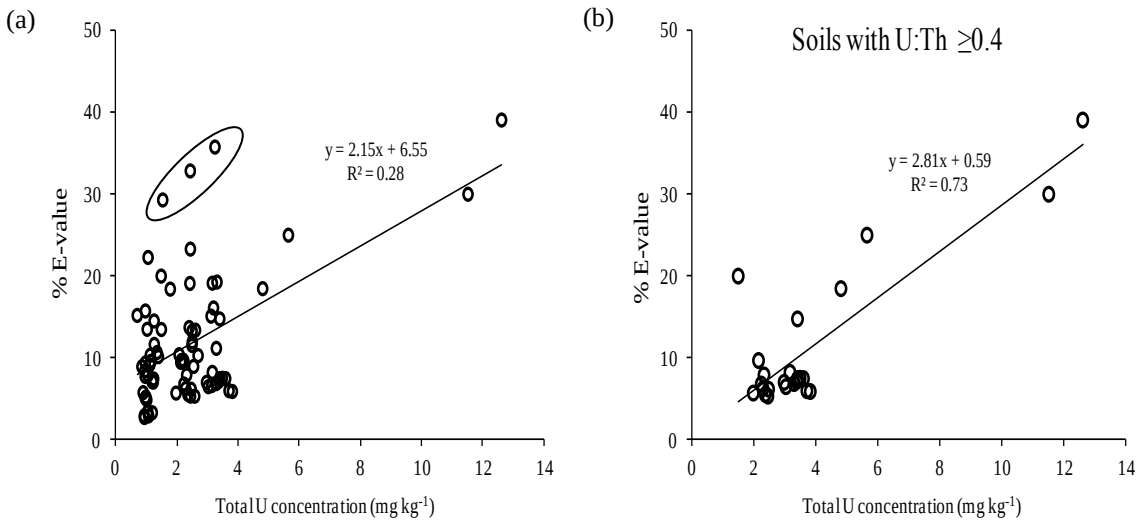

Figure 4.13: Relationship between ^{238}U(VI) %E-value (% of total U content) and total soil U concentration (mg kg^{-1}) in all soils studied (a; n = 77) and only soils with U/Th ratio greater than 0.4 (b; n =24).

In some of the soils with no sign of U enrichment (U/Th ≤0.3) %E-value also increased with total U concentration; these soils (n = 3) had relatively large FeOx concentrations (>45 g kg^{-1}). The values of %U lability were also found to be significantly correlated with FeOx concentration across the entire data set, as shown in Figure 4.14.

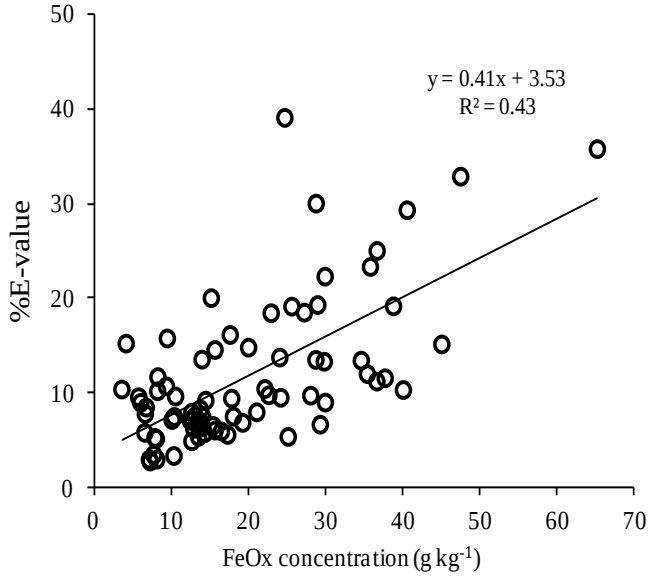

Figure 4.14: Relationship between ^{238}U(VI) %E-value (% of total U content) and FeOx concentration (g kg^{-1}) in the soils studied (n = 77).

4.3.7 Multiple linear regression model to predict U lability

Stepwise regression was used to model the isotopically exchangeable ^{238}U pool as a function of the soil variables thought most likely to affect U availability in soils (Equation 4.1): total U content (U_{tot}, mg kg^{-1}), pH, %SOM, available phosphate (P, mg kg^{-1}), %clay and Fe, Al, Mn-oxide concentrations (g kg^{-1}). The stepwise regression was implemented by incremental inclusion of the independent variables in the model, setting the condition for inclusion that the t-value (the coefficient of the predictor divided by the standard error of the coefficient) was greater than 1.0. Through this process pH, %clay, Al and Mn-oxide concentrations were eliminated as non-significant predictors when applied to the whole dataset; Table 4.6 shows the resulting values of the optimised coefficients, t-value, P-value, standard deviation error of the estimates (S) and R^2 associated with combinations of the soil parameters in Equation 4.1. The fit of the model is indicated by the residual standard deviation (RSD) between measured and predicted %E-values and the correlation coefficient (r).

Table 4.6: Results of multiple stepwise regression to predict %E-value from FeOx (g kg^{-1}), %SOM, available-P concentration (mg P kg^{-1} soil) and total U concentration (mg kg^{-1}). Regression coefficients (k_0, k_1, k_2, k_3 and k_4; Equation 4.1), P values, and goodness of fit parameters; RSD and correlation coefficient (r value, predicted vs measured %E-value) are shown in the table.

	Constant *(K_0)*	FeOx (k_1)	%SOM (k_2)	Avail-P (k_3)	Total U (k_4)
Coefficient	1.18	0.34	0.33	-0.022	0.91
t-value		6.97	4.64	-5.17	2.75
P-value		0.000	0.000	0.000	0.007
S		5.86	5.27	4.61	4.41
R^2		42.33	54.05	65.35	68.64
RSD			4.35		
r			0.86		

Together, the soil variables (Fe-oxide, %SOM, available-P and Total U concentration) explained 68.6% of the variance in the isotopically exchangeable U (Table 4.6). Figure 4.15 shows that the predicted U lability was in reasonable agreement with the measured values (r = 0.86 and RSD = 4.35%).

The performance of multiple regression model used to predict %E-values might be improved by including further soil variables, such as cation exchange capacity (CEC). For example, Vandenhove et al. (2007a) applied a multiple linear regression model to predict soil solution U concentration and found that including soil solution K concentration and exchangeable Mg and Ca improved the model prediction. At the same time the authors acknowledged that the complex data requirements of such models make them difficult to apply in predictive modelling.

In the current study, it was found that Fe-oxide content had the most significant effect on %E-value prediction and accounted for the largest proportion of total variance in %E-value (42.3%), followed by SOM (11.7%) and available-P (11.3%). Pett-Ridge et al. (2007) reported that adsorption on amorphous Fe-oxides is the dominant control on U mobility in soils due to their high surface area and sorption capacity and their ubiquity as grain coatings. Phillips et al. (2007) found a positive significant correlation between U and Fe, Al and Mn oxides extracted by 2 M nitric acid from fractured shale under field conditions. Although total soil U concentration provided a significant contribution to %E value prediction ($P < 0.01$) in the current dataset, it only explained 3.3% of the total variance in predicting %E-value. The improvement achieved by including total U in the model was most pronounced in soils with U/Th radio >0.4 which again supports the hypothesis that (non-geogenic) added UO_2^{2+} occupies labile sites. The relatively low dependence of %E-value on total soil U concentration for most soils in this study is probably due to the absence of (a range of) external U sources. Rodrigues et al. (2010) used 0.43 M HNO_3 to assess the chemically reactive pool of a broad range of toxic elements, including U, in 136 polluted and non-polluted soils and found that total U concentration provided a good prediction of U reactivity. The inclusion of pH and %clay in the regression model did not improve the model performance, while including % organic carbon improved the prediction of U reactivity, indicating the large sorption capacity of soil organic matter for U.

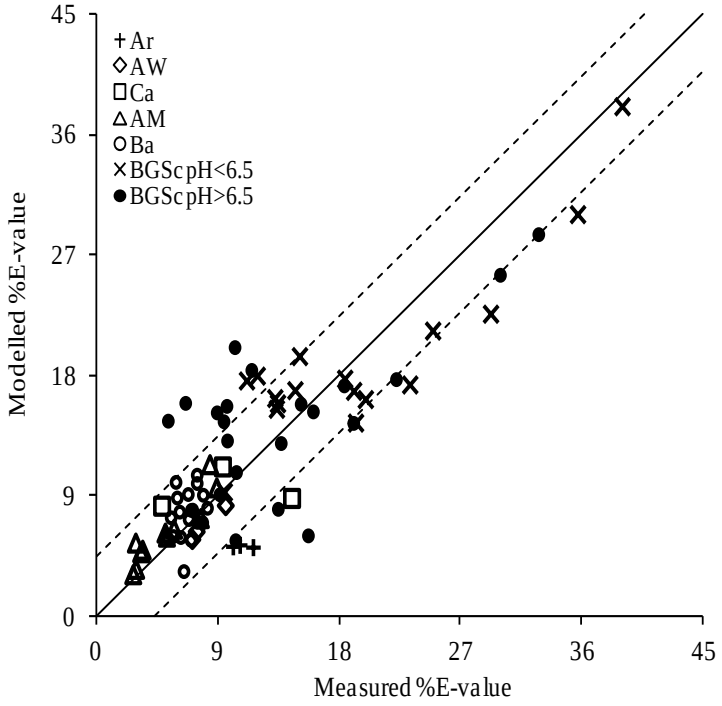

Figure 4.15: Predicting ^{238}U lability (%E-value) from soil variables; FeOx content, %SOM, available-P and total metal concentration;

%E-value = k_0 + k_1 (FeOx) + k_2 (%SOM) + k_3 (available-P) + k_4 (Total U)
for Arable (Ar; +), Acidic Woodland (AW; ◊), Calcareous (Ca; □), Acidic Moorland (AM; Δ), Biosolid-amended (Ba; ○), BGSc pH<6.5 (×) and BGSc pH>6.5 (●) soils, (n = 77). The solid line is the 1:1 relation and dashed lines represent the 1:1 line ± RSD.

4.3.8 Comparison of isotopically exchangeable U with chemically extracted fractions

In this section isotopically exchangeable ^{238}U is compared with the amount of U extracted by four single extraction methods using the following reagents: 1.0 M CH_3COONH_4, 0.05 M EDTA, 0.43 M HNO_3 and 1% TMAH. Figure 4.16 shows a comparison of ^{238}U %E-values with the proportion (%) of U extracted by each method averaged for each of the five soil groups in the first set of soils and also for the BGSc (pH<6.5 and pH >6.5) soils. The amounts of U solubilised by the four extractants were significantly different between soil groups ($P < 0.001$). Thus E-values for UO_2^{2+} did not correspond consistently with any single chemical extraction procedure although the degree of correspondence was soil-dependent.

Ammonium acetate extracted uranium; U_{Ac}

Ammonium acetate extracted the least U: 0.9% of total soil U content on average. This extractant has been used to predict plant uptake of U (Sheppard and Evenden, 1992). It is likely that NH_4^+ displaces only exchangeable UO_2^{2+} although CH_3COONH_4 may also have a small solubilizing effect on specifically adsorbed U through changes in ionic strength and weak complex formation with acetate.

EDTA extracted uranium; U_{EDTA}

Extraction with EDTA released more U than CH_3COONH_4 by an average factor of 1.45. However, although EDTA is widely known as a powerful extractant for many cationic metals in soils (Rauret, 1998; Degryse et al., 2009) the stability constant ($\log_{10}$ value) for a 1:1 EDTA-UO_2^{2+} complex is only 7.4 which is extremely low compared to the Ca-EDTA complex ($\log_{10}K = 10.7$). Furthermore, the presence of the EDTA-$U^{VI}O_2$ complex is limited above pH 6.5 due to formation of U-hydroxyl and carbonate species (Francis et al., 2000). Thus, extraction with both ammonium acetate and EDTA underestimated the E-value, on average dissolving only 7.3% and 10.5% of the isotopically exchangeable U across all the soils. Elias et al. (2003) found that 1 M $NaHCO_3$ at pH 8.3 was a more effective extractant for U(VI) than the organic complexing agents Na-EDTA and Na-citrate in several types of contaminated

sediment. This is probably a consequence of the high stability and solubility of uranyl carbonate complexes compared to U-EDTA and U-citrate complexes.

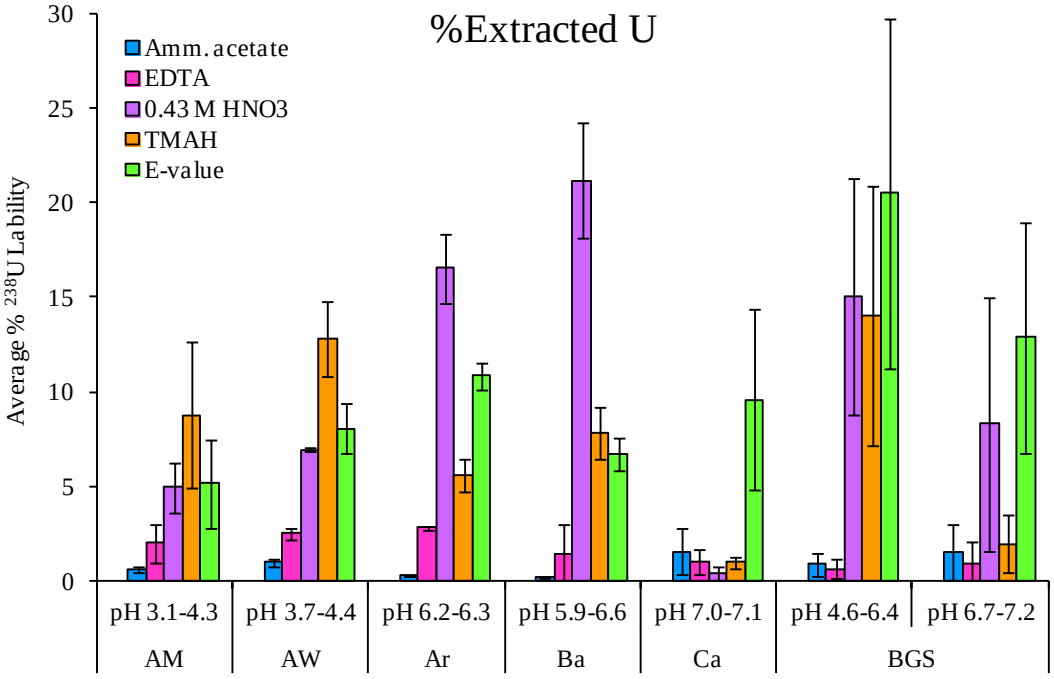

Figure 4.16: Comparison of the isotopically exchangeable U pool with chemical extraction using 1 M CH_3COONH_4, 0.05 M EDTA, 0.43 M HNO_3 and 1% TMAH. The error bars show the standard deviation within each group of soils.

Nitric acid extracted uranium; U_{Nit}

On average, across the whole range of soils studied the strong acid extractant, 0.43 M HNO_3, overestimated the E-value by 4%. With the exclusion of biosolid-amended and arable soils (Ba and Ar), 0.43 M HNO_3 underestimated the E-value, releasing on average 73% of the isotopically exchangeable U across the range of soils studied. The value of U_{Nit} was very similar to the E-value (U_E) for AW and AM soils below pH 5 ($r = 0.85$, $P < 0.01$) (Figures 4.16 and 4.17a) and therefore extraction with 0.43 M HNO_3 might be suitable for acidic and organic woodland soils, as suggested by Tipping et al. (2003).

Nitric acid extraction overestimated the E-value in the Ba soils (by an average factor of 3.2) and arable (Ar) soils (by an average factor of 1.5). For both soil groups combined U_{Nit} was significantly correlated with extracted phosphate ($r = 0.92$, $P <$

0.01). The Ba soils contained extremely large amounts of phosphate from over a century of sewage sludge application, while the Ar soils were enriched with P from long term application of phosphate fertilizers (see Chapter 3 for details). Takeda et al. (2006b) used eight chemical extraction methods to investigate the extractability of 28 elements including U in 16 arable soils and found that the average % U extracted by 1 M HNO_3 (43.5% of total U) and 0.1 M HNO_3 (6.8%) were both higher than the proportion extracted by 1 M ammonium acetate (1.3%) and 0.05 M EDTA (0.73%). Langmuir (1997) reported that uranyl phosphates may accumulate in soils below pH 7 while Singh et al. (2010) suggested that U forms surface complexes with secondary phosphate phases such as hydroxyapatite. It is also thought that phosphate may increase U(VI) adsorption to Fe^{III} oxides by the formation of uranyl–phosphate–Fe(III) oxide ternary surface complexes (Payne et al., 1996; Cheng et al., 2004; Singh et al., 2010). Arey et al. (1999) used sequential extraction to investigate the ability of hydroxyapatite to immobilize U(VI) in two contaminated sediments. They showed that apatite addition transferred significant amounts of highly labile U to less labile phases. The authors attributed this to the precipitation of secondary phosphate phases which can be extracted under acidic conditions (0.01 M $NH_2OH.HCl$ + 0.1 M HNO_3, pH 1.26; sequential extraction step) that favour phosphate dissolution. Takeda et al. (2006a) showed a link between soil U content and phosphate fertilizer application to cultivated andosols, by comparison with neighbouring non-agricultural soils.

TMAH extracted uranium; U_{TMAH}

The alkaline extractant (TMAH) underestimated the E-value, on average dissolving 63.3% of the isotopically exchangeable U across all the soils (Figures 4.16 and 4.17b). This underestimation was most pronounced in calcareous (Ca) soils and in the BGSc soils with pH >6.5. TMAH is expected to dissolve all organically complexed UO_2^{2+}, by solubilising flocculated humic and fulvic acids, and therefore U_{TMAH} was just slightly higher than E-values in the AW, AM and Ba soils (Figures 4.16 and 4.17b). However, TMAH appeared to underestimate E-value in the Ar and BGSc soils and, in common with all the other extractants, in the Ca soils.

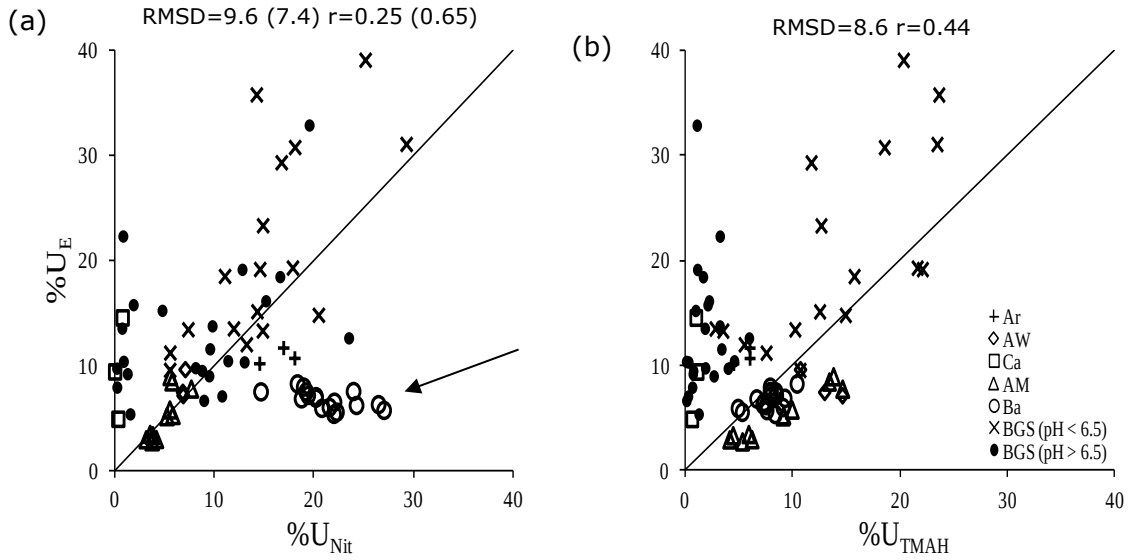

Figure 4.17: Relationships between isotopically exchangeable ^{238}U ($\%U_E$) and (a) U extracted with 0.43 M HNO_3 ($\%U_{Nit}$) and (b) 1% TMAH ($\%U_{TMAH}$). Soils include Arable (Ar; +), Acidic Woodland (AW; ◊), Calcareous (Ca; □), Acidic Moorland (AM; Δ), Biosolid-amended (Ba; ○), BGSc pH <6.5 (×) and BGSc pH >6.5 (●) groups, (n = 77). The numbers in parentheses in (a) show the RMSD and r values if Ba soils (indicated by the arrow) are excluded. The solid line represents the 1:1 relationship.

On average, over all groups of soils, CH_3COONH_4, EDTA and TMAH underestimated E-value by factors of 13.7, 9.5 and 1.6, respectively, while HNO_3 overestimated E-value by only a factor of 1.04. The percentage of uranium extracted by all four extractants fell considerably below the E-value in the calcareous soils. Although 0.43 M HNO_3 gave the best estimate of E-value overall, the $\%U_E$ correlation with $\%U_{TMAH}$ was higher than with $\%U_{Nit}$ and the root mean square difference (RMSD) was smaller for $\%U_{TMAH}$, because the data were in general closer to the 1:1 line, as shown in Figure 4.17a and b. For Ba soils, in particular, the difference between U_E and U_{Nit} was large, and excluding these soils strongly increased the correlation coefficient and decreased the RMSD (Figure 4.17a) between $\%U_E$ and $\%U_{Nit}$.

The ratio of ^{238}U E-value to U extracted by HNO_3 (U_E:U_{Nit}) as a function of soil carbonate content and soil pH

Figure 4.18a and b shows the ratio of U_E to U_{Nit} as a function of the soil carbonate content and soil pH. The results suggest that soils with carbonate content higher than 2% will show large deviations between isotopically exchangeable U and U_{Nit}. Except for one soil (indicated by the arrow; Figure 4.18a) with 9.6% carbonate content and pH 7.12, the deviation between U_E and U_{Nit} was high for soils with >2% carbonate content. This may be attributed to the high organic matter content (39%) in this soil; most of the reactive UO_2^{2+} may be bound to the soil organic matter rather than association with $CaCO_3$. Although the deviation between U_E and U_{Nit} was high at pH >7 (Figure 4.18b), the ratio of U_E:U_{Nit} for soils with pH >6.5 was not significantly correlated with soil pH, but highly significantly correlated with carbonate content. For example, isotopically exchangeable U was close to U_{Nit} for some soils with pH >7 and <2% carbonate content. These results contradict previous observations that 0.43 M HNO_3 overestimated the isotopically exchangeable metal fraction (Zn, Ca, Pb) in calcareous soils due to the mobilization of the non-labile metal pool by dissolving carbonate binding phases (Degryse et al., 2009; Marzouk et al., 2013).

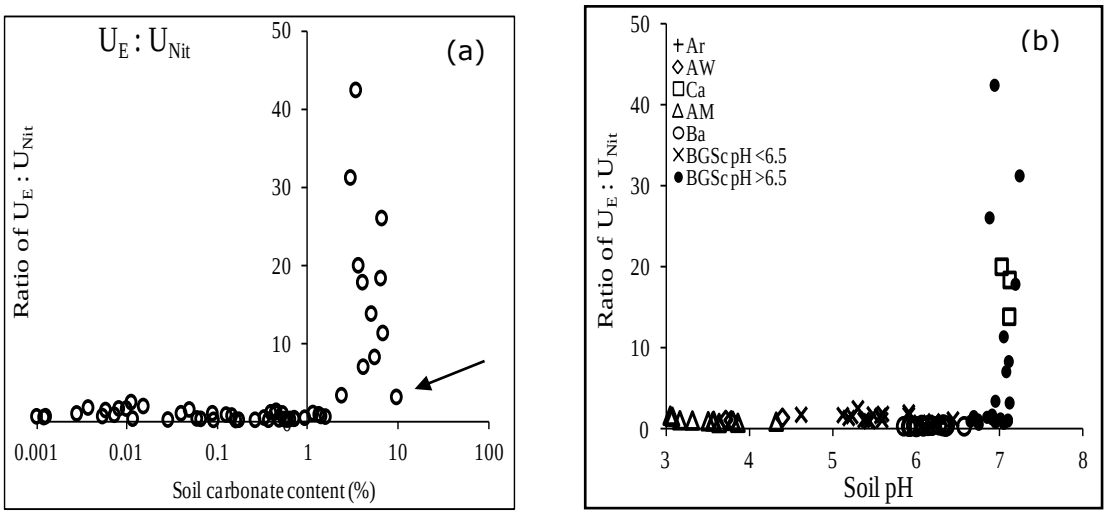

Figure 4.18: Ratio of ^{238}U E-value to U extracted by HNO_3 (U_E:U_{Nit}) as a function of (a) soil carbonate content (%) (note the logarithmic scale on the x axis) and (b) soil pH. Soils include Arable (Ar; +), Acidic Woodland (AW; ◊), Calcareous (Ca; □), Acidic Moorland (AM; Δ), Biosolid-amended (Ba; ○), BGSc pH <6.5 (×) and BGSc pH >6.5 (●) groups.

Flaws in the E-value protocol and chemical extraction methods

The high E-value measured in Ca soils compared to the four estimates of extractable U may highlight a flaw in the E-value protocol or the lack of specificity of chemical extractants and a substantial dependency of chemical extractants on soil properties. The flaw in the E-value protocol may be attributed to one, or more, of at least three possible mechanisms, all of which would tend to increase the apparent E-value: (i) precipitation of the spike isotope (^{233}U) immediately following addition to the soil suspension (ii) migration of the ^{233}U spike into more slowly reacting pools of ^{238}U in calcareous soils over the four day equilibration period compared to the short chemical extraction period allowed (2 – 4 hr) or (iii) dissolution of native ^{238}U from the slightly acidifying effect of adding the ^{233}U spike. The low recovery of U_{Nit} in the Ca soils would suggest that the final problem listed is perhaps unlikely. In addition, the effects of spike concentration and pH on E-value were studied (Section 4.3.4) for four soils, including a Ca soil and it was found that neither the amount of spike, nor pH value, produced a statistically significant effect on measured %E-value. Ammonium acetate and EDTA underestimated the E-value in all soil groups. TMAH dissolves the organically-complexed U but organic matter is not expected to be the major U-binding phase in most calcareous soils; U is more likely to be bound to the carbonate and Fe-oxide binding phases. Furthermore, the high pH value produced by TMAH is likely to increase UO_2^{2+} binding to Fe oxides which may offset solubilisation as carbonate and humic complexes - this may explain why $U_{TMAH} < U_E$. The underestimation of U_E by extracting U_{Nit} in calcareous soils may be explained if the relatively short time of soil equilibration with HNO_3 (2 hr) was insufficient to extract all labile U fractions from soil binding phases. For example, Marinussen et al. (1997a and b) used extraction with 0.43 M HNO_3 for 20 hr to assess the fraction of extractable heavy metals in soils. To confirm this explanation, the proportion of U_{Nit} was determined as a function of equilibration time (2, 4, 6, 16, 24, 48, 72, 96, 120 hr; Section 4.2.4) in six different soils including 3 calcareous soils (Ca-Ar, Ca-W, Ca-G) with carbonate content ≥ 6% as shown in Figure 4.19a. For calcareous soils, U_{Nit} increased with equilibration time; this was most pronounced in the calcareous-grassland (Ca-G) soil. In the calcareous arable (Ca-Ar), woodland (Ca-W) and grassland (Ca-G) soils, the fraction of U_{Nit} increased by factors of 5.1, 5 and 112, respectively, over the 120 hr equilibration time; U_{Nit} increased by ≥80% after 16 hr. Although U_{Nit} increased with equilibration time,

the maximum extracted amount at 120 hr still represented only 28, 36, and 36% of U_E in the Ca-Ar, Ca-W and Ca-G, respectively. In contrast to calcareous soils, in acidic soils (pH <6; AW, AM, Ba) U_{Nit} only slightly increased with time in AW and AM soils and was fairly constant in the Ba soil (Figure 4.19a). Figure 4.19b shows the soil pH measured in HNO_3 soil suspension as a function of equilibration time. For acidic soils, the pH dropped directly (at 2 hr) to the pH of the nitric acid extractant (pH 0.5) and remained constant over the equilibration time, U_{Nit} was not correlated with the pH value of the acidic soils. However, for the calcareous soils the pH values of the HNO_3 soil suspensions were high (pH 5.4 on average) and increased with equilibration time from 4.9 at 2 hr to 5.7 at 120 hr. In calcareous soils U_{Nit} was significantly correlated with soil pH ($r \geq 0.96$ $P < 0.001$). This contrast between calcareous and acidic soils must be attributed to the buffering capacity of soil carbonates. At the pH values of the Ca soil suspensions in 0.43 M HNO_3, it is likely that UO_2^{2+} initially released from dissolved carbonate phases was then substantially re-adsorbed by humus and Fe oxides. This represents a major flaw in the nitric acid extraction scheme when applied to calcareous soils. Similarly, Rodrigues et al. (2010) reported that 0.43 M HNO_3 extraction is an easy, rapid and reproducible method with limitations in the application to calcareous soils (>10% lime) due to the large buffering capacity of $CaCO_3$. To conclude, adaptation of the 0.43 M HNO_3 extraction method according to the initial soil carbonate content, possibly involving adjustment of the pH during extraction and minimizing the solid to liquid ratio, may be necessary to achieve consistent results. The mode of operation of the HNO_3 extraction protocol is entirely due to changes in pH value and so, because soils differ in the suspension pH values produced depending on their buffer capacities and initial pH values, the method is intrinsically flawed.

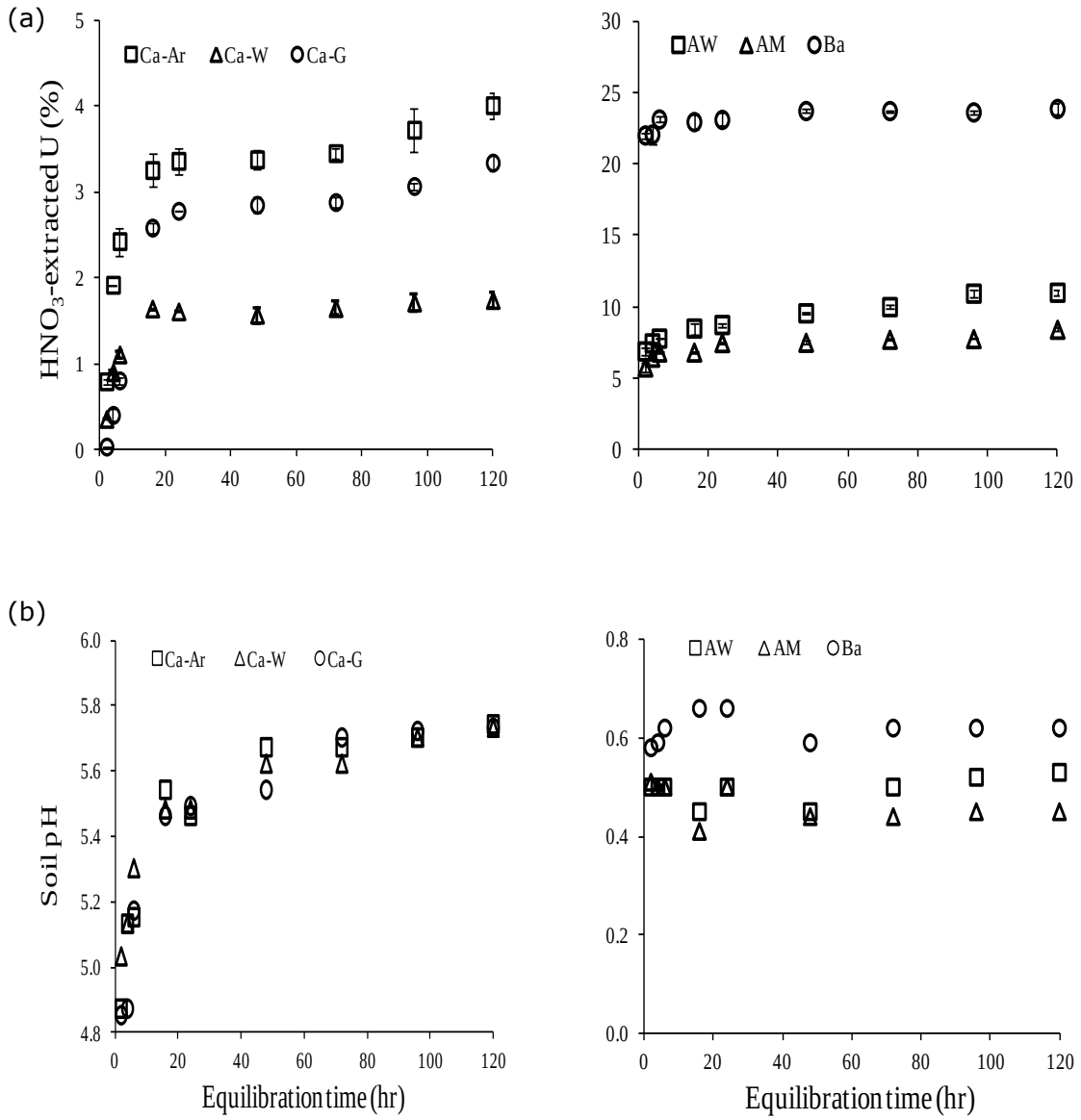

Figure 4.19: Proportion of 0.43 M HNO_3 extracted U (U_{Nit}) (a) and soil pH measured in HNO_3 soil suspension (b) as a function of equilibration time for six soils. Calcareous arable, woodland and grassland (Ca-Ar; □, Ca-W; Δ, Ca-G; ○), Acidic Woodland (AW; □), Acidic Moorland (AM; Δ) and Biosolid-amended (Ba; ○).

4.3.9 Evaluation of chemical extraction approaches for the characterization of reactive thorium

This section investigates the fractionation of Th in the two sets of soils described in Section 4.2.1, using the four single extraction methods previously applied to uranium. Figure 4.20 shows a comparison of Th fractions (% of soil total Th) extracted by the four single extractants (1 M CH_3COONH_4, 0.05 M EDTA, 0.43 M HNO_3 and 1% TMAH) from each of the five soil groups in the first set of soils and also for the BGSc soils (pH <6.5 and pH >6.5). The amounts of Th solubilised by the four extractants differed significantly (P <0.001) between soils. The average extractability of the four extractants followed the order: Th_{Ac} (0.08±0.13%) < Th_{Nit} (1.5±1.73%) < Th_{EDTA} (3.1±2.44%) < Th_{TMAH} (4.6±4.48%). Across all the soils studied, the proportions of Th_{Ac}, Th_{EDTA} and Th_{TMAH} (% of total Th) were significantly correlated (P <0.001), while Th_{Nit} was not correlated with the others (P >0.05).

Ammonium acetate extracted thorium; Th_{Ac}

Ammonium acetate extracted the least Th: 0.08% of total soil Th on average. Ammonium acetate releases the adsorbed cationic metal fraction from soil surface exchange sites but may also solubilize specifically adsorbed Th through changes in ionic strength, weak acetate complex formation and possibly changes in humic and fulvic acid solubility. For other metals M_{Ac} may be considered to approximate a 'bioavailable' fraction, but CH_3COONH_4 may not release the entire biologically available proportion of soil metal (Mclaughlin et al., 2000; Singh, 2007) depending on its effect on specifically adsorbed (but labile) metal fractions.

Nitric acid extracted thorium; Th_{Nit}

The strong acid extractant, 0.43 M HNO_3, released more Th than CH_3COONH_4 by an average factor of 18. Dilute nitric acid lowers the soil pH and hence partially dissolves cationic metals bound to Fe oxides and organic matter and contained within carbonate and phosphate minerals (Laing, 2010a). However, solubilization of thorium by 0.43 M HNO_3 may be limited by the flocculation of humic and fulvic acid at extremely low pH values if the main stable form of Th in solution, in the absence of synthetic chelating agents, is organically complexed Th. The difference between Th_{Ac} and Th_{Nit}

was most pronounced in the Ba soils compared with other soil groups. For the AW, AM and Ca soils, Th_{Nit} was only slightly higher (an average factor of 1.4) than Th_{Ac}. However, for the calcareous soils the pH value of the HNO_3 soil suspension was high (pH 5.4 on average), the nitric acid was neutralized by the $CaCO_3$ (see previous section). At the pH value of the Ca soil suspensions in 0.43 M HNO_3, it is likely that initially released Th^{4+} was substantially re-adsorbed by humus and Fe oxides. Therefore, nitric acid extraction was not effective in calcareous soils at the solid : solution (1:10) ratio used.

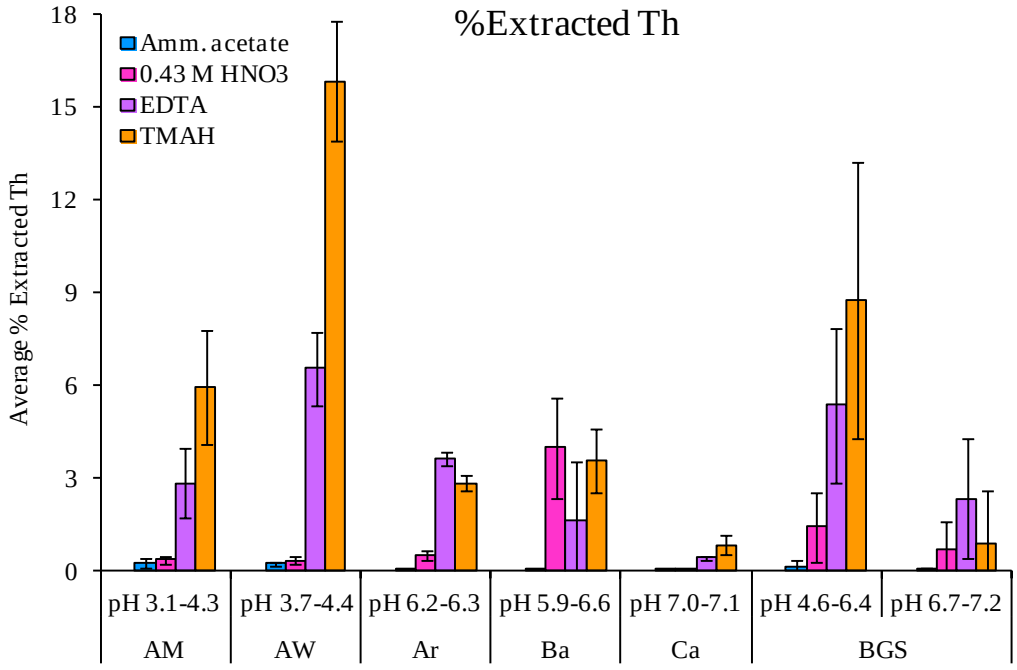

Figure 4.20: Comparison of the chemical extraction methods (1 M CH_3COONH_4, 0.05 M EDTA, 0.43 M HNO_3 and 1% TMAH) used for measuring available Th in soils in this study (n = 77). The error bars show standard deviation within each group of soils.

EDTA extracted thorium; Th_{EDTA}

The proportion of Th_{EDTA} was on average 3.1%; EDTA released more Th than CH_3COONH_4 and 0.43 M HNO_3 by average factors of 38 and 2, respectively. Synthetic chelating agents such as EDTA solubilize Th by complex formation depending on the stability of the EDTA-Th complex formed and the lability of Th in the soil. The stability constant (log_{10} value) for a 1:1 EDTA-Th complex is 23.6; the stability of this complex has been reported over a wide pH range (2.5-10.8) (Rao and

Rao, 1957; Cartwright et al., 2007). Langmuir et al. (1980) reported that Th forms an extremely strong complex with EDTA; one EDTA group can completely satisfy the coordination requirements of Th^{4+} ion. Thus, EDTA might be expected to represent a reasonable extraction method for Th since, unlike strong acids and weak acid salts (HNO_3, CH_3COONH_4), it is capable of stabilizing the extracted Th in solution and should be relatively unaffected by secondary soil factors such as the pH buffer power of the soil or the dissolution of fulvic acid in the extractant.

TMAH extracted thorium; Th_{TMAH}

The alkaline extractant (TMAH) released on average 4.6% (0.006 - 17.9%) of the total Th across all the soils (Figure 4.20), representing 1.5 times Th_{EDTA}. TMAH is expected to dissolve all organically-complexed Th, by solubilising humic and fulvic acids complexed Th. This is a different mode of action from any of the previous extractants in that the Th solubilized is probably retained in its original (organically) bound form but the humic and fulvic acid Th fractions are dissolved 'intact'. Thus, $\%Th_{TMAH}$ is expected to be high in organic soils. A possible consequence of the mode of action associated with Th_{TMAH} dissolution is that not all Th_{TMAH} may be regarded as 'reactive' since much of it has been solubilised in its bound form and has not, in fact, reacted with the extractant. Again, this is in contrast to Th_{EDTA}, Th_{Nit} and Th_{Ac} and possibly also to U_{TMAH} as UO_2^{2+} is expected to be much more weakly bound to humus and may be dissolved as carbonate complexes in the TMAH reagent. On the other hand, it can at least be said that Th_{TMAH} provides a contrast with Th bound into primary minerals in the soil since humus bound Th has at some point reacted with the indigenous soil humus acids. Given that most labile soil Th is expected to be humus-bound, Th_{TMAH} may also provide an appropriate input to geochemical speciation/fractionation models as the reactive Th pool.

Comparison of Th extractability using single extraction methods

Although Th_{Nit} was higher than Th_{Ac} for all soils, it was on average (1.5% of total Th) lower than Th_{EDTA} (3.1 %) and Th_{TMAH} (4.6%). With the exception of the Ba soils, all other soil groups showed low Th_{Nit} compared to Th_{EDTA} and Th_{TMAH}; in Ba soils Th_{Nit} was very similar to Th_{TMAH} and higher than Th_{EDTA}. This may be attributed to the

extremely high phosphate concentration in this soil category from over a century of sewage sludge application (Section 4.3.7) and the formation of Th-phosphate fractions and/or ternary surface complexes such as Th-phosphate-Fe^{III}oxide. Across all soils, values of Th_{Nit} were positively correlated with nitric acid extracted phosphate ($r = 0.77$ $P < 0.001$), while Th_{Ac}, Th_{EDTA} and Th_{TMAH} were negatively correlated with phosphate even with the exclusion of the Ba soils from the correlation analysis. Takeda et al. (2006b) investigated the extractability of 28 elements, including Th, in 16 arable soils using a range of chemical extraction methods including 1 M CH_3COONH_4, 0.1 M HNO_3 and 0.05 M EDTA. They found that the average Th extractability followed the order: Th_{Ac} (0.03%) < Th_{Nit} (0.08%) < Th_{EDTA} (1.6%); Th_{EDTA} was approximately double Th_{Nit} in agreement with the current study. In this study, the Th_{TMAH} fraction was higher than Th_{EDTA} in acidic organic soils (AM, AW, Ba, BGSc pH <6.5), and in calcareous-woodland and grassland soils with high organic matter contents, Th_{TMAH} was almost twice Th_{EDTA}, except for some Ba soils rich in SOM content Th_{TMAH} was on average 40 times Th_{EDTA} (Figure 4.21a and b). However, in soils with high pH and low organic matter content (Ar and BGSc pH >6.5) Th_{EDTA} was higher than Th_{TMAH} particularly in BGSc pH >6.5 (Figure 4.21a and b). As mentioned before, TMAH dissolves organically-complexed Th but organic matter is not expected to be the major Th-binding phase in soil at high pH and low organic matter content; Th is more likely to be bound to the Fe-oxide binding phases. Furthermore, the high pH value produced by TMAH is likely to increase Th^{4+} binding to negatively charged binding sites. This may explain why $Th_{TMAH} < Th_{EDTA}$ in Ar and BGSc pH >6.5.

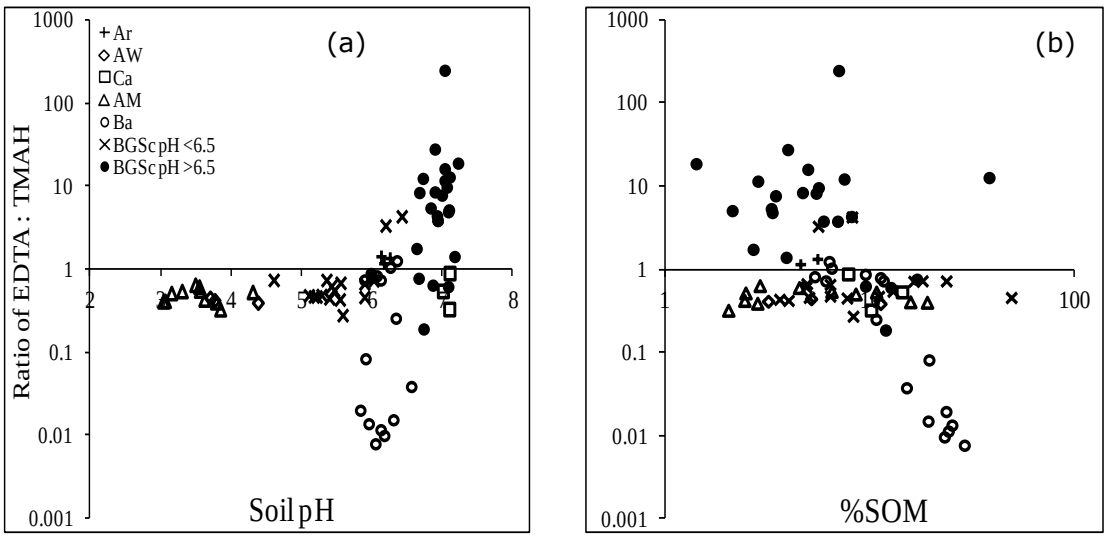

Figure 4.21: Ratio of EDTA extracted Th to TMAH extract (Th_{EDTA}:Th_{TMAH}; log scale) as a function of (a) soil pH and (b) %soil organic matter (%SOM; log scale). Soils include Arable (Ar; +), Acidic Woodland (AW; ◊), Calcareous (Ca; □), Acidic Moorland (AM; Δ), Biosolid-amended (Ba; ○), BGSc pH <6.5 (×) and BGSc pH >6.5 (●) groups, (n = 77).

4.3.10 Influence of soil characteristics on the extractability of Th

Table 4.7 shows correlations between individual soil characteristics and the proportion of Th_{Ac}, Th_{Nit}, Th_{EDTA} and Th_{TMAH}. Soil pH, available phosphate and carbonate content were negatively correlated with Th_{Ac}, Th_{EDTA} and Th_{TMAH}. These negative correlations were expected. The adsorption of Th onto soil binding phases increases markedly with increasing pH (above 2), with maximum adsorption (95-100%) being attained at pH values above 5.5-6.5 (Langmuir, 1980). Under alkaline conditions, Th strongly adsorbs onto negative binding sites, thus minimizing the labile fraction. However, there was no significant correlation between SOM and Th_{EDTA} or Th_{TMAH}, against expectation, which may be attributed to the influence of the biosolid-amended soils (Ba). In Ba soils both SOM and available phosphate were positively correlated ($r = 0.8$, $P < 0.001$); thus the negative correlation between extractable Th and SOM probably arose from the influence of phosphate. Excluding the Ba soils data resulted in a significant positive correlation between SOM and Th_{EDTA} ($r = 0.35$, $P < 0.05$), Th_{TMAH} ($r = 0.47$, $P < 0.01$) and enhanced the positive correlation with Th_{Ac} ($r = 0.58$, $P < 0.001$). Organic matter is an important binding phase for reactive Th in soils (Langmuir and Herman, 1980; Kaplan and Knox, 2003; Guo et al. 2008). In contrast to Th_{Ac}, Th_{EDTA} and Th_{TMAH}, Th_{Nit} was positively correlated with phosphate; this may

be due to the Ba soils, since the low pH of nitric acid dissolved the Th-phosphate phases. Arey et al. (1999) reported that secondary phosphate phases can be extracted under acidic conditions that favour phosphate dissolution. In the current study, other soil properties such as Fe-oxide (FeOx), %clay and total Th were not significantly correlated with extractable Th, but Th_{Ac} was negatively correlated with total Th concentration as shown in Table 4.7.

Table 4.7: Correlation between soil properties and the fraction of Th extracted using: 1 M ammonium acetate (Th_{Ac}), 0.43 M HNO_3 (Th_{Nit}), 0.05 M EDTA (Th_{EDTA}) and 1% TMAH (Th_{TMAH}). Significant values are shown in bold italics where P-value is <0.05.

Soil variables	%Extracted Th			
	$\%Th_{Ac}$	$\%Th_{Nit}$	$\%Th_{EDTA}$	$\%Th_{TMAH}$
pH	***-0.69 (<0.001)***	0.10 (>0.05)	***-0.31 (<0.01)***	***-0.80 (<0.001)***
Avail-P (mg kg^{-1})	***-0.31 (<0.01)***	***0.77 (<0.001)***	***-0.41 (<0.001)***	***-0.29 (<0.05)***
% $CaCO_3$	***-0.27 (<0.05)***	***-0.28 (<0.05)***	***-0.36 (<0.001)***	***-0.42 (<0.001)***
%SOM	***0.33 (<0.01)***	***0.53 (<0.001)***	-0.09 (>0.05)	0.11 (>0.05)
Th_{total} (mg kg^{-1})	***-0.40 (<0.001)***	-0.02 (>0.05)	0.15 (>0.05)	-0.02 (>0.05)
FeOx (g kg^{-1})	-0.22 (>0.05)	-0.05 (>0.05)	0.21 (>0.05)	0.07 (>0.05)
%clay	-0.21 (>0.05)	-0.16 (>0.05)	0.05 (>0.05)	-0.09 (>0.05)

4.3.11 Multiple linear regression model to predict Th extractability

Stepwise regression was used to model %Th extractability measured using CH_3COONH_4, EDTA, TMAH and HNO_3 as a function of the soil variables likely to affect Th extractability in soils (Equation 4.1). Only significant predictors ($P < 0.05$) were included to predict Th extractability. The resulting values of the optimised coefficients are shown in Table 4.8. The fit of the model is indicated by the residual standard deviation (RSD) between measured and predicted extracted Th and the correlation coefficient (r) (Table 4.8).

Ammonium acetate extracted thorium; Th_{Ac}

Soil pH and available-P coefficients indicated a negative effect on $\%Th_{Ac}$. Soil pH had the most significant effect on the prediction of $\%Th_{Ac}$ and accounted for the largest proportion of total variance in %extracted Th, followed by available-P (Table 4.8). Apart from soil pH and available-P, the inclusion of %SOM, total soil Th content and $\%CaCO_3$ improved the model prediction by 10.8, 2.3 and 1.6%, respectively.

EDTA extracted thorium; Th_{EDTA}

Soil pH and available-P were the most important variables for predicting $\%Th_{EDTA}$. Soil pH explained 28.3% of the total variance in $\%Th_{EDTA}$, followed by available-P which explained 18.6% of the variance (Table 4.8). The inclusion of FeOx and AlOx improved the model prediction. Iron oxide content (FeOx) explained 11.7% of the variance in Th_{EDTA} (positive coefficient) suggesting that EDTA was able to partially dissolve Th fixed within soil Fe oxide or Fe oxide coatings, in high pH soils: such behaviour was not observed for other extractants.

TMAH extracted thorium; Th_{TMAH}

Soil pH was the most important soil variable for predicting $\%Th_{TMAH}$ and accounted for 75% of the total variance in Th_{TMAH} (Table 4.8), while including available-P and %SOM to the regression model slightly improved the model prediction by 4 and 0.8%, respectively.

Nitric acid extracted thorium; Th_{Nit}

In contrast to $\%Th_{Ac}$, $\%Th_{EDTA}$ and $\%Th_{TMAH}$, the coefficient for available-P indicated a positive effect on $\%Th_{Nit}$. Available-P accounted for the largest proportion of total variance in $\%Th_{Nit}$ (60%; Table 4.8). The inclusion of $\%CaCO_3$, %SOM and soil pH improved the model prediction by 7.1, 6.3 and 3.4%, respectively. With the exclusion of Ba soils from the regression analysis, available-P was no longer a significant predictor of $\%Th_{Nit}$, whereas %SOM, $\%CaCO_3$ and pH explained 26.6, 20.5 and 10.7% of the total variance in $\%Th_{Nit}$ (Table 4.8). Soil pH was the least important variable for predicting $\%Th_{Nit}$, unlike $\%Th_{Ac}$, $\%Th_{EDTA}$ and $\%Th_{TMAH}$.

Predicting Th extractability

Generally, soil pH was the most important soil variable for predicting $\%Th_{Ac}$, $\%Th_{EDTA}$ and $\%Th_{TMAH}$. This is consistent with Guo et al. (2010) who suggested that soil pH was the major contributor to Th bioavailability for wheat plants, as indicated by a negative coefficient for soil pH in a multiple regression model of Th uptake. In the current study, available-P was also an important variable for explaining the variance in $\%Th_{Ac}$, $\%Th_{EDTA}$ and $\%Th_{TMAH}$ (negative effect). As shown in Table 4.8, phosphate decreased the availability of Th, as discussed above. This may be due to the precipitation of secondary phosphate phases and/or the formation of Th–phosphate–Fe(III) oxide ternary surface complexes. Guo et al. (2010) observed that the addition of hydroxyapatite and sodium pyrophosphate to the soil decreased thorium availability; the available Th was transformed into non-available Th-phosphate/pyrophosphate compounds. Such Th-phosphate complexes dissolve under acidic conditions (Arey et al., 1999), which explains the positive effect of available phosphate in multiple regression modelling of $\%Th_{Nit}$. The optimised empirical model can give reasonably good predictions of extractability of Th by all the reagents investigated, but particularly for $\%Th_{Ac}$ and $\%Th_{TMAH}$ judging from values of r (Table 4.8). The $\%Th_{TMAH}$ was accurately predicted using the lowest number of soil variables (pH, available-P and %SOM), amongst which pH explained most of the variance (75%) in $\%Th_{TMAH}$. Given that most labile soil Th is expected to be humus-bound, TMAH may be the most appropriate extraction method for measuring soil available Th compared with CH_3COONH_4, HNO_3 and EDTA. Figure 4.22 shows that the

predicted Th_{TMAH} was in reasonable agreement with the measured values (r = 0.88 and RSD = 2.18%).

Table 4.8: Multiple linear regression model coefficients, RSD and r values for model prediction of %Th extractability (Th_{Ac}, Th_{Nit}, Th_{EDTA}, Th_{TMAH}) from pH, available-P concentration (mg P kg^{-1} soil), %SOM, total Th concentration (mg kg^{-1}), %$CaCO_3$, FeOx (g kg^{-1}) and AlOx (g kg^{-1}). Values in brackets are the % of total variance explained by individual soil variables. *N.S:* not significant (P >0.05).

%Th extractability	Constant	pH	P-avail	%SOM	Th_{total}	%$CaCO_3$	FeOx	AlOx	RSD	r
$\%Th_{Ac}$	0.44	-0.052	-0.0005	0.008	-0.011	-0.016	*N.S*	*N.S*	0.06	0.88
		(48.2)	*(15.3)*	*(10.8)*	*(2.3)*	*(1.6)*				
$\%Th_{EDTA}$	19	-2.4	-0.001	*N.S*	*N.S*	*N.S*	0.010	-0.99	1.72	0.76
		(28.3)	*(18.6)*				*(11.7)*	*(4.3)*		
$\%Th_{TMAH}$	35.8	-5.0	-0.007	0.052	*N.S*	*N.S*	*N.S*	*N.S*	2.18	0.88
		(74.9)	*(4.0)*	*(0.8)*						
$\%Th_{Nit}$	-1.41	0.307	0.006	0.074	*N.S*	-0.34	*N.S*	*N.S*	0.86	0.87
		(3.4)	*(59.5)*	*(6.3)*		*(7.1)*				
$\%Th_{Nit}$ - Excluding Ba soils	-0.96	0.26	*N.S*	0.067	*N.S*	-0.279	*N.S*	*N.S*	0.51	0.77
		(10.7)		*(26.6)*		*(20.5)*				

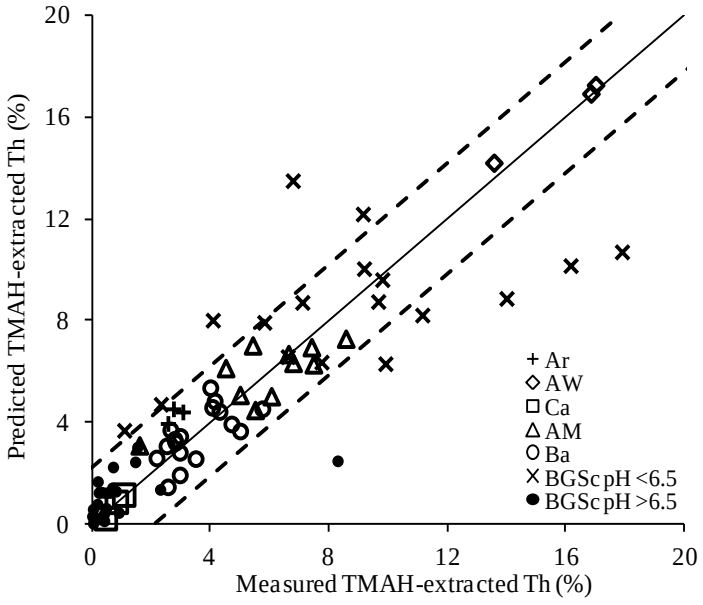

Figure 4.22: Predicting $\%Th_{TMAH}$ (% of total Th) using selected soil variables; pH, available-P and %SOM for Arable (Ar; +), Acidic Woodland (AW; ◊), Calcareous (Ca; □), Acidic Moorland (AM; Δ), Biosolid-amended (Ba; ○), BGSc pH <6.5 (×) and BGSc pH >6.5 (●) soils, (n = 77). The solid line is the 1:1 relationship and dashed lines represent the 1:1 line ± RSD.

4.3.12 Isotopically exchangeable Th

An important line of research to enhance understanding of soil Th dynamics would be the measurement of isotopically exchangeable Th and a comparison of Th E-values with existing single extraction methods. Two preliminary experiments were undertaken during the course of this project to test the validity of the isotopic dilution technique (ID) for measuring labile soil Th and to optimise the composition of the soil suspending solution with minimum disturbance to the soil system.

Testing the isotopic exchangeability of ^{232}Th adsorbed on Amberlite IR-120 resin

A preliminary experiment was undertaken to test the validity of ID for measuring ^{232}Th. The ^{232}Th E-values were measured on an indifferent resin exchange system in which all the (added) ^{232}Th present was in a labile form. Compared to U(VI) (UO_2^{2+}), retaining Th in solution is problematic and so it was thought necessary to include an organic complexing agent to have sufficient Th in solution to allow robust analysis of isotopic ratios. Samples of Amberlite IR-120 were equilibrated with 0.01 M KH-phthalate containing aliquots of ^{232}Th for 24 hr; the KH-phthalate solution was used to try to simulate a natural soil system containing DOC in soil solution which can form strong complexes with Th. The resin suspensions were spiked with different volumes of ^{230}Th spike solution and equilibrated for a further 24 hr to allow isotopic equilibration between ^{232}Th and ^{230}Th. The (^{230}Th/^{232}Th) ratio was assayed by ICP-MS.

Figure 4.23 shows, as a function of ^{230}Th spike concentration, the ratio of (i) the total ^{232}Th added to the E-value for ^{232}Th in Amberlite IR-120 resin suspensions and (ii) the ratio of measured resin-adsorbed ^{232}Th to predicted adsorbed ^{232}Th from the ^{230}Th spike distribution coefficient. Both variables should have a value of 1.0 if there is complete isotopic equilibrium and the adsorbed ^{232}Th is entirely labile and not bound irreversibly to the resin. There was no significant effect of ^{230}Th concentration and both variables were close to 1.0, confirming the validity of the isotopic dilution protocol, analysis and calculation under the conditions employed.

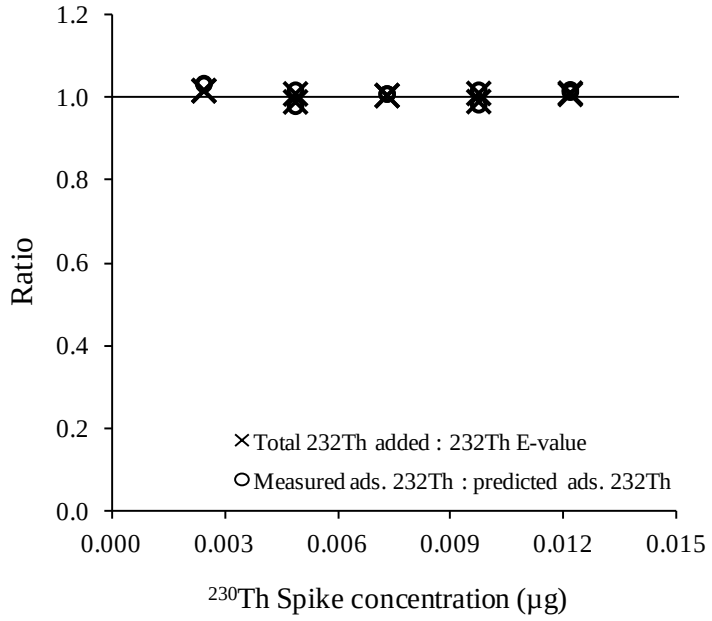

Figure 4.23: The ratio of total (added) ^{232}Th to the measured ^{232}Th E-value (×) and the ratio of measured resin-adsorbed ^{232}Th to predicted adsorbed ^{232}Th (○) from the ^{230}Th spike distribution coefficient; both variables are shown as a function of ^{230}Th concentration (µg).

Preliminary investigation: optimising the composition of the suspending solution for measuring soil ^{232}Th E-value

To measure the concentration of labile Th in soils and to try to optimise the composition of the soil suspending solution with minimum disturbance of the soil system, sub-samples of three soils were equilibrated with different EDTA concentrations (0.05, 0.1, 0.5, 1.0, 5 and 10 mM) for 1 day. The Ar, AM and Ba soils were chosen for this investigation to cover a range of ^{232}Th K_d values across the two sets of soils. The soil suspensions were then spiked with ^{230}Th tracer and equilibrated for a further 3 days prior to the assay of the isotope ratio (^{230}Th/^{232}Th). In the Ar and AM soils, the concentration of Th in solution increased with increasing EDTA concentration (Table 4.9), particularly at the larger concentrations (5 and 10 mM), as a result of complexation of EDTA with Th, while Th concentration was nearly constant in the Ba soil. There was no significant effect of increasing EDTA concentration on the Ba soil E-value (Table 4.9). However, in the Ar and AM soils, although there was no significant effect on the E-value up to concentrations of 1.0 mM EDTA, a significant increase in E-values was observed when EDTA was used at larger concentrations (5 and 10 mM). Generally, the E-value for Th appeared to be

unaffected by using EDTA in small concentrations (e.g. 0.1 mM) but larger concentrations of EDTA may solubilise some of the non-labile Th pool. Thus EDTA can be used in small concentrations to avoid analytical problems associated with measuring E-values for soils with high pH and low dissolved Th concentrations.

The next step would have been to add a range of small concentrations of EDTA (0.1, 0.01 and 0.001 mM) to soil suspensions in 0.01 M $Ca(NO_3)_2$ to refine our understanding of the effect of EDTA addition on E-values. Unfortunately, the tracer isotope (^{230}Th) was not available to carry out this step at that time.

Table 4.9: The effect of EDTA concentration on the amount of ^{232}Th extracted and on the E-value of ^{232}Th for Arable (Ar), Acidic Moorland (AM) and Biosolid-amended (Ba) soils. Standard errors of two replicates are given in parentheses.

		^{232}Th (µg kg^{-1})	
Soil	EDTA (mM)	Extracted	E-value
Arable (Ar)	0.05	2.6 (0.03)	472 (4.2)
	0.1	2.9 (0.05)	479 (1.3)
	0.5	4.0 (0.06)	473 (2.7)
	1	9.3 (0.02)	475 (5.8)
	5	69 (0.52)	524 (11.3)
	10	195 (0.30)	653 (5.5)
Acidic Moorland	0.05	3.0 (0.02)	110 (0.7)
(AM)	0.1	3.7 (0.01)	114 (0.8)
	0.5	6.2 (0.02)	120 (0.5)
	1	15 (0.04)	112 (0.6)
	5	209 (0.68)	217 (6.3)
	10	215 (1.18)	271 (7.6)
Biosolid-amended	0.05	1.5 (0.003)	199 (1.9)
(Ba)	0.1	1.5 (0.002)	205 (1.1)
	0.5	1.4 (0.003)	220 (1.2)
	1	1.0 (0.001)	215 (1.3)
	5	1.4 (0.003)	220 (1.4)
	10	1.6 (0.004)	222 (1.2)

4.4 CONCLUSIONS

An optimised approach to measuring isotopically exchangeable ^{238}U(VI), with ^{233}U(VI) as the spike isotope, was based on a number of preliminary experiments. The first experiment tested the basic principle of the isotopic dilution technique, using suspensions of Amberlite IR-120 resin spiked with ^{238}U(VI), and demonstrated the validity of the technique with a measured %lability value of 99.9% over a range of spike isotope (^{233}U(VI)) concentrations.

A preliminary experiment in which isotopic equilibration was determined over a period of 5 days for four soils with different characteristics indicated little practical change in E-value after four days of contact with the spike isotope. Therefore four days was adopted as the standard time for isotopic equilibration under aerobic conditions. In practice, very little change in E-value was found across a wide range of spike concentrations (Rss values). The results obtained demonstrated that even a small amount of the spike isotope ^{233}U(VI) added to the soil suspension, equivalent to just 5% of the E-value, produced low uncertainty in the E-value (≤ uncertainty at high spike amounts) determination and allowed accurate detection of isotope ratios and concentrations.

The presence of non-labile SCP-^{238}U(VI) in soil suspensions used to measure E-values, identified by comparing solution (E_{soln}) and resin (E_{resin}) assays, led to a small but significant overestimation of the true E-value (2.2% on average), even in soils with high pH and carbonate contents. In soils with exceptionally high phosphate and well humified organic matter contents, there appeared to be a greater presence of non-labile SCP-^{238}U. Thus, in the Biosolid-amended (Ba) soils from a sewage processing farm, the true E-value was overestimated by 20%. The presence of non-labile SCP-^{238}U was significantly related to P and DOC in the filtered soil solution (<0.2 μm), suggesting that 'nano-particulate' SCP-^{238}U might be associated with phosphate and organic colloids.

The E-value for ^{238}U(VI) ranged from 2.7 to 39.1 % of the total soil ^{238}U content in the soil samples studied (n = 77). The results obtained indicated that some soil properties had a systematic effect on the lability of ^{238}U(VI). The values of %U

lability were found to be significantly positively correlated with Fe-oxide concentration across the entire data set and also positively correlated with %SOM, indicating the large sorption capacity of soil organic matter for U. Approximately 69% of the variance in the isotopically exchangeable U was explained by the variation in concentrations of Fe-oxide, SOM and available phosphate. Iron oxide content had the most significant effect on prediction of %E-value and accounted for the largest proportion of total variance in %E-value (42.3%).

The amounts of U solubilised by the four chemical extractants (U_{Ac}, U_{Nit}, U_{EDTA}, U_{TMAH}) were significantly different between soil groups ($P < 0.001$). Thus E-values for U(VI) did not correspond consistently with any single chemical extraction procedure although the degree of correspondence was soil-dependent. On average, over all groups of soils, CH_3COONH_4, EDTA and TMAH underestimated E-value by factors of 13.7, 9.5 and 1.6, respectively, while HNO_3 overestimated E-value by only a factor of 1.04. The value of U_{Nit} was very similar to the E-value (U_E) for AW and AM soils below pH 5 and therefore extraction with 0.43 M HNO_3 might be suitable for acidic and organic woodland soils. However, extraction with 0.43 M HNO_3 overestimated the E-value in Ba and Ar soils, probably due to the solubilisation of U held within phosphate phases in both soil groups. Soils with carbonate content higher than 2% showed large deviations between isotopically exchangeable U and U_{Nit} due to the buffering capacity of soil carbonates, the nitric acid was largely neutralized by the $CaCO_3$. This represented a major flaw in the nitric acid extraction scheme when applied to calcareous soils.

The amounts of Th solubilised by the four extractants differed significantly ($P < 0.001$) between soils. The average extractability of the four extractants followed the order: Th_{Ac} 0.08% < Th_{Nit} 1.5% < Th_{EDTA} 3.1% < Th_{TMAH} 4.6%. Across all the soils studied, the proportions of Th_{Ac}, Th_{EDTA} and Th_{TMAH} were significantly correlated ($p < 0.001$), while Th_{Nit} was not correlated with the others ($P > 0.05$). Solubilization of Th by 0.43 M HNO_3 may be limited by the flocculation of humic and fulvic acid at extremely low pH values if the main stable form of Th in solution is organically complexed Th. As found for U, nitric acid extraction was not effective in calcareous soils because the nitric acid was substantially neutralized by the $CaCO_3$, thus it was

likely that much initially released Th^{4+} was re-adsorbed by humus and Fe oxides. Thorium extractability was reasonably well predicted from multiple linear regression model using soil properties. Approximately 78%, 63% and 80% of the variability in $\%Th_{Ac}$, $\%Th_{EDTA}$ and $\%Th_{TMAH}$ were explained by the variation in soil properties: soil pH was the most important soil variable for predicting $\%Th_{Ac}$, $\%Th_{EDTA}$ and $\%Th_{TMAH}$ followed by available-P; both pH and available-P were negatively correlated with Th extractability. Given that most labile soil Th is expected to be humus-bound, TMAH may be the most appropriate extraction method for measuring soil available Th compared with CH_3COONH_4, HNO_3 and EDTA.

5 CONTINUOUS LEACHING APPROACH FOR THE STUDY OF URANIUM AND THORIUM FRACTIONATION IN SOILS

5.1 INTRODUCTION

A wide range of extraction procedures for trace metals in soils and sediments have been developed in the past; they can be broadly classified into sequential (SEP) and single-extraction procedures (Tessier et al., 1979; Quevauviller, 1998; Jimoh et al., 2004; Kurosaki et al., 2002). All extraction procedures that utilize a 'batch' approach are effectively based on the establishment of a new equilibrium between the solid and solution phases. Although SEPs have been shown to be *reproducible* for trace metals and radionuclide partitioning (Tessier et al., 1979; Schultz et al., 1998; Kurosaki et al., 2002) they suffer from several logistical and conceptual limitations. They are often time consuming, prone to contamination and to artefacts such as metal re-adsorption and re-distribution among phases during extraction. As a result, it is widely accepted that the geochemical phases quantified in the SEP steps are actually operationally defined (Whalley and Grant, 1994; Gómez-Ariza et al., 1999; Bermond, 2001; Jimoh et al., 2004; Kurosaki et al., 2002). Kurosaki et al. (2002) considered that SEPs are indirect methods for determining contaminant partitioning. Moreover, the batch procedures are unable to provide information about the kinetics of leaching processes and chemical association between elements (Buanuam et al., 2006; Kurosaki et al., 2002). Because naturally occurring processes are always dynamic, recent studies have focused on the development of alternative methods to mimic the environmental processes more accurately than classical batch extraction procedures (Miró et al., 2005; Buanuam et al., 2006). Miró et al. (2005) proved that the dynamic (non-equilibrium) based extraction method can be used as an alternative for trace metal partitioning. Thus a continuous-flow extraction system for the leaching, association and partitioning of trace elements has been recently proposed (Shiowatana et al., 2001; Fedotov et al., 2002; Kurosaki et al., 2002; Jimoh et al., 2004). Dynamic column leaching experiments have been widely used for determining metal and DOM mobility in soil and sediment to try to mimic field leaching conditions and to obtain data on a realistic time-scale (Anderson et al., 2000; Wisotzky and Cremer, 2003; Ashworth and Alloway, 2004).

One possible way to minimize the limitations accompanied with traditional batch techniques is to use a continuous-flow extraction method. One of the key advantages of a continuous leaching process is that solution flow through the system will allow immediate removal of extracted metal thereby minimizing the possibility of metal re-adsorption to the solid phase. Leaching of trace metals in the soil environment is profoundly affected by pH which is one of the most important factors affecting trace metal mobilization in soil. Continuous acid leaching will gradually decrease the soil pH as the acid saturates the soils buffering capacity resulting in progressive metal mobilization due to decreasing negative surface charge and increased proton competition for adsorption sites (Beauchemin et al., 2002; Jimoh et al., 2004). Furthermore, metal oxides (Fe, Mn, Al hydrous oxides) that adsorb trace metals are gradually dissolved at low pH values (Hinsin et al., 2002; Buekers et al., 2007). Thus, elements (both adsorbents and adsorbates) showing the same release pattern as a function of pH decrease could indicate a close association.

In this chapter, a continuous leaching method was developed and applied to two contrasting soils: Biosolid-amended (Ba) and Acidic Moorland (AM). The leaching rates of U and Th, as well as other trace and major elements were measured by fraction collection and assay by ICP-MS. Leached Th and U concentrations were compared with batch single extracted metal (M_{Ext}) or labile metal (U_E) concentrations.

The primary objectives of this study were therefore to:

(i) develop a simple continuous leaching approach to U and Th fractionation;

(ii) determine and compare the release patterns of Th and U and some major and trace elements, in order to investigate possible metal associations through similarities in the release patterns and correlation analysis;

(iii) Compare released Th and U concentrations obtained by the continuous leaching approach to that obtained using batch extraction techniques (M_{Ext}) or isotopic dilution (U_E).

5.2 MATERIALS AND METHODS

5.2.1 Soil samples

In this chapter, two contrasting soils were used. The first soil investigated was the Biosolid-amended Arable topsoil collected from Field 8 (8C), while the second one was the Acidic Moorland topsoil collected from under Scots Pine (*Pinus sylvestris*). The origins and characteristics of the two soils have been described in Chapters 2 and 4.

5.2.2 Soil column leaching experiment

Soil (1 g < 2 mm) was placed in a small column with a 1.6 cm inside diameter and 10 cm length, the leaching solution (0.05 M HNO_3 or 0.1 M CH_3COONH_4 (pH 4.5)) was supplied to the top of the column by peristaltic pump at a rate of 0.42 ml min^{-1}. A disc of coarse filter paper was placed at the base of the column to prevent the outflow of soil particles, while one at the top of the soil ensured that added leaching solution was spread evenly over the soil surface. The soil packing in the column was loose enough to allow free drainage but sufficiently well consolidated so the structure of the re-packed sample (macropores, etc.) would not be changed during the leaching process. Prior to acid leaching, the soil column was saturated with water applied at a rate of 0.42 ml min^{-1}. The acid leachate was then applied and the column effluent was collected in 115 fractions of 6.4 ml each (5.8 and 6.3 pore volumes of Ba and AM soils, respectively) using an automatic fraction collector. Thus, the fractions were collected over a period of 27 hour. The small amount of soil used (1.0 g) was chosen to ensure complete removal, or at least substantial depletion, of elements of interest; larger samples would have required longer leaching times, and possibly risked re-adsorption within the column of soil during transit of the leaching solution. Nevertheless, the flow rate was quite slow to increase the solution-mineral contact time and to amplify the chemical reaction signatures.

Both soils were leached with dilute nitric acid (0.05 M HNO_3) either with, or without, initially washing the soil with 128 ml of 1 M NH_4NO_3 to remove exchangeable cations. A proportion of Ca exists in weakly held exchangeable forms in soil and so acid leaching would preferentially release Ca^{2+} from exchange sites and confound any

attempt to identify associations between Ca solid phases (carbonates or phosphates) and adsorbed or occluded trace metals. Thus, ammonium nitrate was used to initially remove exchangeable Ca^{2+}, and other exchangeable cations. The pH of all soil fractions was measured (Section 2.2.1). The concentration of P was measured colorimetry (Section 2.2.9). Fractions were diluted 1:2 with 2 % nitric acid and multi-element analysis including Th and U was undertaken by ICP-MS (Model X-Series^{II}, Thermo-Fisher Scientific, Bremen, Germany) operating in collision cell mode (7% hydrogen in helium) to reduce polyatomic interferences. Internal standards included Ge (50 µg L^{-1}), Rh (10 µg L^{-1}) and Ir (10 µg L^{-1}) in 2 % TAG HNO_3. External Th and U calibration standards (Claritas-PPT grade CLMS-2, SPEX Certiprep, Stanmore, UK) were used in the concentration range 0-10 µg L^{-1} (Section 2.5.1).

5.3 RESULTS AND DISCUSSION

In this chapter fractionation and elemental association of U, Th and some major and trace elements in two contrasting soils were studied using a continuous leaching method. This method not only evaluates the mobility or potential environmental impact of U and Th, but also allows correlations between release patterns of different elements to be studied. The following sections examine correlations between the leaching behaviour of metals using correlation matrices and cluster analysis to interpret elemental associations revealed by the leaching patterns. Elemental ratio plots are used to confirm any associations between elements and to provide more information on the metal binding. Finally, U and Th release patterns are compared with the fixed U and Th values provided by the batch and isotope exchange methods described in chapter 4.

Leachate pH

The pH values of the leachates collected from Ba and AM soil columns are shown in Figures 5.1a and b. Leaching of the Ba and AM soils with nitric acid resulted in a rapid decrease of soil pH to 2.2 and 1.7 in the first 5.8 and 6.3 pore volumes (the first leached fraction) of Ba and AM soils, respectively (Figure 5.1a). The pH reached an equilibrium value of 1.34 after 47 or 63 pore volumes, respectively. Ammonium acetate leaching produced different final soil pH values (Figure 5.1b). For the Ba soil,

the pH decreased from 4.7 in the first 5.8 pore volumes to reach an equilibrium pH of 4.53 after 47 pore volumes; for the AM soil, the pH increased from 4.12 in the first 6.3 pore volumes to reach an equilibrium pH of 4.53 after 31 pore volumes.

Acid (0.05 M HNO_3) leaching

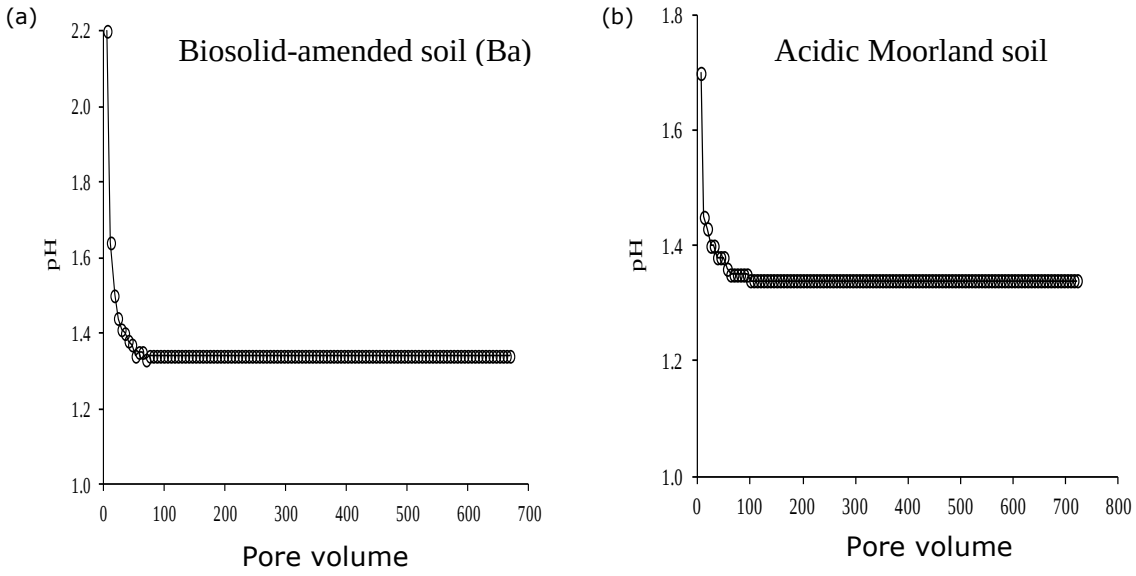

Figure 5.1a: Leachate pH as a function of pore volumes leached for (a) Biosolid-amended (Ba) and (b) Acidic Moorland (AM) soils leached with 0.05 M HNO_3.

0.1 M CH_3COONH_4 leaching

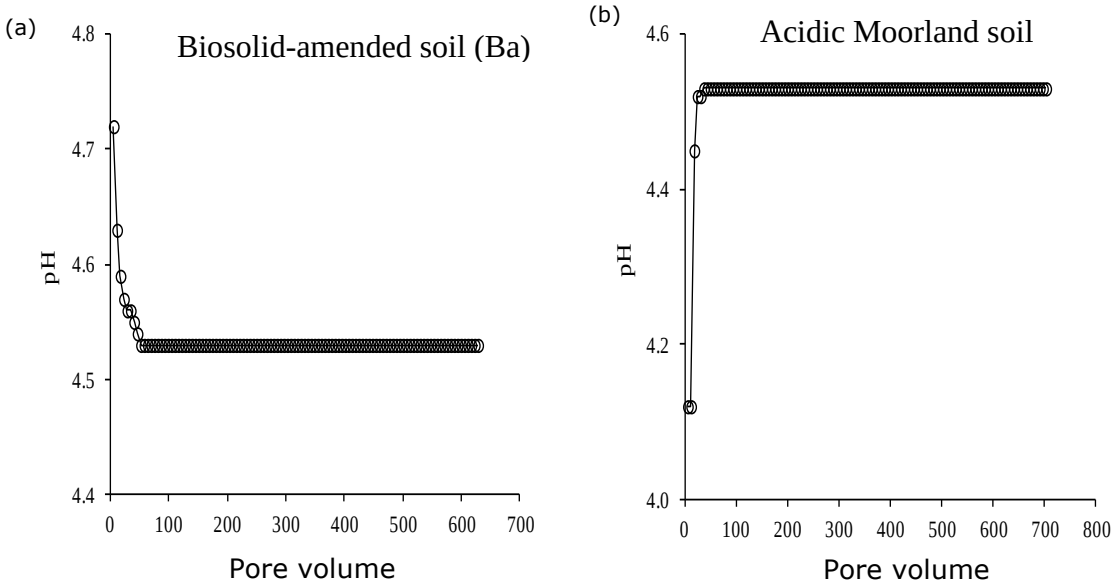

Figure 5.1b: Leachate pH as a function of pore volumes leached for (a) Biosolid-amended (Ba) and (b) Acidic Moorland (AM) soils leached with 0.1 M CH_3COONH_4 (pH 4.5).

5.3.1 Correlation and cluster analysis

Nitric acid continuous leaching

Tables 5.1 and 5.2 show the correlation matrices for metals released from the Biosolid-amended (Ba) and Acidic Moorland (AM) soils leached with 0.05 M HNO_3, after first removing the exchangeable cations with 1 M NH_4NO_3 solution. For both soils, the Pearson correlation coefficients demonstrated a significant positive correlation ($P < 0.001$) between metal concentrations and pH of the leachates (Tables 5.1 and 5.2), except for Mo in AM soil, was not significantly correlated with other metals and pH. For Th and U in the Ba soil, the strongest correlation was found between Th and Ti and between U, Pb and Th. In the AM soil, the strongest correlation was found between Th and Al and between U, Fe, P and Pb. These correlations were supported by cluster analysis presented as a dendrogram in Figure 5.2.

The cluster analysis of Ba soil metal data suggests two main groups (Figure 5.2a). The first one included two sub-clusters: one of these included only Mo, while the other one was further sub-divided into two sub-clusters including Ca, As, P (suggesting the presence within the Ba soil of Ca-phosphate/arsenate minerals) and a range of trace metals Mn, Ni, Sr, Zn, Cd. The second group also included two sub-clusters, one of which was further divided in two sub-clusters (Mg, K, Co and Al, Cu, Cr, Ba, Se), whereas the other group included elements likely to be associated with adsorption on Fe oxides (Ti, Th, Pb, U, Fe). The strong grouping of As, P and Ca strongly suggests substitution of arsenate into Ca-phosphate minerals (Tu and Ma, 2003; Kabata-Pendias, 2010); the Ba soil has exceptionally high inorganic phosphate concentrations. The clustering of Cd and Zn may be due to isomorphous substitution of Cd for Zn in sulphide minerals such as sphalerite (Nakhone and Young, 1993) but in the Ba soil this probably reflects the common industrial origin of these metals. A highly significant correlation was also found between Mg, K and Co, probably due to association with clay. Du et al. (2012) investigated the mode of occurrence and mobility of Ti and Th in intensely weathered lateritic regolith in Western Australia and reported that Ti and Th were affected by transformation of resistant minerals and incorporation into secondary phosphate minerals and sorption or co-precipitation with Al and Fe oxides; this may explain the grouping and strong positive correlation

between Ti, Th and Fe. Thorium, like tetravalent actinides, adsorbs strongly onto Fe-oxides (Murphy et al., 1999; Reiller et al., 2002; Reiller et al., 2005; Degueldre and Kline., 2007; Seco et al., 2009; Melson et al., 2012). Figure 5.2a and Table 5.1 show a highly significant correlation between U and Pb, both of which were correlated with Fe. Lyons (1964) investigated the distribution of Th and U in three early palaeozoic plutonic series in new Hampshire (USA) and found that Pb was highly significantly correlated with uranium. Significant correlations between U, Pb and Fe suggest association of U and Pb with Fe-oxyhydroxides (Table 5.1) (McKenzie, 1980; Waite et al., 1994; Phillips et al., 2007; Pett-Ridge et al., 2007; Duff et al., 2002; Curtis et al., 2004, 2006). Stubbs et al. (2006) investigated the solid phase hosts for U in two contaminated soils using electron microprobe analysis and transmission electron microscopy and identified three distinct solid phase hosts for U: Fe-oxyhydroxides, barium- and lead-bearing mixed Mn-Fe oxides and discrete uranium phosphates. In all three solid phase hosts, U was associated with phosphorus.

Cluster analysis of the AM soil data (Figure 5.2b) showed two main groups. The first group consisted of two sub-clusters; one of these included only Mo while the other included two sub-clusters, (Mg, Mn, Ca, Sr, Co, Zn and K, Ni, Ba, Al, Th). The second group comprised Ti, Cu, Pb, Fe, U, Se, P, As and Cr. The highly significant correlation of Mg, Mn, Ca, Sr, Co and Zn suggests an association with clay or Mn oxides. In particular adsorption of Co^{2+} can be followed by oxidation to Co^{3+} and isomorphic substitution for Mn^{III} in Mn^{IV} oxides (McLaren et al., 1986; Ma and Hooda, 2010). The strong correlation/grouping of Th and Al suggests an association of Th with clay or Al hydrous oxides, while the highly significant correlation of Ti, Pb, Fe, U, Se, P, As and Cr suggests an association with Fe oxides. The significant correlation between Cr and Fe might be explained by isomorphic substitution of Cr^{3+} for Fe^{3+} in Fe oxides; the ferric ion has a similar radius (0.067 nm) and geochemical properties to Cr^{3+}. Sphene minerals can accept as much as 80 percent of available U, probably by isomorphic substitution with Ca; during soil weathering processes U and Ti can adsorb or co-precipitate with Fe oxides (Lyons, 1964; Deer et al., 1992). The significant correlation between U, Fe and P suggests the formation of U(VI)-phosphate-Fe(III) ternary surface complexes on Fe oxides. The U(VI)-phosphate interactions are important in controlling UO_2^{2+} mobility in both natural and polluted

environments (Cheng et al., 2004; Phillips et al. 2007; Stubbs et al., 2006), but this interaction depends on a number of factors such as pH, phosphate and U(VI) concentrations. If phosphate and U(VI) concentrations are sufficiently high, U(VI) can precipitate as uranyl phosphate solids (Singh et al., 2010). The extent of phosphate adsorption on the surfaces of iron oxides and oxyhydroxides decreases with increasing pH (Arai and Sparks, 200; Nilsson et al., 1992). At low pH, U(VI)-phosphate species adsorb to Fe-oxide forming ternary surface complexes (Payne et al., 1996; Cheng et al. 2004; Phillips et al. 2007; Singh et al., 2010), while at high pH, U adsorption *decreases* in the presence of phosphate due to the formation of soluble uranyl phosphate complexes (Cheng et al., 2004).

Table 5.1: Correlation matrix for the metals released and solution pH of the Biosolid-amended (Ba) soil leached with 0.05 M HNO_3 after removing the exchangeable cations with 1 M NH_4NO_3; n = 110 collected fractions; P-values < 0.05.

	Na	Mg	K	Ca	Al	Ti	V	Cr	Mn	Fe	Co	Ni	Cu	Zn	As	Se	Rb	Sr	Mo	Cd	Ba	Pb	Th	U
Mg	0.91																							
K	0.89	0.96																						
Ca	0.99	0.95	0.91																					
Al	0.91	0.86	0.95	0.90																				
Ti	0.84	0.92	0.96	0.85	0.91																			
V	0.91	0.88	0.96	0.90	1.00	0.93																		
Cr	0.88	0.87	0.95	0.87	0.98	0.96	0.99																	
Mn	0.94	0.96	0.97	0.96	0.94	0.91	0.95	0.92																
Fe	0.64	0.76	0.84	0.64	0.78	0.94	0.80	0.88	0.74															
Co	0.82	0.94	0.98	0.85	0.90	0.94	0.92	0.91	0.95	0.85														
Ni	0.96	0.93	0.93	0.98	0.92	0.85	0.92	0.88	0.98	0.65	0.89													
Cu	0.91	0.86	0.95	0.89	1.00	0.91	1.00	0.98	0.94	0.77	0.91	0.92												
Zn	0.92	0.81	0.87	0.92	0.93	0.78	0.92	0.88	0.93	0.59	0.82	0.96	0.93											
As	0.98	0.87	0.89	0.96	0.95	0.86	0.94	0.92	0.93	0.68	0.81	0.96	0.94	0.95										
Se	0.84	0.88	0.95	0.84	0.96	0.97	0.97	0.98	0.91	0.90	0.94	0.85	0.96	0.82	0.87									
Rb	0.94	0.87	0.92	0.92	0.96	0.92	0.96	0.96	0.93	0.80	0.87	0.93	0.95	0.92	0.96	0.93								
Sr	0.97	0.91	0.93	0.97	0.96	0.86	0.95	0.92	0.98	0.67	0.88	0.99	0.96	0.98	0.98	0.88	0.95							
Mo	0.70	0.43	0.51	0.64	0.69	0.48	0.65	0.64	0.61	0.38	0.45	0.68	0.69	0.80	0.75	0.55	0.77	0.72						
Cd	0.92	0.80	0.88	0.90	0.97	0.82	0.96	0.92	0.92	0.64	0.82	0.94	0.97	0.98	0.96	0.87	0.94	0.97	0.80					
Ba	0.87	0.88	0.97	0.86	0.99	0.96	0.99	0.99	0.94	0.86	0.95	0.89	0.99	0.88	0.90	0.99	0.94	0.92	0.61	0.92				
Pb	0.79	0.86	0.92	0.79	0.91	0.97	0.93	0.96	0.86	0.95	0.92	0.79	0.91	0.74	0.82	0.99	0.90	0.82	0.49	0.80	0.96			
Th	0.87	0.91	0.96	0.87	0.95	0.99	0.96	0.98	0.92	0.95	0.94	0.87	0.94	0.82	0.89	0.99	0.94	0.89	0.54	0.86	0.98	0.98		
U	0.82	0.86	0.93	0.81	0.92	0.98	0.94	0.98	0.88	0.95	0.92	0.82	0.92	0.77	0.85	0.98	0.93	0.84	0.55	0.83	0.96	0.99	0.99	
P	0.99	0.87	0.88	0.97	0.93	0.84	0.93	0.91	0.92	0.66	0.80	0.95	0.93	0.94	1.00	0.85	0.96	0.97	0.76	0.95	0.88	0.80	0.88	0.84
pH	0.67	0.40	0.44	0.62	0.59	0.37	0.56	0.52	0.55	0.23	0.37	0.64	0.59	0.76	0.69	0.44	0.70	0.68	0.95	0.73	0.50	0.36	0.43	0.42

Table 5.2: Correlation matrix for the metals released and solution pH of the Acidic Moorland (AM) soil leached with 0.05 M HNO_3 after removing the exchangeable cations with 1 M NH_4NO_3; n = 110 collected fractions; P-values < 0.05 except where marked with an asterisk.

	Na	Mg	K	Ca	Al	Ti	V	Cr	Mn	Fe	Co	Ni	Cu	Zn	As	Se	Rb	Sr	Mo	Cd	Ba	Pb	Th	U
Mg	0.62																							
K	0.69	0.92																						
Ca	0.63	1.00	0.94																					
Al	0.68	0.85	0.98	0.86																				
Ti	0.61	0.63	0.83	0.65	0.93																			
V	0.66	0.75	0.94	0.77	0.99	0.96																		
Cr	0.51	0.42	0.62	0.43	0.75	0.89	0.79																	
Mn	0.62	1.00	0.93	1.00	0.85	0.63	0.75	0.42																
Fe	0.59	0.55	0.77	0.57	0.89	0.99	0.93	0.90	0.56															
Co	0.65	1.00	0.96	1.00	0.89	0.69	0.81	0.47	1.00	0.62														
Ni	0.68	0.94	1.00	0.95	0.97	0.82	0.92	0.61	0.94	0.76	0.97													
Cu	0.59	0.56	0.79	0.58	0.90	0.99	0.95	0.90	0.57	0.99	0.63	0.78												
Zn	0.64	1.00	0.95	1.00	0.88	0.67	0.79	0.45	1.00	0.59	1.00	0.96	0.61											
As	0.51	0.35	0.61	0.37	0.76	0.94	0.84	0.90	0.35	0.97	0.42	0.59	0.95	0.40										
Se	0.62	0.63	0.82	0.65	0.92	0.99	0.95	0.89	0.64	0.99	0.69	0.81	0.98	0.67	0.93									
Rb	0.68	0.79	0.93	0.81	0.98	0.97	0.98	0.82	0.80	0.94	0.84	0.93	0.94	0.82	0.84	0.97								
Sr	0.64	1.00	0.94	1.00	0.87	0.66	0.78	0.44	1.00	0.59	1.00	0.96	0.60	1.00	0.39	0.66	0.82							
Mo	0.16*	0.05*	0.10*	0.06*	0.08*	0.03*	0.08*	0.00*	0.05*	0.04*	0.06*	0.07*	0.06*	0.05*	0.03*	0.01*	0.03*	0.06*						
Cd	0.47	0.69	0.67	0.69	0.65	0.54	0.59	0.40	0.69	0.50	0.70	0.68	0.49	0.69	0.37	0.55	0.63	0.69	0.03*					
Ba	0.67	0.97	0.99	0.97	0.95	0.78	0.89	0.56	0.97	0.71	0.99	1.00	0.72	0.98	0.53	0.77	0.90	0.98	0.07*	0.69				
Pb	0.58	0.59	0.79	0.61	0.90	0.99	0.94	0.89	0.59	0.99	0.65	0.78	1.00	0.63	0.94	0.98	0.95	0.62	0.07*	0.51	0.73			
Th	0.68	0.84	0.97	0.86	1.00	0.94	0.99	0.75	0.84	0.89	0.89	0.97	0.91	0.87	0.77	0.93	0.99	0.87	0.08*	0.66	0.95	0.91		
U	0.59	0.56	0.77	0.58	0.89	0.99	0.93	0.90	0.56	1.00	0.62	0.76	1.00	0.60	0.96	0.99	0.95	0.59	0.05*	0.50	0.71	1.00	0.90	
P	0.57	0.52	0.78	0.54	0.89	0.98	0.95	0.88	0.53	0.99	0.59	0.76	0.99	0.57	0.95	0.96	0.92	0.56	0.07*	0.46	0.70	0.98	0.89	0.99
pH	0.53	0.87	0.89	0.88	0.86	0.69	0.80	0.48	0.87	0.61	0.89	0.90	0.66	0.88	0.42	0.67	0.78	0.88	0.17*	0.60	0.90	0.68	0.85	0.63

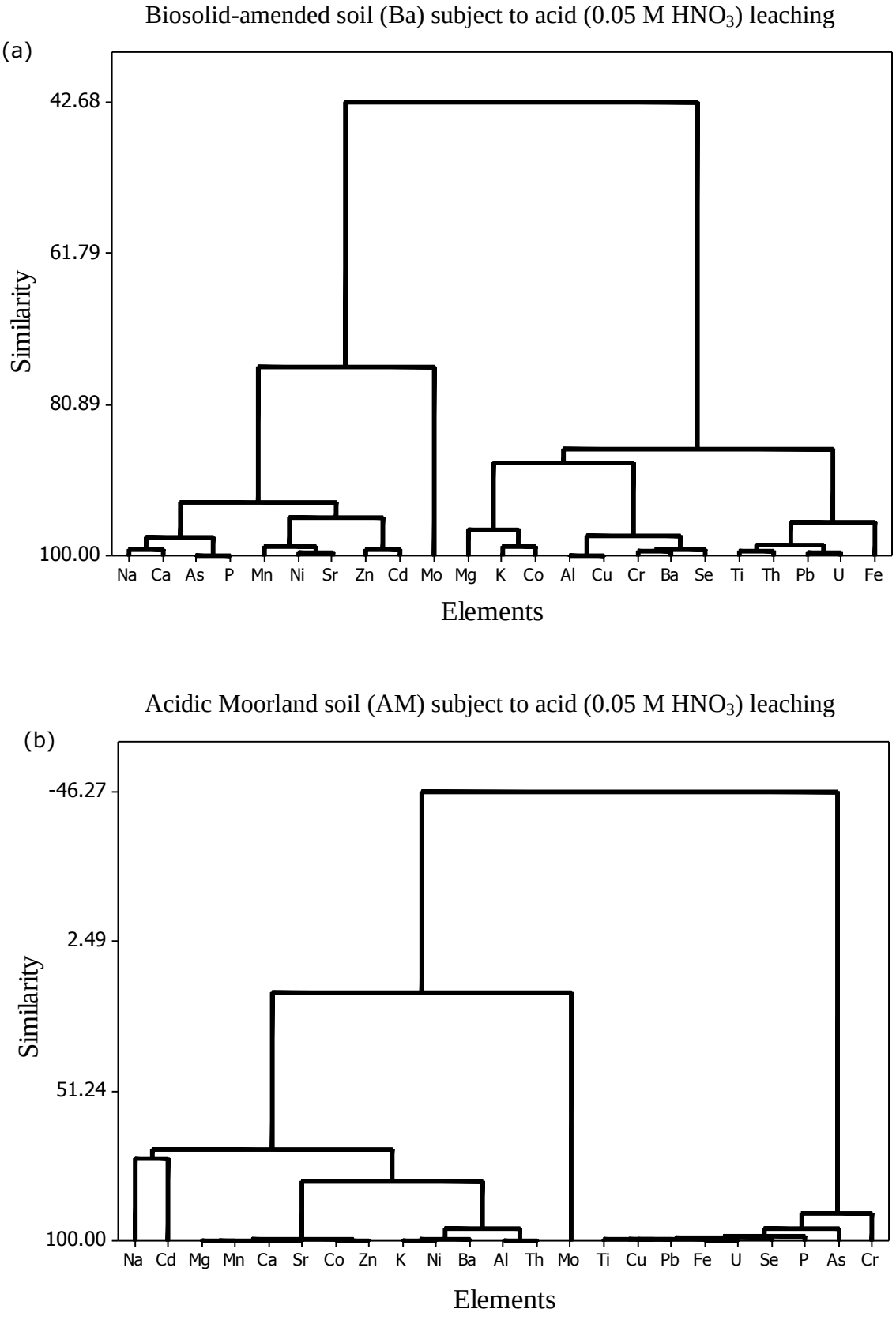

Figure 5.2: Dendrogram obtained by cluster analysis of released metals from (a) Ba and (b) AM soils leached with 0.05 M HNO_3 after removing the exchangeable cations with 1 M NH_4NO_3; n = 110 collected fractions.

Ammonium acetate continuous leaching

Tables 5.3 and 5.4 show the correlation matrices for metals released from the Ba and AM soils leached with 0.1 M CH_3COONH_4 (at pH 4.5). Metals released by CH_3COONH_4 from the Ba soil exhibited correlations with each other and with pH which differed from those derived from the HNO_3-released metal data. Most metals showed a negative correlation with the pH of leachates.

In the Ba soil, Th within the leachate was significantly negatively correlated with Al, Ba, Pb and U and positively correlated with Fe, Mn, Ti and P. Uranium was highly positively correlated with Pb and Ba and weakly positively correlated with Fe, Mn and P. In the AM soil, the strongest positive correlation was found between Th, Fe, Ti, P, Al and Cu and between U, Pb, Al and Ba. Th and U concentrations in the AM soil leachate were positively correlated, in contrast to the Ba soil. These correlations were supported by cluster analysis presented as a dendrogram (Figure 5.3). The cluster analysis of metals released from the Ba soil suggested two main groups (Figure 5.3a). The first group comprised two sub-clusters, one of which included the exchangeable cations Mg and K, while the other one was further sub-divided into four sub-clusters:

i. Ca, Ni, Sr
ii. P, Ti, Cr, Fe, As, Se
iii. Mn, Zn, Co, Cd, Cu and
iv. Th' on its own.

The second group also included two sub-clusters:

i. Al alone and
ii. Ba, Pb, U.

In the Ba soil, Th released by CH_3COONH_4 did not show a close association with any other metals (Figure 5.3); the Th concentrations in leachate were very low compared to those produced by acid leaching and may represent only an exchangeable Th fraction. Like Th, U did not show close association with other metals except Pb and Ba which again suggests geochemical association of U and Pb.

Cluster analysis of metals released from AM soil by CH_3COONH_4 leaching (Figure 5.3b) showed two main groups. The first group consisted of two sub-clusters, one of which included the exchangeable cations Mg and K, while the other one was further subdivided into two sub-clusters, mainly the alkaline-earth cations Ca, Sr and Mn and the trace metals Co, Zn, Ni, Cd, Ba, U and Pb. The second group also consisted of two sub-clusters, one of which included Cr alone whereas the other was further subdivided into two sub-clusters associated with oxide mineralogy and the anions adsorbed on oxides respectively:

i. Al, Ti, Fe, Cu, Th and
ii. P, As, Se.

The strong correlation/grouping of Th, Fe and P (Table 5.4, Figure 5.3b) may indicate the presence of Th-phosphate-Fe (III) oxide ternary surface complexes (Zhang et al., 2006, 2007; Guo et al., 2005); however, the grouping of Th and Cu also suggests adsorption to humus surfaces. Nitric acid leaching of the AM soil did not show a similar association of Th with Fe and P; Th concentrations released by nitric acid were very low compared to those released by acetate and might explain the differences in association.

Table 5.3: Correlation matrix for the metals released and solution pH of the Biosolid-amended (Ba) soil leached with 0.1 M CH_3COONH_4; n = 110 collected fractions; P-values < 0.05 except where marked with an asterisk.

	Na	Mg	K	Ca	Al	P	Ti	Cr	Mn	Fe	Co	Ni	Cu	Zn	As	Se	Sr	Cd	Ba	Pb	Th	U
Mg	0.55																					
K	0.76	0.87																				
Ca	0.53	0.85	0.85																			
Al	-0.71	-0.65	-0.55	-0.66																		
P	0.25	0.52	0.35	0.75	-0.77																	
Ti	0.33	0.56	0.44	0.81	-0.78	0.99																
V	0.95	0.53	0.64	0.53	-0.85	0.44	0.49															
Cr	0.25	0.47	0.35	0.74	-0.75	0.99	0.98															
Mn	0.23	0.66	0.40	0.76	-0.79	0.96	0.95	0.94														
Fe	0.21	0.47	0.33	0.74	-0.72	0.99	0.98	1.00	0.93													
Co	0.30	0.72	0.50	0.83	-0.79	0.96	0.96	0.93	0.99	0.93												
Ni	0.43	0.76	0.64	0.93	-0.80	0.94	0.96	0.92	0.94	0.92	0.97											
Cu	0.37	0.65	0.46	0.80	-0.85	0.98	0.98	0.96	0.98	0.95	0.98	0.96										
Zn	0.16[a]	0.60	0.29	0.65	-0.78	0.93	0.90	0.90	0.99	0.89	0.96	0.87	0.95									
As	0.43	0.62	0.55	0.87	-0.80	0.97	0.98	0.96	0.92	0.95	0.95	0.98	0.97	0.85								
Se	0.58	0.68	0.63	0.88	-0.87	0.92	0.95	0.92	0.88	0.90	0.92	0.97	0.95	0.81	0.98							
Rb	0.57	0.89	0.94	0.97	-0.56	0.57	0.64	0.56	0.61	0.55	0.70	0.82	0.64	0.49	0.73	0.76						
Sr	0.45	0.83	0.74	0.97	-0.75	0.87	0.91	0.86	0.89	0.85	0.94	0.99	0.91	0.81	0.94	0.94						
Cd	0.26	0.74	0.50	0.83	-0.76	0.94	0.94	0.91	0.99	0.91	1.00	0.97	0.97	0.96	0.92	0.89	0.94					
Ba	-0.74	-0.05*	-0.37	-0.29	0.57	-0.29	-0.34	-0.36	-0.14*	-0.31	-0.17*	-0.29	-0.30	-0.08*	-0.40	-0.49	-0.25	-0.09*				
Pb	-0.89	-0.21	-0.45	-0.30	0.70	-0.27	-0.32	-0.29	-0.17*	-0.24	-0.20	-0.31	-0.33	-0.13*	-0.39	-0.51	-0.27	-0.14*	0.92			
Th	0.81	0.57	0.63	0.69	-0.90	0.69	0.74	0.70	0.65	0.67	0.68	0.75	0.76	0.59	0.78	0.86	0.71	0.64	-0.71	-0.79		
U	-0.73	0.03*	-0.41	-0.06*	0.16*	0.27	0.18*	0.22	0.38	0.26	0.31	0.13*	0.22	0.46	0.07*	-0.06*	0.10*	0.36	0.78	0.77	-0.38	
pH	0.86	0.10*	0.34	0.10*	-0.54	0.03*	0.09*	0.04*	-0.04*	-0.01*	-0.01*	0.08*	0.12*	-0.07*	0.17*	0.31	0.05*	-0.07*	-0.78	-0.93	0.65	-0.79

Table 5.4: Correlation matrix for the metals released and solution pH of the Acid Moorland (AM) soil leached with 0.1 M CH_3COONH_4; n = 110 collected fractions; P-values < 0.05 except where marked with an asterisk.

	Na	Mg	K	Ca	Al	P	Ti	Cr	Mn	Fe	Co	Ni	Cu	Zn	As	Se	Sr	Cd	Ba	Pb	Th	U
Mg	0.56																					
K	0.69	0.96																				
Ca	0.46	0.92	0.82																			
Al	0.63	0.84	0.79	0.93																		
P	0.82	0.61	0.65	0.69	0.89																	
Ti	0.66	0.72	0.69	0.84	0.97	0.95																
Cr	0.45	0.29	0.30	0.33	0.43	0.48	0.45															
Mn	0.48	0.96	0.87	0.99	0.91	0.67	0.81	0.32														
Fe	0.73	0.78	0.77	0.87	0.98	0.96	0.99	0.46	0.85													
Co	0.41	0.85	0.75	0.98	0.96	0.73	0.88	0.36	0.95	0.89												
Ni	0.44	0.84	0.74	0.96	0.96	0.75	0.89	0.40	0.93	0.90	0.99											
Cu	0.75	0.68	0.68	0.78	0.94	0.98	0.98	0.48	0.75	0.98	0.81	0.83										
Zn	0.42	0.84	0.73	0.97	0.96	0.74	0.90	0.37	0.94	0.89	1.00	0.99	0.83									
As	0.80	0.65	0.69	0.71	0.90	0.99	0.95	0.46	0.70	0.96	0.74	0.76	0.98	0.75								
Se	0.85	0.66	0.70	0.70	0.88	0.97	0.91	0.47	0.69	0.94	0.71	0.74	0.95	0.72	0.96							
Sr	0.47	0.91	0.81	1.00	0.94	0.71	0.86	0.34	0.99	0.88	0.98	0.96	0.80	0.98	0.73	0.72						
Cd	0.11*	0.34	0.25	0.52	0.50	0.37	0.47	0.18	0.48	0.46	0.55	0.53	0.44	0.55	0.39	0.32	0.53					
Ba	0.31	0.78	0.65	0.95	0.92	0.67	0.85	0.33	0.92	0.84	0.99	0.97	0.77	0.99	0.68	0.65	0.96	0.58				
Pb	0.18*	0.64	0.50	0.87	0.86	0.62	0.81	0.31	0.81	0.78	0.94	0.93	0.72	0.95	0.62	0.57	0.88	0.58	0.98			
Th	0.77	0.71	0.71	0.80	0.95	0.99	0.98	0.48	0.78	0.99	0.83	0.84	1.00	0.84	0.98	0.96	0.81	0.43	0.78	0.72		
U	0.43	0.75	0.64	0.92	0.97	0.81	0.94	0.39	0.88	0.92	0.97	0.97	0.88	0.98	0.81	0.77	0.93	0.57	0.98	0.96	0.88	
pH	-0.90	-0.19*	-0.34	-0.13*	-0.39	-0.74	-0.52	-0.39	-0.14*	-0.55	-0.12*	-0.16*	-0.64	-0.14*	-0.71	-0.74	-0.15*	0.00*	-0.04*	0.04*	-0.64	-0.22

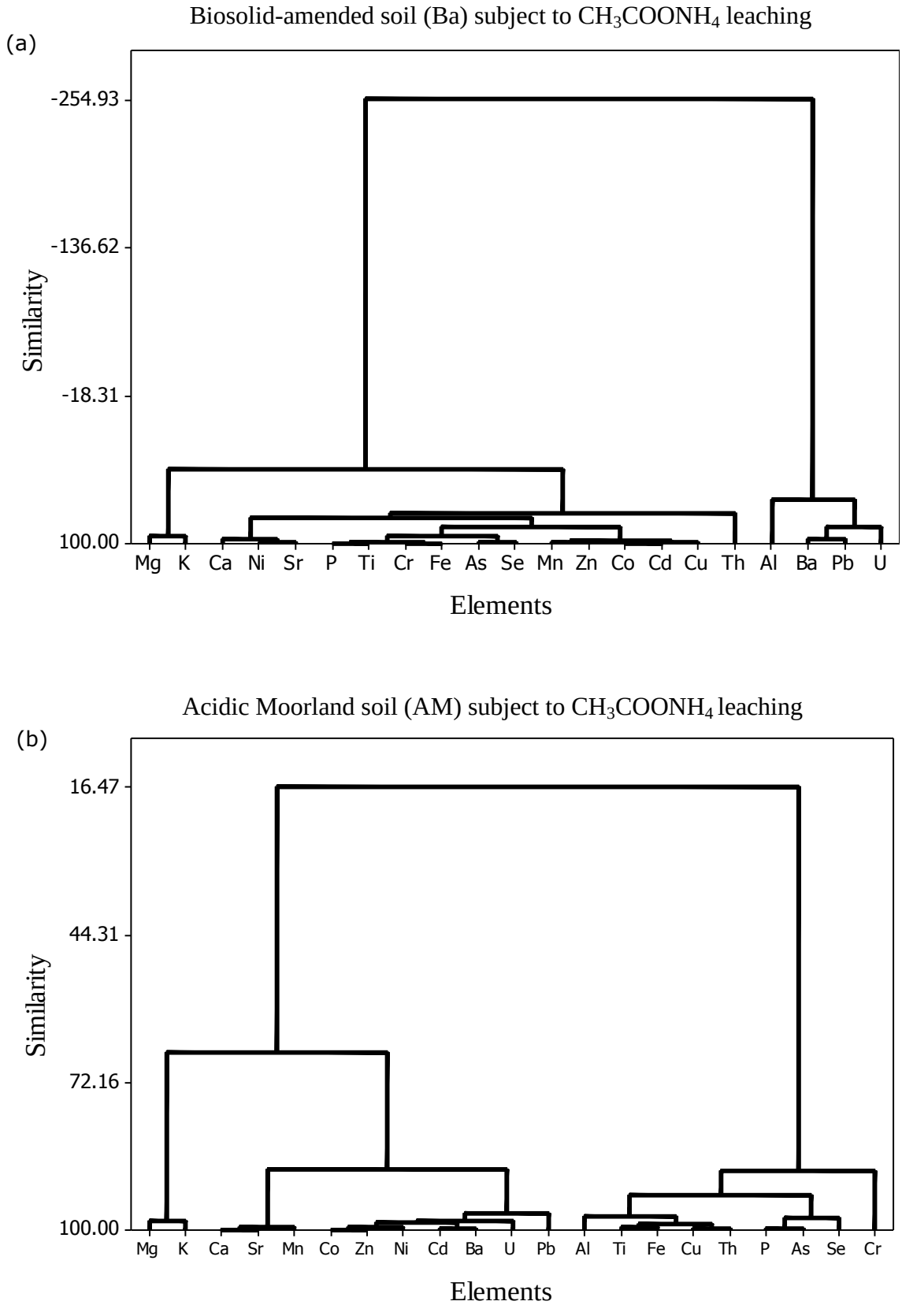

Figure 5.3: Dendrogram obtained by cluster analysis of released metals from (a) Ba and (b) AM soils leached with CH_3COONH_4; n = 110 collected fractions.

5.3.2 Release patterns of U and Th

5.3.2.1 Nitric acid continuous leaching; release patterns of U and Th

The simultaneous monitoring of the release of U, Th and some major and trace elements from soil solid phases can be used to describe how U and Th are bound to the soil. Metals bound to surface exchangeable sites would dissolve more quickly than the metals in the same soil fraction and hence generate a distorted release pattern (Buanuam et al., 2005, 2006). Therefore, only the data obtained from acid leaching of soils initially washed with NH_4NO_3 (to remove the exchangeable metal fraction) are presented. Figures 5.4a and b show the release patterns of U, Th, Fe, Al, Ca and P in the Ba and AM soils continuously leached with 0.05 M HNO_3 for 27 hr. The release pattern for Ca is not shown for the AM soil because almost all the soil Ca had been removed by prior leaching with NH_4NO_3.

In the Ba soil, U, Th and Fe had similar release patterns (Figure 5.4a) and they were correlated to the same degree (r = 0.95; Table 5.1). The similar rate of release and the significant correlation suggest a close association between these metals. Thorium and U exhibited different release patterns to those of Ca and P.

The rate of U and Th release from Ba soil

Figure 5.5a shows the *rate* of U and Th release from the Ba soil as a function of the cumulative amount released. The rate of release showed an initial rapid decline for U and Th in the first 50 pore volumes (the first 2 hr of leaching time (27 hr)), followed by a constant rate of release until 8 hr (200 pore volumes) and finally a gradual and continuous decline in release rate up to the end of the experiment (Figure 5.5a). For U, the initial fast decline in leaching may represent the labile (isotopically exchangeable) U as shown in Figure 5.5a, while the gradual decline may represent the U fraction associated with the resistant solid phase. The resistant solid phase may be Fe-oxide as Fe has a similar release pattern to that of U; the highly 'buffered' region (constant rate of release) between the previous two zones may represent the gradual erosion of occluded U in Fe-oxides. Iron oxide appears effectively to buffer the release of U in response to nitric acid leaching until that supply is exhausted and the rate of U release then declines. The Th released from the Ba soil was less than for the batch-extracted Th (Th_{TMAH}) by a factor of 5.6. TMAH mobilises all organically-complexed Th, by

solubilising humic and fulvic acid complexed Th, whereas the acid leaching is quite ineffective at solubilising inorganic Th and causes flocculation of humic and fulvic acid at the extremely low pH values.

In the AM soil leached continuously with 0.05 M HNO_3 for 27 hr, U, Fe and P had similar rates of release with a rapid initial decline followed by a more gradual decrease as available reserves were depleted (Figure 5.4b); all three elements were significantly correlated to the same degree (r = 0.99; Table 5.2). The similar release patterns and close correlation are consistent with the presence of mixed U(VI)-phosphate-Fe(III) oxide compounds. Thorium and Al exhibited similar release patterns (Figure 5.4b) and a close correlation (r = 1.0, Table 5.2), suggesting association of Th with clay or Al hydrous oxides.

The rate of U and Th release from AM soil

Figure 5.5b shows the rate of U and Th release from the AM soil as a function of cumulative amount released. The rate of release showed an initial rapid decline of U and Th concentrations in the first 8 and 4 hr, respectively, followed by a gradual decrease in the concentrations of U and Th released with time (Figure 5.5b). In contrast to the trend shown for the Ba soil there was no obvious 'buffer' region but rather a continuous decline in release rate. By the end of the experiment, cumulative U and Th released were less than U_E and Th_{TMAH} although extending the leaching time slightly would have released the entire labile U fraction (U_E; Figure 5.5b). By contrast, the amount of Th solubilised was much less than the batch-extracted Th (Th_{TMAH}) by a factor of 53.

Biosolid-amended soil (Ba) subject to acid (0.05 M HNO_3) leaching after prewashing with NH_4NO_3

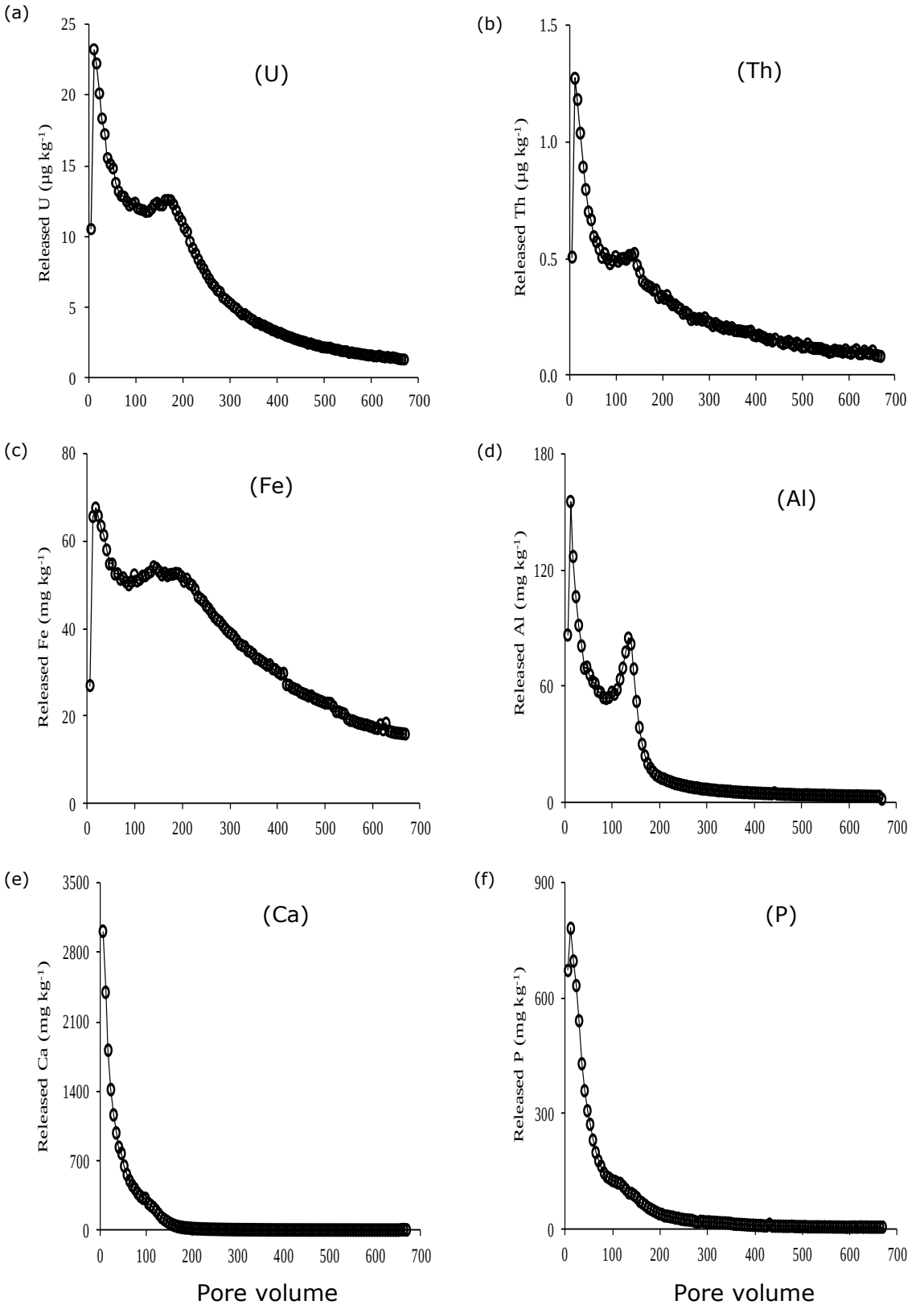

Figure 5.4a: Release patterns of (a) U (µg kg^{-1}), (b) Th (µg kg^{-1}), (c) Fe (mg kg^{-1}), (d) Al (mg kg^{-1}), (e) Ca (mg kg^{-1}) and (f) P (mg kg^{-1}) from the Biosolid-amended (Ba) soil subject to 0.05 M HNO_3 leaching.

Acidic Moorland soil (AM) subject to acid (0.05 M HNO_3) leaching after prewashing with NH_4NO_3

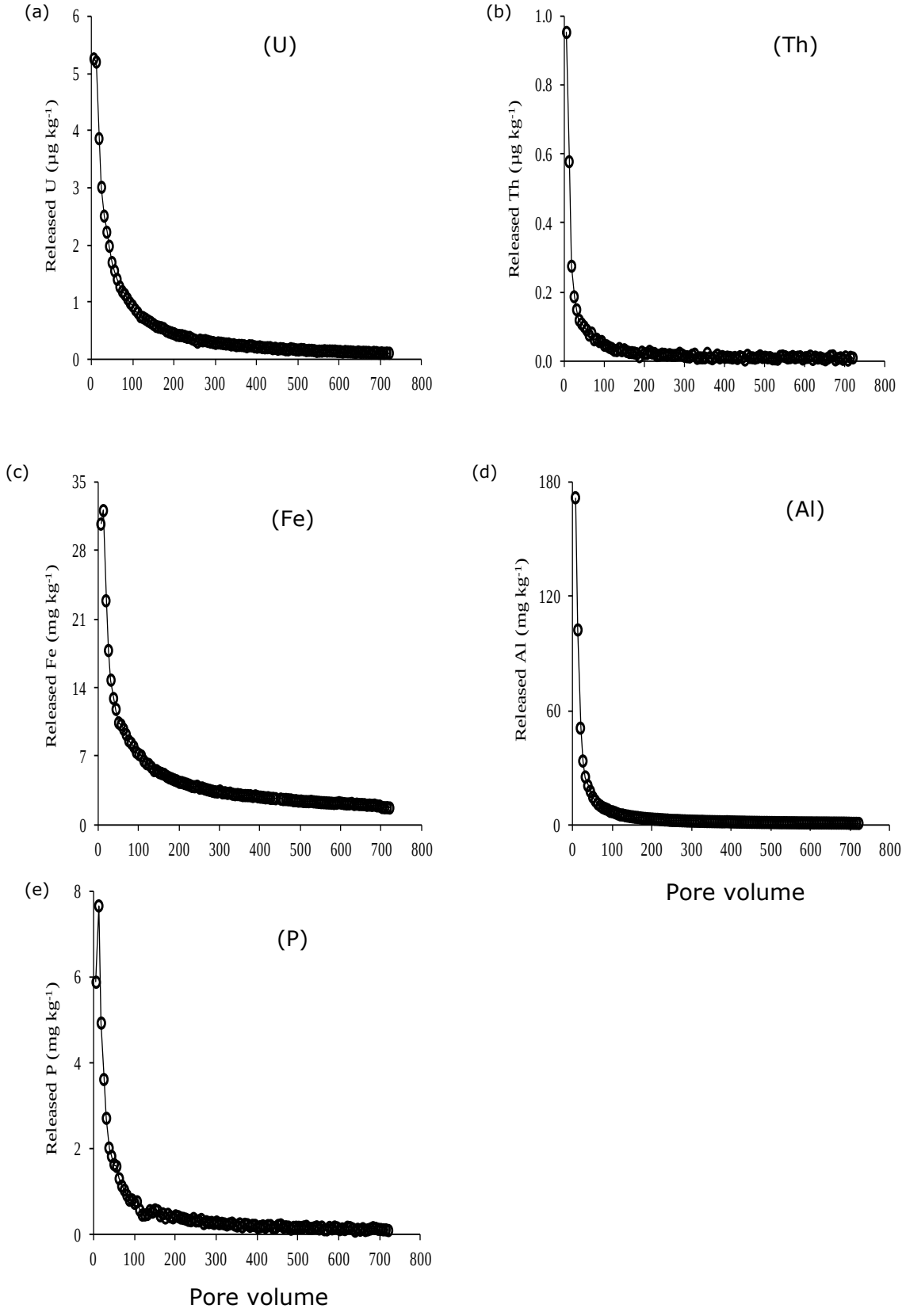

Figure 5.4b: Release patterns of (a) U (µg kg^{-1}), (b) Th (µg kg^{-1}), (c) Fe (mg kg^{-1}), (d) Al (mg kg^{-1}) and (e) P (mg kg^{-1}) from Acidic Moorland (AM) soil subject to 0.05 M HNO_3 leaching.

Biosolid-amended soil (Ba) subject to acid (0.05 M HNO_3) leaching after prewashing with NH_4NO_3

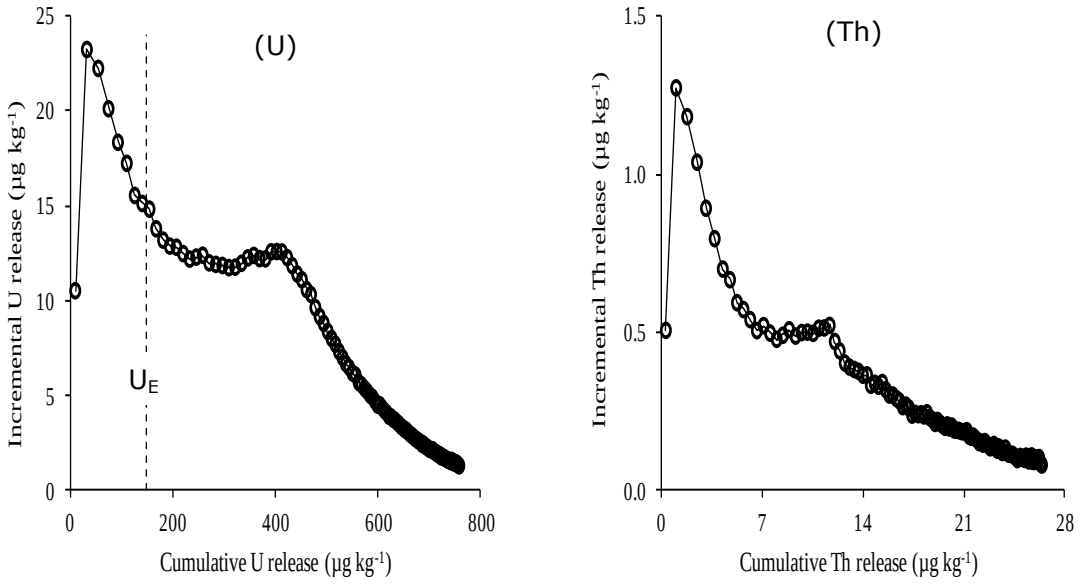

Figure 5.5a: Incremental U and Th release from the Biosolid-amended (Ba) soil as a function of cumulative U and Th (µg kg^{-1}) release by leaching with 0.05 M HNO_3. The dashed line represents labile U ($U_{E)}$ value on the X-axis.

Acidic Moorland soil (AM) subject to acid (0.05 M HNO_3) leaching after prewashing with NH_4NO_3

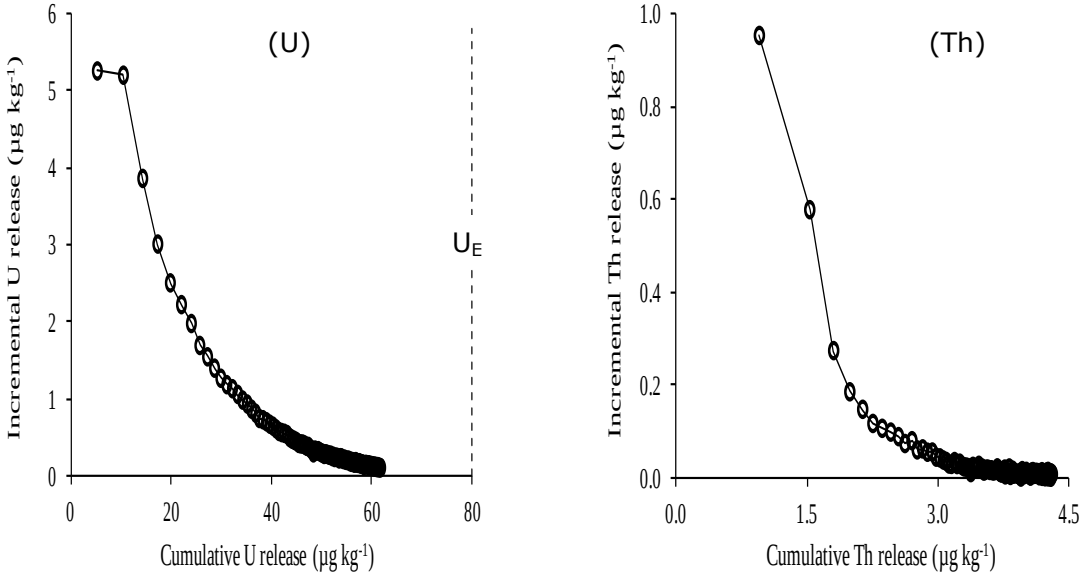

Figure 5.5b: Incremental U and Th release from the Acid Moorland (AM) soil as a function of cumulative U and Th (µg kg^{-1}) release by leaching with 0.05 M HNO_3. The dashed line represents labile U ($U_{E)}$ value on the X-axis.

5.3.2.2 Ammonium acetate continuous leaching; release patterns of U and Th

Figures 5.6a and b show the release patterns of U, Th, Fe, Al, Ca and P in the Ba and AM soils continuously leached with 0.1 M CH_3COONH_4 (pH 4.5) for 27 hr. In AM soil, Ca was detected only in the first 427 pore volumes.

In the Ba soil, the release patterns of U, Th, Fe and Al were different (Figure 5.6a), in agreement with the lack of correlation between U, Fe and Al and the negative correlation between U and Th in the Ba soil (Table 5.3); Th was also negatively correlated with Al and weakly correlated with Fe. Uranium and Th also exhibited different release patterns to those of Ca and P. The low cumulative released Fe and Al concentrations (52 and 144 mg kg^{-1}) compared to nitric acid leaching released concentrations (3600 and 2517 mg kg^{-1}) may explain the lack of similarity between U, Th, Fe and Al release patterns and also the lack of close correlations. In addition, the total concentration of Th released by the end of the leaching experiment was very low compared with the acid leached Th concentration.

The rates of U and Th release from Ba soil

Figure 5.7a shows the rates of U and Th release from the Ba soil as a function of cumulative released amounts. The rate of U release showed an initial rapid increase in U concentration in the first 17 pore volumes, followed by a slow decrease in release rate up to, and beyond, depletion of the labile U pool. The rate of Th release showed an initially fast decline over the first 134 pore volumes (the first 5 hr of leaching time), followed by a relatively constant (and low) rate of release. The cumulative Th released by the end of the experiment was 93× less than batch-extracted Th (Th_{TMAH}).

In the AM soil leached continuously with 0.1 M CH_3COONH_4 (pH 4.5) for 27 hr, U and Al exhibited similar release patterns (Figure 5.6b) and a close correlation (r = 0.97; Table 5.4), suggesting U association with clay or Al hydrous oxides. On the other hand, Th, P and Fe displayed similar release patterns (Figure 5.6b) and were significantly correlated to the same degree (r = 0.99; Table 5.4). Again, the similar release pattern and close association suggests the presence of Th-phosphate-Fe(III) oxides compounds (Zhang et al., 2006, 2007). These results contradict the nitric acid leaching data in which Th and Al and U, P and Fe exhibited similar release patterns.

This may be due to differences in the efficiency of each leaching solution for U and Th. For example, U released by ammonium acetate was 3 times less than that solubilised by nitric acid while the ammonium acetate-released Th concentration was 9.3 times greater than the nitric acid-released Th.

The rate of U and Th release from AM soil

Figure 5.7b shows the rates of U and Th release from the AM soil as a function of cumulative release. The rates of U and Th release showed an initially rapid increase over the first 19 pore volumes, followed by a fast decline until approximately 107 pore volumes, and finally a gradual decline with time (Figure 5.7b). Cumulative released U and Th concentrations were 3.2× and 5.7× less than U_E and Th_{TMAH}, respectively.

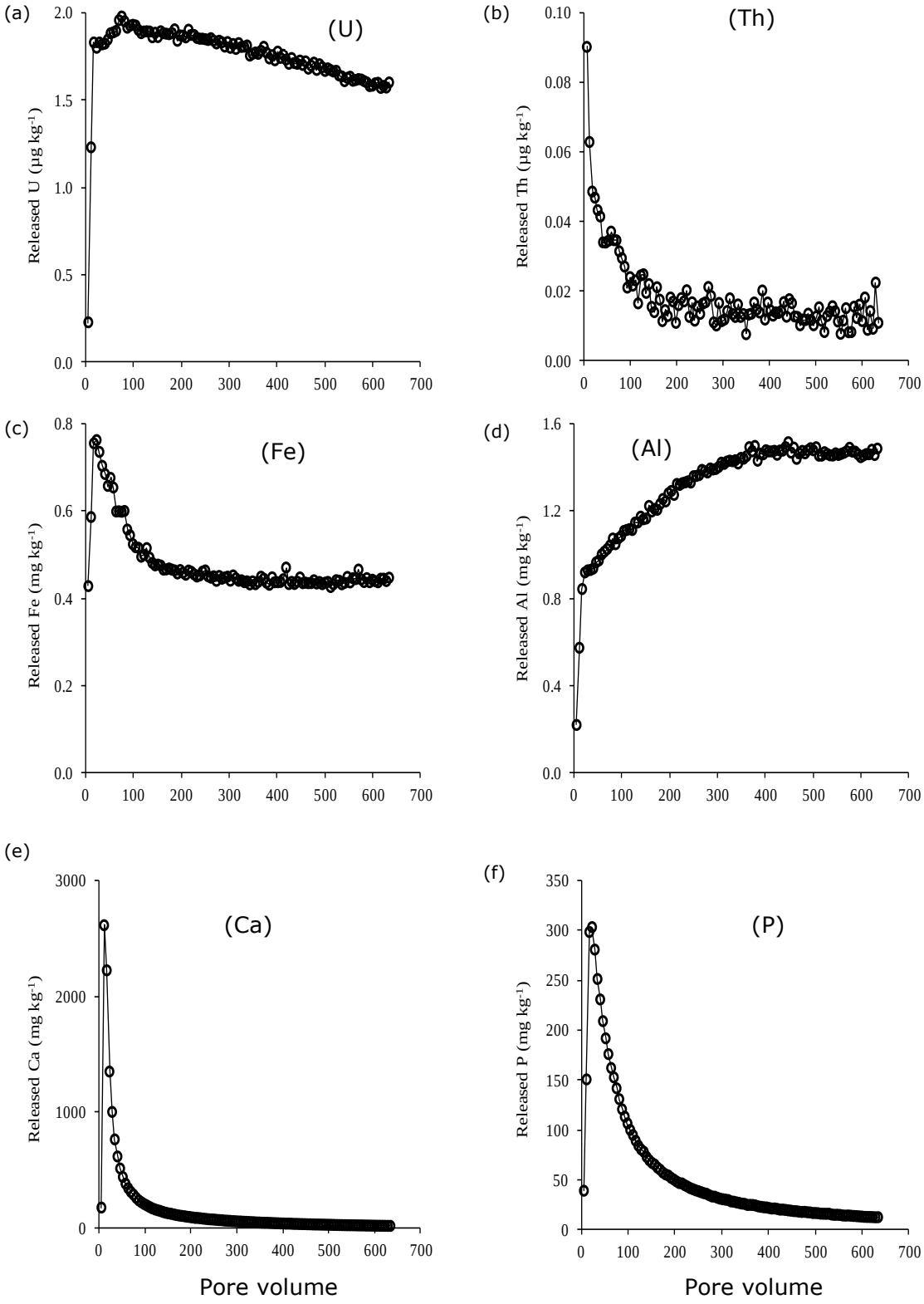

Figure 5.6a: Release patterns of (a) U (µg kg^{-1}), (b) Th (µg kg^{-1}), (c) Fe (mg kg^{-1}), (d) Al (mg kg^{-1}), (e) Ca (mg kg^{-1}) and (f) P (mg kg^{-1}) from the Biosolid-amended (Ba) soil subject to 0.1 M CH_3COONH_4 (pH 4.5) leaching.

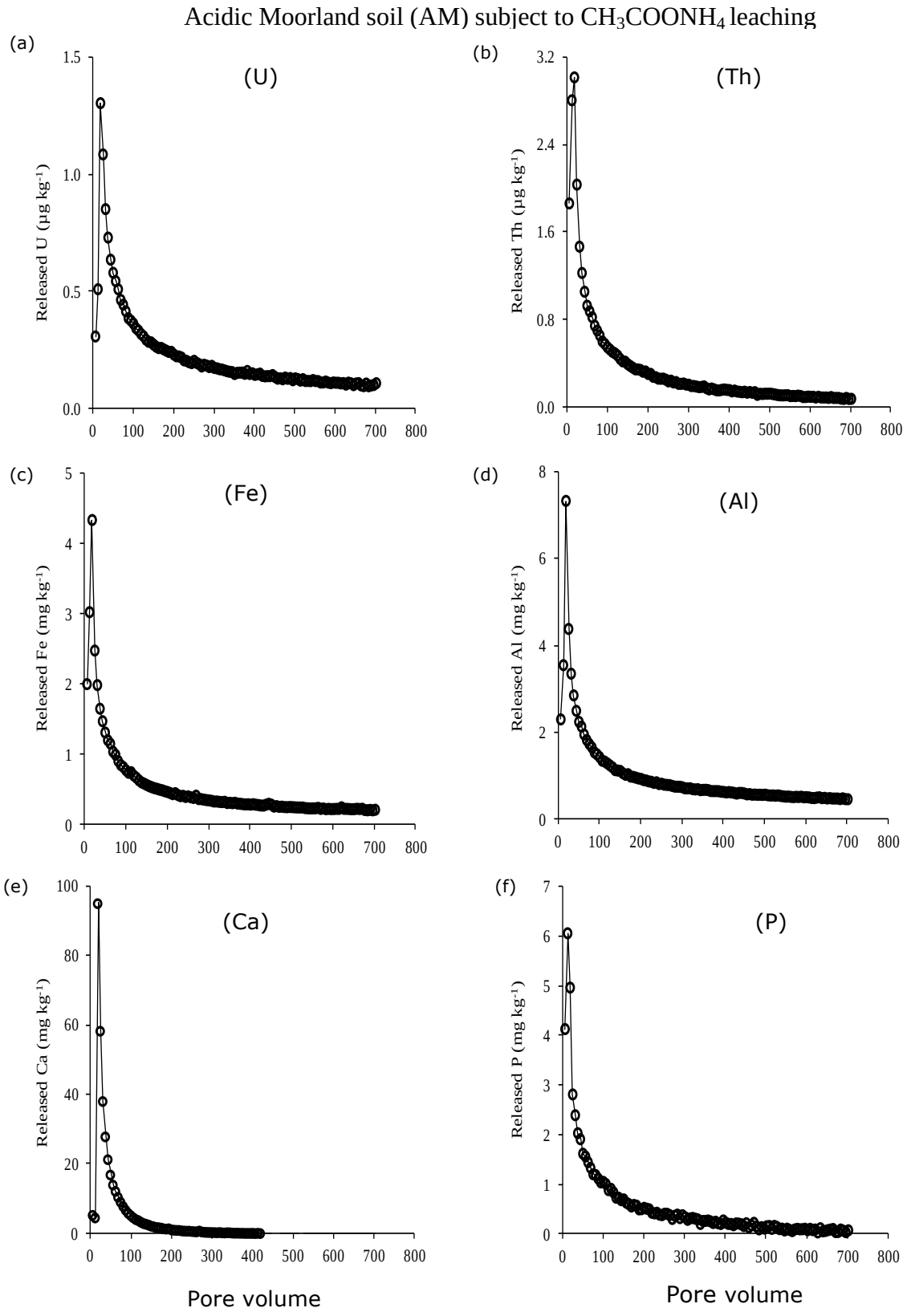

Figure 5.6b: Release patterns of (a) U (µg kg^{-1}), (b) Th (µg kg^{-1}), (c) Fe (mg kg^{-1}), (d) Al (mg kg^{-1}) and (e) P (mg kg^{-1}) from the Acidic Moorland (AM) soil subject to 0.1 M CH_3COONH_4 (pH 4.5) leaching.

Biosolid-amended soil (Ba) subject to CH_3COONH_4 leaching

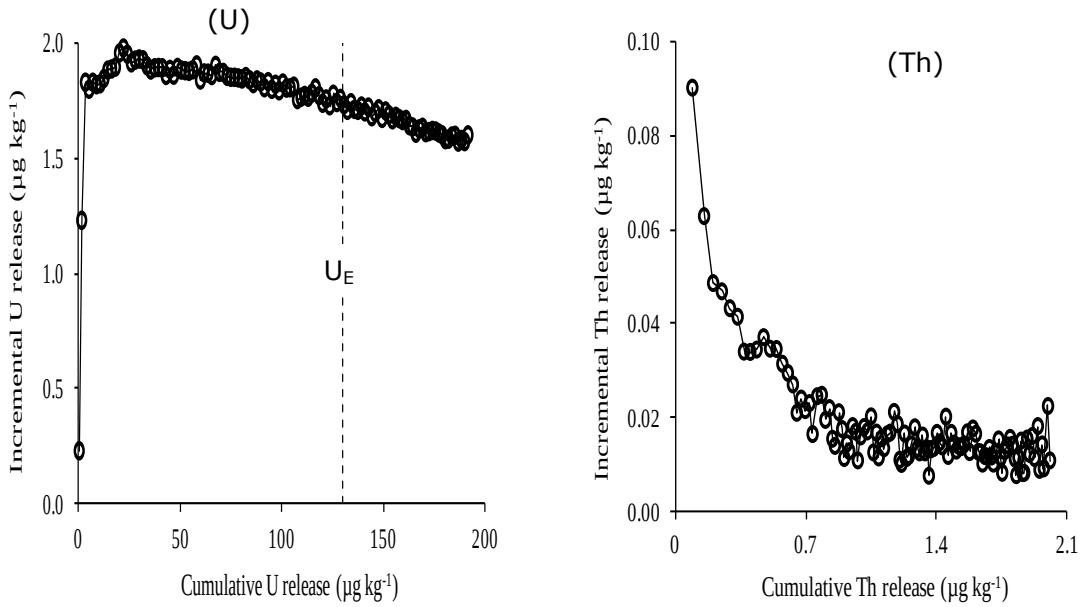

Figure 5.7a: Incremental U and Th release from the Biosolid-amended (Ba) soil as a function of cumulative U and Th (µg kg-1) release by leaching with 0.1 M CH3COONH4 (pH 4.5). The dashed line represents labile U (UE) value on X-axis.

Acidic Moorland soil (AM) subject to CH_3COONH_4 leaching

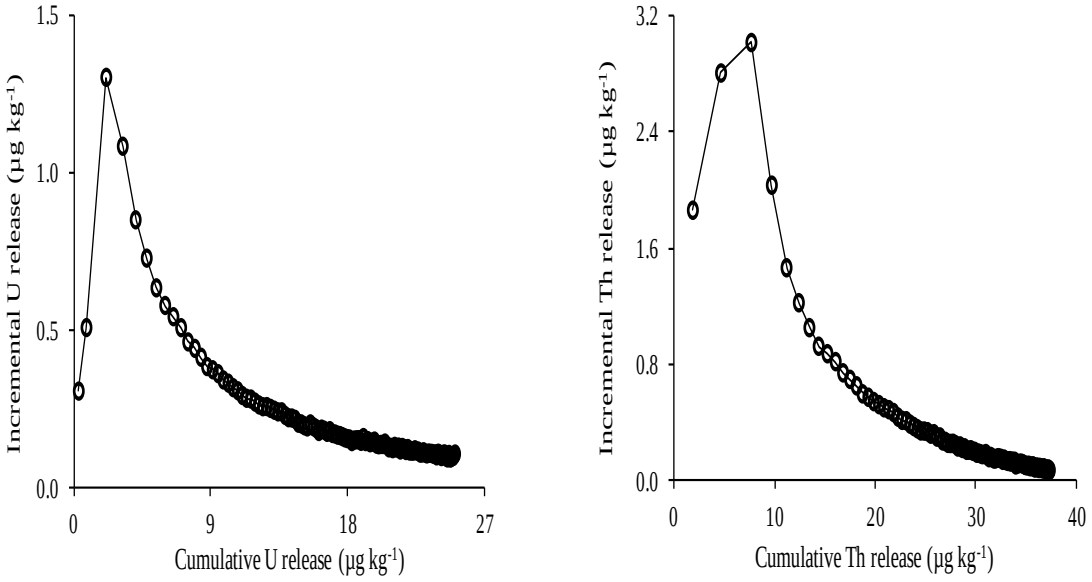

Figure 5.7b: Incremental U and Th release from the Acidic Moorland (AM) soil as a function of cumulative U and Th (µg kg^{-1}) release by leaching with 0.1 M CH_3COONH_4 (pH 4.5).

5.3.2.3 Elemental ratios

Figure 5.8 shows concentration ratios of elements of interest versus the pore volume in the Ba and AM soils continuously leached with 0.05 M HNO_3. In the Ba soil, the elemental ratio of As/P was almost constant for all pore volumes and ranged from 0.99 to 1.03 (Figure 5.8a), indicating the strong association of As and P as would be expected. This result indicates that the continuous leaching approach is a valid and useful means for studying the associations between elements. Uranium in column leachate was present in an approximately 1:1 ratio with Pb (U/Pb varied from 0.97 to 1.02), strongly suggesting a similar association which would be expected to reside in Fe oxides. If U and Pb associate with Fe-oxide, then the high (and nearly equal) U/Fe and Pb/Fe ratios in the early leached fractions and the following gradual decline in ratios with leaching time as shown in Figure 5.8a suggest surface adsorption of U and Pb on Fe-oxides; progressive dissolution of U and Pb reveals underlying Fe-oxide and so the U/Fe and Pb/Fe ratios in solution decline. Although the Th/Fe ratio was less than the U/Fe and Pb/Fe ratios, it followed the same trend also indicating surface adsorption of Th on Fe-oxides. The higher ratio of U/Fe and Pb/Fe than Th/Fe may reflect the industrial origin of U and Pb.

In the AM soil, the elemental concentration ratios (Figure 5.8b) confirm the information obtained from elemental correlation and release patterns. The ratio of Th/Al was almost constant for all pore volumes and varied in the range 1.0 - 1.04 (Figure 5.8b), indicating association of Th with clay or Al hydrous oxides. On the other hand, uranium was present in an approximately 1:1 ratio with P, strongly suggesting a similar association which may be with Fe-oxides. The U/Fe and P/Fe ratios were high in the early leached fractions then declined to the same degree as leaching proceeded. This could indicate the initial release of a surface complex followed by progressive dissolution of Fe-oxide is dissolved as leaching continued. In the Ba and AM soils, adsorption of U on Fe-oxides can be observed. The U/Fe ratio was high in Ba soil compared with AM soil, particularly in the early released fractions, which may indicate some U enrichment in the Ba soil due to the continuous application of sewage sludge. Buanuam et al. (2005) studied the fractionation and elemental association of Zn, Cd and Pb in 79 soils near a Zn mining area using a continuous-flow approach. Soils were divided into 4 groups according to their total

metal content. The authors used elemental ratio plots as a tool for identification of the anthropogenic origin and degree of contamination; the higher the degree of contamination, the higher the Cd/Fe and Pb/Fe elemental ratios in the earlier fractions due to the surface adsorption of Cd and Pb on Fe-oxides.

Biosolid-amended soil (Ba) subject to acid (0.05 M HNO_3) leaching after prewashing with NH_4NO_3

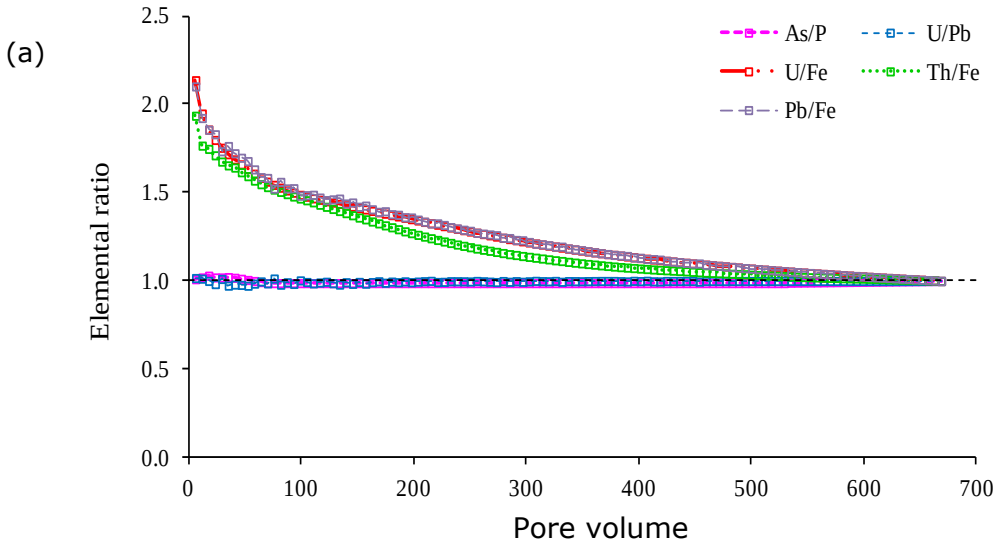

Acidic Moorland soil (AM) subject to acid (0.05 M HNO_3) leaching after prewashing with NH_4NO_3

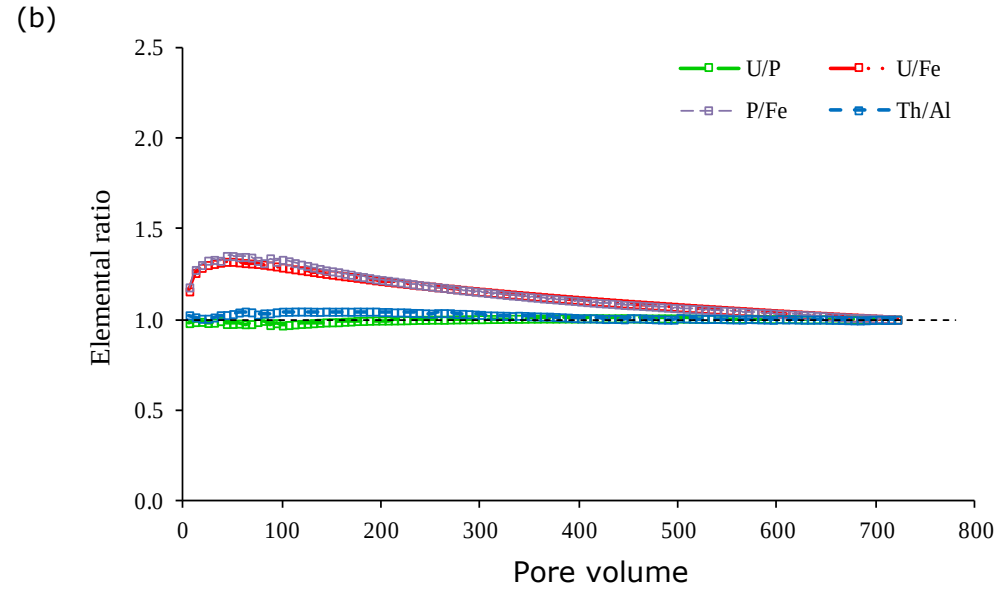

Figure 5.8: Elemental atomic ratio plotted against pore volume in (a) Biosolid-amended and (b) Acidic Moorland soils subject to 0.05 M HNO_3 leaching.

5.3.3 Comparison of U and Th with labile (U_E) and M_{Ext} (M_{Ac}, M_{Nit}, M_{EDTA}, M_{TMAH})

In this section the pattern of solubilised U and Th concentrations from Ba and AM soils subject to continuous leaching with 0.05 M HNO_3 are compared with the fixed U and Th concentrations obtained using batch extraction techniques or isotopic dilution. Figures 5.9 and 5.10 show cumulative U and Th released from the Ba and AM soils by continuous leaching with 0.05 M HNO_3. The labile U (U_E) and the concentrations of U and Th extracted by four batch single extraction methods using 1.0 M CH_3COONH_4 (M_{Ac}), 0.05 M EDTA (M_{EDTA}), 0.43 M HNO_3 (M_{Nit}) and 1% TMAH (M_{TMAH}) (see Chapter 4 for details) are also shown in Figures 5.9 and 5.10 for comparison with continuously leached U and Th.

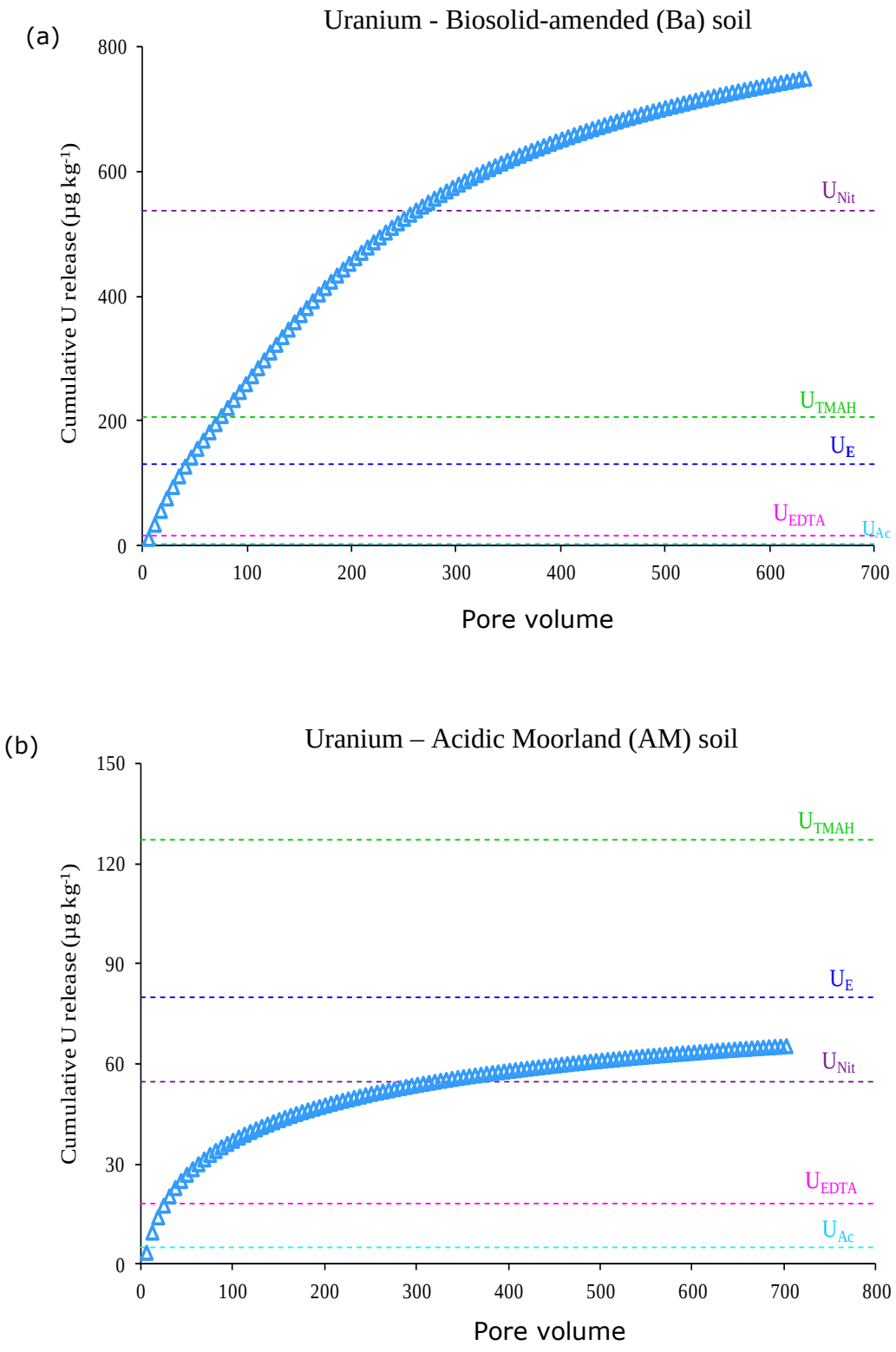

Figure 5.9: Cumulative U (µg kg^{-1}) released from (a) Biosolid-amended (Ba) and (b) Acidic Moorland (AM) soils continuously leached with 0.05 M HNO_3. The labile U (U_E) and U batch-extracted by 1.0 M CH_3COONH_4 (U_{Ac}), 0.05 M EDTA (U_{EDTA}), 0.43 M HNO_3 (U_{Nit}) and 1% TMAH (U_{TMAH}) are shown for comparison.

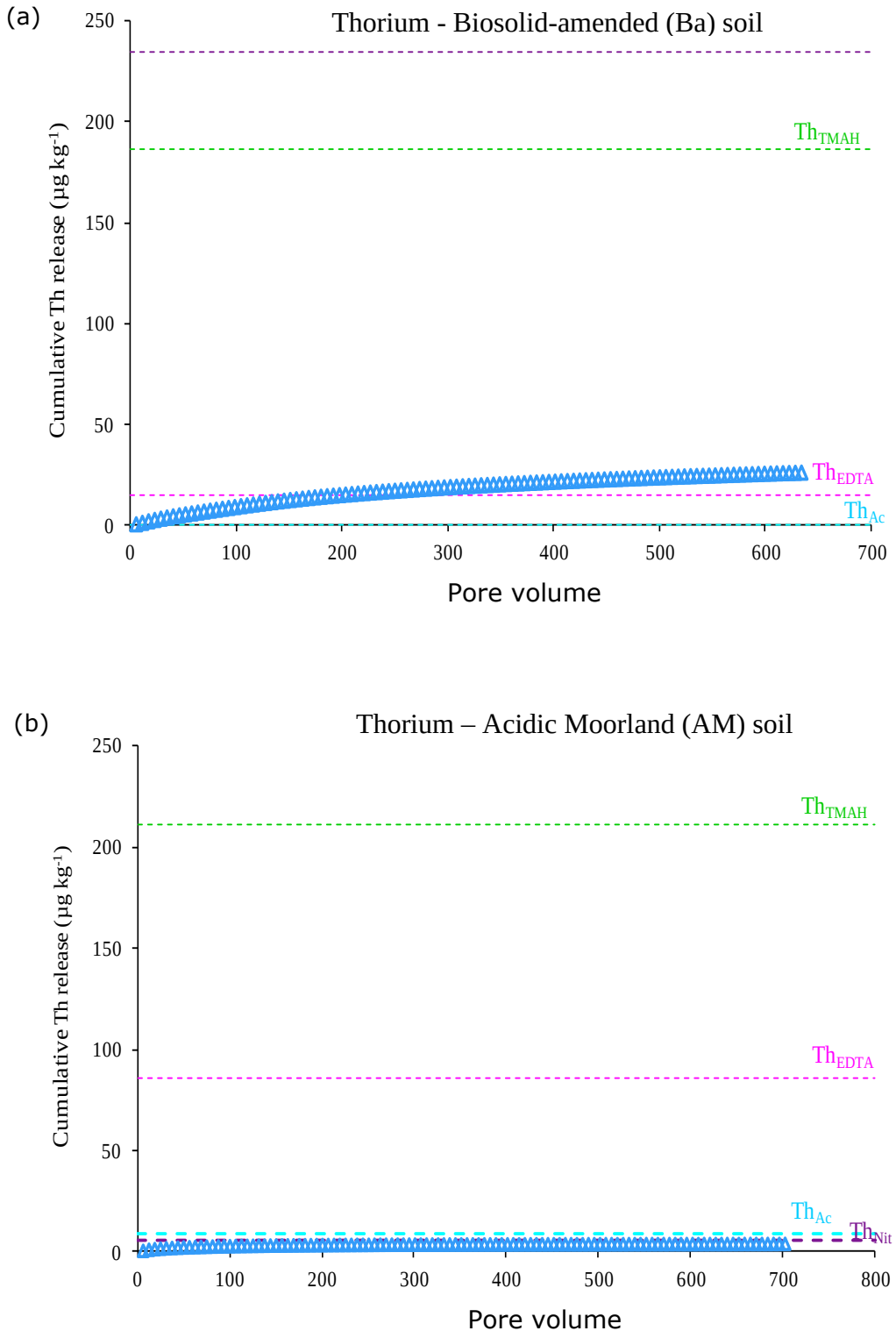

Figure 5.10: Cumulative Th (µg kg^{-1}) released from (a) Biosolid-amended (Ba) and (b) Acidic Moorland (AM) soils continuously leached with 0.05 M HNO_3. The concentration of Th batch-extracted by 1.0 M CH_3COONH_4 (U_{Ac}), 0.05 M EDTA (U_{EDTA}), 0.43 M HNO_3 (U_{Nit}) and 1% TMAH (U_{TMAH}) are shown for comparison.

Comparison of U released by continuous leaching with U_E and U_{Ext} (U_{Ac}, U_{EDTA}, U_{Nit}, U_{TMAH})

Towards the end of the continuous leaching experiment the cumulative U released from AM soil (Figure 5.9) is moving towards the U_E and it is expected that extending the leaching time would have released the entire labile U fraction. The AM soil is a highly weathered sandy soil; U(VI) adsorbed to the mineral surfaces leaches easily while that adsorbed in the micropores or sequester in the sand particles needs more leaching time. In the AM soil all the acid-leached U is labile, whereas in the Ba soil the labile U (U_E) is released in the early leached fractions (the first 8 fractions; Figure 5.9a). This indicates the presence of layers of occluded U in Ba soil held in mineral form, possibly associated with phosphate and Fe-oxides which effectively buffers release of U in response to acid leaching. The Ba soil is rich in secondary phosphate and iron minerals, perhaps produced during the sludge processing, and it might be expected that the U and Th are occluded within these minerals to a greater extent than in the AM soil. Although the cumulative U released from the Ba soil by the end of the leaching experiment was higher than the U concentration obtained by other approaches, it represented only 31% of the total U concentration (U_{tot} = 2.44 mg kg^{-1}).

Comparison of Th released by continuous leaching with Th_{Ext} (Th_{Ac}, Th_{EDTA}, Th_{Nit}, Th_{TMAH})

Figure 5.10 shows the resistance of Ba and AM soil-bound Th to solubilisation by nitric acid. In the Ba soil, while eventually the nitric acid leaching might solubilise as much as EDTA complexation it will never release the Th fraction solubilised by TMAH. In addition, the cumulative Th released from AM soil was much less than Th solubilised by EDTA and TMAH and it appears that nitric acid leaching will never release the Th fractions solubilised by EDTA and TMAH. This suggests very strong bonding of reactive Th to humus, particularly in AM soil, and confirms the weakness of nitric acid as a Th extractant as it causes flocculation of humic and fulvic acid at the extremely low pH values.

5.4 CONCLUSIONS

A continuous leaching method was used to study fractionation and elemental associations of U and Th in two contrasting soils. Compared with batch extraction procedures, the leaching approach dissolves the solid phases sequentially by continuous leaching. It therefore provides more information than single extraction methods on the leaching kinetics, the different sources and associations of metals in soils and the potential reactivity of metals under environmental conditions. The results obtained demonstrate the feasibility of the continuous leaching approach with respect to the simultaneous determination of multiple elements and the evaluation of leaching 'fingerprints'. However, explaining the results with respect to different solid phase fractions is difficult.

The correlation of elements and leaching patterns obtained from the continuous leaching approach revealed close association between U, Pb, Th and Fe in Ba soil and close association between Th, Al and U, P, Fe in AM soil. The rate of U release from Ba and AM soils and the comparison of U released by continuous leaching with U_E showed that all the acid-leached U in AM soil was labile, while in Ba soil the labile U was released in the early leached fractions. These results indicated the presence of layers of occluded U in Ba soil held in mineral form, possibly associated with phosphate and Fe-oxides which effectively buffered release of U in response to acid leaching until that supply was exhausted and the rate of release then declined. The Ba soil is rich in secondary phosphate and iron minerals, perhaps produced during the sludge processing, so it might be expected that the U and Th are occluded within these to a greater extent than in the AM soil.

The data from concentration ratios of U/Fe, Pb/Fe and Th/Fe in Ba soil and U/Fe, P/Fe and Th/Al in AM soil confirm the information obtained from elemental correlation and release patterns; U, Pb and Th appear to be adsorbed on the surface of Fe-oxides in Ba soil, while in AM soil U and P are adsorbed on the surface of Fe-oxides suggests the presence of mixed U(VI)-phosphate-Fe(III) oxide compounds. The U/Fe ratio in Ba soil was high compared to that in AM soil, particularly in the early released fractions, which may indicate U enrichment in the Ba soil due to the continuous application of sewage sludge to the soil.

In both Ba and AM soils the resistance of soil-bound Th to solubilisation by nitric acid was remarkable. It was clear that while eventually the nitric acid leaching might solubilise as much as EDTA complexation it will never release the Th fraction solubilised by TMAH, which suggests very strong bonding of reactive Th to humus.

6 SOLUBILITY AND MOBILITY OF THORIUM AND URANIUM IN SOILS: THE EFFECT OF SOIL PROPERTIES ON THORIUM AND URANIUM CONCENTRATIONS IN SOIL SOLUTION

6.1 INTRODUCTION

Metals exist in soil in different solid-phase forms that vary considerably in terms of mobility and bioavailability; therefore, total concentrations of metals are poor indicators of metal toxicity (Nolan et al., 2003; Clemente et al., 2008). The total dissolved metal or free metal ion concentration in soil solution is acknowledged to be a better indicator of metal bioavailability and toxicity than the total soil metal concentration. Soil solution chemistry provides valuable information about mobility, bioavailability and geochemical cycling of elements in soils. The chemical composition of soil solution is influenced by soil geocolloidal mineralogy, soil characteristics such as pH and Eh, complexation by organic and inorganic ligands, ionic strength and ion competition (Tack, 2010). Soil solution characteristics also depend on the extraction technique used (Tiensing et al., 2001). A thorough understanding of the dynamics of Th and U in soils is required to allow accurate long-term predictions of their mobility. The solid-liquid distribution coefficient (K_d) has been used in risk assessments as a quantitative indicator of environmental mobility of elements in soil. In the literature, most K_d values are derived from spiking experiments; this is often called the 'sorption' K_d value. By contrast, the native K_d (desorption K_d) has the advantage that the soil is more likely to be at equilibrium even for very slow reactions (Sheppard et al. 2009). In nuclear waste risk assessment, native K_d values may be the most applicable, especially for assessment of radionuclides with very long half-lives such as ^{232}Th and ^{238}U. The K_d values for U and Th can vary over several orders of magnitude and are highly dependent on bulk soil characteristics and soil solution geochemistry (EPA 1999; Thibault et al., 1990; Sheppard et al., 2009). Thus, for example, it is well known that pH and carbonate concentration are the two most important factors that influence U K_d values. Uranium speciation is largely a function of pH, which explains the linear correlation found between U log K_d values and pH (Echevarria et al., 2001; Vandenhove et al; 2007a; Sheppard et al., 2009). The U K_d has been shown to increase by five orders of magnitude in the pH range from acidic to neutral (Davis et al., 2004; Curtis et al.,

2006; Um et al., 2010). However, at higher pH values the U K_d declines sharply due to soluble carbonate complex formation (Kohler et al., 2004; Curtis et al., 2006). In contrast to U, there is scarce information on how soil physico-chemical characteristics affect Th mobility and speciation. Therefore, there is a pressing need to investigate the soil factors that determine Th mobility and both solid phase fractionation and liquid phase speciation in soils. Although Th and U K_d values are extremely variable, they vary systematically with key soil variables (Sheppard et al., 2009).

To study and predict the solid-solution partitioning of U and Th in soil, empirically derived relationships can be used. Empirical models relate the partitioning of metal (K_d) to soil properties and usually take the form of a multivariate, linear relationship between logK_d and soil properties (e.g. Sauvé et al., 2000; Degryse et al., 2009). Empirical models based on native K_d are more representative for field conditions and, arguably, provide a better description of metal chemistry than models derived from adsorption studies (Degryse et al., 2003; Sheppard et al., 2009). Although the empirical models require little input data, they should not be used outside the ranges of input data used to derive them (Kohler et al., 2004; Degryse et al., 2009).
In the work reported in this chapter U and Th concentrations in soil solution were measured under aerobic conditions. The soil K_d values were determined, from measured U and Th solubilities, compared with literature values and correlated with soil properties. Free ion activities of Th^{4+} and UO_2^{2+} were predicted using a simple empirical model and a limited number of soil properties.

The primary objectives of this study were therefore to:

(iv) investigate the dominant soil properties controlling U and Th solubility in soils and rank them according to their relative influence to try to reduce the uncertainty linked with the soil K_d values used in risk assessment models;

(v) develop a simple model to predict free ion activities of Th^{4+} and UO_2^{2+};

(vi) compare predictions of U and Th K_d values that are based either on total metal concentrations or on measured reactive metal fractions.

6.2 MATERIALS AND METHODS

6.2.1 Soil samples

In this study, two soil sets were used. The first set (Field Soils) consisted of thirty seven soil samples representing five contrasting local ecosystems; the second dataset (BGSc) included 40 soils sub-sampled from the British Geological Survey (BGS) archive. Both datasets covered a wide range of soil characteristics. The origins and characteristics of these two sets of soils have been described in Chapters 2 and 4.

6.2.2 Soil solution

For Field Soils, soil pore water was extracted from fresh moist soils (< 4 mm) using *Rhizon* soil moisture samplers. Soil pore water samples were collected daily over a period of 6 days in order to measure Th and U concentrations (Th_{pw}, U_{pw}) (see Section 2.3.1 for details). Concentrations of U were also measured in 0.01 M $Ca(NO_3)_2$ soil suspensions (soil : solution ratio 1 g : 20 ml) equilibrated for 7 days as the equilibration time used for measuring E-values. In the second soil set (BGSc), dissolved U and Th concentrations were measured in 0.01 M $Ca(NO_3)_2$ soil suspensions (soil : solution ratio 1 g in 10 ml) shaken for 3 days to reach equilibrium (Section 2.3.2). The concentrations of U in $Ca(NO_3)_2$ extracts may differ from those in pore water extracted from soil columns due to differences in Ca concentration, pH and soil : solution ratio. Degryse et al. (2003, 2009, 2011) suggested that dilute salt extracts provide a good proxy for *in situ* soil solutions and 0.01 M Ca electrolytes has been widely used in this context. Therefore, in the current study, U concentrations in soil solution (U_{pw}) were compared with U concentrations in 0.01 M $Ca(NO_3)_2$ extracts (U_{ext}).

6.2.3 Modelling Th and U free ion activities (FIA) in solution using a multiple linear regression approach

A multiple linear regression model was used to predict the free ion activity of Th^{4+} and UO_2^{2+} in the soil solution (Equation 6.1). It takes into account the labile adsorbed metal concentration in soil, the effect of soil pH and organic matter content (%SOM). The predicted Th^{4+} and UO_2^{2+} activities were compared with the solution

concentrations of these species predicted by WHAM-VII (Section 2.7). The details of WHAM-VII model settings and variables are given in Section 7.2.2.

$$log_{10}(Th^{4+}) \text{ or } log_{10}(UO_2^{2+}) = K_0 + K_{pH}\,(pH) + K_{SOM}\,(\%SOM) + K_{Lab}\,(M_{Lab}) \qquad (6.1)$$

In Equation 6.1, $\log_{10}(Th^{4+})$ and $\log_{10}(UO_2^{2+})$ are the free Th and U activities on a $\log_{10}$ scale (mol L^{-1}); M_{Lab} is labile U concentration measured by ID with the Chelex resin purification step (U_E; Section 2.6.4) or TMAH extracted Th (Th_{TMAH}; Section 2.4.1), (mol kg^{-1}). The data analysis tool *'Solver'* in Microsoft® Excel was used to optimize parameters in the empirical model to find the lowest residual standard deviation value (RSD) between and the two sets of predicted values of free ion activity.

6.2.4 Modelling the solid-liquid distribution coefficient (K_d, K_d^{lab}, $^*K_d^{lab}$) using a multiple linear regression approach

The K_d expresses the distribution of an element between the solid and solution phases within a soil:

$$K_d = \frac{M_{tot}}{M_{soln}} \qquad (6.2)$$

Where M_{tot} is the total U or Th concentration (mg kg^{-1}) in the solid phase and M_{soln} is the concentration of U or Th (mg L^{-1}) in the soil solution at equilibrium with the solid phase. The total U or Th concentration in the solid phase includes both the 'fixed' and 'labile' metal pools and so using them to describe metal partitioning results in higher K_d values than would result from consideration of only U or Th which is actively involved in a dynamic equilibrium between the solid and solution phases. Therefore, K_d can be expressed based on the measured labile metal pool rather than total metal concentration:

$$K_d^{lab} = \frac{M_{Lab}}{M_{soln}} \qquad (6.3)$$

The free metal ion in solution is the most reactive species for reaction and can be regarded as being in equilibrium with the adsorbed labile metal pool on the solid surfaces. Therefore, K_d can also be expressed as the partitioning between the labile metal pool and the free ion activity in equilibrium with this pool:

$$^{*}K_d^{lab} = \frac{M_{Lab}}{(M^{2+})} \quad (6.4)$$

Where M_{Lab} is the labile metal concentration (mol kg^{-1}) measured by isotopic dilution with the Chelex resin purification step (^{238}U E_{resin}; Section 2.6.4) for U and (as a proxy) by extraction with (e.g.) 1% TMAH for Th (Th_{TMAH}; Section 2.4.1). The free metal ion activity (UO_2^{2+}, Th^{4+}; mol L^{-1}) was calculated using WHAM-VII with inputs solely from the 'soil solution' composition – i.e. soil pore water for the Field soils and the 0.01 M $Ca(NO_3)_2$ extract for the BGSc set. A multiple linear regression model was then used to predict $log_{10}K_d$, $log_{10}K_d^{lab}$ or $log_{10}{}^{*}K_d^{lab}$ from available soil properties (pH, soil metal content (M_{soil}; mg kg^{-1}), %SOM, %clay, available phosphate (P-avail; mg kg^{-1}), Fe oxide content (mg kg^{-1}), $\%CaCO_3$, DOC and DIC (mg L^{-1})) according to the following equation:

$$log_{10}K_d,\ log_{10}K_d^{lab}\ or\ log_{10}{}^{*}K_d^{lab} = k_0 + k_1\,(pH) + k_2\,(M_{soil}) + k_3\,(\%SOM) + k_4\,(FeOx) + k_5\,(P\text{-}avail) + k_6\,(\%Clay) + k_7\,(\%CaCO_3) + k_8\,(DOC) + k_9\,(DIC) \quad (6.5)$$

The data analysis tool *'Solver'* in Microsoft® Excel was used to optimize parameters in the empirical model to find the lowest residual standard deviation value (RSD) between and the two sets of predicted values of the solid-liquid distribution coefficient.

6.3 RESULTS AND DISCUSSION

6.3.1 Soil solution chemistry: Th and U solubilities

Effect of time, DOC and DIC on Th and U solubilities

The soil pore water chemical composition can be influenced considerably by the extraction technique used and by the equilibration time applied after wetting the soil (Nolan et al., 2003). Rhizon samplers apply a low negative pressure to the soil, so that soil solution is extracted from the larger pores while the soil physical structure remains intact. Tiensing et al. (2001) and Nolan et al. (2003) reported that Rhizon samplers may be the more suitable technique for assessing the bioavailable fraction of metals in soils by sampling the pore water extracted by plants. Tiensing et al. (2001) recommended the use of Rhizon samplers in ecotoxicity studies. In the current study, Th and U solubilities were measured through time under aerobic conditions in five soil groups (Ar, AW, Ca, AM and Ba; n = 37). Figures 6.1a, b and c show the variation in Th, U, DOC and DIC concentration in the pore waters of Ar, AW, Ca, AM and Ba soils with time. Concentrations of DOC covered a wide range in soils (12 – 418 mg L^{-1}), DOC concentrations were greatest in the topsoils of AM and AW soils (400 mg L^{-1}) and decreased markedly with soil depth to reach 12 mg L^{-1} in AM subsoil. Concentrations of DIC varied from 8 to 119 mg L^{-1} (Figure 6.1), with the highest average values in Ca (94 ± 22 mg L^{-1}) and Ar soils (78 ± 27 mg L^{-1}) followed by Ba (34 ± 10 mg L^{-1}) soil. Solution concentrations of Th and U ranged from 0.001 to 4.02 µg L^{-1} and from 0.002 to 2.94 µg L^{-1}, respectively. The average (± std. dev.) soluble Th in each soil category (Figure 6.1) followed the order: Ba (0.003±0.002 µg L^{-1}) < Ca (0.013±0.007 µg L^{-1}) < Ar (0.028±0.023 µg L^{-1}) < AM (1.27±1.30 µg L^{-1}) < AW (1.46±0.68 µg L^{-1}). By contrast, the concentration of U in solution followed the sequence: Ba (0.081±0.094 µg L^{-1}) < AM (0.13±0.104 µg L^{-1}) < AW (0.22±0.106 µg L^{-1}) < Ar (0.39±0.37 µg L^{-1}) < Ca (1.47±1.27 µg L^{-1}). The results show a variation in Th and U solubilities within each soil category and with time; this variation was consistent with changes in either DOC or DIC concentrations. Figures 6.1a, b and c show a wider range of soluble Th concentrations in AM and AW soils than in other soils (Ar, Ca and Ba). There were greater Th concentrations in the pore water of AM, AW and Ar topsoils than in subsoils, producing a significant positive correlation between Th concentration and both SOM and DOC in these soils ($r > 0.90$, $P < 0.001$).

Pore water Th and DOC concentrations in the Ar soil were lower than in AM and AW soils, though both Th and DOC concentrations were fairly constant with time; this may be attributed to the large buffering capacity of the SOM in the Ar soil. In the calcareous-woodland soil (Ca-W), pore water Th and DOC concentrations were twice those in Ca-Ar and Ca-G soils; although the three Ca topsoils had the same parent material, the land use and/or soil characteristics appear to affect the solubility of Th. In contrast to Th, U concentration in Ca-Ar soil pore water was higher than in Ca-W and Ca-G, producing a significant correlation for dissolved U with SIC and DIC ($r > 0.85$, $P < 0.05$). As found for Th, there were greater pore water U concentrations in AM, AW and Ar topsoils than in subsoils producing a significant correlation for soluble U in AM and AW soils with SOM and DOC in both soils ($r > 0.85$, $P < 0.01$), and a positive correlation for dissolved U in the Ar soil with DIC ($r = 0.96$, $P > 0.05$). Soluble Th and U concentrations in AM and AW soils were significantly correlated ($r = 0.83$, $P < 0.001$) and both correlated with DOC.

Gooddy et al. (1995) measured the concentrations of 48 elements, including Th and U, in the soil solutions of two acid sandy humus-iron podzol profiles (the vegetation consisted of mature and widely spaced Scots pine; the first profile was between trees, the second profile was beneath a pine tree). Soil solutions were extracted from the fresh moist soils using the centrifuge drainage technique. It is therefore useful to compare Th and U concentrations in the AM soil pore water under Heather (*Calluna vulgaris)*, Birch (*Betula pendula)* and Pine *(Pinus sylvestris* L.) (see Section 4.2.1) with the results of Gooddy et al. (1995). Both studies showed depth-dependent changes for DOC, Th and U concentrations in the soil solution. Concentrations of Th and U in the pore water of AM soil profiles were highly correlated with DOC, in agreement with the trend for Th reported by Gooddy et al. (1995) but not for U, particularly in the first soil profile where U was almost uniformly distributed with depth. Thorium concentration in the soil solution was higher than U by an average factor of 8.7 and 5 in the AM and in the Gooddy et al. (1995) soil profiles, respectively. The DOC concentrations in both studies were large. Thus, for strongly organically-bound elements such as Th, complexation by DOC, which enhances Th in soil solution, will compete effectively with binding to SOM, which tends to remove Th from soil solution (Gooddy et al., 1995).

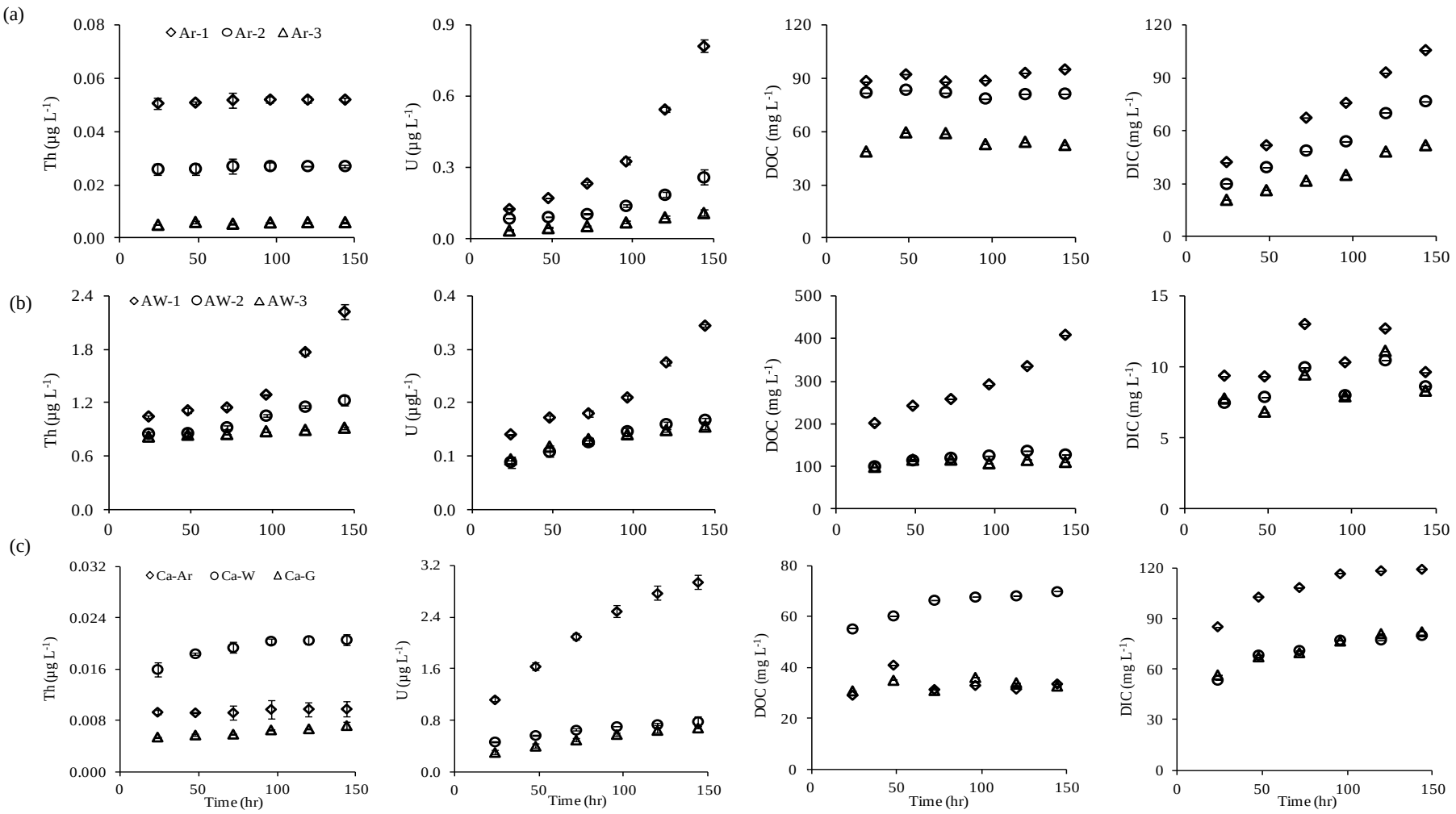

Figure 6.1a: The variation in concentrations of Th (µg L-1), U (µg L-1), dissolved organic and inorganic carbon (DOC and DIC; mg L-1) in soil pore water with incubation time (24, 48, 72, 96, 120 and 144 hr) in (a) Arable soil profile (Ar-1; 0-14 cm, Ar-2; 14-28 cm, Ar-3; 28-42 cm), (b) Acidic Woodland soil profile (AW-1; 0-12 cm, AW-2; 12-24 cm, AW-3; 24-36 cm) and (c) Calcareous topsoils (Arable; Ca-Ar, Woodland; Ca-W, Grassland; Ca-G).

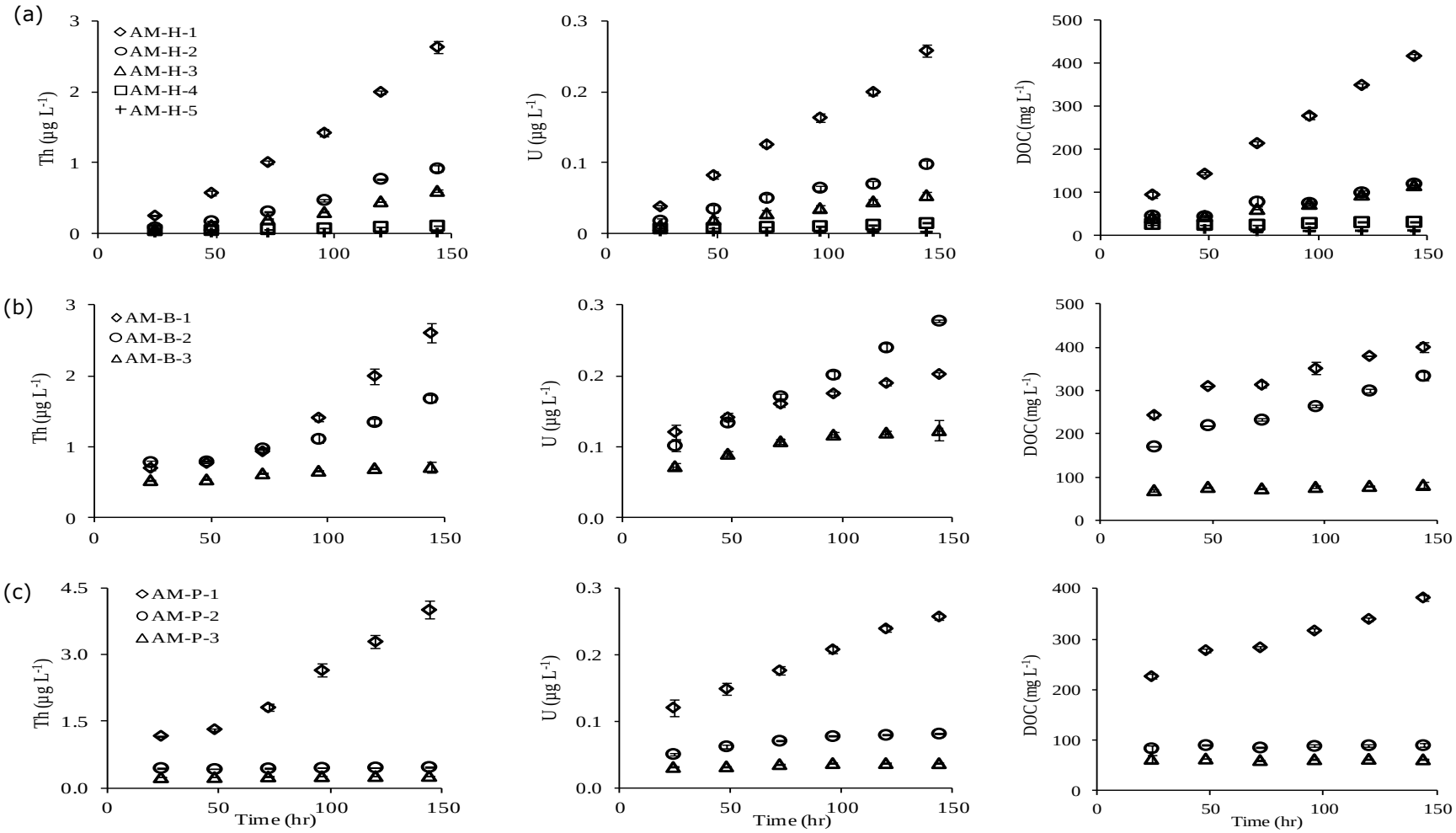

Figure 6.1b: The variation in concentrations of Th (µg L^{-1}), U (µg L^{-1}), dissolved organic and inorganic carbon (DOC and DIC; mg L^{-1}) in soil pore water with incubation time (24, 48, 72, 96, 120 and 144 hr) in an Acidic Moorland soil profile under three contrasting vegetation regimes: (a) *Calluna vulgaris* (AM-H-1; 2-8 cm, AM-H-2; 8-12 cm, AM-H-3; 12-14 cm, AM-H-4; 20-30 cm, and AM-H-5; 30-40 cm), (b) *Betula pendula* (AM-B-1; 0-8 cm, AM-B-2; 10-20 cm, and AM-B-3; 20-35 cm) and (c) *Pinus sylvestris* L. (AM-P-1; 11-15 cm, AM-P-2; 15-35 cm, and AM-P-3; 35-45 cm).

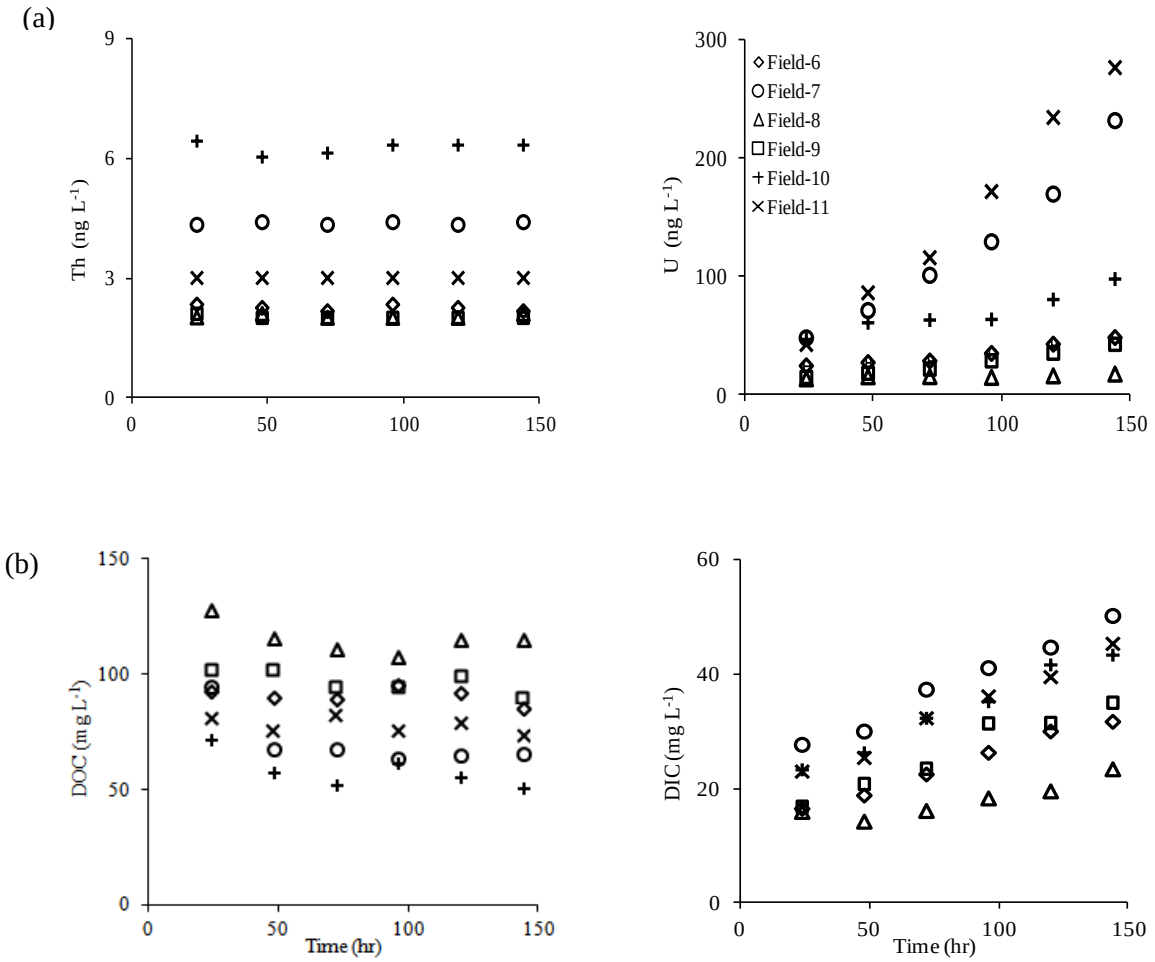

Figure 6.1c: The variation in concentrations of (a) Th and U (ng L^{-1}), (b) dissolved organic and inorganic carbon (DOC and DIC; mg L^{-1}) in soil pore water with incubation time (24, 48, 72, 96, 120 and 144 hr) in Biosolid-amended arable top soils with a range of historical sludge amendment levels: Field 6 (6A, 6B, 6C, and 6D), Field 7 (7A, and 7B), Field 8 (8A, 8B, 8C, 8D, 8E, and 8T), Field 9 (9A, and 9B), Field 10 (10A, and 10B) and Field 11 (11A).

Biosolid-amended arable soils (Ba)

Although the biosolid-amended soils (Ba) showed some indication of U enrichment (Section 4.3.1), they exhibited the lowest Th and U concentrations in soil solution and a narrow range of Th and U concentrations, particularly for Th, which was fairly constant with time (Figure 6.1c). This may be attributed to the relatively constant pH in these soils and their high SOM and extremely high phosphate concentrations. Both Th and U concentrations in soil solution were negatively correlated with DOC concentration, contrary to expectation, especially for Th (Figure 6.2, Table 6.1). In Ba soils (pH >6) U was expected to be positively correlated with DIC concentration due to the formation of uranyl carbonate complexes (Vandenhove et al., 2007a) (Figure 6.2b, Table 6.1). The negative correlation between Th and DOC may be explained by a higher humus content at higher concentrations of DOC; both SOM and DOC were significantly and positively correlated ($r = 0.72$, $P < 0.01$; Figure 6.3). The effects of SOM and DOC may be expected to work in opposition: DOC effectively competes with SOM for complex formation with metals. This would suggest that the stabilization or fixation effects of the SOM dominate over the mobilizing effects of the DOC in the soil solution. However, an alternative explanation may lie in the co-addition of organic matter and phosphate that results from sludge amendment of arable soils. Figure 6.4 shows Th and U concentrations in biosolid-amended arable soil solution as a function of %SOM and available phosphate. As expected, a significant positive correlation was found between %SOM and available phosphate ($r = 0.91$, $P < 0.001$) and soluble Th and U concentrations were negatively correlated with both %SOM and available phosphate (Table 6.1, Figure 6.4). It is possible that both high SOM and available phosphate contents contribute to the low Th and U concentration in soil solution (Vandenhove et al., 2007a; Taboada et al., 2006). In particular, high phosphate concentrations may lead to precipitation of both Th and U-phosphates (Koch-Steindl and Prohl, 2001; Zhang et al., 2006; Cheng et al., 2004; Arey et al., 1999) or enhance Th and U sorption through the formation of ternary surface complexes involving UO_2^{2+} or Th, PO_4^{3-} and Fe oxides (Payne et al., 1996; Vandenhove et al., 2007a; Zhang et al., 2006).

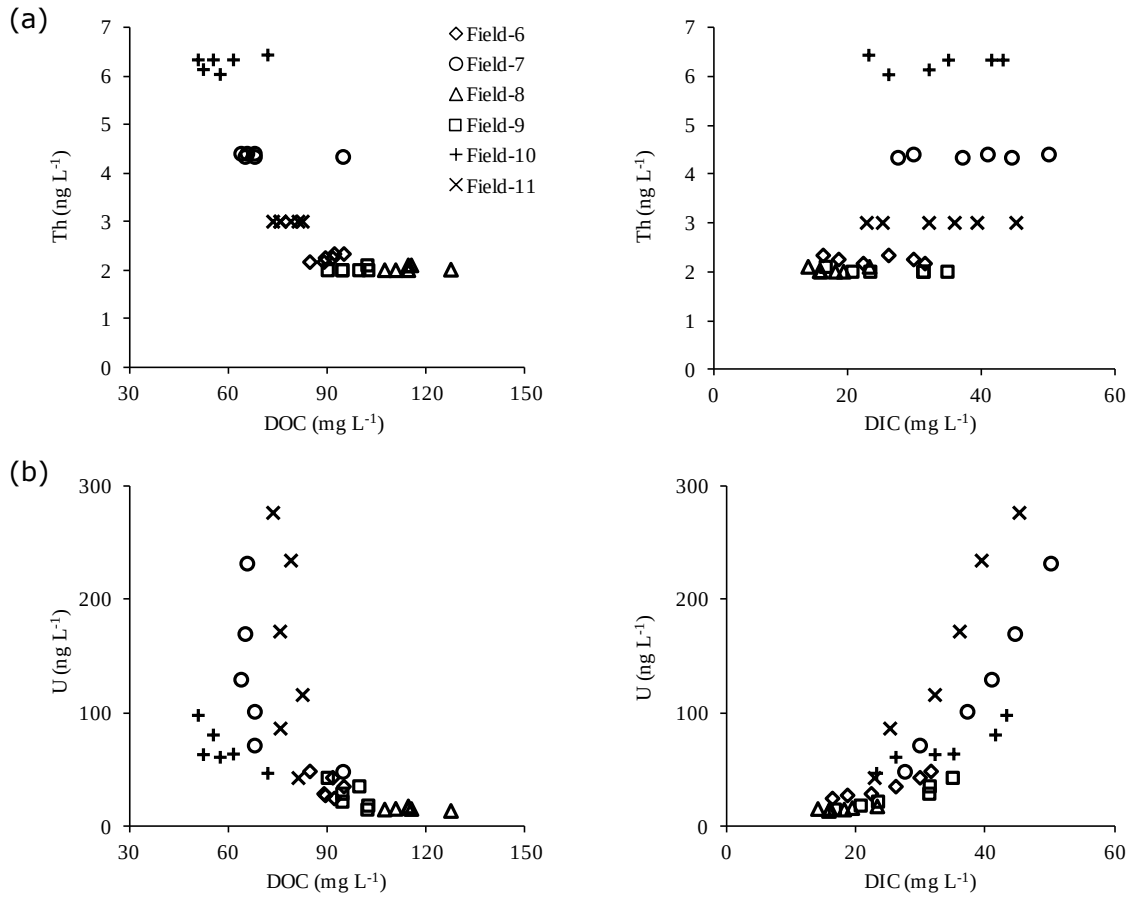

Figure 6.2: Concentration of (a) Th and (b) U (ng L^{-1}) in Biosolid-amended arable soil solution as a function of DOC and DIC (mg L^{-1}). Individual fields (n = 6) are shown over a range of incubation times.

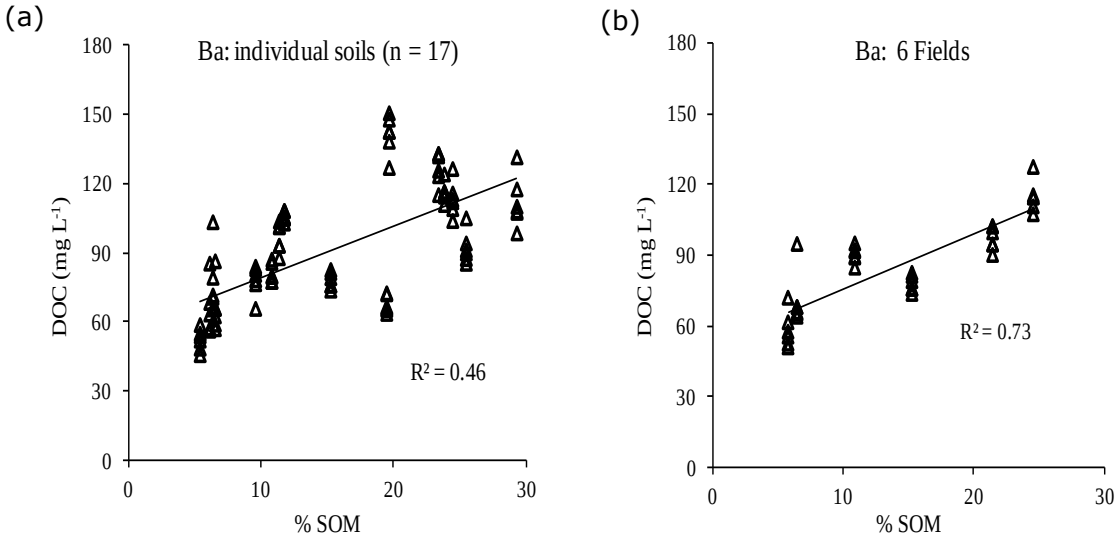

Figure 6.3: Concentration of DOC (mg L^{-1}) in Biosolid-amended arable soil solution as a function of %SOM shown as (a) individual soils (n = 17), or (b) individual fields (n = 6) over a range of incubation times. The solid line is the regression line.

Table 6.1: Correlation analysis (correlation coefficient, r) between Th and U concentrations in Ba soils pore water and soil properties including DOC, DIC, pH, %SOM, available-P, Fe and Al oxides (n = 17 soils and 102 soil solution samples collected at different times); P-values are in brackets.

Soil variable	*Soil solution Th and U concentrations (µg L^{-1})*	
	Th (µg L^{-1})	U (µg L^{-1})
DOC (mg L^{-1})	-0.70 *(<0.001)*	-0.50 *(<0.05)*
DIC (mg L^{-1})	0.73 *(<0.001)*	0.76 *(<0.001)*
pH	0.61 *(<0.05)*	0.67 *(<0.01)*
%SOM	-0.79 *(<0.001)*	-0.52 *(<0.05)*
P-avail (mg kg^{-1})	-0.77 *(<0.001)*	-0.57 *(<0.05)*
FeOx (g kg^{-1})	0.65 *(<0.01)*	0.74 *(<0.001)*
AlOx (g kg^{-1})	-0.77 *(<0.01)*	-0.53 *(<0.05)*
U (µg L^{-1})	0.50 *(<0.05)*	

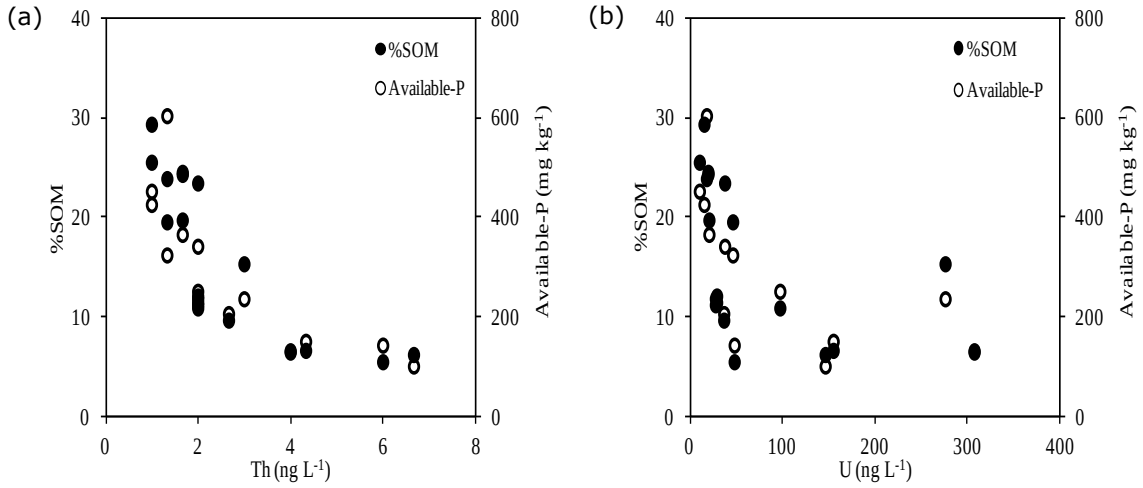

Figure 6.4: Concentration of Th (a) and U (b) (ng L^{-1}) in Biosolid-amended arable soil solution (at 144 hr) as a function of %SOM and available phosphate (mg kg^{-1}).

For most soils, Th solubility increased with DOC concentration. However, the Ba soils illustrate the potential danger in expecting a consistent relationship of this kind to cover all soils when other co-varying (and counteracting) factors may be active, such as DOC and available phosphate, in this case. Concentrations of Th in soil solution exceeded those for U in AM and AW soils, while U concentrations exceeded Th in Ca, Ar and Ba soils, producing a significant positive correlation of U with pH and

DIC, due to the formation of stable soluble uranyl carbonate complexes (e.g. Langmuir, 1978; Waite et al., 1994; Payne et al., 1996; McKinley et al., 2007; Echevarria et al., 2001; Vandenhove et al., 2007a) and a negative correlation of Th with the same soil parameters after the exclusion of the Ba soil.

Comparing concentrations of U in Rhizon-extracted soil pore water (U_{pw}) and 0.01 M $Ca(NO_3)_2$ extracts (U_{Ext}).

The U concentration measured in the 0.01 M $Ca(NO_3)_2$ electrolyte suspension used to determine E-values can be used as a surrogate for pore water U concentration. Degryse et al. (2003, 2011) reported that dilute salt electrolytes can mimic soil solution; 0.01 M $CaCl_2$ extractions provided reasonable estimates of Cd and Zn concentrations in soil pore water isolated by a centrifugation technique. Figure 6.5 shows a comparison between $\log_{10}$ U concentrations (ng L^{-1}) in pore water (U_{pw}) and in 0.01 M $Ca(NO_3)_2$ extractions (U_{Ext}). Overall, there was a positive significant correlation between $\log_{10}U_{pw}$ and $\log_{10}U_{Ext}$ ($r = 0.88$, $P < 0.001$), however they were significantly different (T-test; $P < 0.001$). Thus extraction with 0.01 M $Ca(NO_3)_2$ provides a reasonable estimate of the concentration of U in soil pore water isolated by Rhizon samplers. Concentrations of U in the Ca extract were generally lower than those in the pore water except for three AM soil samples from relatively deep layers in the profile (AM-H-4, AM-H-5 and AM-B-3; Section 4.3.1) with small soluble U and DOC concentrations and small SOM contents. For the AM-H-5 soil with the lowest soil solution U concentration among all the soils (Field soils), the concentration of U was 15 times larger in the $Ca(NO_3)_2$ extract than in pore water. For the other two soils AM-H-4 and AM-B-3 U_{Ext} was 2.1 and 1.3 times larger than U_{pw}. With the exception of these three soils, U_{pw} was on average 2 times greater than U_{Ext} with a maximum of 3.3 times greater. The difference between U_{pw} and U_{Ext} was most pronounced in the AM and AW topsoils. This difference decreased with soil depth and in the deepest layers U_{Ext} was higher than U_{pw}. The general trend seen in Figure 6.5 ($U_{pw} > U_{Ext}$) may be explained by several factors: (i) greater dilution caused by a high solution : soil ratio in the $Ca(NO_3)_2$ extraction; (ii) coagulation of DOC by Ca^{2+} ions limiting the solubility of organic-U complexes; (iii) lower pH and bi-carbonate concentrations in $Ca(NO_3)_2$ limiting the concentration of U-DIC complexes in solution (Yin et al., 2002;

Degryse et al., 2003; Romkens et al., 1996; Degryse et al., 2009). Takeda et al. (2006b) used eight chemical extraction methods (HNO_3 (0.01, 0.1 and 1 mol L^{-1}), 0.05 mol L^{-1} EDTA, 1 mol L^{-1} CH_3COONH_4, 1 mol L^{-1} NH_4NO_3, 0.01 mol L^{-1} $CaCl_2$ and pure water; 1 g soil : 10 ml extractant) to investigate the extractability of 28 elements including Th and U in 16 arable soils. The authors found that water extractable Th and U was not the lowest among the methods; it was higher than NH_4NO_3 and $CaCl_2$ extractable Th and U, probably due to dispersion of colloidal substances in water-extracted solution. However, Meers et al. (2006) investigated the presence of Zn in 29 polluted and unpolluted soils using Rhizon samplers and assessed soil solution speciation of Zn using geochemical models. They also excluded the colloidal fraction as the Rhizon samplers filter out suspended colloids with a diameter of >0.1 µm.

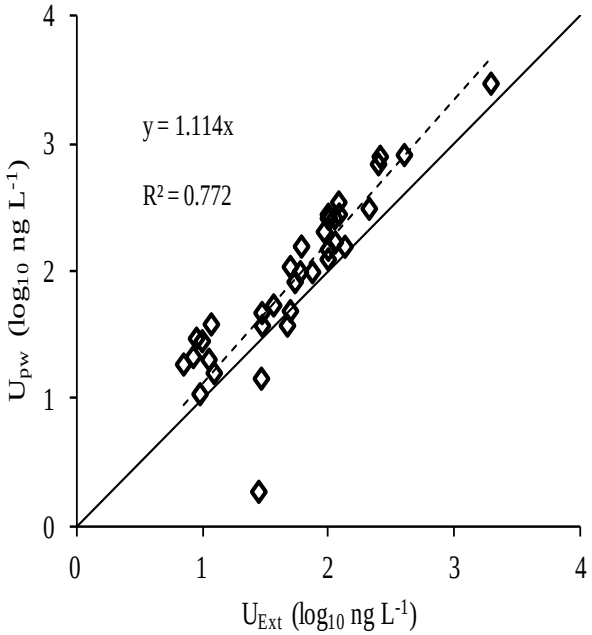

Figure 6.5: Comparison between the concentrations of U (log_{10} ng L^{-1}) in pore water extracted with Rhizon samplers (U_{pw}) and in 0.01 M $Ca(NO_3)_2$ extract (U_{Ext}), (n = 37). The solid line represents the 1:1 line and the dashed line represents the regression line.

6.3.2 Solid solution distribution of Th and U

In this section the factors affecting U and Th soil distribution coefficients are examined for two sets of soils: the Field-collected soils (Field) and soil samples from the British Geological Survey (BGS) archive (BGSc). Tables 6.2 and 6.3 compare the native $\log_{10}K_d$ values for Th and U from the two sets of soils with those in a database of K_d values for Canadian agricultural soils (Sheppard et al., 2007), Swedish soils (Sheppard et al., 2009) and a survey by Thibault et al. (1990) which was the source for K_d values compiled by the IAEA in 1994. Sheppard et al. (2007, 2009) measured the native Th and U K_d values as the ratio of total Th or U on the solid phase to Th or U concentration in soil solution isolated by a centrifugation technique. Native U K_d values were also compared with values determined from U adsorption studies on 13 French soils (Echevarria et al., 2001). The range and average values for Th and U $\log_{10}K_d$ values in this study were generally higher than those reported in the literature (Tables 6.2 and 6.3), particularly for Th (Thibault et al., 1990; Sheppard et al., 2007, 2009; Echevarria et al., 2001), although the order of K_d values (Th > U) in soils was consistent. The variation in $\log_{10}K_d$ values seen between this study and the literature may arise from varying soil characteristics but probably also includes the effect of different techniques used to measure Th and U concentrations in the 'soil solution'. The Th and U K_d values varied over 4 and 3 orders of magnitude over the range of soils studied. The K_d values in each soil category of the Field soils followed the order: Ba > Ca > Ar > AM >AW for Th, and Ba > AM > Ar > AW > Ca for U. The Ba soils exhibited the highest Th and U K_d values, particularly for Th, which may be attributed to the high SOM content and extremely high phosphate concentrations (Section 6.3.1); these soils are examined separately from the other Field soils because of their unusual characteristics. For the second set of soils (BGSc), Th K_d values increased with increasing pH (Table 6.2), while U exhibited the reverse trend (U K_d values decreased with increasing soil pH; Table 6.3). The Th K_d values for AW and AM soils and U K_d values for Ca, Ar, AW and BGSc >6.5 fell in the range of K_d values reported in the literature (Thibault et al., 1990; Sheppard et al., 2007, 2009). Generally, K_d values were on average 7.5 or 12 (Gm or Am) times higher for Th than U.

Table 6.2: Comparison of thorium $log_{10}K_d$ (L kg^{-1}; log_{10} scale) values from the two soil sets studied (Field and BGSc) with values for Canadian agricultural soils (Sheppard et al., 2007), Swedish soils (Sheppard et al., 2009) and data from the survey by Thibault et al. (1990) which was the source for K_d values in the IAEA compilation of 1994. Number of soils (n), geometric mean (Gm), geometric standard deviation (GSD), arithmetic mean (Am), standard deviation (SD), minimum (min) and maximum (max) values are given.

	$Log_{10}K_d$ (Th) (L kg^{-1})						
	n	**Gm**	**GSD**	**Am**	**SD**	**min**	**max**
Thibault et al. (1990)						3.51	4.95
Sheppard et al. (2007)	106	4.49	0.70			2.63	5.76
Sheppard et al. (2009)	7	4.40	0.48	4.70	4.91	3.74	5.40
Current study							
Field soils	37	5.18	1.15	5.95	6.04	2.85	6.71
Field soils excluding Ba soils	20	4.39	0.95	5.19	5.39	2.85	5.99
Arable (Ar)	3	5.39	0.48	5.58	5.39	4.98	5.99
Acidic Woodland (AW)	3	3.67	0.00	3.68	3.08	3.33	3.80
Calcareous (Ca)	3	5.58	0.00	5.61	5.19	5.33	5.82
Acidic Moorland (AM)	11	3.99	0.78	4.81	5.21	2.85	5.79
Biosolid-amended arable (Ba)	17	6.17	0.30	6.26	6.01	5.19	6.71
BGSc soils	40	5.41	0.48	5.63	5.59	4.16	6.18
BGSc < 6.5 (pH)	17	5.11	0.60	5.42	5.55	4.16	6.18
BGSc > 6.5 (pH)	23	5.64	0.30	5.74	5.57	5.04	6.15
Whole dataset	77	5.22	1.08	5.92	6.01	2.85	6.71

Table 6.3: Comparison of uranium $\log_{10}K_d$ (L kg^{-1}) values from the two soil sets studied (Field and BGSc) with values for Canadian agricultural soils (Sheppard et al., 2007), Swedish soils (Sheppard et al., 2009) and data from the survey by Thibault et al. (1990) which was the source for K_d values in the IAEA compilation of 1994. Number of soils (n), geometric mean (Gm), geometric standard deviation (GSD), arithmetic mean (Am), standard deviation (SD), minimum (min) and maximum (max) values are given.

	$Log_{10}K_d$ (U) (L kg^{-1})						
	n	**Gm**	**GSD**	**Am**	**SD**	**min**	**max**
Thibault et al. (1990)						1.18	3.20
Sheppard et al. (2007)	112	2.98	0.81			0.94	4.34
Sheppard et al. (2009)	7	3.60	0.60	3.96	4.16	2.79	4.64
Echevarria et al. (2001)	13	1.63	1.43	2.92	3.10	-0.05	3.50
Current study							
Field soils	37	4.42	0.70	4.89	5.08	2.63	5.81
Field soils-Excluding Ba soils	20	4.01	0.60	4.65	5.10	2.63	5.81
Arable (Ar)	3	4.00	0.30	4.12	4.00	3.23	4.60
Acidic Woodland (AW)	3	3.89	0.00	3.92	3.43	3.52	4.15
Calcareous (Ca)	3	3.08	0.30	3.15	2.85	2.63	3.49
Acidic Moorland (AM)	11	4.29	0.60	4.88	5.22	3.51	5.81
Biosolid-amended arable (Ba)	17	4.93	0.30	5.08	4.97	3.86	5.63
BGSc soils	40	3.99	0.60	4.28	4.35	2.80	4.95
BGSc < 6.5 (pH)	17	4.42	0.30	4.51	4.37	3.72	4.95
BGSc > 6.5 (pH)	23	3.68	0.48	3.96	4.19	2.80	4.88
Whole dataset	77	4.35	0.70	4.84	5.05	2.63	5.81

6.3.3 Soil variables affecting Th distribution coefficient

Table 6.4 shows the correlation between soil properties and Th $\log_{10}K_d$ values for the Field soils and BGSc soils. The K_d values were not measured under the same experimental conditions in the two sets of soils (Section 2.3) and it is expected that soil solution chemical composition will be influenced by the extraction/equilibration technique used. Therefore, there may be operational differences between the two sets of data. Nevertheless, in both sets of soils, soil pH, available-P and FeOx were positively correlated with $\log_{10}K_d$ (Th), while DOC was negatively correlated with $\log_{10}K_d$ (Th). In the Field soils, SOM was positively correlated with $\log_{10}K_d$ (Th) values whereas in BGSc soils SOM was negatively correlated with $\log_{10}K_d$ (Th) values, although excluding Ba soils from the Field soils also resulted in a negative correlation ($r = -0.35$, $P < 0.05$). The positive correlation between $\log_{10}K_d$ (Th) values and pH, FeOx and phosphate may be explained by Th adsorption onto all soil binding phases such as clay, phosphate minerals and especially iron oxides (Waite et al., 1994; Braun et al., 1998; Murphy et al., 1999; Barnett et al., 2000; Jerden and Sinha, 2002; Jerden et al., 2003; Zhang et al., 2006). Moreover, Th can precipitate as secondary phosphate minerals (Braun et al., 1998; Fuller et al., 2002; Zhang et al., 2006; Taboada et al., 2006). Vandenhove et al. (2009) reported that FeOx and MnOx are expected to be more important than alumina-silicate clays for adsorption of Th. The adsorption of dissolved Th onto organic matter, oxyhydroxides and clay increases markedly with increasing pH (above pH 2) with the maximum (complete) adsorption (95-100%) attained at pH values above 5.5-6.5 (Langmuir and Herman, 1980). In alkaline conditions, Th strongly adsorbs onto binding phases with minimal soluble complex formation (Langmuir, 1980). However, in the acidic soils used in the current study (AW and AM) there was accumulation of organic matter, especially in the topsoils, which provides a greater concentration of organic ligands (humic and fulvic acids) in the soil solution and, therefore, increased Th solubility - thus producing a negative correlation of $\log_{10}K_d$ (Th) with SOM and DOM. Vandenhove et al. (2009) reported that Th K_d values are largely texture-independent and classification of K_d values based on soil pH is generally a more appropriate approach to linking distribution coefficient to soil properties. Similarly, there was no significant correlation between Th $\log_{10}K_d$ values and soil clay content in the present data. Prediction of K_d values from only one soil parameter (e.g. soil pH) would seem

unwise given the marked effect of organic matter described above. However, the strength of such a relationship would depend on the correlation between pH and humus content – which is a fairly common feature in some groups of soils. For example a comparison of moorland, woodland, grassland and arable soils is likely to show a strong negative correlation between humus content and pH value.

Table 6.4: Correlations between soil properties and Th and U $\log_{10}K_d$ values (L kg^{-1}) for the Field soils (n = 37 soils; 222 soil solution samples collected over a range of incubation times) and for the BGSc soil set (n = 40); P-values are in brackets.

Soil variable	$Log_{10}K_d$ (L kg^{-1}) calculated based on total metal concentration in solid phase				
	Th $\log_{10}$ K_d (L kg^{-1})		**U $\log_{10}$ K_d (L kg^{-1})**		
	Field soils	BGSc soils	Field soils pH<5	Field soils pH>5	BGSc soils
DOC (mg L^{-1})	-0.55 **(< 0.001)**	-0.83 ***(< 0.001)***	-0.75 ***(< 0.001)***	0.67 ***(< 0.001)***	-0.08 (> 0.05)
DIC (mg L^{-1})	0.36 **(< 0.001)**	0.18 (> 0.05)	0.11 (> 0.05)	-0.92 ***(< 0.001)***	-0.74 ***(< 0.001)***
pH	0.86 ***(< 0.001)***	0.64 ***(< 0.001)***	0.78 ***(< 0.001)***	-0.65 ***(< 0.001)***	-0.61 ***(< 0.001)***
%SOM	0.42 ***(< 0.001)***	-0.63 ***(< 0.001)***	-0.56 ***(< 0.001)***	0.59 ***(< 0.001)***	-0.21 (>0.05)
P_{avail} (mg kg^{-1})	0.72 ***(< 0.001)***	0.49 ***(< 0.05)***	-0.20 (>0.05)	0.82 ***(< 0.001)***	-0.21 (>0.05)
%SIC	0.21 ***(< 0.01)***	0.24 (< 0.05)	-0.01 (> 0.05)	-0.72 ***(< 0.001)***	-0.60 ***(< 0.001)***
FeOx (g kg^{-1})	0.82 ***(< 0.001)***	0.28 ***(< 0.05)***	0.41 ***(< 0.001)***	0.31 ***(< 0.001)***	0.48 ***(< 0. 01)***
%Clay	-0.04 (> 0.05)	0.23 (> 0.05)	0.10 (> 0.05)	0.14 (> 0.05)	-0.01 (> 0.05)
Th_{tot} (mg kg^{-1})	0.62 ***(< 0.001)***	0.26 ***(< 0.05)***	-	-	-
U_{tot} (mg kg^{-1})	-	-	0.31 ***(< 0.01)***	0.75 ***(< 0.001)***	0.09 (> 0.05)

The effect of soil pH on Th distribution coefficient

Figure 6.6 shows $\log_{10}K_d$ values for Th as a function of soil pH; there was a highly significant linear relationship with soil pH for Field soils (Figure 6.6a) showing that increased pH strongly decreased Th solubility:

$$\log_{10}K_d = 0.78\ pH + 0.99,\ (r^2 = 0.74,\ P < 0.001).$$

Although K_d values for the BGSc soils were measured under different conditions, combining the data for both sets of soils also gave a strong linear relationship for the whole dataset (Figure 6.6b) with a remarkably similar regression equation:

$$\log_{10}K_d = 0.72\ pH + 1.25,\ (r^2 = 0.70,\ P < 0.001).$$

Sheppard et al. (2009) compiled three datasets, which provided 39 K_d values for Th, and derived the equation:

$$Log_{10}K_d = 0.35\ pH + 1.90,\ (r^2 = 0.16),$$

which again suggests a similar linear increase of $\log_{10}K_d$ with pH.

In the current study, although Figures 6.6a and b show a significant positive linear relationship between $\log_{10}K_d$ and soil pH, there was a drop in $\log_{10}K_d$ above pH 5.8. Figure 6.6d shows Th $\log_{10}K_d$ values as a function of soil pH for soils with pH >5.8 (Ba, Ca, BGSc pH >6.5) excluding Ar soils: there was a negative linear relationship with soil pH, showing that Th solubility increased above pH 5.8:

$$\log_{10}K_d = -0.58\ pH + 9.73,\ (r^2 = 0.42,\ P < 0.001).$$

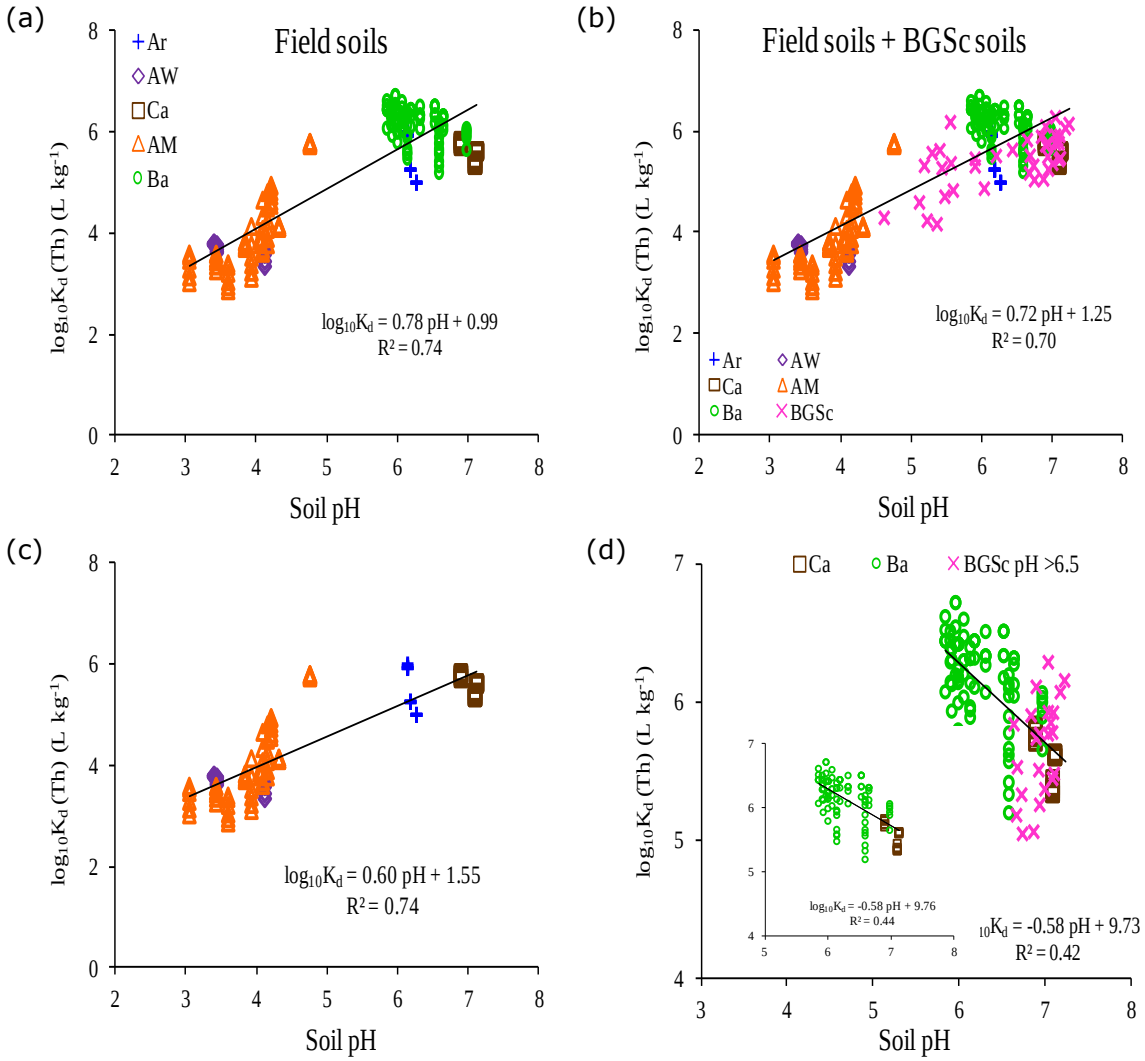

Figure 6.6: Thorium $\log_{10}K_d$ (L kg^{-1}) as a function of soil pH in (a) Field soils, (b) a combined dataset (Field soils + BGSc soils), (c) Field soils excluding Ba soils and (d) only Ba, Ca and BGSc pH >6.5 soils; showing a negative trend with pH. The solid line represents the regression line.

In Ba soils Th $\log_{10}K_d$ was significantly positively correlated with SOM, phosphate and DOC and negatively correlated with pH and DIC. Therefore, in the Ba soils increased Th solubility at high pH may also be due to the negative correlation between pH and SOM, phosphate and DOC. Soils with greater humus content, due to higher sewage sludge application levels, also have greater phosphate loadings and lower pH values – but may have higher $\log_{10}K_d$ values due to bonding to humus and association with phosphate. Unlike Ba and Ca soils, $\log_{10}K_d$ was positively correlated with soil pH ($r = 0.49$, $P < 0.05$) for BGSc pH >6.5. However, a negative linear relationship was found between $\log_{10}K_d$ and DIC ($r^2 = -0.60$, $P < 0.001$). The increase in Th solubility above pH 5.8 is probably due to the formation of negatively charged Th-carbonate

(e.g. $Th(CO_3)_5^{6-}$) and/or Th-hydroxy-carbonate complexes (e.g. $Th(OH)(CO_3)_4^{5-}$, $Th(OH)_3CO_3^-$), which are the dominant Th species above pH 6.5 in the presence of carbonate (Altmaier et al., 2005, 2006; Rand et al., 2008). At low carbonate concentrations in the near neutral pH range, the complexes $Th(OH)_3(CO_3)^-$ and $Th(OH)_2(CO_3)$ were found to be important for the solubility of hydrous thorium oxide $ThO_2 \cdot x\, H_2O$(am) and Th(IV) hydroxide (Rand et al., 2008). The limiting carbonate complex $Th(CO_3)_5^{6-}$ is an important Th species and predominates at pH 8−11 at high carbonate concentrations (e.g. in 0.2 − 2 M $NaHCO_3$ or Na_2CO_3) (Altmaier et al., 2005, 2006). The presence of $Th(CO_3)_5^{6-}$ complex at high carbonate concentration (1.0 M) has been supported by EXAFS measurements, while at low carbonate concentrations (0.1 M) Th-hydroxide-carbonate complex ($Th(OH)(CO_3)_4^{5-}$) predominates showing clearly different spectra (Felmy et al., 1997; Altmaier et al., 2006). In the current study, DIC concentrations ranged from 10^{-4} to 10^{-2} M, therefore, it is unlikely that Th-carbonate ($Th(CO_3)_5^{6-}$) complex contributes to the increased Th solubility above pH 5.8.

Figure 6.7 shows Th $\log_{10}K_d$ values predicted by WHAM-VII as a function of soil pH. A model soil with fixed soil variables (average measured values) except for pH (3 - 8.25) and DOC (0.05 - 0.5 M; in the range of studied soils) was used to investigate the effect of soil pH on Th $\log_{10}K_d$ values under CO_2 partial pressure (0.00038 atm), 10 and 100$\times CO_2$ partial pressure (0.0038 and 0.038), to try to compare that with the general trend across all the soils. The predicted $\log_{10}K_d$ general trend was similar to $\log_{10}K_d$ trend across the combined dataset (Field soils + BGSc soils) (Figure 6.6b), including the flat section at low pH (~3) followed by the rise in $\log_{10}K_d$ with soil pH and then the fall at pH >6. Increasing CO_2 partial pressure from 0.00038 to 0.038 did not affect Th K_d values over a pH range from 3 to 6, although there was a decrease in $\log_{10}K_d$ values at pH >6. According to the WHAM prediction, Th was predominantly bound to DOM below pH 6 with little contribution from Th-hydroxide species, therefore increasing CO_2 partial pressure did not influence $\log_{10}K_d$ values below pH 6. Above pH 6 under CO_2 partial pressure (0.00038 atm) Th was dominantly pound to $Th(OH)_4$ and $Th(OH)_3CO_3^-$, the importance of $Th(OH)_4$ decreased with increasing soil pH (pH >7). At 10 times CO_2 partial pressure $Th(OH)_3CO_3^-$ was the dominant species, while at 100 times CO_2 partial pressure $Th(OH)_3CO_3^-$ predominates only at

6< pH <7.5 and pure Th-carbonate complex $Th(CO_3)_5^{6-}$ predominates at pH >7.5 representing 100% of total Th in solution.

Overall, the results of WHAM-VII predicted $\log_{10}K_d$ and Th speciation support the suggestion that Th solubility increased at pH >6 due to the formation of Th-hydroxy-carbonate. These results contradict the simple hypothesis that Th solubility significantly decreases with increasing pH in the absence of DOM and that at alkaline pH Th exists primarily as the neutral $Th(OH)_4$ complex (Langmuir and Herman, 1980).

Various studies have reported the presence of dissolved thorium-carbonate and hydroxyl-carbonate complexes and their importance to the solution chemistry of Th (Laflamme and Murray, 1987; Östhols et al., 1994; Felmy et al., 1997; Altmaier et al., 2005, 2006). Laflamme and Murray (1987) found elevated concentrations of Th in a range of alkaline lakes; Th concentration was about four orders of magnitude higher than sea water and two orders of magnitude above the solubility limit of ThO_2. The enhanced Th concentration coincided with an increase in carbonate alkalinity; the authors therefore attributed the enhanced Th concentration to the formation of Th-carbonate complexes. Laflamme and Murray (1987) studied the effect of carbonate on Th adsorption to goethite at pH 9.0±0.6 and observed that adsorbed Th began to decrease from 100% at 100 meq L^{-1} carbonate alkalinity until, above 300 meq L^{-1}, no adsorption was observed. The authors attributed the decline in Th adsorption to two factors (i) the competition of CO_3^{2-} and HCO_3^- for surface sites on the Fe oxide and (ii) the formation of soluble negatively charged thorium-carbonate complexes.

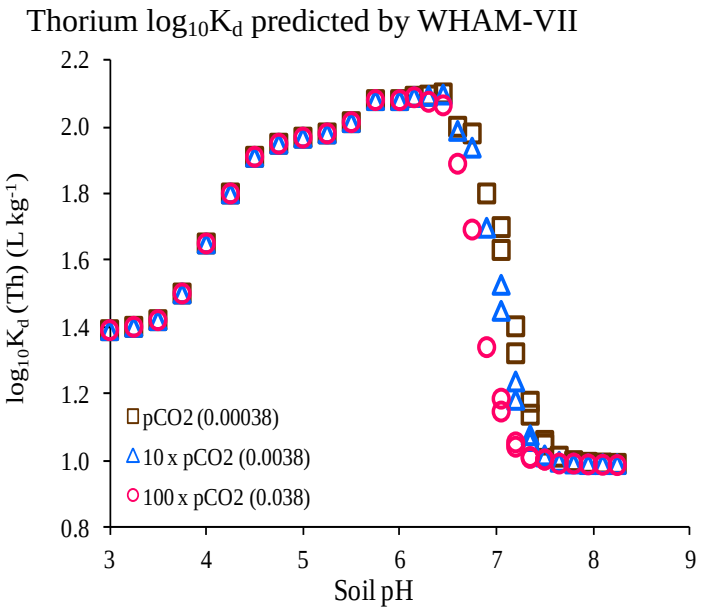

Figure 6.7: Thorium $\log_{10}K_d$ predicted by WHAM-VII as a function of pH for a model soil with fixed soil variables (average measured values) except for pH (3 - 8.25) and DOC (0.05 - 0.5 M; in the range of studied soils). Partial pressure of CO_2 was fixed, K_d was predicted at three different partial pressure values: (□) CO_2 partial pressure (0.00038 atm), (Δ) 10×CO_2 partial pressure (0.0038), (○) 100×CO_2 partial pressure (0.038).

The effect of DOC on Th solubility

The significant positive correlation between $\log_{10}K_d$ for Th and soil pH in both sets of soils was coincident with a significant negative correlation between DOC and $\log_{10}K_d$. Figure 6.8 shows $\log_{10}K_d$ (Th) as a function of DOC for Field soils excluding Ba soils (Figure 6.8a) and for a combined dataset (Field soils + BGSc soils) excluding Ba soils (Figure 6.8b). The significant negative correlation between DOC and $\log_{10}K_d$ was not only observed for AW and AM soils with high DOC concentrations (400 mg L^{-1} on average; Section 6.3.1), but also for Ar, Ca and BGSc soils. Thus soil pH and DOC will be the most relevant parameters to consider when assessing site-specific variability of Th K_d values. However, these soil variables may have a complex interaction. For example, with increasing soil pH, adsorption of Th on soil binding phases is likely to reduce Th solubility but may also mobilise fulvic and humic acids, or biological ligands such as citric acid, which would increase solubility as soluble complexes (Bondietti, 1974; Rancon, 1973; Langmuir, 1980). However, no similar clear interaction has been observed in the current study (both soil solution Th and DOC decreased with increasing soil pH).

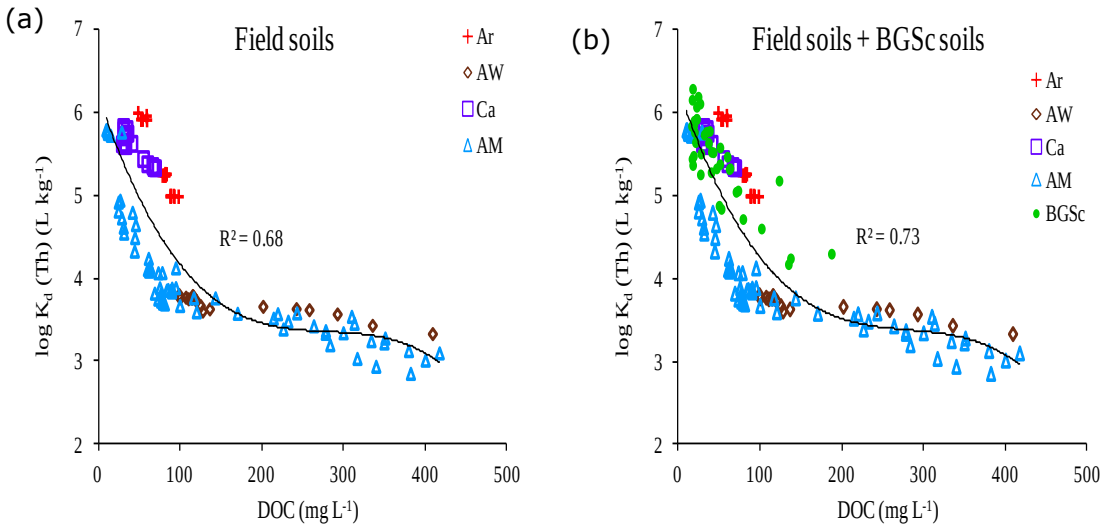

Figure 6.8: Thorium $\log_{10}K_d$ (L kg^{-1}) as a function of DOC (mg L^{-1}) in (a) Field soils and (b) a combined dataset (Field soils + BGSc soils) excluding Ba soils. The solid line represents a third order polynomial fit to the data.

Biosolid-amended arable soils (Ba)

Figure 6.9 shows $\log_{10}K_d$ (Th) as a function of DOC for the Ba soils. In contrast with all other soils, $\log_{10}K_d$ (Th) was positively correlated with DOC ($r = 0.46$, $P < 0.001$) for the Ba soils. This is likely to be a consequence of the high humus and phosphate contents in the Ba soils. As has been discussed in Section 6.3.1, the negative effect of DOC on Th solubility may be explained by the strong correlation between SOM and DOC ($r = 0.72$, $P < 0.01$; Figure 6.3). The (solid) SOM and (aqueous) DOC may work in 'opposite directions' as regards their likely effect on Th solubility. This might suggest that adsorption by the SOM overwhelms the potential mobilizing effects of a greater DOC concentration in the soil solution as soil humus content increases. Alternatively, and perhaps more importantly, a greater humus content in the Ba soils implies higher sewage sludge application levels and so a greater phosphate loading in the soil. This factor may be the principal cause for higher $\log_{10}$Kd values.

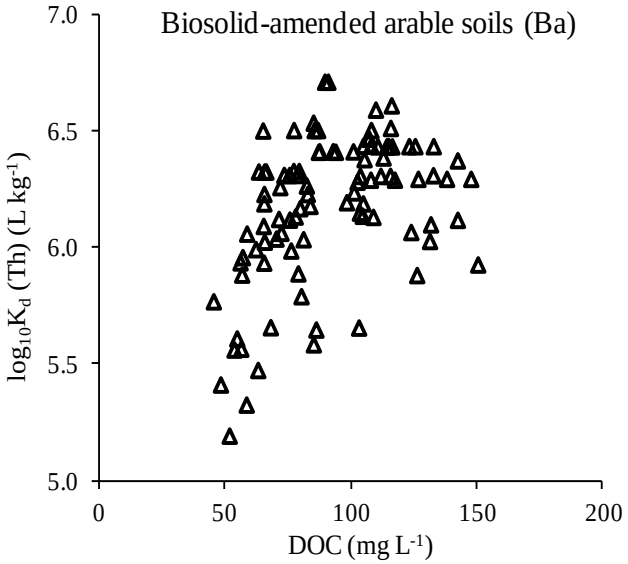

Figure 6.9: Thorium $\log_{10}K_d$ (L kg^{-1}) as a function of DOC (mg L^{-1}) in Biosolid-amended arable soils (Ba).

6.3.4 Soil variables affecting U distribution coefficient

The effect of soil pH on U distribution coefficient

Uranium solubility is strongly dependent on soil pH for reasons similar to those governing Th solubility – changes in affinity for adsorption surface and in solution phase speciation (Ebbs et al., 1998; Shahandeh and Hossner, 2002; Duquene et al., 2006; Vandenhove et al., 2007a). At acidic pH values, the divalent uranyl cation (UO_2^{2+}) predominates and sorption is weak. With increasing pH, the negative charge on mineral and organic binding sites increases, due to the release of protons, and so the adsorption strength of UO_2^{2+} should increase. On the other hand, with rising pH, there is an increase in carbonate concentration, which is probably the most important inorganic complexing ligand for uranium. Thus, above pH 6, the fraction of U(VI) in solution that is complexed with carbonate increases; the carbonate complexes ($UO_2CO_3^0$, $UO_2(CO_3)_2^{2-}$, $UO_2(CO_3)_3^{4-}$) are poorly adsorbed, which enhances U solubility (Langmuir, 1978; Zheng et al., 2003; Koch-Steindl and Pröhl, 2004; Duquene et al., 2006; Vandenhove et al., 2007a). Thus, values of $\log_{10}K_d$ for U show two distinct trends with pH value with a peak in $\log_{10}$Kd just above pH 5, for the reasons discussed above (Table 6.4; Fig 6.10) (Sheppard et al., 2006, 2009; Vandenhove et al., 2007a, 2009). Therefore, in the current study, and because the Field soils cover a pH range from 3 to 7.13, the soil set was divided depending on soil

pH value. Below pH 5, a significant positive relationship was observed between U $\log_{10}K_d$ and soil pH:

$\log_{10}K_d = 1.17\ pH - 0.37,\ r^2 = 0.66,\ P < 0.001$; *Figure 6.10a.*

This is consistent with the hypotheses that adsorption strength of UO_2^{2+} increases with pH value and that below pH 5, UO_2^{2+} is the dominant species in solution. However, no significant influence (Sheppard et al., 2006; Vandenhove et al., 2007a) or only a weak influence ($r^2 = 0.2$; Vandenhove et al., 2009) of pH on $\log_{10}K_d$ values at pH <5.5 or <6 has been reported in previous studies.

Above pH 5 (pH 5.8 - 7.13), a significant negative linear relationship was observed between U $\log_{10}K_d$ and soil pH:

$\log_{10}K_d = -1.22\ pH + 12.10,\ r^2 = 0.56,\ P < 0.001$; *Figure 6.10a.*

due to the formation of soluble uranyl carbonate complexes which increase U solubility at higher pH values. For BGSc soils which covered a pH range from 5.3 to 7.24 except for one soil (pH 4.62), a similar negative linear relationship was obtained between $\log_{10}K_d$ and pH (Figure 6.10b). When combining data for both sets of soils (soils with pH >5) a strong negative linear relationship was again obtained (Figure 6.10c) and the regression equation was similar to the first soil set equation:

$\log_{10}K_d = -1.28\ pH + 12.50,\ r^2 = 0.57,\ P < 0.001$; *Figure 6.10c.*

Echevarria et al. (2001) studied the influence of soil properties on U sorption in 13 French soils covering a pH range from 5.5 to 8.8. No significant effect of clay or organic matter content was found and pH was the only significant factor controlling U K_d values. The authors deduced a linear relationship very similar to the current study:

$\log_{10}K_d = -1.25\ pH + 10.9,\ r^2 = 0.89,$

when adding the $\log_{10}K_d$-pH values of 8 Canadian soils into the regression analysis the same effect on K_d values was again obtained:

$\log_{10}K_d = -1.29\ pH + 11.0,\ r^2 = 0.76.$

They concluded that the difference in behaviour of the uranyl cation (UO_2^{2+}) and UO_2^{2+}-carbonate complexes is so great that it hides any more subtle effect of soil properties on U sorption. Sheppard et al. (2006) compiled K_d values (sorption experiment for 134 soils with a pH range of (4.0 - 8.8) and found a negative linear relation between U $\log_{10}K_d$ and pH for soils with pH >5.5

$$\log_{10}K_d = -1.07\ pH + 9.8,\ r^2 = 0.41.$$

Vandenhove et al. (2007a) explored the dominant soil variables controlling U mobility in 18 ^{238}U-spiked soils, a similar linear decrease in $\log_{10}K_d$ with soil pH was found for soils with pH ≥6 which was again attributed to uranyl carbonate formation:

$$\log_{10}K_d = -1.18\ pH + 10.8,\ r^2 = 0.65.$$

Vandenhove et al. (2009) compiled K_d values (n = 110) and obtained the regression equation:

$$\log_{10}K_d = -0.77\ pH + 7.7,\ r^2 = 0.30,$$

for soils within the pH range 5.5 - 8.8, the correlation parameters are in agreement with the current study.

Overall, the linear relationship between $\log_{10}K_d$ and pH for soils with pH >5 in the current study was similar to that in the literature, even though the authors listed above measured K_d for recently contaminated soils (using a ^{238}U spike). These results demonstrate that soil pH is likely to be the most relevant parameter to assess site-specific variability of U K_d values and associated risk assessments.

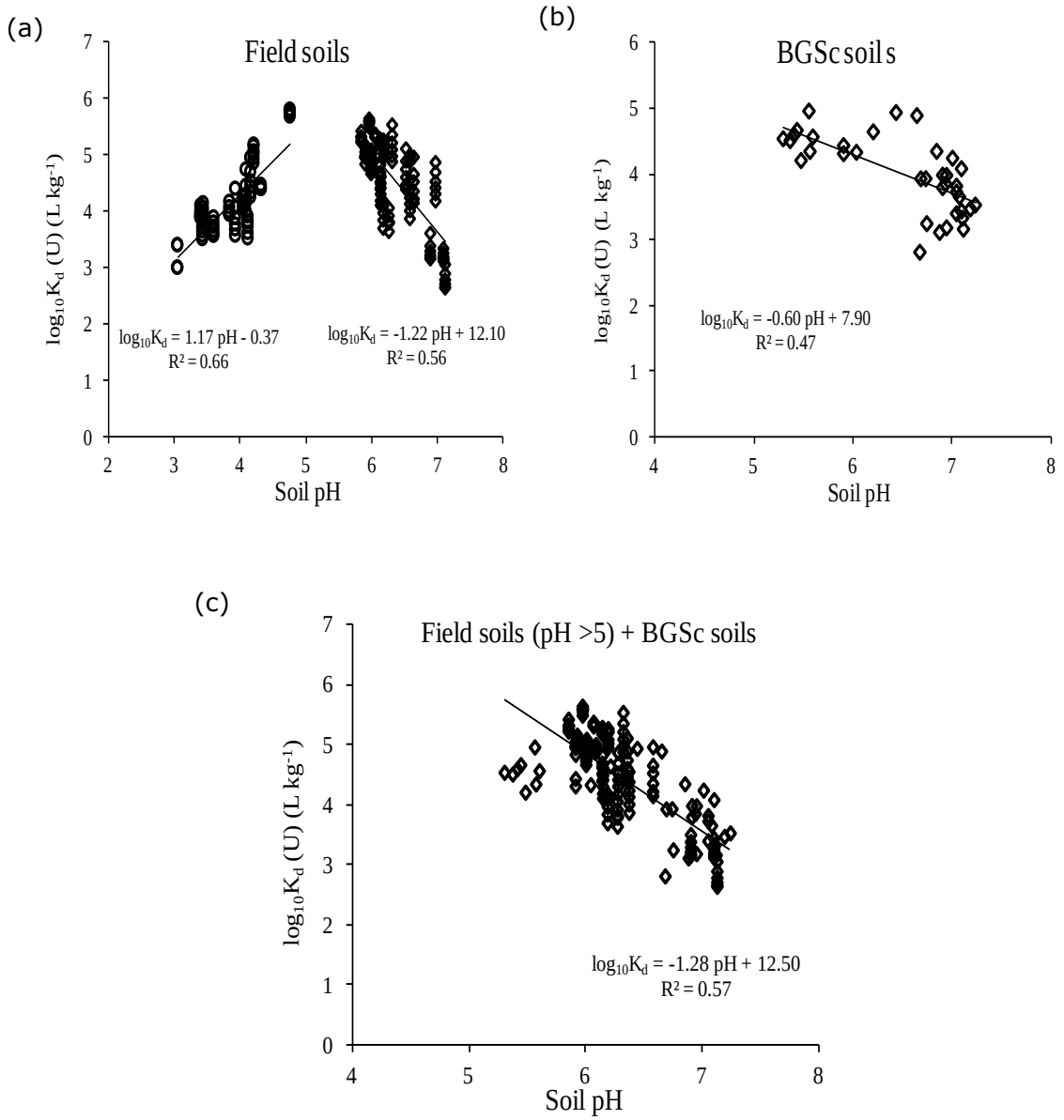

Figure 6.10: Uranium $\log_{10}K_d$ (L kg^{-1}) as a function of soil pH in (a) Field soils pH <5 and pH >5, (b) BGSc soils excluding one soil (pH 4.62) and (c) a combined dataset (Field soils pH >5 + BGSc soils). The solid lines represent linear regressions through each data set.

The effect of DOC and DIC on U distribution coefficient

The significant positive correlation between $\log_{10}K_d$ for U and soil pH in soils with pH <5 was coincident with a significant negative correlation between $\log_{10}K_d$ and DOC (Table 6.4; Figure 6.11). Below pH 5, both DOC and SOM were positively correlated ($r = 0.86$, $P<0.001$) and negatively correlated with U $\log_{10}K_d$ (Table 6.4). It appears that U complexation by DOC will compete effectively with binding to SOM. However, Vandenhove et al. (2007a) observed a significant positive correlation between U K_d and the organic matter content in ^{238}U-spiked soils (pH <6).

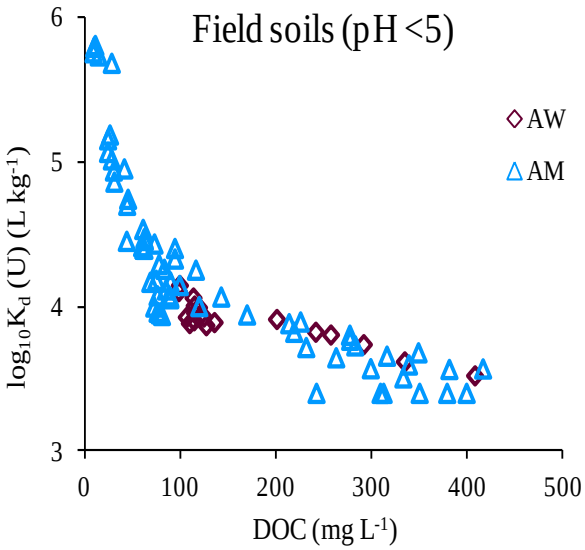

Figure 6.11: Uranium $\log_{10}K_d$ (L kg^{-1}) as a function of DOC (mg L^{-1}) in Field soils pH <5.

The negative linear relationship between U $\log_{10}K_d$ and soil pH in Field soils (pH >5) and BGSc soils was coincident with a significant negative linear relationship between DIC and U $\log_{10}K_d$. Figures 6.12a and b show $\log_{10}K_d$ as a function of dissolved carbonate concentration (DIC) for the Field soils (pH >5) and BGSc soils, respectively. Increased DIC concentration increased U solubility through the formation of soluble uranyl-carbonate complexes at high pH and carbonate concentrations (Ebbs et al., 1998; Shahandeh and Hossner, 2002; Duquene et al., 2006; Vandenhove et al., 2007a). Thus, in agricultural soils (pH >6), soil pH and dissolved carbonate concentration profoundly affect the distribution of U(VI) (EPA, 1999; Davis et al., 2002; Kohler et al., 2004; Vandenhove et al., 2009). Many

agricultural soils are limed to maintain soil pH in the optimum range. The influence of solid calcium carbonate on U(VI) sorption in soils has been investigated by Zheng et al. (2003), who found that $CaCO_3$ resulted in a pronounced suppression of the pH dependent sorption curve in the neutral pH range due to the formation of a very stable neutral uranyl carbonate complex $Ca_2UO_2(CO_3)_3$ in solution.

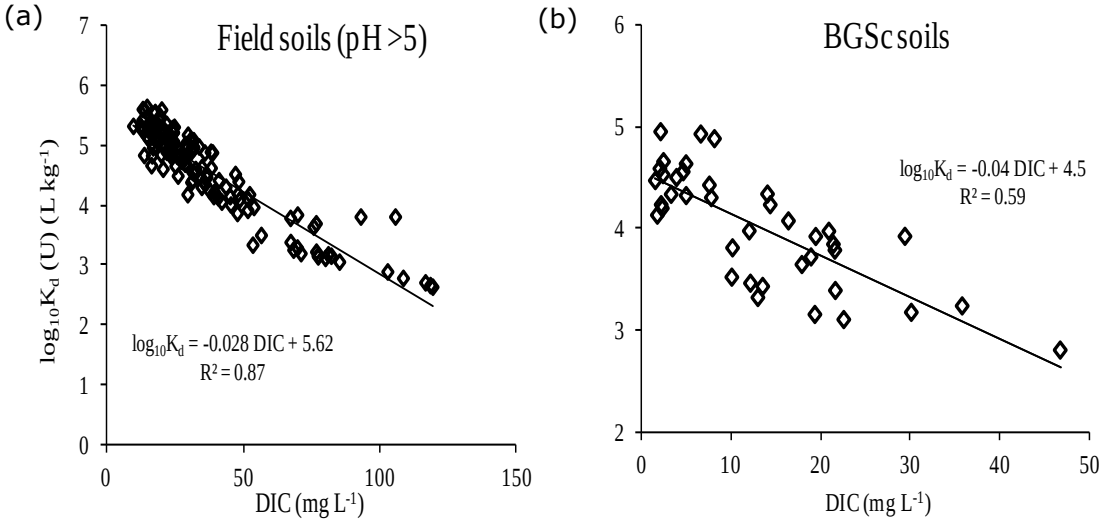

Figure 6.12: Uranium $\log_{10}K_d$ (L kg^{-1}) as a function of DIC (mg L^{-1}) in (a) the Field soils (pH >5) and (b) BGSc soils. The solid lines represent linear regressions through the data sets.

6.3.5 Soil solution speciation

Thorium: overview

Calculated free Th ion activities ranged from as little as 8.3×10^{-13} to 0.4% and from 1.7×10^{-12} to 8.0×10^{-3}% of the total dissolved Th concentration for the Field soils and BGSc soils, respectively. The results showed that the free metal ion represents a very minor solution species for Th, while Th binding to DOM was crucial for Th solubility and varied from 80% in Ca soils to approximately 100% in Ar, AW, AM and Ba soils. In BGSc soils Th binding to DOM and hydroxide (particularly $Th(OH)_4$ species) were the important solution species and ranged from 0.1 to 100% and from 0.2 to 100%, respectively, depending on soil pH and SOM content. In addition, Th-carbonate and particularly Th-hydroxy-carbonate complexes have contributed to Th speciation in Ca and BGSc pH >6.5 soils.

Uranium: overview

Free U(VI) ion activity (UO_2^{2+}) varied from 4.5×10^{-5} to 59% and from 2.4×10^{-3} to 36% of total dissolved U concentration in the Field soils and BGSc soils, respectively. Apart from free ion activity (UO_2^{2+}), U binding to carbonate (4.2×10^{-3} to 98%) and to DOM (1.6 to 97%) represented important U species in soil solution and varied depending on soil pH. In contrast to Th, the free uranyl cation (UO_2^{2+}) represented 38% on average of the total dissolved U in AW and AM soils, which supports the hypothesis that below pH 5.5 the uranyl cation (UO_2^{2+}) predominates (Langmuir, 1978; Ebbs et al., 1998; Curtis et al., 2004; Vandenhove et al; 2007, 2009). In these acidic soils (AW and AM), due to the high DOC concentration, UO_2^{2+} was also complexed with DOC in soil solution (50% of dissolved U, on average).

Empirical modelling of Th and U free ion activity using soil properties

The free ion activity of Th and U was determined from the speciation of soil solution phase using the geochemical speciation model WHAM-VII; all soil solution cation and anion concentrations were used to determine the free ion activity. The observed free ion activity was then related empirically to the soil characteristics that are most likely to control the solid-solution equilibrium of the free ions.

Empirical modelling of Th free ion activity (Th^{4+}) using soil properties

Table 6.5 shows the optimised coefficients (K_0, $K_{pH,}$ K_{SOM}, K_{Lab}), RSD and r values for model prediction of $\log_{10}(Th^{4+})$ using pH, %SOM and U_E as determining variables. Observed and predicted $\log_{10}(Th^{4+})$ values were highly correlated ($r > 0.95$). The coefficient for pH (K_{pH}) indicated a negative effect on $\log_{10}(Th^{4+})$, i.e. a higher soil pH results in a decrease in Th FIA in soil solution. A negative effect from %SOM was only found for the Field soils, while for BGSc soils %SOM content did not significantly affect the FIA. In addition, labile Th (Th_{TMAH}) did not significantly influence the FIA. Soil pH value was the most important soil variable for predicting $\log_{10}(Th^{4+})$ in Field soils and the only significant variable in BGSc soils, explaining 96.2% and 92.1% of the total variance in $\log_{10}(Th^{4+})$ in Field soils and BGSc soils, respectively. Including %SOM into the Field soils regression equation slightly improved the model prediction (Table 6.5).

Empirical modelling of U free ion activity (UO_2^{2+}) using soil properties

Table 6.5 shows the optimised coefficients (K_0, $K_{pH,}$ K_{SOM}, K_{Lab}), RSD and r values for model prediction of $\log_{10}(UO_2^{2+})$ using pH, %SOM and U_E as determining variables:

$$\log_{10}(Th^{4+}) \text{ or } \log_{10}(UO_2^{2+}) = K_0 + K_{pH}\,(pH) + K_{SOM}\,(\%SOM) + K_{Lab}\,(M_{Lab}) \quad (6.1)$$

A strong correlation was found between observed FIA from WHAM-VII speciation of soil solution concentrations and predicted values (r >0.95). The FIA is mainly controlled by the soil pH and followed a single trend with soil pH unlike total U concentration in soil solution which followed a binary trend with pH due to carbonate complex formation (Section 6.3.4). The coefficient for pH (K_{pH}) indicated a negative effect on $\log_{10}(UO_2^{2+})$, i.e. a higher soil pH results in a decrease in (UO_2^{2+}) activity in soil solution. A small negative effect from %SOM was only found for the Field soils, while for BGSc soils %SOM content did not significantly affect the FIA. Soil pH was the most important soil variable for $\log_{10}(UO_2^{2+})$ prediction in both sets of soils, explaining 93% and 89.1% of the total variance in $\log_{10}(UO_2^{2+})$ in Field soils and BGSc soils, respectively. Including %SOM and U_E in the Field soils regression equation slightly improved the model prediction whereas introducing U_E into the BGSc soils regression equation only explained an additional 2.4% of the variance in $\log_{10}(UO_2^{2+})$.

Table 6.5: Linear regression model coefficients, RSD and correlation coefficient (r value, predicted vs measured) for model prediction of $\log_{10}(Th^{4+})$ and $\log_{10}(UO_2^{2+})$ using pH, %SOM and M_{Lab} (Th_{TMAH} and U_E) as determining variables (Equation. 6.1). Values in brackets are the % of total variance explained.

		Constant (K_0)	pH (K_{pH})	%SOM (K_{SOM})	M_{Lab} (K_{Lab})	RSD	r
Field soils	$\log_{10}(Th^{4+})$	2.302	-3.649 *(96.2)*	-0.088 *(1.8)*	-	0.700	0.990
	$\log_{10}(UO_2^{2+})$	-5.008	-1.254 *(93.0)*	-0.035 *(1.2)*	2.497 *(0.34)*	0.377	0.972
BGSc soils	$\log_{10}(Th^{4+})$	6.834	-4.244 *(92.1)*	-	-	0.969	0.960
	$\log_{10}(UO_2^{2+})$	-2.180	-1.548 *(89.1)*	-	0.285 *(2.4)*	0.405	0.957

The variables contribute significantly (P <0.01) to the regression.

Overall, Th and U free ion activities (log_{10} values) were accurately predicted using pH as the main variable and with only a very small contribution from %SOM and labile metal concentration (Table 6.5, Figure 6.13). This confirms the dominant role of pH in the partitioning and speciation of Th and U in soils. The difference between the predicted and observed free ion activity was less than 1 order of magnitude, except for a few U outliers (Figure 6.13). Thorium and U exhibited the same trend in terms of the distribution of free ion activity values among different soil groups, with the lowest free ion activity for Ca, Ba and BGSc pH >6.5 soils and the highest for AW and AM soils (Figure 6.13).

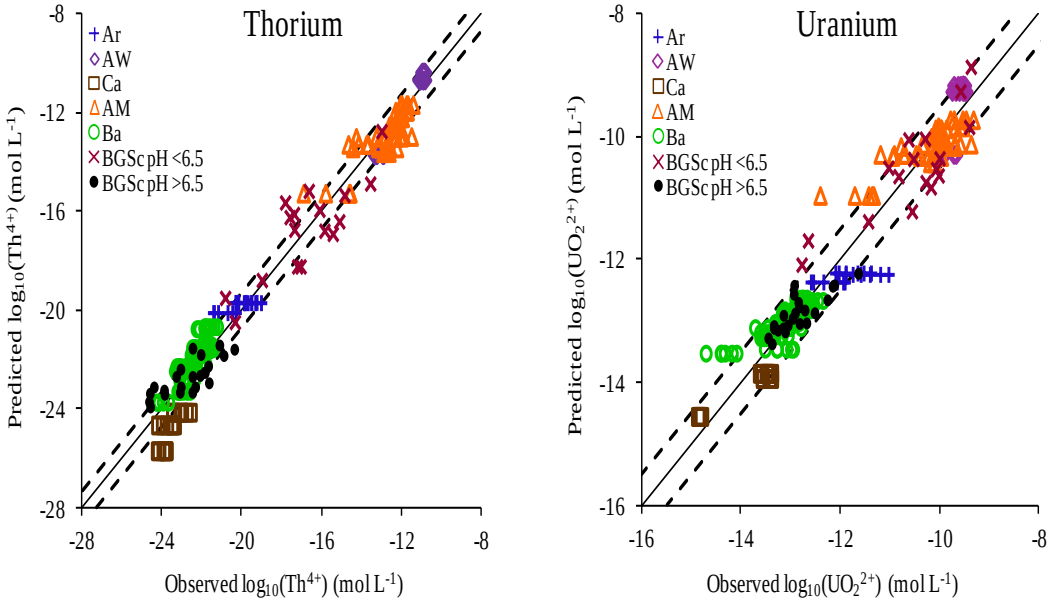

Figure 6.13: The free ion activity of Th^{4+} and UO_2^{2+} (log_{10} (mol L^{-1})) predicted from an optimised form of equation (6.1) compared with the observed free ion activity calculated using WHAM-VII for speciation of solution phase data for Arable (Ar; +), Acidic Woodland (AW; ◊), Calcareous (Ca; □), Acidic Moorland (AM; Δ), Biosolid-amended (Ba; ○), BGSc pH <6.5 (×) and BGSc pH >6.5 (●) soils, (n = 77). The solid line represents the 1:1 relationship and dashed lines represent ± RSD for the model.

6.3.6 Modelling Th and U K_d, K_d^{lab}, $^*K_d^{lab}$ values using soil properties

Solid-liquid distribution coefficients discussed below were based on (i) the ratio of total metal concentration in soil to that in the soil solution (K_d) (ii) the ratio of adsorbed reactive (labile) metal concentration in soil to total metal concentration in soil solution (K_d^{lab}) or (iii) the ratio of labile adsorbed metal to free metal ion activity in the soil solution phase ($^*K_d^{lab}$) calculated using WHAM-VII.

Stepwise regression was used to model Th and U $\log_{10}K_d$ values (K_d, K_d^{lab}, or $^*K_d^{lab}$) as a function of the soil variables thought most likely to affect Th and U solubility in soils (Equation 6.5): soil pH, %SOM, available phosphate (P-avail, mg kg^{-1}), DOC and DIC (mg L^{-1}), %$CaCO_3$, soil metal content (mg kg^{-1}), and Fe-oxide concentration (g kg^{-1}). Optimised regression coefficients, RSD and r of the predicted versus measured values are summarized in Tables 6.6 and 6.7 for Th and U, respectively. In general the regression results indicated that a limited number of soil variables were able to accurately explain the variance in $\log_{10}K_d$, $\log_{10}K_d^{lab}$ and $\log_{10}{}^*K_d^{lab}$ values.

$$\log_{10}K_d,\ \log_{10}K_d^{lab} \text{ or } \log_{10}{}^*K_d^{lab} = k_0 + k_1(pH) + k_2(M_{soil}) + k_3(\%SOM) + k_4(FeOx) + k_5(P\text{-}avail) + k_6(\%Clay) + k_7(\%CaCO_3) + k_8(DOC) + k_9(DIC) \quad (6.5)$$

Thorium: Prediction of K_d, K_d^{lab}, $^*K_d^{lab}$

Soil pH was the most important variable, explaining 74.1% and 40.5% of the total variance in $\log_{10}K_d$ for the Field soils and BGSc soils, respectively. The coefficient for pH indicated a positive effect on $\log_{10}K_d$ values, i.e. a higher pH results in a decrease of Th solubility. Introducing available-P, DOC, total Th and %SOM into the regression model explained a further 11%, 5.1%, 1.6% and 0.5% of the variance in $\log_{10}K_d$, respectively, in the Field soils, while in BGSc soils %SOM was the only significant variable with soil pH and explained a further 22% of the variance in $\log_{10}K_d$ values. A small positive effect from %SOM was only found for the Field soils; a positive effect was also found for available-P (increased %SOM and phosphate content decreased Th solubility). This positive effect was ascribed to the influence of the Ba soils; with exclusion of Ba soils from the regression analysis both %SOM and phosphate content were found to be non-significant variables and Th K_d values were explained by pH (71.2%), DOC (14.1%) and total Th (1.2%).

Table 6.6: Linear regression model coefficients, RSD and correlation coefficient (r value, predicted vs measured) for model prediction of Th $\log_{10}K_d$, $\log_{10}K_d^{lab}$, $\log_{10}{}^{*}K_d^{lab}$ (L kg^{-1}) from soil properties. The regression equations were fitted with K_d values that were based on total Th concentration (K_d = Th_{tot}/Th_{soln}) or on Th_{TMAH} concentration (K_d^{lab} = Th_{TMAH}/Th_{soln}, and ${}^{*}K_d^{lab}$ = $Th_{TMAH}/(Th^{4+})$). Values in brackets are the % of total variance.

		Constant	pH	P-avail	%SOM	DOC	Th_{soil}	RSD	r
Field soils	$\log_{10}K_d$	2.08	0.394	0.002	0.023	-0.004	0.203	0.32	0.96
			(74.1%)	*(11)*	*(0.48)*	*(5.1)*	*(1.6)*		
	$\log_{10}K_d^{lab}$	1.49	0.203	0.003	-	-0.003	0.244	0.35	0.94
			(19.2)	*(58.5)*		*(4.3)*	*(5.7)*		
	$\log_{10}{}^{*}K_d^{lab}$	-7.73	3.264	0.005	-	-	0.326	0.64	0.99
			(94.8)	*(2.9)*			*(0.4)*		
BGSc soils	$\log_{10}K_d$	3.48	0.344	-	-0.027	-	-	0.33	0.79
			(40.5)		*(22)*				
	$\log_{10}K_d^{lab}$	7.16	-0.534	-	-0.023	-	-	0.42	0.71
			(36.5)		*(13.5)*				
	$\log_{10}{}^{*}K_d^{lab}$	-7.30	3.306	-		-	-	*0.95*	*0.94*
			(88.0)						

All entered variables contributed significantly (P <0.01) to the regression.

The solid-liquid distribution was also expressed with respect to the reactive Th (Th_{TMAH}; K_d^{lab}) instead of the total Th concentration (K_d) and with respect to the free ion activity instead of total solution concentration (${}^{*}K_d^{lab}$). The K_d value was higher than K_d^{lab} by an average factor of 37, while ${}^{*}K_d^{lab}$ was much higher than K_d and K_d^{lab} by average factors of 6.2×10^{10} and 1.9×10^{12}, respectively, due to the extremely low free ion activity values (Th^{4+}) calculated using WHAM-VII. Empirical regression modelling was also undertaken for K_d^{lab} and ${}^{*}K_d^{lab}$. Although better prediction is expected for K_d^{lab} describing the equilibrium between the reactive metal pool and solution phase, no improvement in the prediction of Th solubility (judging from values of RSD, r values, % of total variance) was found by using Th_{TMAH} instead of total Th concentration as the numerator in the distribution coefficient. This probably results from compensating factors included within the regression parameters explaining the variance in K_d values (Table 6.6). The value of Th_{TMAH} is highly pH dependent (a negative effect of pH on Th_{TMAH}; Section 4.3.9), thus the variation in reactive Th fraction between soils in the modelling of K_d will be accounted for by the pH coefficient in Equation 6.5. This may also explain the surprising negative effect of

pH on $\log_{10}K_d^{lab}$ in BGSc soils. There was a significant negative effect of pH on Th_{TMAH} ($r = -0.8$, $P < 0.001$) in BGSc soils. By contrast, better prediction was found for ${}^{*}K_d^{lab}$ which describes the equilibrium between the reactive Th pool and the free Th^{4+} ion in solution phase. A limited number of soil variables were included for predicting $\log_{10}{}^{*}K_d^{lab}$ compared to $\log_{10}K_d$ and $\log_{10}K_d^{lab}$. For BGSc soils, pH was the only significant variable and explained 88% of the variance in $\log_{10}{}^{*}K_d^{lab}$, while soil pH explained 94.8% of the variance in the Field soils $\log_{10}{}^{*}K_d^{lab}$. Introducing available phosphate and total Th into the regression contributed only 2.9 and 0.4% of the variance, respectively, in predicted $\log_{10}{}^{*}K_d^{lab}$ values (Table 6.6). Sheppard et al. (2007) performed stepwise regression between Th $\log_{10}K_d$ for Canadian agricultural soils versus soil pH, clay content and %SOC: pH was the only significant variable with a positive effect on $\log_{10}K_d$ ($r^2 = 0.24$). Sheppard et al. (2009) combined Th K_d datasets; Canadian soils, Thibault et al. (1990) datasets, along with data from Sheppard and Hawkins (1991), the stepwise regression of those combined datasets included only pH as a significant variable with $r^2 = 0.16$. Overall, comparison of measured and predicted $\log_{10}K_d$, $\log_{10}K_d^{lab}$, $\log_{10}{}^{*}K_d^{lab}$ values (Figure 6.14) shows that the empirical model was able to accurately predict Th solubility. The difference between the predicted and measured $\log_{10}K_d$, $\log_{10}K_d^{lab}$, $\log_{10}{}^{*}K_d^{lab}$ values was less than 1 order of magnitude for all soils.

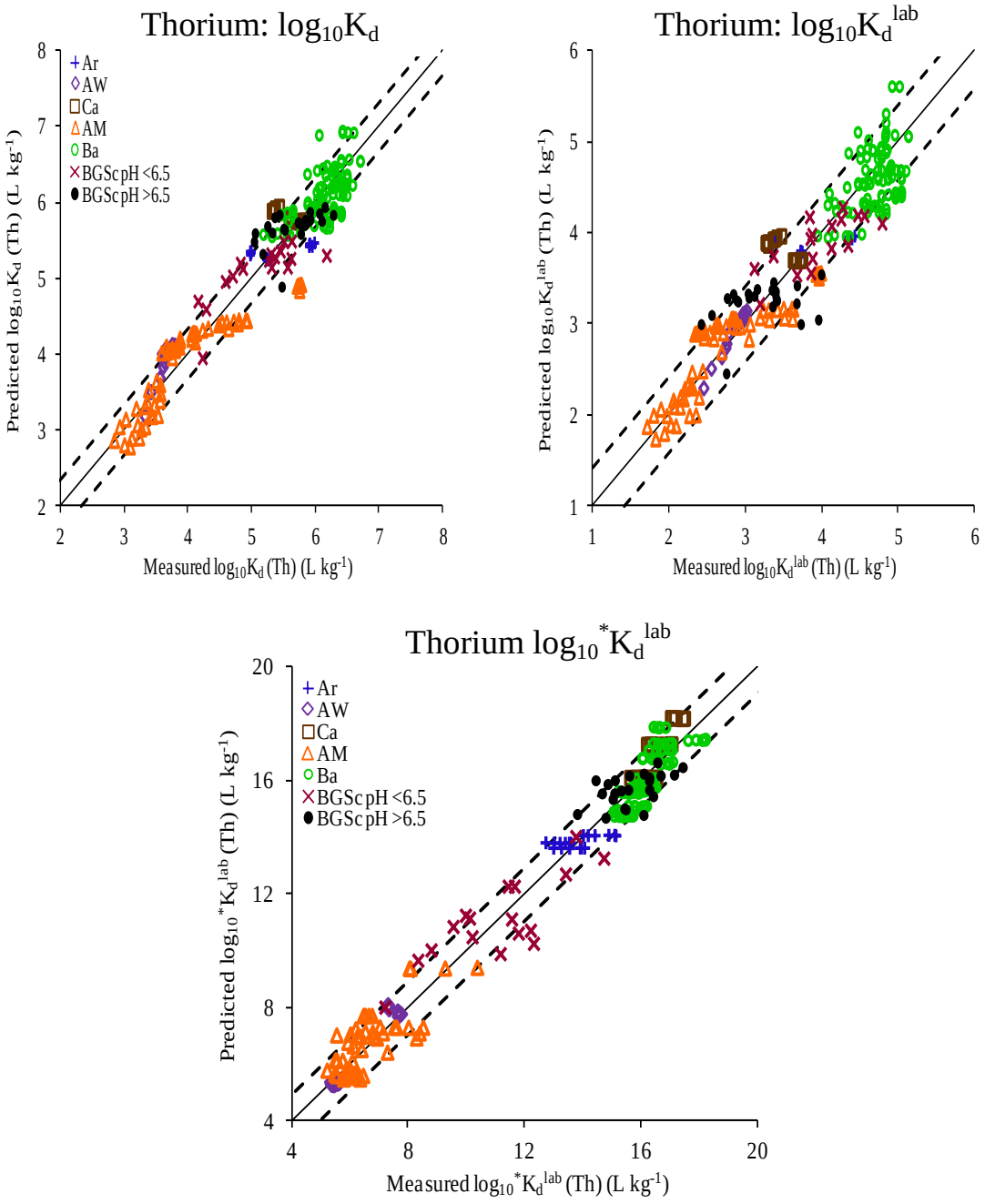

Figure 6.14: Comparison of measured and predicted values of Th $\log_{10}K_d$, $\log_{10}K_d^{lab}$, $\log_{10}{}^*K_d^{lab}$ (L kg^{-1}) using a multiple linear regression model. The solid line represents a 1:1 line and dashed lines represent ± RSD (the larger RSD for Field soils or BGSc soils) for the model fit. The two sets of soils were modelled separately because of differences in methodology (Section 6.3.3). Optimization parameters are given in Table 6.6.

Uranium: Prediction of K_d, K_d^{lab}, ${}^*K_d^{lab}$

As noted before, K_d for U showed two contrasting trends with pH value (Section 6.3.4), therefore two stepwise regressions were developed for the Field soils (pH <5 and pH >5). Below pH 5, pH was the dominant soil variable and accounted for the largest proportion of the total variance (60.5%) in $\log_{10}K_d$ (Table 6.7), followed by

DOC (18.2%). The contributions from available phosphate content, %SOM and total U content were statistically significant but these variables explained only a very small proportion of the total variance in $\log_{10}K_d$ values. The coefficient for pH indicated a positive effect on $\log_{10}K_d$, i.e. increased pH decreased U solubility. By contrast, the coefficient for pH indicated a negative effect on $\log_{10}K_d$ values for the Field soils above pH 5 and BGSc soils. Moreover, soil pH was not the dominant soil variable above pH 5; DIC explained 87.5% and 54.4% of the variance in $\log_{10}K_d$ for Field soils (pH >5) and BGSc soils respectively. Apart from DIC, the significance of soil properties on predicting $\log_{10}K_d$ appeared to be soil-specific. For example, introducing the significant variables (available phosphate, total U and pH) into the regression model explained 5.2%, 1.9% and 1.6% of the variance in $\log_{10}K_d$, respectively, in Field soils (pH >5), while adding $\%CaCO_3$, DOC and soil pH contributed 14.6%, 7.4% and 4.9% of variance in $\log_{10}K_d$ for BGSc soils (Table 6.7). The Field soil data were also fitted to a single regression: neither pH nor DIC were the most important variables for $\log_{10}K_d$, instead, available phosphate was the most important variable, explaining 43.8% of the total variance in $\log_{10}K_d$, followed by DIC and DOC which contributed significantly and accounted for 20.2% and 17.3% of the variance, respectively. It appears that using a single regression to predict $\log_{10}K_d$ for all the Field soils, which cover a pH range from 3.0 to 7.13, masked the strong binary trend of pH on $\log_{10}K_d$ (See section 6.3.4 for details) and also, to some extent, the effect of DIC. Therefore, it is preferable to divide the dataset by pH and develop two regression models for U $\log_{10}K_d$ values. Sheppard et al. (2009) managed the Canadian dataset in two stepwise regressions; pH >5.5 (182 soils), pH and clay content were the significant variables, while for pH <5.5 (30 soils) there was no significant variable. The data from the review by Sheppard et al. (2006) and references therein, which includes almost all the data from Thibault et al. (1990), were also managed in two regressions. Above pH 5.5 (123 soils), pH, SOC and clay*pH interactions were the significant variables, while below pH 5.5 (24 soils), only soil pH was the significant variable. EMRAS (2008) reported that U K_d values varied with pH and were classified based on soil pH.

Table 6.7: linear regression model coefficients, RSD and correlation coefficient (r value, predicted vs measured) for model prediction of U $\log_{10}K_d$, $\log_{10}K_d^{lab}$, $\log_{10}{}^{*}K_d^{lab}$ (L kg^{-1}) from soil properties. The regression equations were fitted with K_d values that were based on total U concentration ($K_d = U_{tot}/U_{soln}$) or on labile U concentration ($K_d^{lab} = U_E/U_{soln}$ and ${}^{*}K_d^{lab} = U_E/(UO_2^{2+})$). Values in brackets are the % of total variance.

		Constant	pH	P-avail	%SOM	DIC	DOC	U_{soil}	$\%CaCO_3$	RSD	r
Field soils											
pH <5	$\log_{10}K_d$	0.21	0.907	-0.004	0.042	-	-0.004	0.704	-	0.23	0.92
			(60.5)	*(3.1)*	*(2.3)*		*(18.2)*	*(1.1)*			
	$\log_{10}K_d^{lab}$	-1.29	0.778	-0.006	0.066	-	-0.003	1.230	-	0.23	0.89
			(47.3)	*(13.6)*	*(7.4)*		*(7.0)*	*(4.8)*			
	$\log_{10}{}^{*}K_d^{lab}$	-2.78	1.005	-0.002	0.108	-	-0.003	1.947	-	*0.28*	*0.85*
			(36.5)	*(8.5)*	*(7.3)*		*(9.2)*	*(10.1)*			
pH >5	$\log_{10}K_d$	6.28	-0.273	0.001	-	-0.017	-	0.181	-	0.15	0.98
			(1.6)	*(5.2)*		*(87.5)*		*(1.9)*			
	$\log_{10}K_d^{lab}$	5.17	-0.292	0.001	-	-0.017	-	3.392	-	0.15	0.97
			(1.8)	*(0.97)*		*(81.3)*		*(11.7)*			
	$\log_{10}{}^{*}K_d^{lab}$	-5.69	1.933	0.001	-	-0.013	-	2.948	-	*0.19*	*0.97*
			(53.2)	*(30.8)*		*(7.1)*		*(2.0)*			
pH 3.0 – 7.13	$\log_{10}K_d$	4.16	0.167	0.001	0.026	-0.018	-0.004	-	-0.154	0.28	0.93
			(1.4)	*(43.8)*	*(1.2)*	*(20.2)*	*(17.3)*		*(1.7)*		
	$\log_{10}K_d^{lab}$	2.77	0.138	0.001	0.035	-0.012	-0.004	-	-0.184	0.29	0.90
			(1.4)	*(52.7)*	*(2.1)*	*(4.0)*	*(6.9)*		*(14.5)*		
	$\log_{10}{}^{*}K_d^{lab}$	-2.43	1.476	-	0.028	-0.014	-	-	-	0.33	*0.98*
			(92.6)		*(2.8)*	*(1.2)*					
BGSc soils											
BGSc soils	$\log_{10}K_d$	7.06	-0.369	-	-	-0.016	-0.008	-	-0.091	0.25	0.90
			(4.9)			*(54.4)*	*(7.4)*		*(14.6)*		
	$\log_{10}K_d^{lab}$	6.79	-0.460	-	-	-0.019	-0.007	-	-0.084	0.27	0.91
			(6.2)			*(60.6)*	*(1.5)*		*(14.1)*		
	$\log_{10}{}^{*}K_d^{lab}$	-1.93	1.274	-	-		-0.003	-	-	*0.34*	*0.96*
			(90.3)				*(0.7)*				

All entered variables contributed significantly (P <0.01) to the regression.

Uranium solid-liquid distribution coefficients were also expressed with respect to the labile pool (U_E; Kd^{lab}) instead of total U concentration (K_d) and with respect to the free ion (UO_2^{2+}) activity instead of total solution concentration ($^*K_d^{lab}$). As found for Th, the K_d value was higher than K_d^{lab} by an average factor of 17, while $^*K_d^{lab}$ was higher than K_d and K_d^{lab} by average factors of 205 and 3,555, respectively. Uranium $\log_{10}K_d^{lab}$ and $\log_{10}{}^*K_d^{lab}$ were also modelled as a function of measured soil properties (Table 6.7). There was no obvious advantage in using U_E instead of total U concentration to predict U solubility (K_d^{lab}; Table 6.7). This may seem against expectation, but the lack of any clear advantage in using the labile U pool to predict K_d value probably results from compensating factors included within the regression parameters explaining the variance in K_d value. The variation in U lability between soils with pH will be subsumed into the regression of K_d by the pH coefficient, as noted for heavy metals by Tye et al. (2003) and Degryse et al. (2009). Unlike $\log_{10}K_d$ and $\log_{10}K_d^{lab}$, $\log_{10}{}^*K_d^{lab}$ followed a single trend with soil pH because UO_2^{2+} activity decreased continuously with increasing soil pH. Therefore, $^*K_d^{lab}$ which describes the equilibrium between the labile U pool and the free (UO_2^{2+}) ion in solution phase can be predicted by a single regression model (regardless of pH range) with a limited number of soil variables. There was a marginally better prediction for $\log_{10}{}^*K_d^{lab}$ than $\log_{10}K_d$ and $\log_{10}K_d^{lab}$: soil pH explained 92.6% and 90.3% of the variance in U $\log_{10}{}^*K_d^{lab}$ for the Field soils and BGSc soils, respectively. Apart from pH, the inclusion of %SOM and DIC slightly improved the prediction of $\log_{10}{}^*K_d^{lab}$ for Field soils. For BGSc soils, DOC was the least important variable compared with soil pH and explained only 0.7% of the variance in $\log_{10}{}^*K_d^{lab}$.

Overall, U $\log_{10}K_d$, $\log_{10}K_d^{lab}$, $\log_{10}{}^*K_d^{lab}$ values were accurately predicted using soil variables: pH and DIC were the dominant predictors, in agreement with the suggestion that pH and dissolved carbonate concentrations are the two most important factors to influence U K_d values (EPA 1999; Thibault et al., 1990; Curtis et al., 2004; Sheppard et al., 2009). Comparison of measured $\log_{10}K_d$, $\log_{10}K_d^{lab}$ and $\log_{10}{}^*K_d^{lab}$ with predicted values (Figure 6.15) showed good agreement and accurate prediction of U solubility within one order of magnitude of the measured values for the Field soils (pH <5 and >5) and BGSc soils.

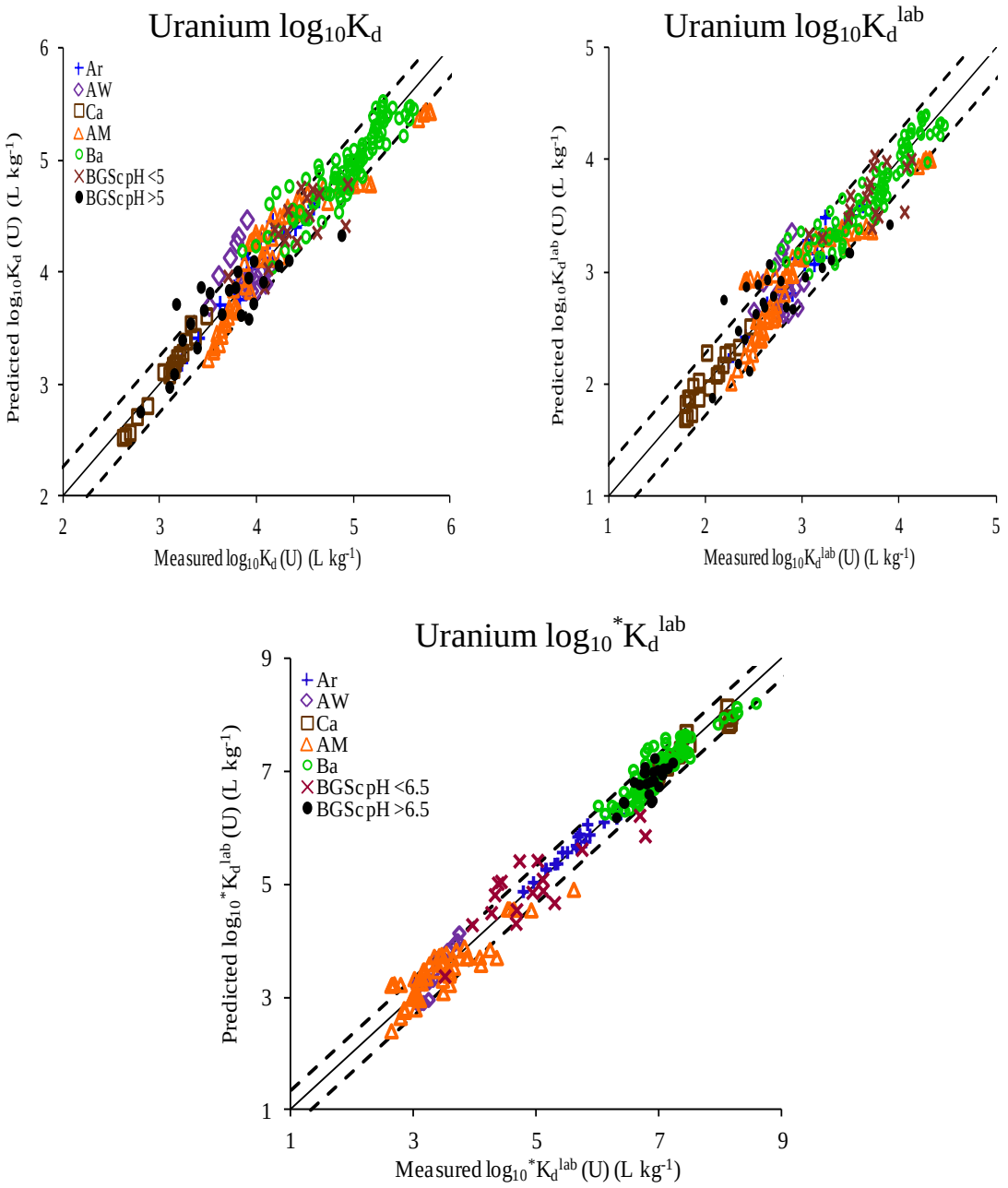

Figure 6.15: Comparison of measured and predicted values of U $\log_{10}K_d$, $\log_{10}K_d^{lab}$, $\log_{10}{}^{*}K_d^{lab}$ (L kg^{-1}) using a multiple linear regression model. The solid line represents a 1:1 line and dashed lines represent ± RSD (the largest RSD for Field soils pH <5, pH >5 or BGSc soils) for the model fit. The Field soils pH <5 (AW, AM), pH >5 (Ar, Ca, Ba) and the BGSc soils were modelled separately because of differences in methodology (Section 6.3.3). Optimization parameters are given in Table 6.7.

6.4 CONCLUSIONS

To predict U and Th solubility there appeared to be only marginal advantages in using the labile metal fraction in preference to total soil U and Th content, or in basing the K_d value on the free metal ion activity in soil solution rather than the total concentration in solution. Thus, because it is preferable to include only routinely measured soil properties in empirical models, it might be more applicable to predict Th and U solid liquid distribution using the simple form of the K_d value. However, this depends on the purpose behind the prediction of K_d values. When the objective is to predict metal leaching and transport, the total Th and U solution concentration, rather than the free ion activity must be known (K_d). On the other hand, if the objective is to calculate risks to micro-fauna and aquatic organisms, predict plant uptake, or to calculate the geochemical phase present in the soil, then free metal ion activity may be more important than the total solution concentration. Furthermore, although the optimised empirical models based on simple K_d values can provide adequate predictions of Th and U solubilities, they may be not applicable beyond the range of soil properties which applied when measured – especially if solution speciation varies (Degryse et al., 2009; Ivezić et al., 2012). So, for example, the prediction of a simple K_d value for U above pH 5 will fail if the partial pressure of CO_2 (and bicarbonate concentration) differs from those present during the measurements used to parameterise the original regression equation. Similarly, prediction of a K_d value for Th depends almost entirely on DOC falling in a range similar to that in the soils used to parameterise the regression equation. In both these cases, the prediction of $\log_{10}{}^{*}Kd^{lab}$ should be much more robust but, of course, accurate solution speciation is then required to convert ${}^{*}Kd^{lab}$-predicted free ion activities to total solution concentrations. Hence the need for internally consistent geochemical speciation models.

7 USE OF THE GEOCHEMICAL SPECIATION MODEL WHAM-VII TO PREDICT SOLUBILITY AND SPECIATION OF URANIUM AND THORIUM

7.1 INTRODUCTION

Complex formation between trace metals and organic and inorganic ligands in the soil solution phase affects metal mobility, bioavailability and sorption to soil surfaces (Bednar et al., 2007). Uranium and Th form stable complexes with dissolved organic matter, DOM (Glaus et al., 1997; Saito et al., 2004; Casartelli and Miekeley, 2003; Zhang et al., 1997; Jackson et al., 2005; Wu et al., 2004) and, as a result, can undergo transport (McCarthy et al., 1998; Artinger et al., 1998; Artinger et al., 2000; Schussler et al., 2001). Soil solution Th and U speciation depends on soil physico-chemical characteristics (Langmuir and Herman, 1980, Taboada et al. 2006, Vandenhove et al., 2007; Gustafsson et al., 2009). For example, it is widely accepted that the low U(VI) K_d values seen in alkaline soils (Echevarria et al., 2001; Vandenhove et al., 2007, 2009) and the mobility of U(VI) in aquifers at circumneutral to alkaline pH values is due to the formation of soluble uranyl-carbonate complexes, $UO_2(CO_3)_2^{2-}$ and $UO_2(CO_3)_3^{4-}$ (Hsi and Langmuir, 1985; Waite et al., 1994; Pabalan et al., 1998; Barnett et al., 2000). Furthermore, recent studies of U(VI) geochemistry have focused on the important role of $Ca_2UO_2(CO_3)_3$ and $CaUO_2(CO_3)_3^{2-}$ complexes in U(VI) aqueous chemistry at neutral to alkaline pH values due to their large formation constants (Brooks et al., 2003; Zheng et al., 2003; Dong and Brooks, 2006; Kelly et al., 2007). In addition, Ca-U(VI)-CO_3 complexes have been reported to inhibit microbial reduction of U(VI) (Brooks et al., 2003; Wang et al., 2004) which would also have the effect of increasing solubility. Thorium can form Th-carbonate and/or Th-hydroxy-carbonate complexes under neutral to alkaline conditions depending on pH and carbonate concentration; such complexes may be responsible for the increased Th solubility reported in alkaline soils (Lafiamme and Murray 1987; Östhols et al. 1994; Rai et al., 1994; Felmy et al., 1997; Altmaier et al., 2005, 2006; Rand et al., 2008). Soil temperature and microbial mineralization processes may also influence the solubility and speciation of trace metals in the soil solution (Cornue et al., 2007, 2011) through modifying the soil physico-chemical properties (e.g. pH, ionic strength, dissolved organic and inorganic carbon concentration), which in turn will influence

the solubility and speciation of Th and U in the soil solution (Langmuir and Herman, 1980, Taboada et al. 2006, Vandenhove et al., 2007; Curtis et al., 2006; Um et al., 2010) and sorption on solid phases (Waite et al., 1994; Braun et al., 1998; Murphy et al., 1999; Wazne et al., 2003; Hongxia et al., 2006; Fox et al., 2006; Chen et al., 2007). Therefore, understanding of the speciation of Th and U in the soil solution and the soil parameters and processes that influence Th and U dynamics in soil is necessary for comprehensive risk assessments. Modelling of trace metal solubility and speciation is now becoming increasingly common in research and risk assessment.

To study and predict the solid-solution partitioning of U and Th in soil, two approaches can be used: empirically derived relationships (described in detail in Chapter 5) and mechanistic geochemical speciation models. Mechanistic models that describe solid-solution interactions comprehensively, and take into account the variation in soil solution geochemistry and competitive binding to both the soil solid phase and ligands in solution, are more reliable and can cover a wider range of soil conditions than empirical models (Tipping et al., 2003). In addition, mechanistic models provide detailed information about solution speciation and metal partitioning in the whole soil which is not possible with empirical predictions of bulk K_d values. Surface complexation models (SCM) have been used to describe the adsorption of U(VI) contaminants on sediment and compared to U K_d values; it has been reported that the SCM better reflect the dynamic behaviour of a complex aquifer system (Kohler et l., 1996 and 2004; Davis et al., 2006; Curtis et al., 2006; Um et al., 2010). However, mechanistic geochemical models demand a large number of input variables, some of which may be difficult to measure. Prime examples include the ‘reactive metal fraction’, which is used as a predictor of metal concentration and speciation in the soil solution, and the concentration of active adsorption phases (organic matter content, clay content and mineral oxides) (Buekers et al., 2008). Inevitably, assumptions are required to quantify model variables such as the ‘active organic matter fraction’ and the ‘reactive surface area’ of Fe oxides (Degryse et al., 2009).

In this chapter the geochemical speciation model WHAM-VII was used to provide a mechanistic prediction of both fractionation in the solid phase and speciation (of U and Th) in the solution phase. The WHAM model has been used to investigate the

fractionation and solubility of a range of metals in soils (Tipping et al., 2003; Marzouk et al., 2013) but not, to date, to predict solubility of Th and U in whole soils. Stockdale and Bryan (2012) and Stockdale et al., (2013) investigated the binding of Th^{4+}, UO_2^{2+} and NpO_2^{+} with DOM under the high pH regimes expected in cementitious disposal using equilibrium dialysis over a pH range from ~9 to 13. The results were compared with predictions from WHAM-VII to test the effectiveness of the model and to demonstrate the utility of the model for predicting binding to DOM under these conditions. The extraction methods used to define reactive metal fractions are critical inputs for these models. In the current comparative study, predictions of solubility for U were based on isotopically exchangeable U (U_E), total soil U content (U_{tot}), U extracted by 1 M CH_3COONH_4 (U_{Ac}), 0.05 M EDTA (U_{EDTA}), 0.43 M HNO_3 (U_{Nit}) and 1% TMAH-extractable U (U_{TMAH}). For Th, predictions were based on Th_{Ac}, Th_{EDTA}, Th_{Nit}, Th_{TMAH} and Th_{tot}. In addition, U and Th solubilities and solution speciation under different soil temperatures and redox conditions were investigated. Finally, the extent of binding of Th and U to DOM in soil pore water and the distribution of these elements within DOM molecular size fractions were studied for contrasting soils using 'size exclusion chromatography' coupled to ICPMS (SEC-ICP-MS).

The primary objectives of this study were therefore to:

(i) evaluate the effectiveness of the mechanistic speciation model WHAM-VII to predict solid-solution partitioning and solubility of Th and U in two data sets covering a wide range of soil properties;

(ii) assess the relationship between soil temperature and Th and U complexation in order to predict the impact of soil temperature on the speciation of Th and U in the soil solution;

(iii) investigate the extent of binding of Th and U to DOM in soil pore water and compare the results with WHAM-VII predictions.

7.2 MATERIALS AND METHODS

7.2.1 Soil samples

In this study, two sets of soils were used. The first dataset (Field soils) consisted of 37 soil samples representing five contrasting local ecosystems; the second dataset (BGSc) included 40 soils sub-sampled from the British Geological Survey (BGS) archive. Both datasets covered a wide range of soil characteristics. The origins and characteristics of these two sets of soils have been described in Chapters 2 and 4.

7.2.2 WHAM-VII modelling

Modelling Th and U solubility, speciation and fractionation

WHAM-VII was used to predict Th and U concentrations in pore water from the first soil set over a period of 6 days (see Section 2.3.1 for details) and in the solution phase of suspensions of the second soil set (BGSc); the second soil set was suspended in 0.01 M $Ca(NO_3)_2$ (soil : solution ratio 1: 10) and shaken for 3 days to reach equilibrium (Section 2.3.2). The isotopically exchangeable ^{238}U E_{soln} (U_E; Section 2.6.4) was used as an estimate of the total reactive U concentration. Output from WHAM includes U and Th speciation, fractionation and total dissolved concentration. The predicted U and Th concentrations in solution were compared with the measured values to assess the performance of the model. The model settings and variables are listed in Table 7.1.

Predicting free ion activity

The observed free ion activities of UO_2^{2+} and Th^{4+} used in calculating $^{*}K_d^{lab}$ values (Equation 6.4) were calculated using WHAM-VII applied only to soil solution data. With the exception of (the inclusion of) particulate binding phases, all variables and settings were the same as those used to predict solubility and speciation in whole soil (Table 7.1).

Table 7.1: Summary of the variables and settings of WHAM-VII used for modelling Th and U solubility, speciation and fractionation in whole soils and in the soil solution.

Modelling U and Th solubility and speciation in soil	
Variables	**Settings**
Soil condition	
Suspended particulate matter (SPM)	First soil set: - BGSc soil set: 100 g L^{-1}; 1 g soil in 30 ml $Ca(NO_3)_2$
Temperature (K)	289.15 K; 16 ^oC
PCO_2(atm)	Atmospheric partial pressure (3.83×10^{-4} atm)
Soil pH	Measured in 0.01 M $Ca(NO_3)_2$ soil suspension.
Adsorption phase (g L^{-1}):	
Humic and fulvic acid	Estimated from total organic carbon (TOC; Section 2.2.5).
Fe, Al and Mn oxides	Dithionite-Citrate-Bicarbonate extraction (DCB; Section 2.2.8) converted to assumed $Fe_2O_3.H_2O$, Al_2O_3 and MnO_2 content.
Clay content	First soil set: estimated from known soil texture BGSc soil set: measured by laser granulometry (Section 2.2.3).
Colloidal fulvic acid	Estimated from measured DOC (Section 2.2.5).
Dissolved major cations, some trace elements and anions concentration (mol L^{-1})	
(Na, Mg, Al, K and Ca), (Ni, Cu, Zn, Cd and Pb), (Cl^-, NO_3^- and SO_4^{2-})	First soil set: concentration measured in soil pore water (Section 2.3.1); BGSc soil set: concentration measured in 0.01 M $Ca(NO_3)_2$ extract (Section 2.3.2);
Al^{3+} activity	Precipitation option for Al: i.e. allow $Al(OH)_3$ to precipitate if Al is a measured solution component.
Fe^{3+} activity	Precipitation option for Fe: assumes that Fe^{3+}activity is controlled by $Fe^{III}(OH)_3$ solubility; calculated within the model as a function of pH.
Dissolved carbonate	Estimated from total inorganic carbon measured in first soil set pore water and in BGSc soil set 0.01 M $Ca(NO_3)_2$ soil suspensions (Section 2.2.5)
Reactive Th and U concentration (mol L^{-1})	
Total Th concentration	Estimated from extraction with 1 M CH_3COONH_4 (Th_{Ac}), 0.05 MEDTA (Th_{EDTA}), 0.43 M HNO_3 (Th_{Nit}) or 1% TMAH (Th_{TMAH})
Total U concentration	Estimated from E-value (U_E) or extraction with 1 M CH_3COONH_4 (U_{Ac}), 0.05 MEDTA (U_{EDTA}), 0.43 M HNO_3 (U_{Nit}) or 1% TMAH (U_{TMAH})
Other settings	
Charge balance option	Do <u>not</u> charge balance, i.e. measured pH value used
Activity correction	Deby-Huckel equation used to estimate activity coefficients
WHAM database	Standard solute and phase binding databases
Modelling free ion activity	
Th and U concentration (mol L^{-1}) in soil solution	First soil set: concentration measured in soil pore water (Section 2.3.1); BGSc soil set: concentration measured in 0.01 M $Ca(NO_3)_2$ extract; soil solution ratio was 1 g to 10 ml
Other variables and settings are the same as above except the emission of particulate binding phases.	

7.2.3 The effect of soil temperature on Th and U dynamics and speciation in the soil solution phase

The soil used in this study was a biosolid-amended arable soil (Field 8, soil 8T; see Sections 4.2.1 and 4.3.1 for details). Fresh moist soil (500 g, < 4 mm) was packed into 15 cm wide neck plastic columns in triplicate and saturated with MilliQ water (soil (g): solution (ml) ratio was 2.2 : 1). The soil was incubated for 47 days at a range of temperatures (5, 10, 16, 25, and 30 ^{o}C) in well ventilated incubators. The incubation temperatures were chosen based on the annual variation of soil temperature at different soil depths reported by Wu and Nofziger (1999). The soil solution was extracted using Rhizon soil moisture samplers (see Section 2.3.1 for details) at 1, 5, 11, 19, 28, 40, and 47 days. Immediately after sampling the soil solution pH was measured (Section 2.2.1). The soil solution composition (concentrations of Th, U, Fe, Mn, Ca and Mg, DOC and DIC, anions) was determined (Sections 2.5.1, 2.2.5, 2.2.6).

7.2.4 SEC-ICP-MS analysis

The settings for SEC are described in detail in Chapter 2, Section 2.5.2. Soil pore water samples of 100 µl were injected into the mobile phase (0.1 M Tris buffer, pH 8.2) with a flow rate of 1 ml min^{-1}. Samples were introduced directly from the SEC column to the nebuliser of the ICP-MS for Th and U analysis. To quantify Th and U speciation in soil pore water Th and U calibration curves were constructed using a standard addition approach. It is unlikely that inorganic standards could survive transition through the SEC given the pH of the mobile phase; therefore, HA was used as a carrier for Th and U standards. Initially, EDTA (0.01 M) was used as a carrier for Th and U standards, but this approach did not produce consistent recoveries or sensitivities (cps/ppb) for Th and U. This may have been due to the dissociation of EDTA complexes during elution and the consequent adsorption of Th and U to the column gel phase. However, this behaviour was more pronounced for U than Th, probably due to the low stability constant of U-EDTA complexes and the greater likelihood that hydrogen bonding can take place between the free uranyl cation (UO_2^{2+}) and the column matrix. Calibration standards were prepared by adding known concentrations of Th and U (ICP-MS standard solutions) to 1.0 g L^{-1} solution of humic

acid. The final concentrations of Th and U in standard solutions were 5 and 10 µg L^{-1}. The entire chromatogram of Th and U was integrated using PlasmaLab software (Version 2.5.1.276, Thermo Electron, 2003) and blank-subtracted to produce calibration curves for Th and U as counts per second (CPS) versus concentration with r^2 >0.99. All soil pore water samples and calibration standards were run in duplicate.

The humic acid used as a carrier for Th and U standards was previously extracted from soil from a coniferous plantation in Leicestershire (Benscliffe Wood, SK519123) using sodium hydroxide as described by Marshall et al. (1995). Stock HA solution (8 g L^{-1}) was prepared by dissolving the freeze dried sample in 0.5 M NaOH and adjusting the pH value to 7.0 with nitric acid (50%).

7.3 RESULTS AND DISCUSSION

7.3.1 Predicting Th and U concentrations in soil solution using WHAM-VII

The performance of WHAM-VII in predicting Th and U concentrations in soil solutions from the two sets of soils was evaluated by comparing predicted with measured values of $-\log_{10}(Th_{soln})$ and $-\log_{10}(U_{soln})$. The model was parameterized with chemically extracted metal (M_{Ext}; eg Th_{TMAH}), isotopically exchangeable U (U_E) or total soil metal concentration (M_{total}) as input variables. A full set of input variables is shown in Section 2.7. Generally, Th and U solubility predictions based on M_{total} were less successful than those based on Th_{Ext} and U_E. In contrast to the empirical models (Section 6.3.6), the difference between WHAM-VII predictions using U_E or Th_{TMAH} and M_{total} was very clear.

7.3.1.1 Comparing Th solubility predicted using WHAM with Th_{Ext} or Th_{total} as inputs

Figure 7.1 shows measured against predicted values of Th concentration in solution (pTh_{soln}; $-\log_{10}$ (mol L^{-1})) for the two sets of soils, using chemically extracted Th (Th_{Ac}, Th_{EDTA}, Th_{Nit}, Th_{TMAH}) or total soil Th content (Th_{total}) as the reactive Th pool in the soil. Table 7.2 shows the relative predictive power of the different approaches using four indices to evaluate the accuracy of the model prediction:

- the average bias (ΔpTh_{soln} or ΔpU_{soln}) in measured and modelled values of $p(M_{soln})$;
- the median ratio (P/M) of predicted:measured values of $p(M_{soln})$;
- the residual standard deviation (RSD) of predicted from measured values of $p(M_{soln})$;
- the correlation coefficient (r) for predicted vs measured values of $p(M_{soln})$.

The solubility prediction based on total Th concentration was less successful (higher RSD and bias from the 1:1 line; Figure 7.1 and Table 7.2) than prediction based on extractable Th, in marked contrast to the empirical model used to predict Th solubility (Section 6.3.6). Using Th_{total} as a proxy for 'reactive' Th in the soil overestimated the concentration of soluble Th in all soil groups, the overestimation was much more pronounced in BGSc soils, particularly BGSc soils with pH values >6.5. By contrast, the prediction of Th solubility based on Th_{Ext} depended on the method used to estimate the labile fraction. For example, using Th_{Ac} as the input variable generally

underestimated the soluble Th concentration (RSD = 4.25, ΔpTh_{soln} = -1.82). This was as expected, because Th_{Ac} is unlikely to represent the entire labile Th fraction in soil (Section 4.3.8), although Th solubility in BGSc soils was predicted reasonably well. A poor correlation was found between measured and predicted Th solubility when Th_{Nit} was used as the input variable (r = 0.21, RSD = 1.65); this failing seemed to extend beyond the poor prediction of soluble Th concentration in Ca soils due to the 'capacity failure' of the nitric acid extraction method in calcareous soils (Section 4.3.8). Among the four extracted fractions of Th (Th_{Ac}, Th_{EDTA}, Th_{Nit}, Th_{TMAH}), the model gave a better prediction using Th_{TMAH} as the input with a relatively low deviation from the 1:1 line (RSD = 0.82) and high correlation coefficient (r = 0.82). This is in agreement with the previous suggestion that Th_{TMAH} may provide a reasonable estimate of the reactive Th pool (Section 4.3.8) which may be dominated by humus-bound forms of Th. The use of Th_{EDTA} as the labile Th pool gave better predictions than Th_{Ac}, Th_{Nit} and Th_{total}, but produced greater scatter of the modelled data and a lower correlation coefficient than Th_{TMAH}. Overall, the fit of modelled values of pTh_{soln} to measured data showed a strong dependency on the choice of Th_{Ext} method used to estimate labile Th. This suggests that there is scope for further refinement of methods used to estimate the reactive Th pool in soil.

Table 7.2: Summary of goodness of fit parameters for predicting solution concentration of Th (pTh_{soln}) using either chemically extracted Th (Th_{Ac}, Th_{EDTA}, Th_{Nit}, Th_{TMAH}) or total Th concentration (Th_{total}) as input variables to WHAM-VII.

	Input variable	ΔpTh_{soln}	Median P/M	RSD	r
Thorium	Th_{Ac}	-1.82	1.20	4.25	0.88
	Th_{EDTA}	0.28	0.98	1.00	0.73
	Th_{Nit}	0.04	0.97	1.65	0.21
	Th_{TMAH}	**0.66**	**0.92**	**0.82**	**0.82**
	Th_{total}	2.20	0.78	5.51	0.67

ΔpTh_{soln} = pTh_{soln} measured - pTh_{soln} predicted
Median P/M = predicted ($-\log_{10}$ (M))/measured ($-\log_{10}$ (M))

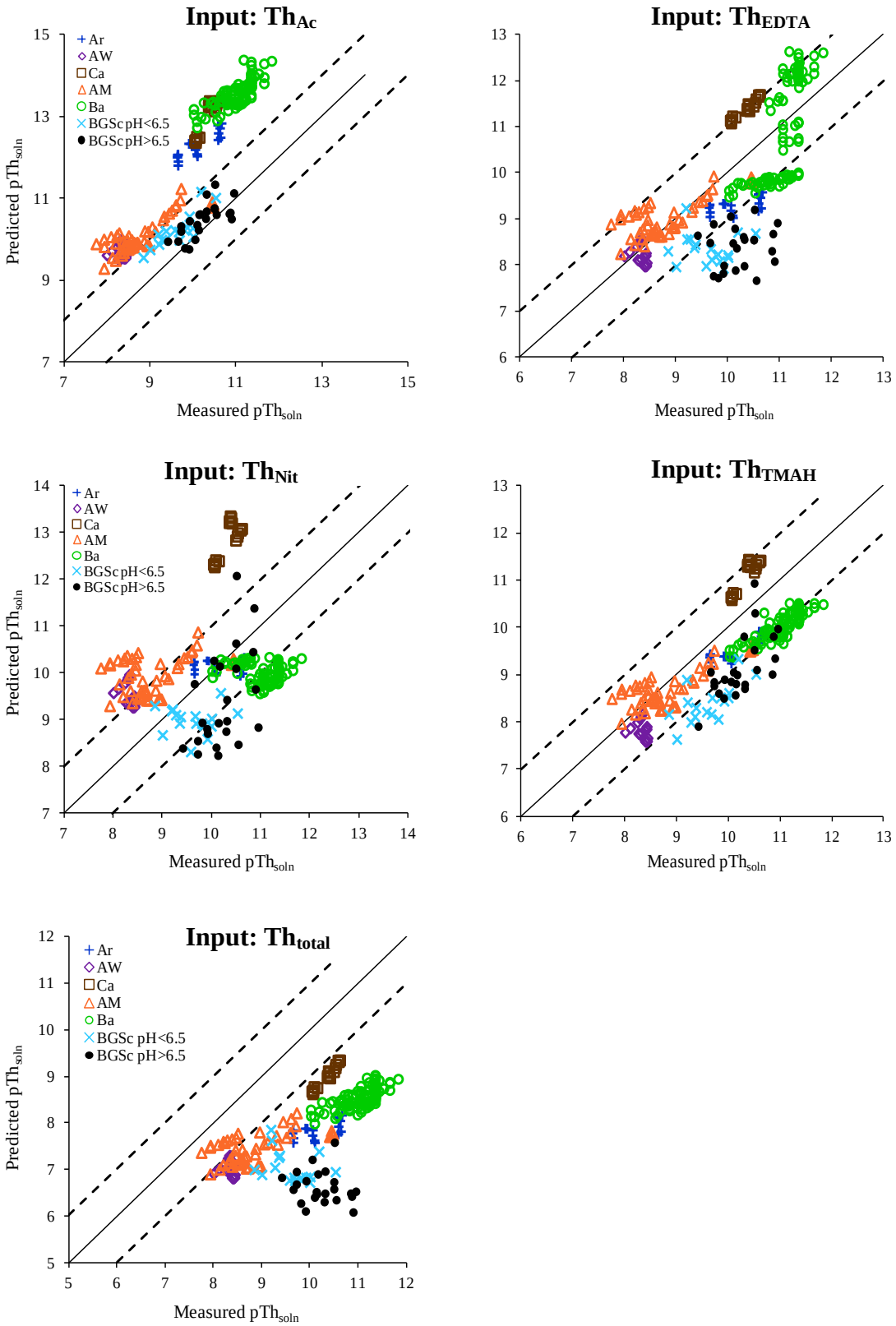

Figure 7.1: Thorium concentrations (pTh_{soln}) in soil solution predicted by WHAM-VII against measured values for Arable (Ar; +), Acidic Woodland (AW; ◊), Calcareous (Ca; □), Acidic Moorland (AM; Δ), Biosolid-amended (Ba; ○), BGSc pH <6.5 (×) and BGSc pH >6.5 (●) soils. Values of Th_{Ac}, Th_{EDTA}, Th_{Nit}, Th_{TMAH} or Th_{total} were used as input variables for the model. The solid line is the 1:1 relation and dashed lines indicate ± one order of magnitude.

7.3.1.2 Predicting total Th solution concentration from Th_{TMAH}

The WHAM-VII model predicted Th solubility reasonably well for both sets of soils, particularly for the Field soils using Th_{TMAH} as the reactive Th pool (Figure 7.1). The value of RSD was less than 1 $\log_{10}$ unit and the average bias (ΔpTh_{soln}) was 0.66. Except for some outliers in the BGSc and Ba soils, the predicted values of Th solution concentration were within one order of magnitude of the measured values. Thorium concentrations were, on average, overestimated by the model, although soluble Th concentrations in Ca soils and a few AM soils were underestimated. It is possible that Th extraction with TMAH may result in an overestimation of the reactive Th pool if some of the humus-bound Th is non-reactive, causing an overestimation of predicted solubility. Using Th_{EDTA} as the reactive Th pool also overestimated Th solubility (using WHAM) in the same soils. Overestimation of Th solubility may be due to the fact that the WHAM model cannot account for dissolution of otherwise non-labile Th by extractants; this may include Th occluded within mineral-humus assemblages, released by TMAH, or Th contained within mineral phosphate phases dissolved by EDTA, for example. The best prediction of Th solubility was found in AW and AM (pH $\leq$4.4) soils (RSD = 0.27, ΔpTh_{soln} = 0.28, median P/M = 0.97). Therefore, predictions are likely to be better for soils in which humus is the predominant adsorption surface than for soils with complex combinations of organic and mineral geocolloids. It has been reported that prediction of trace metal solubility using multi-surface models is more successful when solid-solution partitioning is dominated by soil organic matter (Weng et al., 2002; Cances et al., 2003; Marzouk et al., 2013). Smith et al. (2004) suggested that the properties of the cation binding sites on humic substances in acid washed peat appear very similar to those of isolated humic substances.

7.3.1.3 Comparing WHAM-predicted U solubility using U_E, U_{Ext} or U_{total} as inputs

When applying multi-surface geochemical models to natural systems, a number of choices have to be made with respect to the variables required as model inputs. Dijkstra et al. (2004) and Groenenberg et al. (2012) reported that the available metal concentration, mineral (hydr)oxide content and the active fraction of solid and dissolved organic matter represent sources of uncertainty. Thus, it is important to test

the model sensitivity to these choices. In this study, the prediction of U solubility using U_E as the reactive U concentration was compared to the use of U_{Ext} (U_{Ac}, U_{EDTA}, U_{Nit}, U_{TMAH}) and U_{total}. Figure 7.2 shows predicted U solubility data against measured values; Table 7.3 compares the relative predictive power of the different approaches (ΔpU_{soln}, Median P/M and RSD values) for the two sets of soils and also excluding Ca soils and BGSc pH >6.5 soils. In general, U solubility prediction based on U_{total} was less successful than prediction based on U_E but more successful than prediction based on U_{Ext} (Figure 7.2 and Table 7.3). However, U solubility prediction was also soil-specific. Using U_{total} overestimated the solution U concentration on average, however, the solubility at high pH, in Ca (Ca-Ar and Ca-G) and BGSc pH >6.5 soils, was slightly underestimated (ΔpU_{soln} = -0.77, RSD = 0.71). This may seem surprising but it must mean that model factors outwith the estimation of the reactive U pool affected the result, otherwise reactive U would have to exceed the total soil U content. As a result, all forms of chemically extracted U, and U_E, resulted in an underestimate of the soluble U concentration in these soils. Excluding Ca and BGSc pH >6.5 soils improved the prediction of solubility giving a lower RSD and average bias from the 1:1 line (ΔpU_{soln}) when U_{Ext} or U_E was used as the input variable (Table 7.3). Excluding those soils did not improve the model prediction when U_{total} was used as the reactive U pool (Table 7.3). The underestimation of measured solubility may be due to overestimation of some of the binding phases (particularly humus and Fe oxide content), which implies over-prediction of U binding on these phases. With increasing soil pH the proportion of U binding on mineral oxides increases, therefore, the DCB method (Section 2.2.8) may have extracted more Fe than was actually present in the Fe oxide phase in Ca and BGSc pH >6.5 soils. An alternative explanation is that the model overestimated the U binding to solid phases because the default binding constants for U are too high. In particular, the constants for U bonding to Fe oxide may be at fault because Fe oxide is the dominant reactive surface for U in Ar, Ba, Ca and BGSc soils (from 65 to 99% of labile U is bound to Fe oxide) - not in AW and AM soils (39% on average of labile U is bound to Fe oxide). Therefore, the default model parameters might need to be adjusted before model application to whole soils, especially the description of U adsorption affinity to Fe oxides with increasing pH. Unfortunately, there are no literature publications describing modelling of U solubility in whole soils to compare with the current study. The underestimation of U solubility

in near-neural and alkaline soils was unexpected. WHAM-VII considers a limited number of geocolloidal binding phases and, besides those already considered in the current study (clay, HA and FA, Fe, Mn, and Al oxides), there are also silica and quartz binding phases. However, the WHAM model does not account for other potential binding phases in soils which may be regarded as active surfaces for U adsorption - especially in high pH soils. For example, calcite ($CaCO_3$), which may be an important binding phase for U in the Ca soils and BGSc pH >6.5 soils, and hydroxyapatite ($Ca_5(PO_4)_3(OH)$) which may be important in Ba and Ar soils. In contrast to what was observed, the exclusion of these phases from the model might be expected to cause *overestimation* of soluble metal concentration.

The model gave a better prediction of U solubility when U_E was used as the reactive U pool (lower RSD and ΔpU_{soln}) compared to using U_{Ac}, U_{EDTA}, U_{Nit}, U_{TMAH} and U_{total} as proxies for 'reactive uranium'. In contrast to the empirical models (Section 6.3.6), the differences in model predictions between using U_E and U_{total} were highly significant. Using U_{Ext} (U_{Ac}, U_{EDTA}, U_{Nit}, U_{TMAH}) as input variables gave inferior predictions with a much higher RSD and bias from the 1:1 line (Table 7.3). In fact, using U_{Ac} and U_{EDTA} gave the least successful predictions of U solubility; U concentrations were underestimated by ≥2 orders of magnitude (RSD >4) in Ar, Ca, Ba and BGSc soils, although soluble U concentrations in AW and AM soils were predicted reasonably well (Figure 7.3). On the other hand, using U_{Nit} and U_{TMAH} gave better predictions than using U_{Ac} and U_{EDTA} with much lower RSD values and deviations from the 1:1 line; excluding Ca and BGSc pH >6.5 soils improved the model prediction (< RSD and ΔpU_{soln} values; Table 7.3). Using U_{Nit} and U_{TMAH} underestimated U solubility in Ca and BGSc pH >6.5 soils by ≥2 orders of magnitude. This underestimation was most pronounced in Ca soils when U_{Nit} was used as an input variable (RSD = 12.2, ΔpU_{soln} = -3.4), due to the flaw in the nitric acid extraction scheme discussed previously (Section 4.3.8). It can be concluded that, with the exception of Ca and BGSc pH >6.5 soils, solution U concentrations are predicted reasonably well by WHAM-VII using U_{Nit} or U_{TMAH} as the reactive U pool: apart for a few outliers, the predicted solution concentrations were within one order of magnitude of the measured values. Overall, using U_E as the input variable in the model gives better prediction of U solubility than other measures of 'reactive' U (U_{total}, U_{Ac}, U_{EDTA}, U_{Nit}, and U_{TMAH}). The next section will discuss in detail the prediction of U solubility from U_E.

Table 7.3: Summary of goodness of fit parameters for predictions of solution concentration of U using U_{Ac}, U_{EDTA}, U_{Nit}, U_{TMAH}, E-value (U_E) or total U concentration (U_{total}) as input variables to WHAM-VII.

		All data from the two sets of soils included			Ca and BGSc pH >6.5 soils excluded		
	Input variable	ΔpU_{soln}	Median P/M	RSD	ΔpU_{soln}	Median P/M	RSD
Uranium	U_{Ac}	-1.74	1.21	4.12	-1.54	1.20	3.43
	U_{EDTA}	-1.30	1.15	3.09	-0.98	1.12	1.99
	U_{Nit}	-0.36	1.00	1.59	0.09	0.98	0.35
	U_{TMAH}	-0.51	1.04	1.77	-0.08	1.02	0.69
	U_E	**-0.38**	**1.04**	**0.85**	-0.13	1.03	0.46
	U_{total}	0.73	0.93	1.45	1.00	0.91	1.62

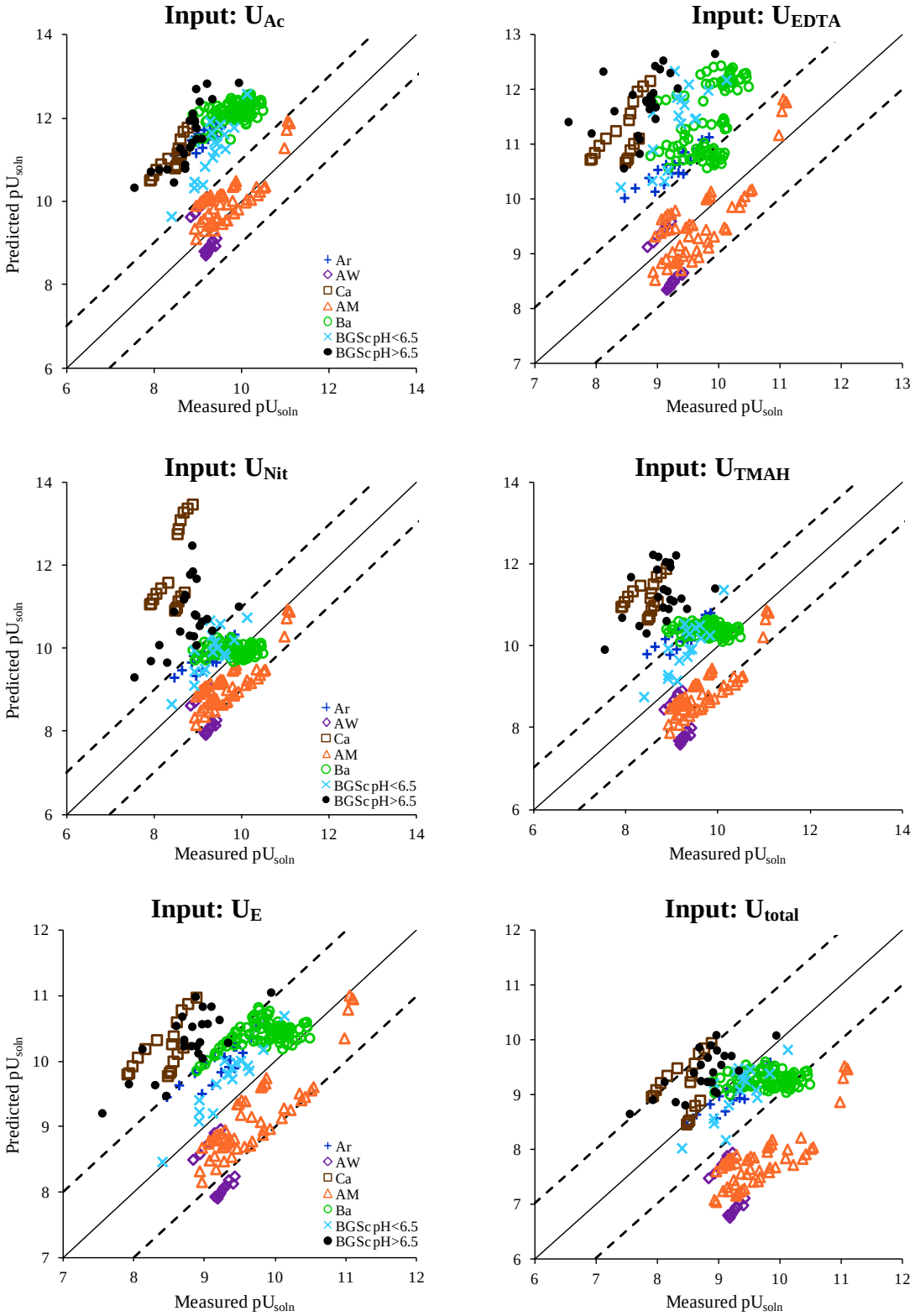

Figure 7.2: Uranium concentrations (pUsoln) in soil solution predicted by WHAM-VII against measured values for Arable (Ar; +), Acidic Woodland (AW; ◊), Calcareous (Ca; □), Acidic Moorland (AM; Δ), Biosolid-amended (Ba; ○), BGSc pH <6.5 (×) and BGSc pH >6.5 (●) soils. The values of UAc, UEDTA, UNit, UTMAH, UE or Utotal were used as estimates of 'reactive uranium' in WHAM-VII. The solid line is the 1:1 relation and dashed lines indicate ± one order of magnitude.

7.3.1.4 Predicting total U solution concentration from U_E

Uranium concentrations were, on average, underestimated by the WHAM-VII model using U_E as the input variable (RSD =0.85; ΔpU_{soln} = -0.38 (Table 7.3)). Except for Ca, BGSc pH >6.5 and a few outliers in the AW soil (subsoil), the predicted solution concentrations of U were within one order of magnitude of the measured values (Figure 7.2). Among all soil groups, the model overestimated solubility in AW and AM soils (ΔpU_{soln} = 0.64; RSD = 0.55), which probably implies underestimation of U binding to humus as the dominant reactive surface in AW and AM soils. In the Ca and BGSc pH >6.5 soils, U solubility was underestimated by less than two orders of magnitude (ΔpU_{soln} = -1.8, RSD = 3.2 for Ca soils; ΔpU_{soln} = -1.5, RSD = 2.5 for BGSc pH >6.5 soils). The underestimation of U solubility in soils with pH >5 may be attributed to the overestimation of U binding to Fe oxide; the level of underestimation may be expected to increase with increasing soil pH and with increased binding to Fe oxide phase as predicted by the WHAM-VII model. One provisional way to investigate underlying causes of model failure is to examine trends in error as a function of predicted fractionation; this approach is discussed below.

7.3.2 Modelling Th and U binding on solid phases

Thorium and U fractionation in the solid phase is provided by WHAM-VII as part of the overall speciation calculations undertaken by the model. As discussed above, the model overestimated Th solubility (ie. underestimated solid phase binding) and underestimated U solubility (ie. overestimated solid phase binding) on average when using Th_{TMAH} and U_E as estimates of the reactive Th and U pools in soil. Therefore, the solid phase fractionation of U and Th, as predicted by WHAM-VII, was examined to assess which binding phases appeared to cause the greatest deviation between measured and predicted solution concentrations.

7.3.2.1 Thorium and uranium fractionation in soils as a function of pH and binding phase content

Figure 7.3 shows the contribution of different binding phases to the sorption of metal in different soil groups. The fractionation was modelled by WHAM-VII and includes the association of metal with SOM (HA+FA), Fe and Al oxides (FeOx+AlOx) and

clay; the metal in the solution phase includes colloidal FA-bound forms. Although there was a large variation in SOM content (Section 4.3.1), organic matter was (predicted to be) the predominant reactive surface for Th; most of the Th (80-99.9%) was absorbed on organic matter across the soil groups (Figure 7.3a). These results are consistent with the well-known importance of organic matter in the complexation of Th (Langmuir and Herman, 1980; Kaplan and Knox, 2003; Reiller et al., 2002 and 2003; Guo et al. 2008). The contribution of adsorption by clay and Fe and Al oxides to overall adsorption is generally small; binding to clay was only significant in very acidic soils (AW and AM), while binding to Fe and Al oxides was only significant in BGSc pH >6.5 soils which contain large amounts of Fe oxide compared to other soil groups (Section 4.3.1). It may therefore be reasonable to ascribe errors in predicted solubility of Th primarily to deficiencies in modelling of binding to humus – although, of course, it could be argued that the lack of importance attributed to the other binding phases may also be the cause of such errors.

Predicted U fractionation was more complex than that of Th (Figure 7.3b); organic matter bound U declined as pH increased with a concomitant increase in U bound to the Fe oxide phase. Organic matter was the most important adsorbent for U in very acidic soils (AW and AM; pH 3.1-4.4); however, at soil depths with low organic matter content there was a significant contribution from Fe oxides to overall U adsorption. By contrast, Fe oxide was the predominant reactive surface in Ar, Ba, Ca and BGSc soils. The Ba and Ca-W soils contain large concentrations of organic matter, thus the fraction of U bound to SOM was greater than in Ar and BGSc soils with a similar range of pH values. The U fraction adsorbed to clay was very small and only significant in AW and AM soils. Many studies have reported the importance of hydrous iron oxides for U(VI) sorption, uranium(VI) forms strong surface complexes with ferrihydrite and goethite, when pH > 5 (Hsi and Langmuir, 1985; Waite et al., 1994; Duff and Amrhein, 1996; Payne et al., 1996; Lenhart and Honeyman, 1999; Gustafsson et al., 2009). As a result of the common existence of ferric oxyhydroxides in soils and sediments and their affinity for UO_2^{2+}, they represent the most important potential sorbents for U, whereas organic matter (in peat, for example) is of secondary importance (Langmuir, 1997). It has been suggested that at low pH the weakening of U adsorption to iron oxides significantly enhances mobility and transport (Langmuir,

1997), whereas at high pH values adsorption is much stronger (Koch-Steindl and Pröhl, 2001). Thus, examination of errors in predictions of solubility across the range of soil properties (pH, FeOx and humus content) may indicate the *origin* of the error.

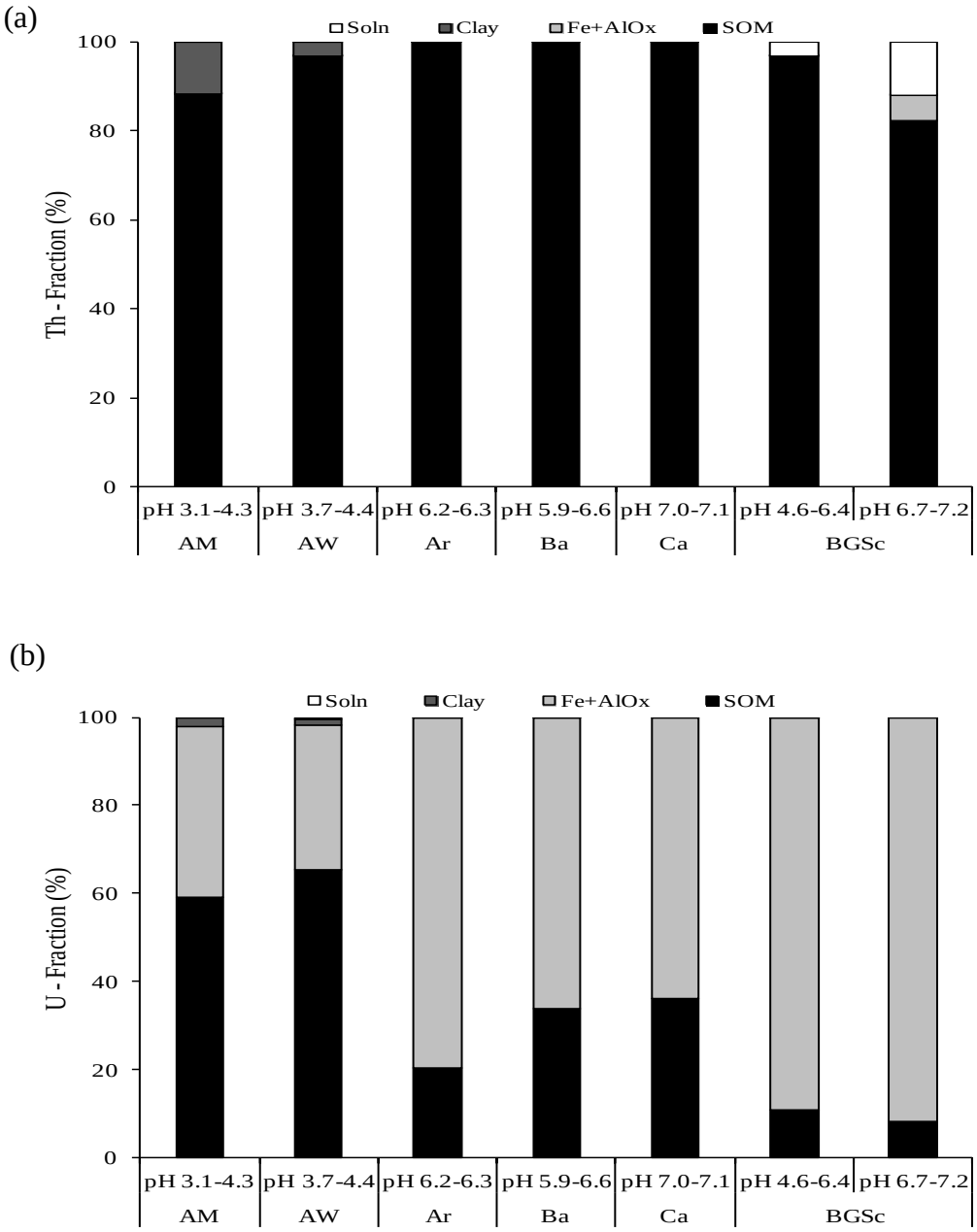

Figure 7.3: Average Th (a) and U (b) distribution between solid phase organic matter (SOM; 'particulate' HA+FA), Fe and Al (hydr)oxides (FeOx + AlOx), clay and the solution phase (Soln). Soils include; Arable (Ar), Acidic Woodland (AW), Calcareous (Ca), Acidic Moorland (AM), Biosolid-amended (Ba), BGSc pH <6.5 and BGSc pH >6.5. The fractionation was predicted by WHAM-VII parameterized using U_E and Th_{TMAH} as input variables.

7.3.2.2 The bias in Th solubility prediction as a function of soil pH and binding phases

The difference between measured and predicted Th solubility (ΔpTh_{soln}) as a function of soil pH and Th proportions bound to geocolloidal phases (SOM, FeOx and clay) is shown in Figure 7.4. There was a strong relationship between model performance and soil pH, especially with the exclusion of Ca soils. The model both underestimated Th solubility at low pH (pH ≈ 3.0) soils and overestimated solubility in high pH soils, excluding Ca soils (Figure 7.4a) which showed the reverse trend. Because Th is predicted to be almost exclusively adsorbed on humus, there was no consistent trend in model performance and organically bound Th (Figure 7.4b) or with any of the minor binding phases (FeOx and Clay; Figure 7.4c and d).

The trend in Figure 7.4a strongly suggests that the pH-dependence of Th binding to humus is underestimated – that is, solubility is consistently overestimated at high pH and the increase in binding strength per unit pH increase is underestimated. If this were increased then the trend in ΔpM_{soln} would flatten and gravitate to the zero on the Y-axis. At the same time, because values of ΔpTh_{soln} fall below zero at low pH, where humus charge (Z) approaches zero, it may be that a greater 'intrinsic stability constant' (which applies when Z=0) for Th binding to humic acid is also needed. However, it must also be acknowledged that, because almost all Th in solution is present as DOC complexes, increasing (in the model) the strength of binding to humus at high pH could have the effect of increasing solubility as more stable DOC-Th complexes. Crucial to the overall outcome would be the effect of pH on DOC solubility and the difference in pH-dependence of binding between humic and fulvic acid, if we associate DOC mainly with FA and the solid phase humus mainly with HA. The Ca soils fall outside this general trend and it is difficult to ascribe an obvious reason for this.

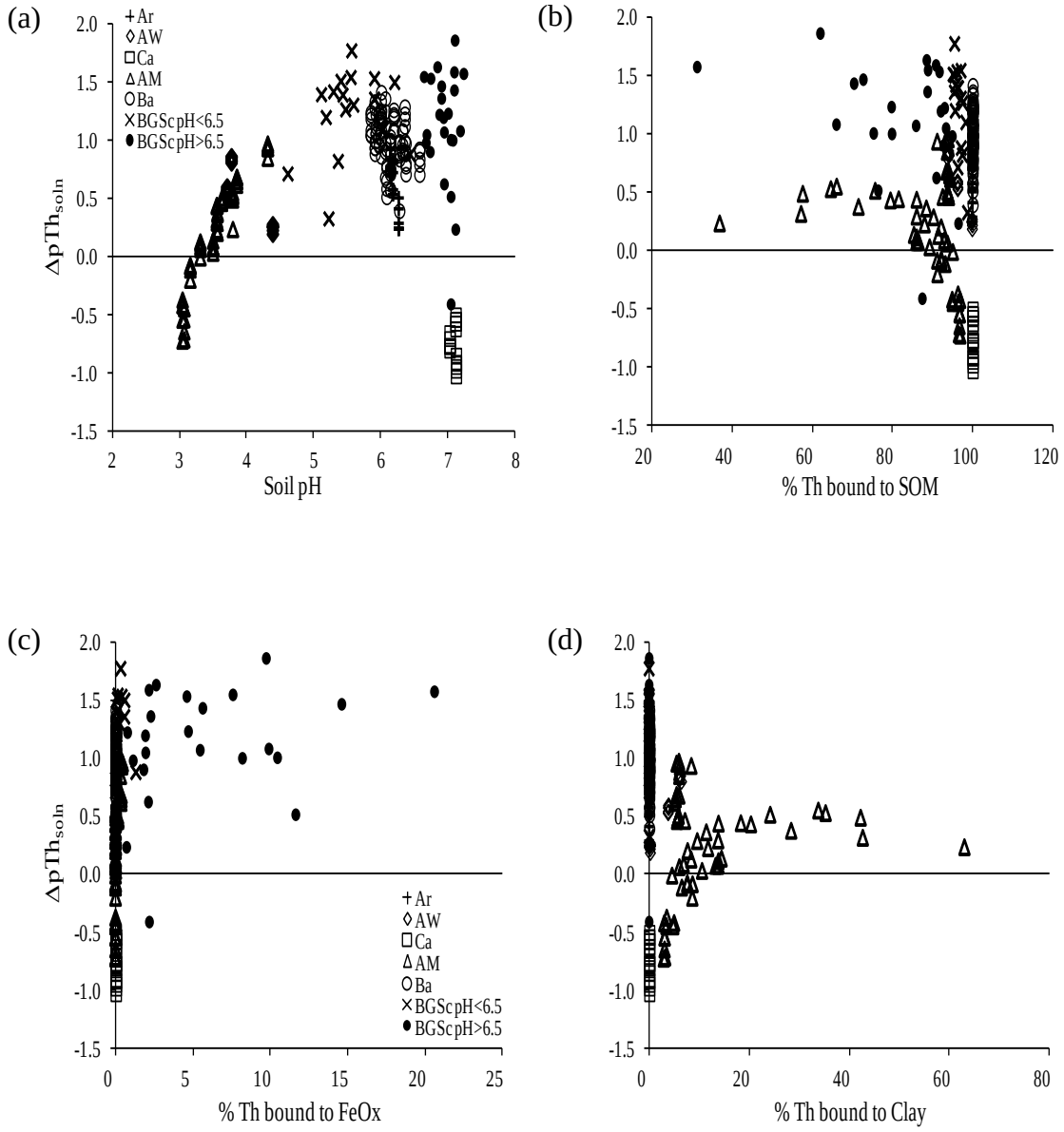

Figure 7.4: Difference between measured and predicted Th solubility (ΔpTh_{soln}) against (a) soil pH and Th proportion bound to (b) SOM, (c) FeOx and (d) clay. Solubility was predicted by WHAM-VII parameterized using Th_{TMAH} as input variable.

7.3.2.3 The bias in U solubility prediction as a function of soil pH and binding phases

Figure 7.5 illustrates the difference between measured and predicted U solubility (ΔpU_{soln}) as a function of soil pH and the proportions of U bound to geocolloidal phases (SOM, FeOx and clay). There was a strong relationship between model performance and soil pH; the model both overestimated solubility below pH 5 (AW and AM soils) and underestimated solubility in high pH soils (pH >5; Ar, Ca, Ba and BGSc soils) (Figure 7.5a). The fractionation of U is much more varied than that of Th – and perhaps more difficult to interpret. Humus is the predominant reactive surface for U in AW and AM soils at low pH but FeOx is the main adsorption surface for soils above pH 5 (Ar, Ca, Ba, and BGSc soils). Figure 7.5b shows an increase in AW and AM bias with increasing SOM-bound U and a corresponding decrease in bias with increasing Fe oxide-bound U fraction, or with increasing pH (Figure 7.5c). WHAM predicts about 80, 66, 64, and 90% of U, on average, is bound to Fe oxide in Ar, Ba, Ca ad BGSc soils, respectively. Ba and Ca (especially Ca-W) soils contain relatively high organic matter content (16 and 10% respectively), therefore SOM-bound U in these soils represents about 35% comparing to 20% and 9% in Ar and BGSc soils. Despite these differences in predicted fractionation between humus and Fe oxides, the trend in bias with pH (Figure 7.5a) seems quite coherent across all soils: solubility is overestimated at low pH and underestimated at high pH. Considering the overall trend with pH and the general change in fractionation with pH, indicates three provisional conclusions: (i) U binding strength to humus is under-estimated at low pH; (ii) U binding to Fe oxides is overestimated at high pH; (iii) in contrast to the trend for Th, the pH-dependence of U binding strength is over estimated.

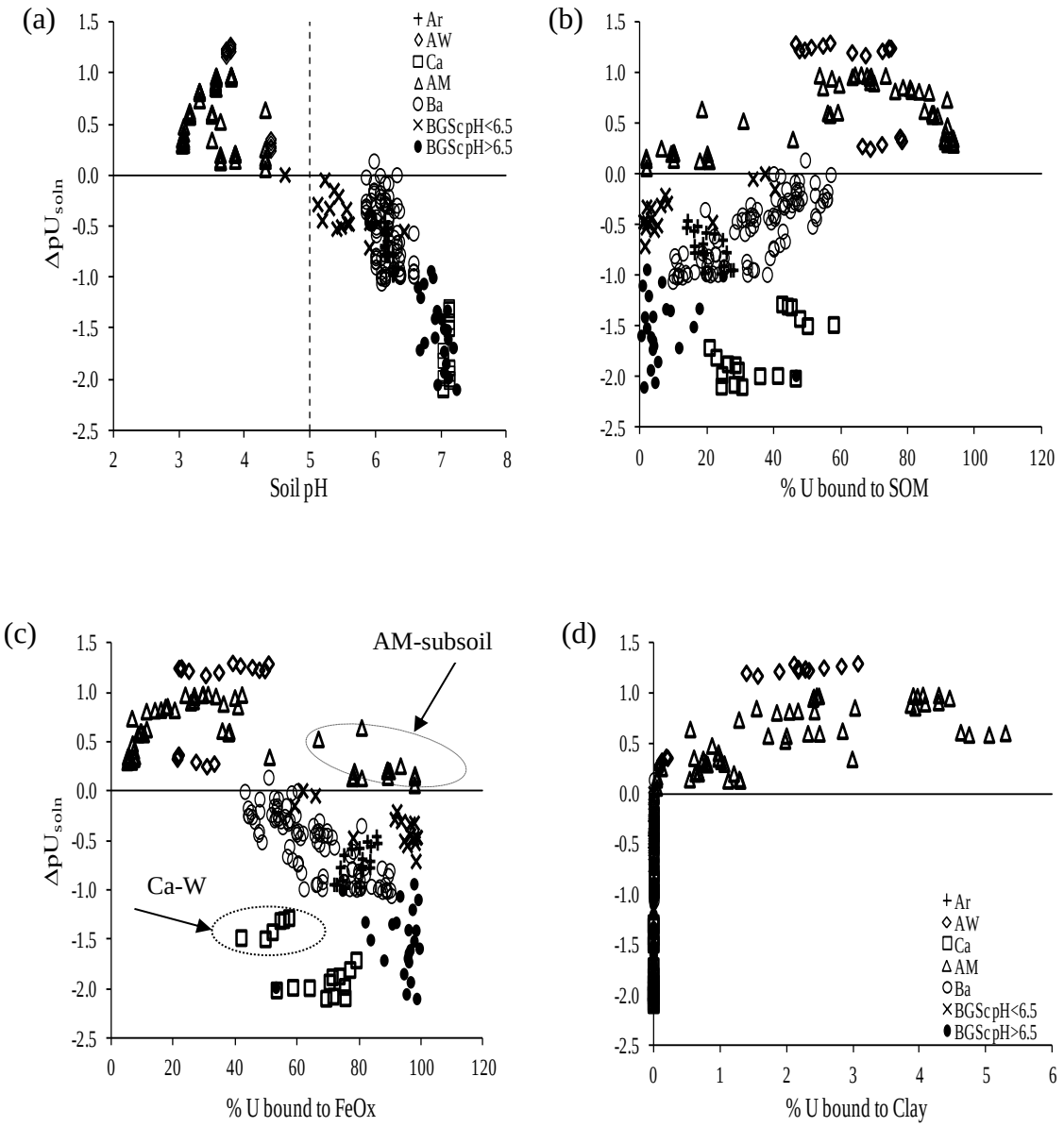

Figure 7.5: Difference between measured and predicted U solubility (ΔpU_{soln}) against (a) soil pH and the proportion of U bound to (b) SOM, (c) FeOx and (d) clay. Solubility was predicted by WHAM-VII parameterized using U_E as input variable.

7.3.2.4 Testing the model sensitivity to the variables affecting U solid - solution distribution

Results from the previous section suggested that better simulations of solubility could be achieved by alteration of the fundamental binding constants for Th and U with HA, FA and Fe/Al oxides. However, alteration of the model parameter database would require justification based on a study of the isolated geocolloid behaviour; changing the database in response to whole soil studies is contrary to the principles of the assemblage model. However, it is reasonable to examine the possible range of key input variables to determine whether these could explain the bias seen in Figures 7.4 and 7.5. Soils with pH >5 were tested for model sensitivity to (i) Fe oxide surface area and (ii) dissolved carbonate concentration. These soils were selected because of their high average bias in ΔpU_{soln} and the two variables because Fe oxide is predicted to be the dominant reactive surface while dissolved carbonate plays a critical role in the distribution of U(VI) between Fe oxide surfaces and the solution phase (Tripathi , 1983; Hsi and Langmuir, 1985). It has been found that the reactive surface area of hydroxides is a sensitive parameter for modelling trace metal solubility, especially in neutral and alkaline soils and in soils rich with Fe-oxyhydroxides, such as weathered tropical soils (Buekers et al., 2008). The surface areas of soil Fe-oxyhydroxides are probably larger than that of synthetic oxyhydroxides. For example, Eusterhues et al. (2005) determined that the surface area of Fe-oxyhydroxides in soil was in the range 200-800 $m^2\ g^{-1}$, calculated based on surface area measurements of soils before and after removal of Fe-oxyhydroxides. The default value of Fe oxide surface area in WHAM is 600 $m^2\ g^{-1}$ and so, because U solubility was underestimated in soils with pH >5, the surface area was adjusted to 400 and 200 $m^2\ g^{-1}$ (within the literature range). Table 7.4 shows the improvement in prediction of solubilityusing default and adjusted surface areas. A slight decrease in ΔpU_{soln}, Median P/M and RSD was achieved by decreasing the Fe oxide surface area in Ca soils, while in BGSc pH >6.5 soils only ΔpU_{soln} slightly decreased. Thus, U solubility was still underestimated after adjusting the surface area to 400 or 200 $m^2\ g^{-1}$. It would therefore seem to be necessary to adjust the binding constant that describes U sorption affinity to Fe oxide to achieve better solubility prediction.

Table 7.4: Performance of WHAM-VII modelling U solubility in calcareous (Ca) and BGSc pH >6.5 soils using default and adjusted FeOx surface areas.

		FeOx surface area		
		Default surface area (600 m^2 g^{-1})	Adjusted surface area (400 m^2 g^{-1})	Adjusted surface area (200 m^2 g^{-1})
Calcareous soils (Ca)	ΔpU_{soln}	-1.77	-1.68	-1.57
	Median P/M	1.23	1.22	1.20
	RSD	3.22	2.91	2.54
BGSc pH >6.5	ΔpU_{soln}	-1.53	-1.48	-1.47
	Median P/M	1.18	1.18	1.18
	RSD	2.51	2.51	2.51

Table 7.5 shows the improvement in U solubility prediction achieved by increasing the dissolved carbonate input to the model by factors of 5 and 10 greater than the measured values. Both levels of carbonate inputs improved the model prediction in both Ca and BGSc pH >6.5 soils. Increasing the carbonate concentration by a factor of 10 produced a lower average bias, RSD values close to zero and median P/M values of 1.00 and 1.04 for Ca and BGSc pH >6.5 soils. In the neutral to alkaline pH range, U(VI) is strongly adsorbed in the absence of dissolved CO_2 (Hsi and Langmuir, 1985; Langmuir, 1997), but in the presence of dissolved CO_2, uranyl carbonate complexes ($UO_2CO_3^0$, $UO_2(CO_3)_2^{2-}$, $UO_2(CO_3)_3^{4-}$) strongly reduce U(VI) adsorption. WHAM-VII accounts for the three uranyl carbonate species listed above but these may not represent a complete mass balance. It has been recently reported that U(VI) adsorption would also be expected to decrease through the formation of $CaUO_2(CO_3)_3^{2-}$ and $Ca_2UO_2(CO_3)_{3(aq)}$, carbonate complexes (Bernhard et al., 2001; Brooks et al., 2003; Curtis et al. 2004; Zheng et al., 2003; Fox et al., 2006).

Table 7.5: Performance of WHAM-VII modelling U solubility in calcareous (Ca) and BGSc pH >6.5 soils using measured dissolved carbonate, five times dissolved carbonate and 10 times dissolved carbonate.

		Dissolved carbonate		
		Measured	5× measured	10×measured
Calcareous soils (Ca)	ΔpU_{soln}	-1.77	-0.48	0.08
	Median P/M	1.23	1.08	1.00
	RSD	3.22	0.33	0.09
BGSc pH >6.5	ΔpU_{soln}	-1.53	-0.79	-0.30
	Median P/M	1.18	1.09	1.04
	RSD	2.51	0.71	0.15

To conclude, a mechanistic geochemical speciation model (WHAM-VII) can be used to predict Th and U solubility in whole soil and allow for changes in soil conditions, such as soil temperature, solid:solution ratio, ionic strength, metal ion competition etc. Predictions of Th and U solubility using M_{total} to represent the reactive meal fraction were less successful than using Th_{Ext} and U_E; in contrast to the empirical models the difference in WHAM-VII predictions using U_E or Th_{TMAH} and M_{total} was very clear. Among the four extracted fractions of Th (Th_{Ac}, Th_{EDTA}, Th_{Nit}, Th_{TMAH}), the model gave a better prediction using Th_{TMAH} as the reactive Th fraction. The results showed a strong dependency of Th solubility prediction on the choice of Th_{Ext} method used to estimate labile Th. This suggests that there is scope for further refinement of methods used to estimate the reactive Th pool in soil. Overestimation of solution Th concentration from WHAM-II was observed, and was correlated with soil pH. The results obtained suggest that the pH-dependence of Th binding to humus (Th was predicted to be almost exclusively adsorbed on humus) is underestimated – that is, solubility is consistently overestimated at high pH and the increase in binding strength per unit pH increase is underestimated.

The model gave a better prediction of U solubility when U_E was used as the reactive U pool compared to using U_{Ext} and U_{total} as proxies for 'reactive uranium'. Solution U concentration was, on average, underestimated by the WHAM-VII model using U_E as the input variable. Solubility was overestimated at pH <5 (AW and AM soils) and underestimated at pH >5 (Ar, Ca, Ba and BGSc soils). Fractionation information from WHAM indicated three provisional conclusions: (i) U binding strength to humus is underestimated at low pH; (ii) U binding to Fe oxides is overestimated at high pH; (iii) in contrast to the trend for Th, the pH-dependence of U binding strength is overestimated. In soils with pH >5, U solubility was still underestimated after decreasing the Fe oxides surface area to 400 or 200 $m^2 g^{-1}$. It would therefore seem to be necessary to adjust the binding constant that describes U sorption affinity to Fe oxide to achieve better solubility prediction. On the other hand, prediction of U solubility was improved by increasing the dissolved carbonate input to the model by factors of 5 and 10 the measured values.

7.3.3 The effect of soil temperature on solubility and speciation of Th and U

Temperature may influence the dynamics of metals through direct effects on chemical reaction rates and through moderation of the soil microbial activity (Almas et al., 1999; Cornu et al., 2008, 2011). Soil temperature effects on microbial mineralization processes can also cause changes in the dissolution/precipitation of minerals such as Fe and Mn hydroxides, soil organic matter decomposition and the solubility and speciation of metals in soil solution. In this section the effect of soil temperature on temporal changes in soil solution composition of the biosolid-amended arable (Ba) soil was investigated. During a 48-day period, soil pore water solutions were sampled from Ba soil incubated at 5, 10, 16, 25 or 30 °C (Section 7.2.3). The soil solution pH and the concentrations of DOC, DIC, Fe, Mn, NO_3^-, Ca, Mg, Th and U were monitored at 1, 5, 11, 19, 28, 40 and 48 days (see Section 7.2.3 for details).

7.3.3.1 Major element and carbon composition of the soil solution

The solution pH and the concentration of NO^{3-}, Fe, Mn, DIC and DOC (Figure 7.6) varied significantly with incubation time and with soil temperature ($P < 0.001$) and generally exhibited the temperature-dependent trend expected for a soil undergoing the onset of anaerobic conditions (Cornu et al., 2007, 2008, 2011; Parat et al., 2009). Solution pH increased over time by about 1.0 unit to reach 7.6 after 19 days of incubation at 30 °C, pH also increased with the rise in soil temperature (Figure 7.6a). The increase in solution pH was much more pronounced at 25 and 30 °C, the pH increased by just 0.17 unit at 5 °C, while at 30 °C the pH increased by 0.91 unit. A rise in pH is expected as redox potential falls in non-calcareous soils, because of the proton:electron stoichiometries of most reduction reactions in soils (Kirk, 2004). Solution NO_3^- concentration decreased steeply with incubation time and with rise in soil temperature (Figure 7.6b). The initial NO_3^- concentration (229 mg L^{-1} on average over all temperatures) declined to values at or below the quantification limit depending on soil temperature, in keeping with the progressive denitrification expected in flooded soils (Cornu et al., 2007, 2008). The Ba soil is high in nitrate, and in readily decomposable N-rich organic residues, because of its history of sewage sludge application.

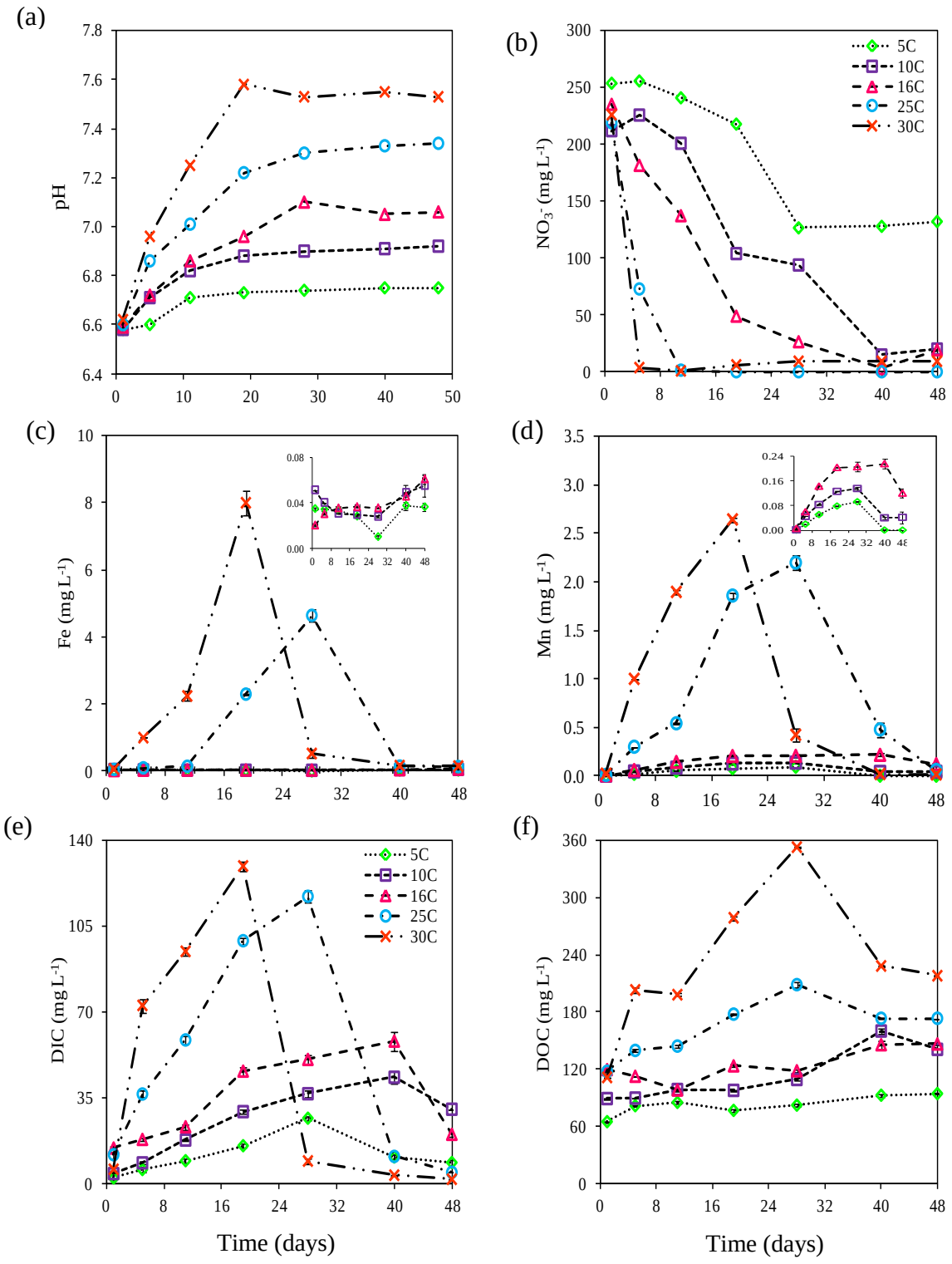

Figure 7.6: Time-dependent trend in (a) pH and the concentration of (b) NO_3^-, (c) Fe, (d) Mn, (e) DIC and (f) DOC in soil solution for incubation temperatures of 5 (◊), 10 (♦), 16 (Δ) 25 (O) and 30 °C (×). The error bars denote standard errors of three replicates.

The concentration of Fe was low and nearly constant over time for 5, 10 and 16 °C, while at 25 and 30 °C Fe concentration increased sharply with time to reach 4.6 and 8 mg L^{-1} at 28 and 19 days, respectively, then decreased steeply towards the end of incubation period. Solution Mn concentration showed broadly the same pattern (Figure 7.6d). Again, this is a pattern that might qualitatively be expected as reduction initially causes dissolution of Fe^{III} and Mn^{IV} oxides but the rise in pH and bicarbonate then leads to precipitation of ferrous carbonate. The concentration of DIC initially increased significantly with time, at a rate proportional to soil temperature (Figure 7.6e). The carbonate concentration then steeply declined with time in a clear temperature-dependent pattern. Again, this suggests a carbonate precipitation reaction or it could simply indicate slow dissipation following initially rapid production (Kirk, 2004). Solution DOC concentration (Figure 7.6f) was high and generally increased significantly with the rise in soil temperature, although a decline after 28 days was evident in the two highest temperatures. DOC is likely to be liberated partly as a result of microbial decay reactions generally but also because of increased solubility at high pH and liberation from adsorption sites on Fe and Mn oxides following their reductive dissolution.

7.3.3.2 Effect of soil temperature on solubility and speciation of uranium and thorium

Total solution U and Th concentrations varied significantly with incubation time and with soil temperature ($P < 0.001$). Uranium concentration increased by up to a factor of 65, whilst Th concentration increased only by up to a factor of 7.2. Figures 7.7a and b show the variation in solution U and Th concentrations over time at different soil temperatures; the correlation coefficients between both Th and U concentrations and soil solution physico-chemical parameters of interest (pH, DOC, DIC, Fe, Mn, NO_3^- Ca and Mg) are listed in Table 7.6.

Uranium: solubility and speciation under variable soil temperature

Under reducing conditions, U(VI) solubility may increase due to the formation of soluble carbonate complexes (Francis et al., 2000; Wan et al., 2005; Gavrilescu et al., 2009). Alternatively, reduction of U(VI) to U(IV) would result in precipitation of relatively insoluble uraninite (UO_2) (Langmuir, 1978; Wan et al., 2005; Gu and Chen, 2003; Gu et al., 2005). Solution U concentration (Figure 7.7a) transitorily increased with time during the first 28 (4-fold increase), 40 (9-fold increase), 40 (8-fold increase), 28 (33-fold increase) and 19 (18-fold increase) days of incubation at 5, 10, 16, 25 and 30 °C respectively, and then steeply decreased over time up to a final concentration less than 0.08 µg L^{-1} at the end of the incubation period. Solution U concentration followed the same trend as DIC and Mn concentrations over time, and at different temperatures, producing a highly significant positive correlation between U and both DIC and Mn concentrations (Table 7.6) across the range of conditions and sample times. Uranium was also positively correlated with other indices of reducing conditions (pH, DOC, Fe) and negatively correlated with NO_3^- (Table 7.6). The major consequence of microbial respiration, and the onset of reducing conditions, was therefore increased solubility of U(VI) as (bi)carbonate complexes rather than reduction to insoluble U(IV) forms (Francis et al., 2000; Wan et al., 2005; Gavrilescu et al., 2009).

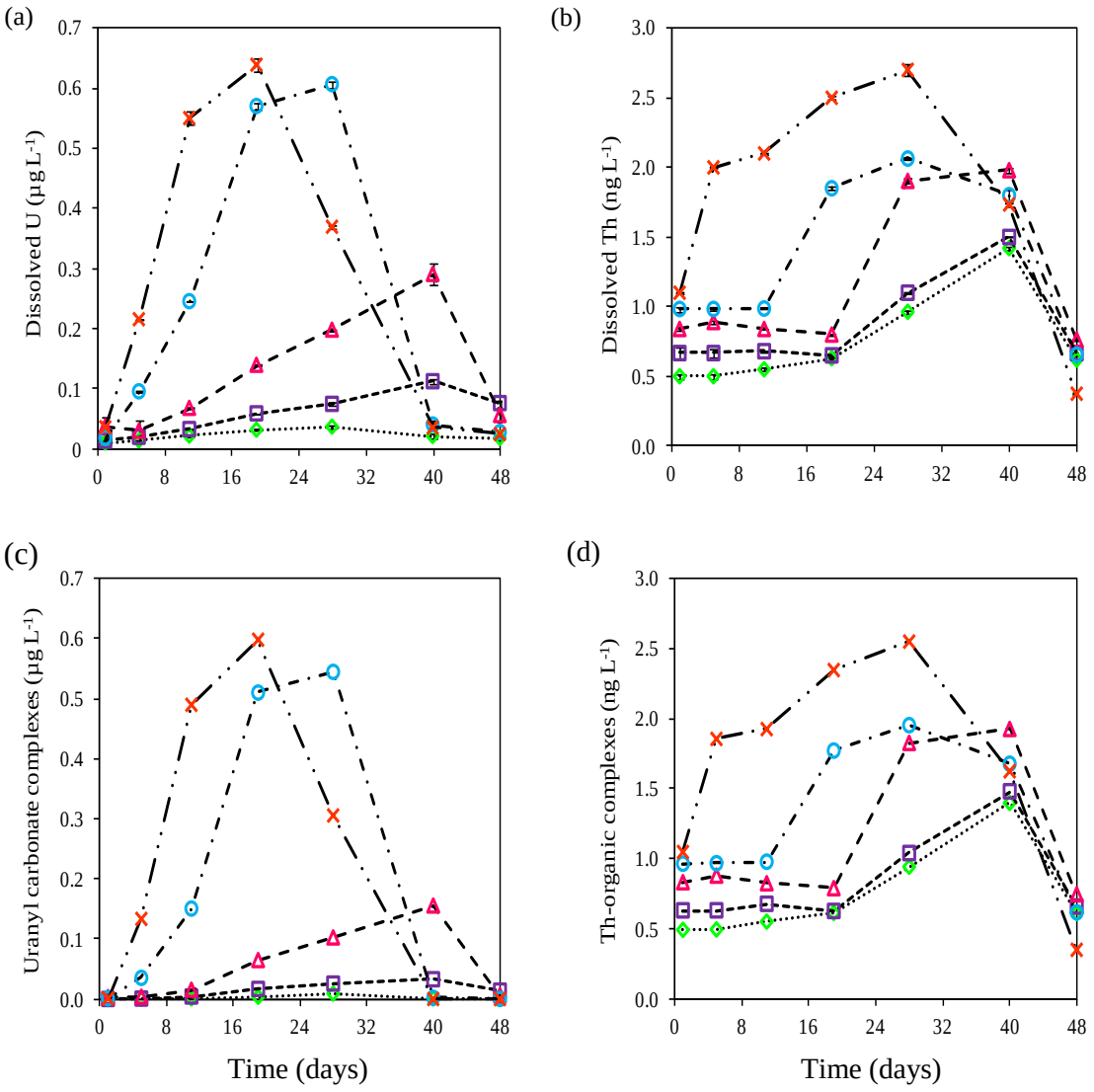

Figure 7.7: Concentrations in soil solution of (a) U (µg L^{-1}) and (b) Th (ng L^{-1}) and WHAM-VII predicted concentrations of (c) uranyl carbonate complexes (µg L^{-1}) and (d) Th-organic complexes (ng L^{-1}) as a function of incubation time at 5 (◊), 10 (♦), 16 (Δ) 25 (O) and 30 °C (×). The error bars denote standard errors of three replicates.

Uranium is a less energetically favourable electron acceptor when Ca-U(VI)-CO_3 complexes are present (Brooks et al., 2003), therefore, the presence of Ca^{2+} even at low concentration (0.45 mmol) can significantly inhibit microbial reduction U(VI) (Brooks et al., 2003). Moreover, the presence of nitrate (Istok et al., 2003; Senko et al., 2002) or other electron acceptors such as Fe(III) and Mn (IV) oxides (Wieling et al., 2000; Fredrickson et al., 2002) can significantly hinder the bio-reduction of U(VI) depending on the availability and redox potential of the electron acceptor. Wan et al. (2005) reported that bio-reduced U(IV) in sediment was re-oxidized under sustained

reducing conditions because bicarbonate accumulation promoted the formation of very stable uranyl carbonate complexes under neutral to slightly alkaline conditions. In the current study, microbial respiration rates initially exceeded the rate of CO_2 dissipation but when the initial rate of organic matter decomposition fell there was a steep decline in DIC (Figure 7.6e) and in U concentration (Figure 7.7a). This may simply have been due to loss of the U(VI)-solubilizing ligand (HCO_3^-). However, it is also possible that, during this phase, the decrease in U solubility may indicate reduction of U(VI) to U(IV) and then precipitation as insoluble uraninite (UO_2).

Figure 7.8 shows that U should have existed as U(VI) (uranyl carbonate complexes) at the beginning of the incubation experiment at the different temperatures. However, with increasing the incubation time, the pH increased and soil redox potential decreased. It appears that U(VI) was reduced to U(IV) forming a mixed-valence U oxide $U_4O_{9(cr)}$ (U(IV) + U(V); Kvashnina et al., 2013) which will completely reduce to U(IV) ($UO_{2(cr)}$) with decreasing redox potential. Precipitation of reduced U as uraninite has been reported to explain the decrease in U solubility observed in soils under anaerobic conditions (Langmuir, 1978; Wan et al., 2005; Gu and Chen, 2003; Gu et al., 2005). It has been shown that reduced U(IV) is usually poorly crystallized and occurs in the form of nano-particulates of <0.2 μm diameter (Suzuki et al., 2002) or surface precipitates (Giammar et al., 2001). Studies have also demonstrated that the presence of organic matter enhances U(VI) reduction rates under anaerobic conditions because humic substances can act as electron mediators or 'shuttles' between microorganisms and redox sensitive metals or metal oxides. Humic acid has been found to be more effective than fulvic acid in enhancing the U(VI) reduction rate (Lovley, 1996; Royer et al., 2002; Gu and Chen, 2003; Gu et al., 2005).

The formation of uranyl carbonate complexes under the experimental reducing conditions was supported by modelling speciation using the geochemical model WHAM-VII (Figure 7.7c). Soil solution U was found to be complexed with organic matter and carbonate depending on DIC concentration. As shown in Figure 7.7c uranyl carbonate complexes followed exactly the same trend as DIC ($r = 0.91$, $P < 0.001$) and U ($r = 0.98$, $P < 0.001$) and represented 1-25%, 1-35%, 9-54%, 7-90% and 2-94% of the total solution U concentration at 5, 10, 16, 25 and 30 °C, respectively; the remaining solution U concentration was bound to organic complexes.

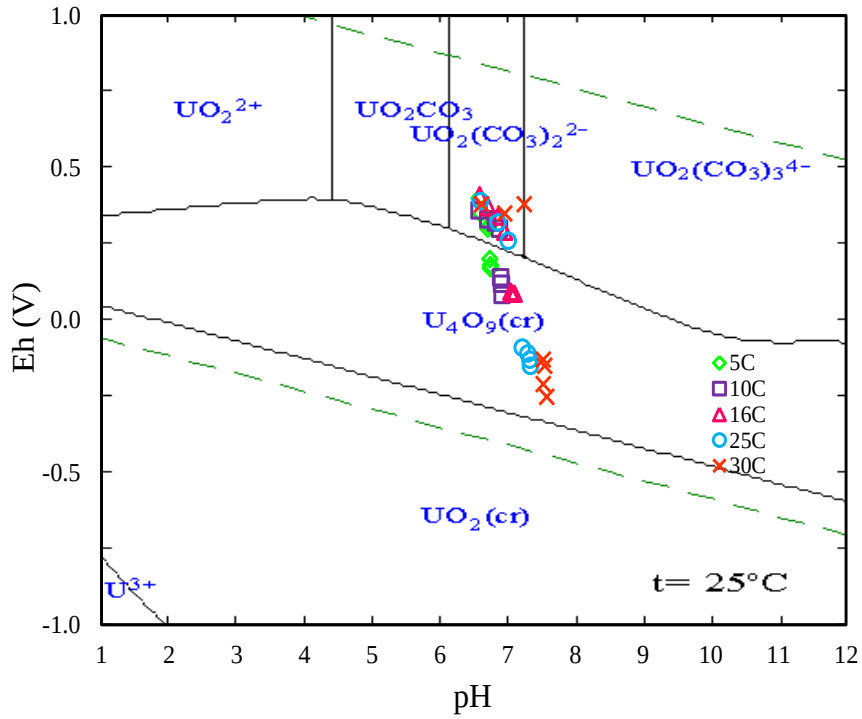

Figure 7.8: Eh-pH diagram for U. The Eh was calculated from measured pH and Fe^{2+} free ion activity (calculated from WHAM-VII, using the total Fe measured in solution as input) assuming that Fe^{2+} ion activity in solution is controlled by the reductive solubilisation of solid ferric hydroxide $Fe(OH)_3$:

$pE = log\ K_r - log(Fe^{2+}) - 3pH$, ($\log K_r$ (solubility constant) = 15.87)

Table 7.6: Correlation coefficients (r) between Th and U concentrations in soil solution and pH, the concentrations of DOC, DIC, Fe, Mn, NO_3^- Ca and Mg (35 soil solution samples were collected at 7 different times and 5 different temperatures); P-values are in brackets, significant p-values are in bold italic.

Soil variable	*Soil solution Th and U concentrations (µg L^{-1})*	
	Th (µg L^{-1})	U (µg L^{-1})
pH	0.62 ***(<0.001)***	0.57 ***(<0.001)***
DOC (mg L^{-1})	0.74 ***(<0.001)***	0.62 ***(<0.001)***
DIC (mg L^{-1})	0.64 ***(<0.001)***	0.91 ***(<0.001)***
Fe (µg L^{-1})	0.58 ***(<0.001)***	0.77 ***(<0.001)***
Mn (µg L^{-1})	0.67 ***(<0.001)***	0.92 ***(<0.001)***
NO_3^- (mg L^{-1})	-0.61 ***(<0.001)***	-0.58 ***(<0.001)***
Ca (mg L^{-1})	-0.18 (>0.05)	-0.21 (>0.05)
Mg (mg L^{-1})	-0.14 (>0.05)	-0.18 (>0.05)
U (µg L^{-1})	0.77 ***(<0.001)***	

Thorium: solubility and speciation under variable soil temperature

Solution Th concentration also varied with time depending on soil temperature (Figure 7.7b); Th concentration was relatively constant during the first 5, 19, 19 and 11 days of incubation then transitorily increased with time until 40, 40, 40 and 28 days at 5, 10, 16 and 25 °C, respectively; after that Th concentration steeply decreased over time till the end of incubation. At 30 °C, the Th concentration increased during the first 28 days of incubation (2.5-fold increase) and then steeply decreased over time till the end of the incubation period. There was a strong positive correlation between Th concentration and pH and concentrations of DOC, DIC, Mn and Fe in solution but a negative correlation with NO^{3-} concentration (Table 7.6). The concentration of Th consistently increased with soil temperature, the impact of temperature was pronounced between 10 and 16 °C and between 25 and 30 °C. The relatively low Th solubility (0.38 – 2.7 ng L^{-1} over all measurements) may be attributed to the extremely high phosphate concentration in Ba soil from over a century of sewage sludge application and the inclusion of Th within phosphate precipitates and/or formation of ternary surface complexes such as Th-phosphate-Fe^{III}oxide (Zhang et al., 2006) (Section 6.3.1). In contrast to U, the increase in Th concentration over the incubation time, and with soil temperature, was most consistent with the increase in DOC concentration (r = 0.74; Table 7.6). This suggests the formation of Th-organic complexes in soil solution under reducing conditions – although there was clearly considerable co-variance between DIC and DOC, especially in the early stages of the incubation. It has been reported that the organic matter released in solution immediately after rewetting air-dried soil has a relatively low affinity for metals in comparison with natural organic matter (Amery et al., 2007; Cornu et al., 2011). However, the composition of DOM has been found to change to include more aromatic compounds (high affinity for metals) during soil incubation and with the rise in soil temperature under anaerobic conditions (Amery et al., 2007; Cornu et al., 2011). Like U, Th was positively correlated with pH, DOC, DIC, Fe and Mn and negatively correlated with NO_3^-. A significant positive correlation was found between solution Th and U concentrations (Table 7.6). The decrease in organic carbon, perhaps due to microbial mineralization, or re-adsorption, explains the steep decline in Th concentration after the initial increase. The trend in decrease of Th solubility differed from that of U. Thorium has only one oxidation state (+IV) so the decrease in Th

concentration cannot have been due to precipitation of a reduced form. Alternatively, the steep decrease in Th solubility may be due to re-adsorption of Th onto reductively modified mineral surfaces (Grybos et al., 2007). Also, under the progressively reducing conditions the solution pH increased from 6.6 to 7.6 which would increase negative surface charge on soil geocolloids and thereby increase Th adsorption onto Fe-oxides and humus. With increasing pH, Th adsorption to organic matter may also be expected to decrease due to the dissolution of soil organic matter and the formation of Th-organic complexes (Langmuir and Herman, 1980; Nash and Choppin, 1980; Miekeley et al., 1985; Avena and Koopal, 1998; Grybos et al., 2007). However, Reiller et al. (2002) reported that at pH >7, sorption of Th onto Fe-oxides is enhanced as compared to Th-organic matter complexation (in solution) because the competition is in favour of the surface sites (Reiller et al., 2002).

Thorium speciation in the soil solution under reducing conditions and at different soil temperatures was predicted by WHAM-VII using the solution properties. The significant positive correlation observed between Th and DOC concentrations and the suggestion of the formation of Th-organic complexes in soil solution was strongly supported by the speciation results. As shown in Figure 7.7d, Th-organic complexes followed the same trend as solution Th concentration ($r = 0.98$, $P < 0.001$) over the period of the incubation and at all soil temperatures. The concentration of Th-organic complexes predicted by WHAM-VII varied from 92 to 100% of the total dissolved Th.

Overall, soil temperature probably affected the dynamics of Th and U partly by moderating the microbial mineralization processes occuring in soil which in turn strongly moderated soil physico-chemical parameters, such as pH, DOC, DIC, NO_3^-, Fe and Mn, which are known to profoundly affect the solubility and speciation of trace elements (Adriano, 2001; Cornu et al., 2008, 2011). It is well recognised that temperature affects microbial activity in soils (Qiu et al., 2005); over the range studied (5 – 30^{o}C), soil microbial activity can be assumed to be increased at higher temperatures (Qureshi et al. 2003). The rise in soil temperature increased the initial flush of DOC and DIC concentration in solution, by promoting microbial C-mineralization and thereby hastened the onset of anaerobic conditions. Moreover, the rise in soil temperature may enhance the DOC complexing capacity for metals by

promoting the selective mineralization of easily degradable, UV-inactive hydrophilic compounds (Marschner and Bredow, 2002; Cornu et al., 2008).

To conclude, the early stages of the incubation trial demonstrate the possible effect of wetting and drying cycles on Th and U solubility. In field soils, it seems likely that if an extended dry period is followed by substantial rainfall, there is likely to be a flush of microbial activity leading to short-term mobilization of U and Th into solution at levels one or two orders of magnitude greater than the normal aerobic pore water concentrations. Given the relatively strong adsorption of U, and especially Th, by most topsoils, it may be that such (redox) cycles provide the greatest opportunity for transport of both elements down the soil profile as U-carbonate and Th-fulvic complexes. Furthermore, the normal lab-based measurement of a fixed K_d value would clearly underestimate the capacity for such migration in field soils.

7.3.4 Investigating the speciation of Th and U in soil pore water using coupled SEC-ICP-MS

In this section size exclusion chromatography (SEC) coupled to ICP-MS was used to verify complexation of Th and U with organic matter in soil pore water samples extracted by Rhizon soil moisture samplers from the Field soils (Ar, AW, Ca and AM) following a range of incubation times (see Section 2.3.1 for details). The relatively high level of DOC found in these soils (Section 6.3.1) suggests that Th and U speciation may be significantly affected by complex-formation with DOM, particularly for Th. Several studies have shown that Th and U can form strong complexes with DOM (Langmuir, 1980; Glaus et al., 1997; Saito et al., 2004; Goody et al., 1995; Kaplan and Knox, 2003; Jackson et al., 2005). Under neutral to alkaline conditions, and in the presence of high carbonate concentrations, U(VI)–DOM complexes are relatively unimportant compared to uranyl carbonate and calcium uranyl carbonate complexes (Ranville et al., 2007; Gustafsson et al., 2009). However, at acidic pH values, although the free divalent uranyl cation (UO_2^{2+}) predominates in the absence of DOM (Koch-Steindl and Pröhl, 2004), U(VI) complexation to DOM is important in most soils (Gustafsson et al., 2009). The potential for DOM-Th interaction is indicated by the strong positive correlation between Th and DOC ($r = 0.90$, $P < 0.001$) across all soil groups. By contrast, U was not significantly correlated with DOC for the entire dataset but there was a strongly positive correlation in AW and AM soils (low pH; $r \geq 0.91$, $P < 0.001$), a weak correlation in Ar soils (neutral pH; $r = 0.64$, $P < 0.05$), and a negative correlation in Ca soils (high pH; $r = -0.36$, $P < 0.05$).

Thorium and uranium distribution in size fractions

Thorium chromatograms for the AW topsoil and AM-H soil profile under (*Calluna vulgaris)* (2-8 cm, 8-12 cm, 12-14 cm) pore water samples are shown in Figure 7.9, while U chromatograms for AM, AW, Ca-Ar and Ca-W topsoils pore water are shown in Figure 7.10. The chromatograms shown in Figures 7.9 and 7.10 all presented reasonably clear signals but some soil pore waters produced undetectable Th and U concentrations. Thorium was detected in the pore water of all soils except for Ca-Ar, Ca-G, and AM-H subsoil (30 – 40 cm); the dissolved Th concentrations in these soils were only 0.01 µg L^{-1} on average (Section 6.3.1). In the AM-H soil profile under

Calluna vulgaris (2 - 8 cm, 8 – 12 cm, 12-14 cm) soil pore water Th was detected in both the excluded volume (elution at ~ 7 min) and in the later eluting fraction, whereas in pore water from Ar, AW, Ca-W, AM-B (*Betula pendula)* and AM-P (*Pinus sylvestris*) soils, Th was not detected in the excluded volume (high MW forms). Thorium was only detected in the excluded volume after 72 hr incubation (at 96 and 144 hr) of soil AM-H-1 (2 -8 cm) and after 96 hr incubation (at 144 hr) for AM-H-2 and AM-H-3 (8 – 12 cm, 12-14 cm) soils (Figure 7.9).

Uranium was detected in the pore water of all soils except for AM-H subsoil (30 – 40 cm), Ar soils following the first 96 hr of incubation and AM-soils following 24 or 48 hr of incubation. As was found for Th, U was detected in both the excluded volume (elution at ~ 7 min) and in the later eluting fraction for the AM-H soil profile under *Calluna vulgaris* (2 - 8 cm, 8 – 12 cm, 12-14 cm). In the pore water from Ar (at 120 and 144 hr), AW, Ca, AM-B (*Betula pendula)* and AM-P (*Pinus sylvestris*) soils, U was not detected in the excluded volume. As was found for Th, U was only detected in the excluded volume after 72 hr of incubation (at 96 and 144 hr) in AM-H-1 soil and after 96 hr of incubation (at 144 hr) in AM-H-2 and AM-H-3 soils.

The first narrow peak observed in AM soil pore water, at approximately 7 minutes, (Figures 7.9 and 7.10) represents the excluded fraction (> 300,000 Da). Following that, a broader peak attributable to DOC-bound Th and U was seen in all soil pore water chromatograms. The elution time was dependent on soil type: eg ~ 12.5 – 17 min in AW soils, ~ 14 – 17 min in AM soils and ~ 16 – 17 min in Ca soils. The elution time and width of the peaks reflect the distribution of molecular mass of the pore water organic matter (DOC) but are also the product of organic matter interactions with the column matrix involving mechanisms such as hydrophobic adsorption (Asakawa et al., 2011), charge repulsion or charge attraction which all lead to changes in retention time (Chin and Gschwend, 1991; Pelekani et al., 1999; Jackson et al., 2005). The excluded fractions may represent association of Th and U with an inorganic colloidal phase or with organic components >300,000 Da, whereas the later eluted fraction represents Th and U associated with lower molecular mass soil organic matter fractions. Th and U chromatograms for Acidic Moorland (AM) soils were compared with chromatograms for (i) humic acid (coniferous plantation) used as a

carrier for Th and U standards (residual only and standard-spiked at 5 and 10 µg L^{-1} Th and U; Section 7.2.4) (Figure 7.11) and with (ii) an alkaline extraction of Acidic Moorland soil under *Calluna vulgaris* (2 - 8 cm) (1 g soil : 10 ml 0.1 M NaOH) (Figure 7.12). In the Humic acid and AM soil alkaline extract (Figures 7.11 and 7.12) Th and U were both detected in the excluded volume (eluted at ~ 7 min) and in the later eluted fraction. The first narrow peak represents the excluded fraction consisting of humic-bound forms of Th or U with MW ranges larger than 300,000 Da. The broad peak eluted after that (~ 8 – 14 min) reflects the distribution of molecular masses of the HA and extracted organic matter but are also the product of HA and extracted organic matter interactions with the column matrix as discussed above for soil pore water organic matter (DOC). In the AM soil pore water, the Th and U excluded fraction eluted at approximately the same time (~ 7 min) as the excluded fraction of the humic acid and the alkaline extract of the AM soil.

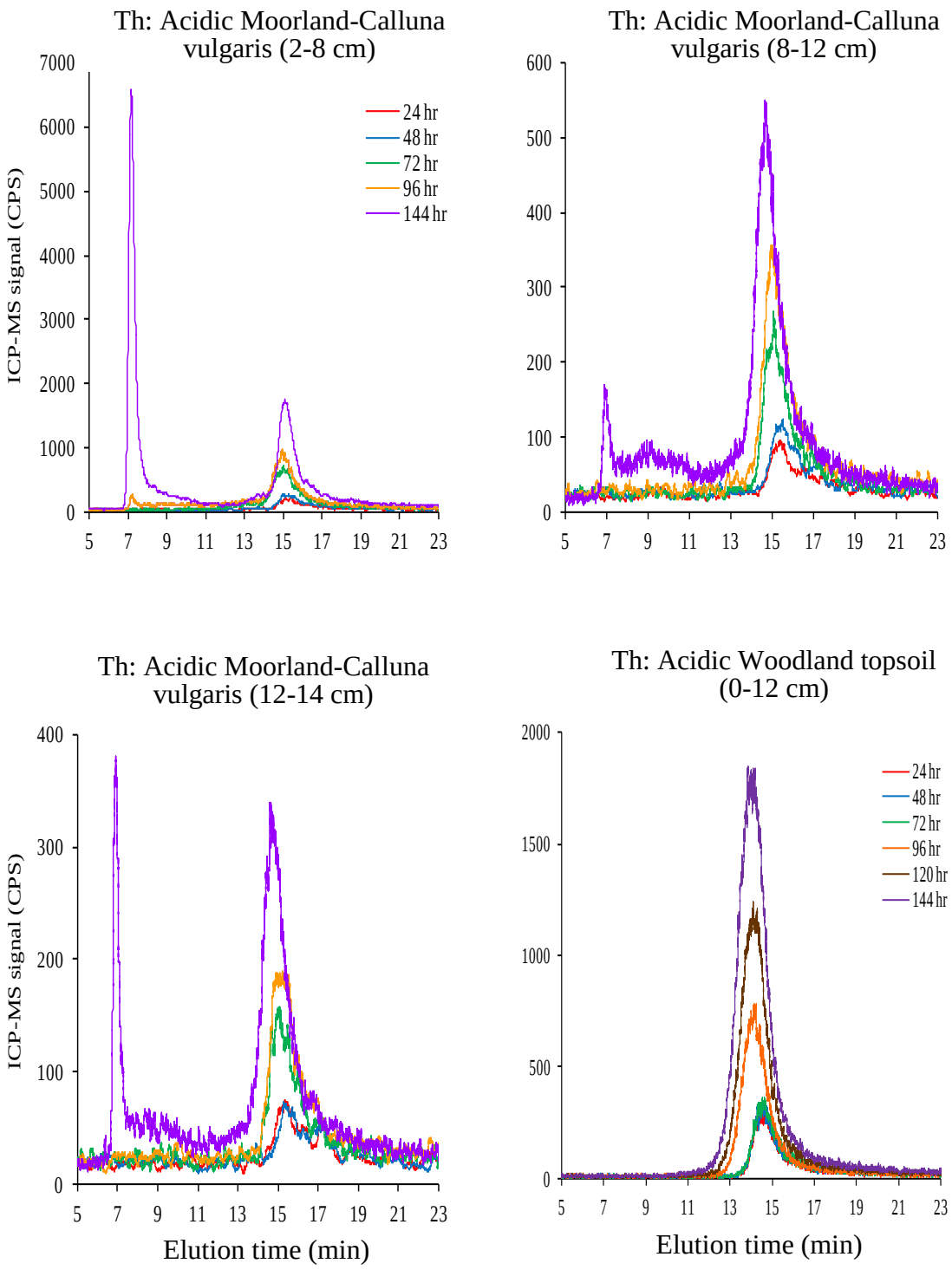

Figure 7.9: SEC-ICP-MS chromatograms of Th in soil pore water at different incubation times (24, 48, 72, 96 and 144 hr for AM soils; 24, 48, 72, 96, 120 and 144 hr for AW soil). Soils include: Acidic Moorland soil profile under *Calluna vulgaris* (2-8 cm, 8-12 cm, 12-14 cm) and Acidic Woodland topsoil (0-12 cm).

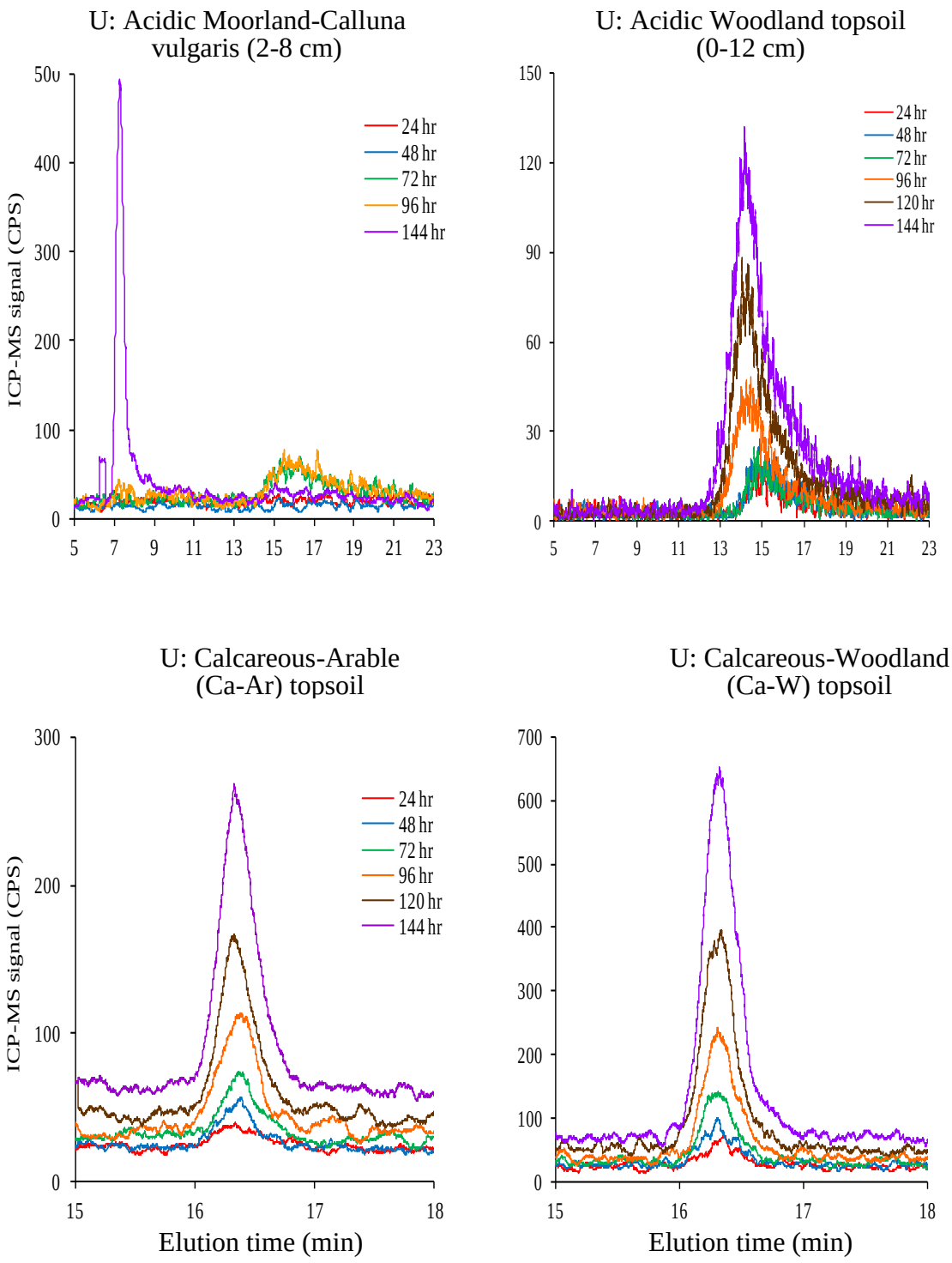

Figure 7.10: SEC-ICP-MS chromatograms of U in soil pore water at different incubation times (24, 48, 72, 96 and 144 hr for AM soils; 24, 48, 72, 96, 120 and 144 hr for AW and Ca soils). Soils include: Acidic Moorland soil under *Calluna vulgaris* (2-8 cm), Acidic Woodland topsoil (0-12 cm), Calcareous-Arable (Ca-Ar) and Woodland (Ca-W) topsoils.

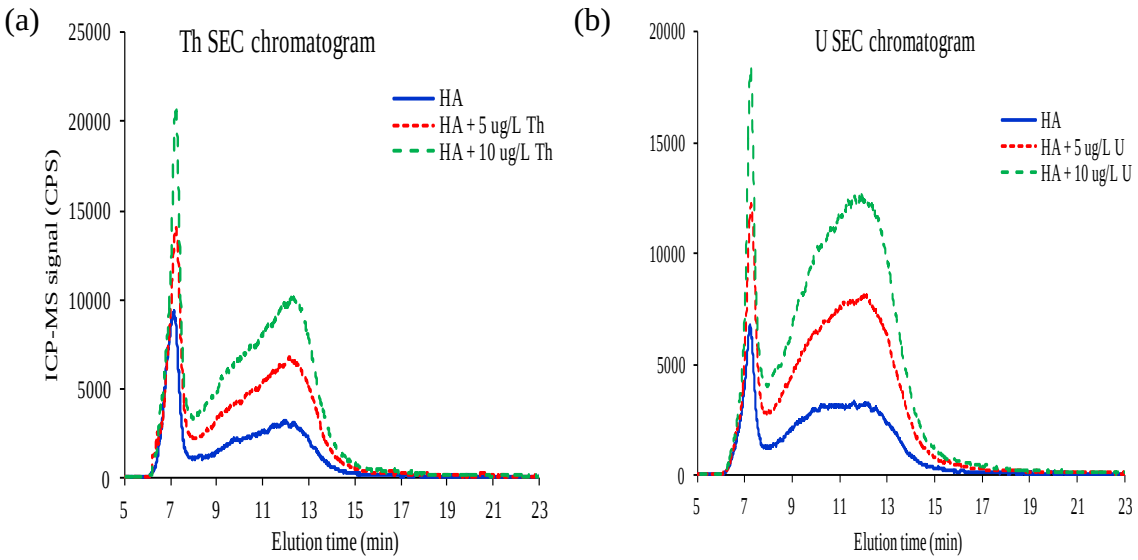

Figure 7.11: SEC-ICP-MS chromatograms of (a) Th and (b) U in a humic acid solution used as a carrier for Th and U standards. The chromatograms show the presence of residual Th and U in the humic acid preparation and the two standard additions (5 and 10 µg L^{-1} Th and U).

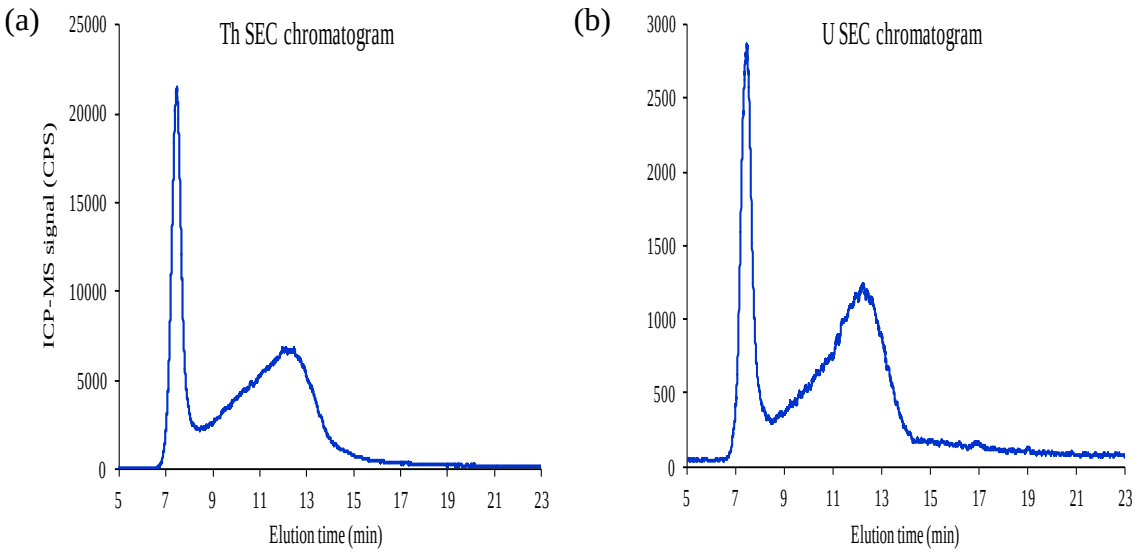

Figure 7.12: SEC-ICP-MS chromatograms of (a) Th and (b) U in an alkaline extract of the Acidic Moorland soil under *Calluna vulgaris* (AM-H-1; 2-8 cm).

Comparing Th and U chromatograms for the acidic soils (AW and AM) showed that Th is more strongly associated with dissolved organic matter than U. Although DOM-Th and DOM-U fractions exhibited broadly the same elution profiles and molecular size distributions, there was a big difference in the peak height and the concentrations associated with DOM. This was in agreement with the AM soil alkaline extract in

which OM-Th and OM-U fractions (Figure 7.12) also exhibited the same elution profiles and molecular mass distributions but the Th concentration greatly exceeded the U concentration. This confirms that Th is mainly and more strongly bound to organic matter (DOM and SOM) in acidic soils than U and also confirms the vital role of dissolved organic matter for the mobilization and geochemical cycling of Th (Casartelli and Miekeley, 2003). This finding could also explain the high concentration of total dissolved Th in AW and AM soils compared to U concentration in the same soils (Section 6.3.1). The chromatograms show a clear effect of soil depth on the concentration of DOM-Th and DOM-U complexes, particularly in the AW and AM soils. The peak height and ICP-MS signal intensity decreased with soil depth due to the decrease in DOC concentration causing a corresponding decrease in concentrations of soluble DOM-Th and DOM-U complexes.

There were clear differences between the soils in terms of the range of molecular weights of the DOM-Th and DOM-U fractions. As shown above (Figures 7.9, 7.10), an 'excluded' organic metal (high MW DOM-Th and DOM-U) fraction was detected in only three AM soils, at one time point in two of them and two time points in the third one. Moreover, Th and U concentrations associated with the excluded fraction were low compared to concentrations associated with the lower molecular mass fractions (except for U in AM-H-1). The broader peak observed in all soil pore water chromatograms is attributable to a wider range of low MW DOM-Th and U fractions. Calcareous soils had the lowest range of molecular sizes (eluted at ~ 16 – 17 min) compared to AW, Ar (~ 12.5 – 17 min) and AM (~ 14 – 17 min) soils.

The chromatograms (Figures 7.9 and 7.10) show a clear effect of incubation time on Th and U fractions associated with dissolved organic matter: the peak height increased with incubation time and this effect was much more pronounced after 48 or 72 hr incubation time. This is almost certainly related to the progressive increase in DOC concentration with incubation time. The incubation time affected both peak height and also peak position; this was clear in the AM, AW and Ar soils. For example, DOM-Th and U peaks in AM and AW soils shifted to a shorter elution time after 48 and 72 hr incubation, indicating the slow solubilisation of high molecular size organic matter fractions with time. In AM soils under *Calluna vulgaris* an organic peak appeared in

the excluded volume after 96 and/or 144 hr incubation time; this peak was attributed to the slow solubilisation rate of higher molecular mass organic matter with time. The excluded peak (high MW fraction) appeared in AM soils under one vegetation type (*Calluna vulgaris)* and did not appear under the other two vegetation types *(Betula pendula and Pinus sylvestris*). This appears to indicate an effect of vegetation type on the nature and molecular mass distribution of the soil DOM and hence on the complexation of Th and U with DOM.

The effect of soil incubation time on Th and U complexation

Figures 7.13a and b show the SEC-ICP-MS measured concentrations of DOM-Th and DOM-U complexes in soil pore water as a function of incubation time for Ar, AW, Ca (Figure 7.13a) and AM soils (Figure 7.13b). The results show variation in Th and U concentrations associated with DOM within each soil category and with time; the variation was consistent with changes in measured DOC. The trend in DOM-Th followed that of measured Th concentration in the soil pore water (Section 6.3.1; Figures 6.1a and b) and both variables were significantly positively correlated with DOC ($r > 0.85$, $P < 0.001$). This again supports the hypothesis that DOM normally controls the speciation of Th in soil pore water (Langmuir, 1980; Taboada et al., 2006). By contrast, DOM-U did not follow the same trend as that of soil pore water U (Section 6.3.1; Figures 6.1a and b). For example, U concentration in soil pore water was higher in Ca-Ar than in Ca-W and Ca-G soils and correlated with DIC, whereas DOM-U concentration was higher in Ca-W than in Ca-Ar and Ca-G soils in correlation with DOC concentration (DOC concentration in Ca-W was higher than in Ca-Ar and Ca-G soils). There was no significant correlation between concentration of total dissolved U and DOM-U complexes but DOM-U concentration was strongly correlated with DOC ($r = 0.87$, $P < 0.001$). It should be noted that both total dissolved U and DOM-U were positively correlated ($r = 0.87$, $P < 0.001$) in AW and AM soils rich in DOC. This may be explained by the fact that DOM-U complexes are not the most important U species in soil pore water, depending on soil physico-chemical characteristics (pH, DIC and DOC) (Reszat and Hendry, 2007; Ranville et al., 2007; Gustafsson et al., 2009).

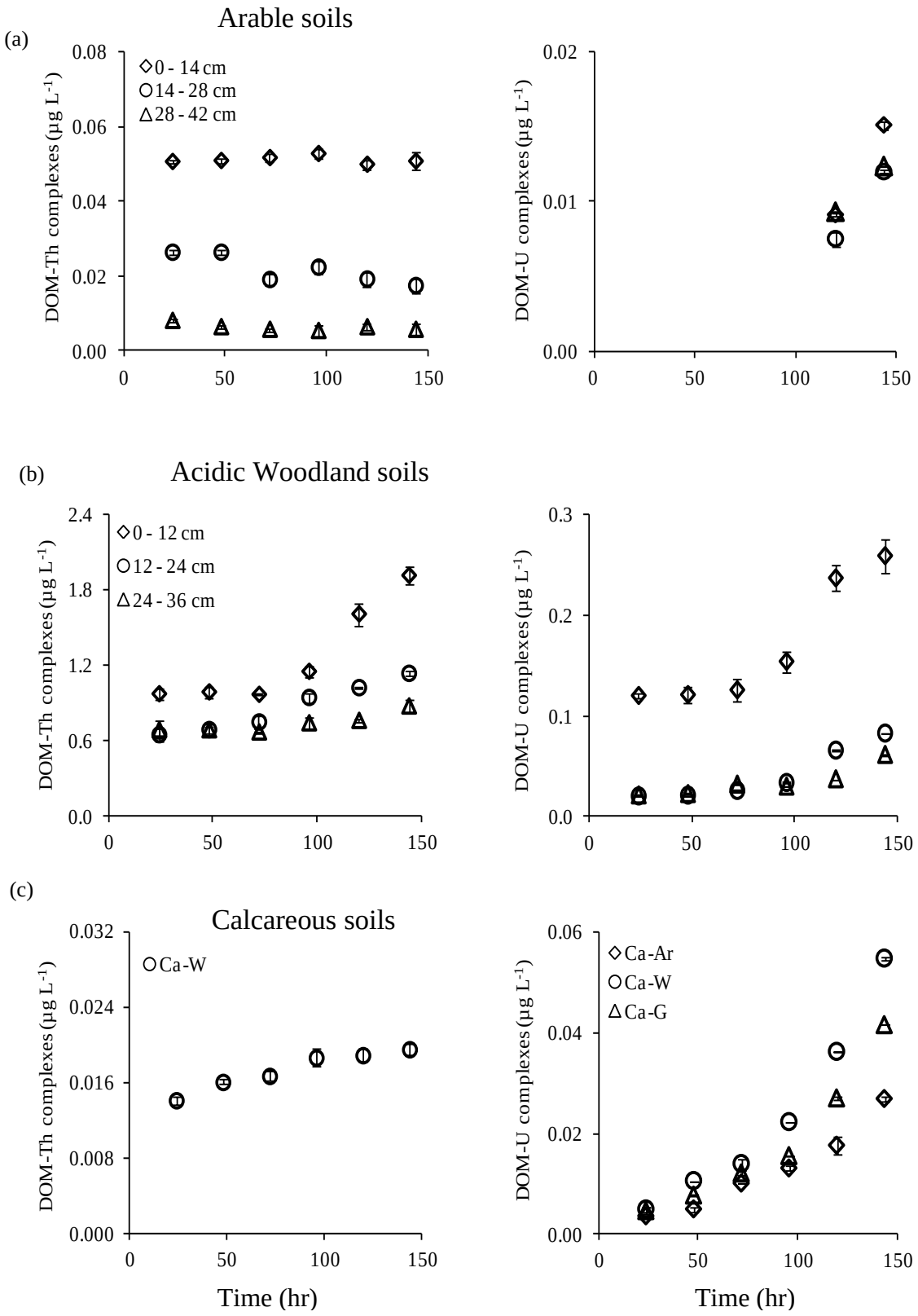

Figure 7.13a: The variation in SEC-ICP-MS measured concentrations of DOM-Th and DOM-U complexes (µg L^{-1}) in soil pore water with incubation time (24, 48, 72, 96, 120 and 144 hr) in (a) Arable soil profile (0-14 cm, 14-28 cm, 28-42 cm), (b) Acidic Woodland soil profile (0-12 cm, 12-24 cm, 24-36 cm) and (c) Calcareous topsoils (Arable; Ca-Ar, Woodland; Ca-W, Grassland; Ca-G).

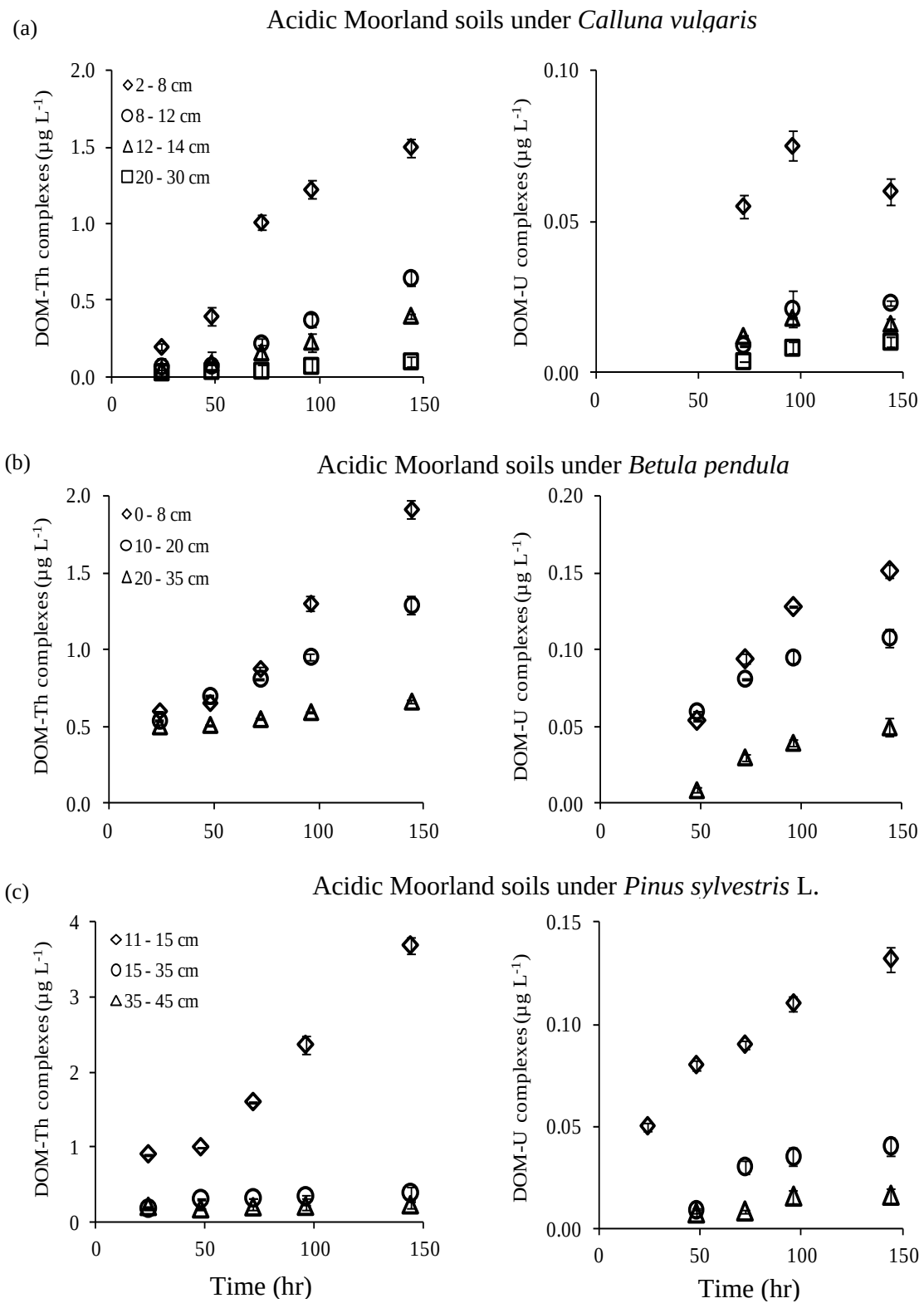

Figure 7.13b: The variation in SEC-ICP-MS measured concentrations of DOM-Th and DOM-U complexes (µg L^{-1}) in AM soils pore water with incubation time (24, 48, 72, 96 and 144 hr). The Acidic Moorland soil profile was under three contrasting vegetation regimes: (a) *Calluna vulgaris* (2-8 cm, 8-12 cm, 12-14 cm, 20-30 cm), (b) *Betula pendula* (0-8 cm, 10-20 cm, 20-35 cm) and (c) *Pinus sylvestris* (11-15 cm, 15-35 cm, and 35-45 cm).

Thorium and uranium recovery

Figures 7.14a and b compare the SEC-recovered Th and U to pore water Th and U concentrations measured directly (Section 6.3.1). As shown in Figure 7.14a pore water Th and recovered Th concentrations were closely correlated ($r^2 = 0.98$). The recovery of Th varied among soil categories and ranged from 39% in the AM subsoil to an apparent figure of 123% in Ar soils; the average recovery across all soils was 85%. The average recovery (minimum-maximum; average) of Th in each soil category followed the order: Ar (65-123%; 97%) > AW (76-112; 87%) > AM (39-123; 82%) > Ca-W (58-88; 74%).

The U recovery varied from 0.3% in Ca soils to 85% in AW soils (average = 30%). The average recovery (minimum-maximum; average) of U in each soil category followed the order: AM (10-80; 45%) > AW (14-85; 37%) > Ar (2-7%; 4%) > Ca (0.3-7; 2%). The U recovery was low compared to Th, particularly for Ar and Ca soils. This is because the SEC was not efficient at eluting the free uranyl cation, or labile complexes such as inorganic species (e.g. uranyl carbonates) or possibly very low molecular weight organic complexes. This may be a consequence of U adsorption to the column through hydrogen bond formation between the uranyl cation (UO_2^{2+}) and the gel matrix; labile U complexes can dissociate to release UO_2^{2+} during transition through the column. Jackson et al. (2005) studied the fractionation of U in four contaminated sediment water extracts using SEC and indicated the presence of (i) a significant fraction of U bound to DOM (22-29%), (ii) a fraction greater than the exclusion limit of the column and co-eluted with Al (0.1-53%), (iii) unrecovered 'labile' U complexes (25-78%). Jackson et al. (2005) reported that separation on SEC is only applicable to strong metal-DOM complexes. The affinity of free metal ions, arising from dissociation of labile complexes, for the column gel phase produced diffuse and unpredictable elution patterns. A smaller recovery of U compared to Th is consistent with Th being more strongly bound to organic matter; complexation of U by carbonate in near neutral and alkaline soils (e.g. Ar and Ca soils) makes U more vulnerable to apparent losses in the column. Low U recovery (2%) was also reported by Ranville et al. (2007) in a study using Asymmetrical Flow Field-Flow Fractionation (AsFlFFF) to assess the partitioning of U to DOC in ground water samples, the authors ascribed the low U recovery to the presence of U as free uranyl

cations and inorganic complexes (e.g. $UO_2CO_3^-$, $UO_2(CO_3)_2^{2-}$) in ground water samples.

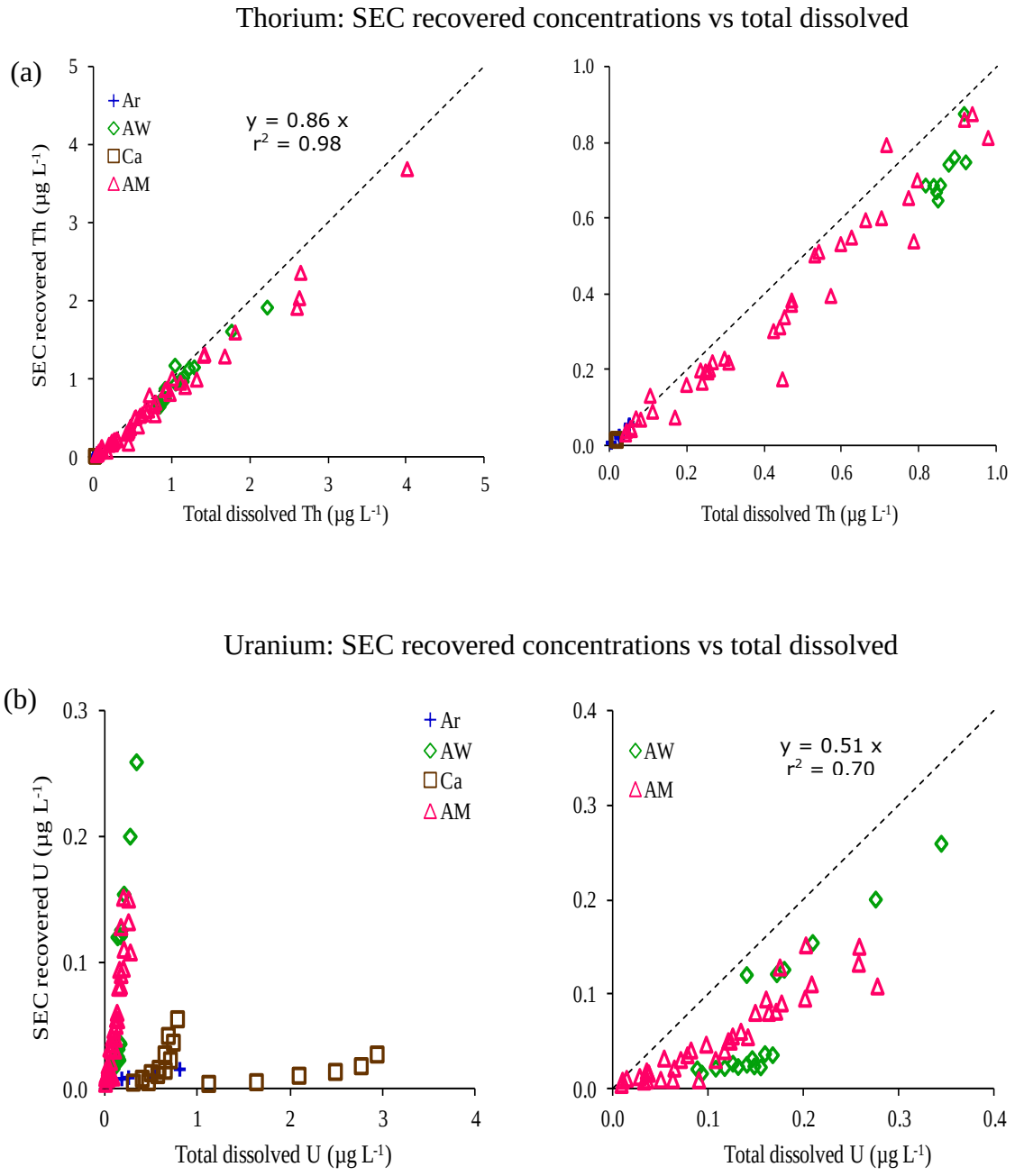

Figure 7.14: SEC-recovered (a) Th and (b) U against total dissolved Th and U concentrations (µg L^{-1}) for Arable (Ar; +), Acidic Woodland (AW; ◊), Calcareous (Ca; □) and Acidic Moorland (AM; Δ) soils. The dashed line is the 1:1 relation. The left-hand and right-hand graphs are on different scales, right-hand graphs show the small Th and U concentration range.

Comparing SEC-ICP-MS measured DOM-Th and DOM-U to WHAM-VII predicted DOM-Th and DOM-U

The DOM associated Th determined by SEC (85% on average of soil pore water Th) was in good agreement with the results of geochemical modelling (94% on average of soil pore water Th), the predicted DOM-Th complexes were closely correlated with the measured values (r^2 = 0.97; Figure 7.15a). There was good agreement between measured and predicted DOM-U complexes in AM and AW soils (Figure 7.15b), particularly for AW soils (Measured DOM-U = 0.98 predicted DOM-U, r^2 = 0.99). On the other hand, predicted concentrations of DOM-U complexes were higher than the measured values in Ar and Ca soils by an average factor of 12 and 6, respectively.

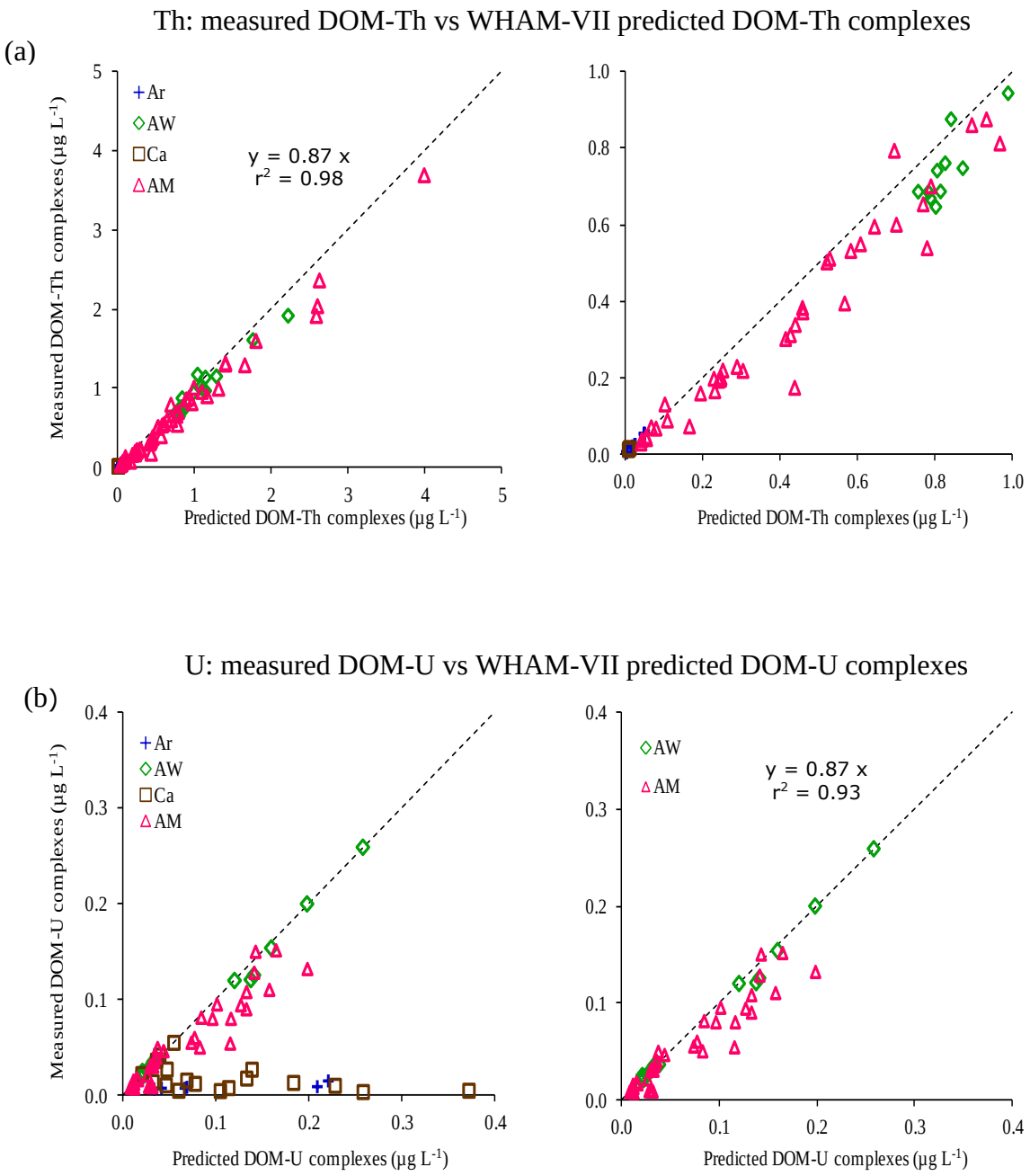

Figure 7.15: SEC-ICP-MS measured (a) DOM-Th and (b) DOM-U complexes against WHAM-VII predicted values (µg L^{-1}) for Arable (Ar; +), Acidic Woodland (AW; ◊), Calcareous (Ca; □) and Acidic Moorland (AM; Δ) soils. The dashed line is the 1:1 relation. The left-hand and right-hand graphs are on different scales; right-hand graphs show the small DOM-Th concentration range and DOM-U complexes for only AW and AM soils.

To conclude, there was a clear difference between the soils in terms of the range of molecular masses of DOM-Th and DOM-U fractions. The results showed a clear effect of soil depth on DOM-Th and DOM-U complexes, particularly in AW and AM soils. The peak height and ICP-MS signal intensity decreased with soil depth due to the decrease in DOC concentration and hence the decrease in DOM-Th and DOM-U complexation. Soil incubation time affected not only concentrations of DOM-Th and DOM-U complexes but also the molecular mass distribution. With increasing incubation time, the DOM-Th and DOM-U peaks shifted to a shorter elution time, indicating the slow solubilisation rate of high molecular mass organic matter fractions. In addition, there was a clear effect of vegetation type in AM soils on the nature of DOM and its molecular mass distribution, hence on the complexation of DOM to Th and U. This is likely to be related to different degrees of humification in the soil and/or different levels of flocculation/aggregation of DOM with polyvalent metals.

The good recovery of Th and the agreement between SEC-ICP-MS measured DOM-Th and WHAM-VII predicted DOM-Th complexes confirms the importance of dissolved organic matter for Th complexation and solubility in soil pore water and the efficiency of SEC for the measurement of DOM-Th complexation at natural DOC and Th concentrations. However, DOM complexes may be of limited importance for U complexation, especially in near-neutral and calcareous soils (Ar and Ca). Uranium appeared to be present as either labile complexes or free uranyl cation in soil pore water, which suggests that U is likely to be much more bioavailable than Th. The speciation technique used was efficient for measuring the strong metal-DOM complexes (in this case, Th), but may be limited by the potential interaction of weakly complexed DOM-U due to adsorption and dissociative interactions with the gel matrix of the column.

8 CONCLUSIONS

The ability to predict transfer of radionuclides to surface and ground water, and uptake by plants and other biota depends mainly on understanding the mechanisms involved in radionuclide interactions with different components of agricultural and natural ecosystems. The current work tried to enhance understanding and prediction of U and Th dynamics in soils with a wide range of characteristics. The approach used in this thesis tested the application of isotope dilution technique (ID) as a means of measuring the *labile* U(VI) pool in soils. Uranium lability was investigated for two sets of soils. The first set (Field soils) consisted of thirty seven soil samples representing five contrasting local ecosystems; the second dataset (BGSc) included 40 soils sub-sampled from the British Geological Survey (BGS) archive and covered a wider range of soil characteristics. The U isotope dilution results were compared with four different single extraction methods to assess the use of the latter to estimate the labile U(VI) pool in soils. In addition, Th reactivity in the two sets of soils was investigated using the four single extraction methods applied to uranium. A multiple linear regression model was used to predict Th and U reactivity from relevant soil characteristics. A dynamic continuous leaching based approach was used to study the fractionation and elemental associations of U and Th in contrasting soils, as an alternative approach to the classical batch extraction procedures. The solubility and fractionation of Th and U, in batch suspensions and in soil columns, were predicted using multiple linear regression and the mechanistic geochemical model WHAM-VII (Tipping et al., 2011). Inputs to the predictive models included labile U and Th fraction measured by ID or from single extraction approaches. Finally, the extent of binding of Th and U to DOM in soil pore water and the distribution of these elements within DOM molecular size fractions were studied for contrasting soils using 'size exclusion chromatography' coupled to ICP-MS (SEC-ICP-MS). Interpretation of the acquired results provided new insights into the dynamics of U and Th in soils and the relationships between soil properties, U and Th geochemistry and lability.

8.1 Solubility and speciation of Th and U in soils

Solubility of Th and U varied between soils, influenced by pH, DOC, DIC and phosphate concentrations. The K_d values for Th and U varied by 4 and 3 orders of

magnitude respectively over the range of soils studied. In acidic soils (pH <5) K_d values for U were 1.2 to 5.2 times greater than for Th. Solubility of Th and U decreased with soil depth and differences between Th and U mobility were greater in the upper soil layers. In mildly acidic and calcareous soils (pH > 5 < 8), K_d values for Th were significantly higher than for U. The formation of soluble uranyl carbonate complexes give rise to a strong positive correlation between U and DIC concentrations in soil solution, especially under anaerobic conditions at high CO_2 partial pressure and also at high temperatures which encouraged microbial activity and led to mobilization of U into solution at levels one or two orders of magnitude greater than the normal aerobic pore water concentrations. Thorium and U K_d values diverged with soil pH, due to enhanced U solubility as carbonate complexes and stronger Th adsorption in the solid phase. However, there was evidence of increasing Th solubility at pH >5.8 due to the formation of Th-hydroxy-carbonate complexes. The solubility of U and Th was accurately predicted from empirical model using soil variables; pH and DIC were the primary predictors of U solubility, whereas pH and DOC were the predominant predictors of Th solubility.

The speciation of Th and U in the pore water of contrasting soils, measured using SEC-ICP-MS, indicated that Th solubility was dependent on DOM-Th complex formation. Dissolved Th and DOM-Th complexes were closely correlated. However, there were clear differences between soils with respect to the range of molecular masses of DOM-Th fractions in soil pore water. By contrast, U complexation with DOM was more variable, especially with increasing soil pH. Uranium appeared to be present as either labile complexes or free uranyl cations in soil pore water, which suggests that U is likely to be much more bioavailable than Th.

8.2 Labile U and Th fractions in soils

Isotopically exchangeable $^{238}U(VI)$ (E-values) in the soils studied varied from 2.7 to 39.1% of the total U content. The results obtained indicated that some soil properties had a systematic effect on the lability of $^{238}U(VI)$. There was no significant correlation between soil pH and U lability, however, co-variance with soil adsorption phases, Fe-oxide and organic matter, may control and explain the variance in U lability. A resin purification step was used to determine the presence of non-labile SCP-$^{238}U(VI)$

formed during E-value assay; significant amounts of non-labile SCP-^{238}U were associated with suspended nano-particulate colloids < 0.2 µm suspended in the solution phase and produced an error of 20% in the estimation of labile ^{238}U in biosolid-amended soils. This was significantly related to the high phosphate and DOC concentrations in filtered solutions from the biosolid-amended soils suggesting an association with fixed forms of ^{238}U. For the remaining soils, the true E-value was overestimated by 2.2%; non-labile SCP-^{238}U was significantly correlated with pH and DIC, suggesting that carbonate colloids in soils with high pH may have been responsible.

The amount of U solubilised by four chemical extractants (U_{Ac}, U_{Nit}, U_{EDTA}, U_{TMAH}) were significantly different between soil groups ($P < 0.001$). Therefore, E-values for U(VI) did not correspond consistently with any single chemical extraction procedure although the degree of correspondence was soil-dependent. On average, over all groups of soils studied, CH_3COONH_4, EDTA and TMAH underestimated E-value by factors of 13.7, 9.5 and 1.6, respectively, while HNO_3 overestimated the E-value by only a factor of 1.04 on average. Uranium extracted by HNO_3 was very similar to the E-value (U_E) below pH 5 and higher than in biosolid-amended and arable soils and was significantly correlated with extracted phosphate; nitric acid may dissolve uranyl phosphate minerals in these soils. On the other hand, TMAH-extracted U was slightly higher than, or equal to, labile U (E-value) in acidic soils (pH <6), whereas in near neutral and calcareous soils U_{TMAH} was lower than labile U. It appears that TMAH is able to dissolve exchangeable and organically complexed, but not carbonate-associated, uranium. Overall, HNO_3 gives the best estimate of E-value compared to other extractants. However, HNO_3 overestimated the E-value in phosphate enriched soils and underestimated E-value, in common with all the other extractants, in the Ca soils. The results revealed a major flaw in the nitric acid extraction scheme when applied to calcareous soils ($CaCO_3$ >2%) due to the large buffering capacity of $CaCO_3$.

The amounts of Th solubilised by the four chemical extractants (Th_{Ac}, Th_{Nit}, Th_{EDTA}, Th_{TMAH}) were significantly different between soil groups ($P < 0.001$). Overall, the average extractability of the four extractants followed the order: Th_{Ac} (0.08%) < Th_{Nit}

(1.5%) < Th_{EDTA} (3.1%) < Th_{TMAH} (4.6%). Although the proportions of Th_{Ac}, Th_{EDTA} and Th_{TMAH} were significantly correlated, Th_{Nit} was not correlated with the others (P >0.05). These results indicate the limitation and weakness of HNO_3 due to the the flocculation of humic and fulvic acid at extremely low pH values if the main stable form of Th in solution is organically complexed Th. In addition, nitric acid was not effective in calcareous soils. The extractability of Th (%Th_{Ac}, %Th_{EDTA}, %Th_{TMAH}) was accurately predicted from soil characteristics using an empirical model; soil pH and available-P were the predominant predictors of Th extractability. Given that most labile soil Th is expected to be humus-bound, TMAH may be the most appropriate extraction method for measuring soil available Th compared with CH_3COONH_4, HNO_3 and EDTA.

Comparing isotopically exchangeable $^{238}U(VI)$ with single extraction methods indicated that isotope dilution technique is probably the most appropriate method to quantify the 'chemically reactive' or 'labile' U pool in soils. Measuring the 'labile' U(VI) by isotopic exchange is preferable to single extraction measurements as no assumptions are required about the nature of the extracted phases. Chemical extraction methods have different modes of operation and substantial dependency on soil properties (e.g. pH, SOM, phosphates, $CaCO_3$). Therefore, the efficiency of chemical extractants vary with soil type and soil properties; it appears that there is no chemical extraction method can estimate the labile U pool in different soil types and under all soil conditions. However, the ID technique can discriminate between labile and non-labile U pools in soils without dependence on soil properties and with minimal disturbance to the soil system.

8.3 Predicting U and Th solubility from E-value and Th_{TMAH}

Including isotopically exchangeable U as an input parameter, to represent the reactive U fraction in soil, improved the prediction of U solubility in the geochemical model WHAM-VII compared to using the total soil U concentration or the pools extractable by CH_3COONH_4, EDTA, HNO_3 and TMAH as surrogates for 'reactive uranium'. The WHAM model generally overestimated solubility at low pH (pH <5) and underestimated it at high pH (pH >5) values. Fractionation information from WHAM indicated that the pH-dependence of U binding strength is overestimated.

Solubility of Th in whole soil was predicted reasonably well by the WHAM-VII model when Th_{TMAH} was used as an input parameter in preference to total Th content and Th_{Ac}, Th_{EDTA}, Th_{Nit}. Generally, Th solubility prediction showed a strong dependency on the choice of Th_{Ext} method used to estimate labile Th. This suggests that there is scope for further refinement of methods used to estimate the reactive Th pool in soil. The model generally overestimated Th solubility, the fractionation results showed that the pH-dependence of Th binding to humus (Th was predicted to be almost exclusively adsorbed on humus) was underestimated – that is, solubility was consistently overestimated at high pH and the increase in binding strength per unit pH increase was underestimated.

8.4 IMPLICATIONS

The isotopic dilution technique discriminates between labile and non-labile metal pools in soil and can be applied without disturbance of the solid-solution equilibrium. The current study developed the ID technique for measuring isotopically exchangeable (labile) $^{238}U(VI)$ in soil and demonstrated that ID is a robust technique for measuring labile U under different soil conditions. Including the labile U in empirical model and in mechanistic geochemical WHAM-VII model improved the prediction of solid-solution distribution of U. Therefore, ID can potentially be used in soil remediation processes to investigate the reversibility and fixation of U binding onto soil, sediments and synthetic solid phases.

Isotopically exchangeable U can be used to accurately describe solid-liquid distribution coefficient, K_d, which in turn can be used in environmental safety assessment as a quantitative indicator of U environmental mobility and uptake from soil by plants. Moreover, U K_d values calculated using measured isotopically exchangeable U can be applied in site investigations for localisation of repository for radioactive waste.

Finally, the variation in isotopically exchangeable metal fraction in soil explains and dominates the variation in metal toxicity and can be used as a conservative estimate of the change in toxicity upon soil aging (Smolders et al., 2009).

REFERENCES

ADRIANO, D. C. 2001. *Trace Elements in Terrestrial Environments: Biogeochemistry, Bioavailability, and Risks of Metals,* Springer.

AHNSTROM, Z. A. S. & PARKER, D. R. 2000. Cadmium reactivity in metal-contaminated soils using a coupled stable isotope dilution−sequential extraction procedure. *Environmental Science & Technology,* 35**,** 121-126.

ALMAS, A., SINGH, B. R. & SALBU, B. 1999. Mobility of cadmium-109 and zinc-65 in soil influenced by equilibration time, temperature, and organic matter. *J. Environ. Qual.* , 28**,** 1742–1750.

ALMÅS, Å. R., LOFTS, S., MULDER, J. & TIPPING, E. 2007. Solubility of major cations and Cu, Zn and Cd in soil extracts of some contaminated agricultural soils near a zinc smelter in Norway: modelling with a multisurface extension of WHAM. *European Journal of Soil Science,* 58**,** 1074-1086.

ALTMAIER, M., NECK, V., DENECKE MELISSA, A., YIN, R. & FANGHÄNEL, T. 2006. Solubility of $ThO_2 \cdot xH_2O$(am) and the formation of ternary Th(IV) hydroxide-carbonate complexes in $NaHCO_3$-Na_2CO_3 solutions containing 0−4 M NaCl. *Radiochimica Acta.*

ALTMAIER, M., NECK, V., MÜLLER, R. & FANGHÄNEL, T. 2005. Solubility of $ThO_2 \cdot xH_2O$(am) in carbonate solution and the formation of ternary Th(IV) hydroxide-carbonate complexes. *Radiochimica Acta,* 93**,** 83-92.

AMERY, F., DEGRYSE, F., DEGELING, W., SMOLDERS, E. & MERCKX, R. 2007. The copper-mobilizing-potential of dissolved organic matter in soils varies 10-fold depending on soil incubation and extraction procedures. *Environmental Science & Technology,* 41**,** 2277-2281.

ANDERSON, P., DAVIDSON, C. M., DUNCAN, A. L., LITTLEJOHN, D., URE, A. M. & GARDEN, L. M. 2000. Column leaching and sorption experiments to assess the mobility of potentially toxic elements in industrially contaminated land. *Journal of Environmental Monitoring,* 2**,** 234-239.

ANJOS, C., MAGALHÃES, M. C. F. & ABREU, M. M. 2012. Metal (Al, Mn, Pb and Zn) soils extractable reagents for available fraction assessment: Comparison using plants, and dry and moist soils from the Braçal abandoned lead mine area, Portugal. *Journal of Geochemical Exploration,* 113**,** 45-55.

ARAI, Y. & SPARKS, D. L. 2001. ATR–FTIR Spectroscopic Investigation on Phosphate Adsorption Mechanisms at the Ferrihydrite–Water Interface. *Journal of Colloid and Interface Science,* 241**,** 317-326.

AREY, J. S., SEAMAN, J. C. & BERTSCH, P. M. 1999. Immobilization of uranium in contaminated sediments by hydroxyapatite addition. *Environmental Science and Technology,* 33**,** 337-342.

ARTINGER, R., KIENZLER, B., SCHÜßLER, W. & KIM, J. I. 1998. Effects of humic substances on the 241Am migration in a sandy aquifer: column experiments with Gorleben groundwater/sediment systems. *Journal of Contaminant Hydrology,* 35**,** 261-275.

ARTINGER, R., RABUNG, T., KIM, J. I., SACHS, S., SCHMEIDE, K., HEISE, K. H., BERNHARD, G. & NITSCHE, H. 2002. Humic colloid-borne migration of uranium in sand columns. *Journal of Contaminant Hydrology,* 58**,** 1-12.

ARTINGER, R., SEIBERT, A., MARQUARDT, C. M., TRAUTMANN, N., KRATZ, J. V. & KIM, J. I. 2000. Humic colloid-borne Np migration: influence of the oxidation state. *Radiochim. Acta,* 88**,** 609–612.

ASAKAWA, D., IIMURA, Y., KIYOTA, T., YANAGI, Y. & FUJITAKE, N. 2011. Molecular size fractionation of soil humic acids using preparative high performance size-exclusion chromatography. *Journal of Chromatography A,* 1218**,** 6448-6453.

ASAKAWA, D., KIYOTA, T., YANAGI, Y. & FUJITAKE, N. 2008. Optimization of Conditions for High-Performance Size-Exclusion Chromatography of Different Soil Humic Acids. *Analytical Sciences,* 24**,** 607-613.

ASHWORTH, D. J. & ALLOWAY, B. J. 2004. Soil mobility of sewage sludge-derived dissolved organic matter, copper, nickel and zinc. *Environmental Pollution,* 127**,** 137-144.

ATKINSON, N. R., BAILEY, E. H., TYE, A. M., BREWARD, N. & YOUNG, S. D. 2011. Fractionation of lead in soil by isotopic dilution and sequential extraction. *Environmental Chemistry,* 8**,** 493-500.

AVENA, M. J. & KOOPAL, L. K. 1998. Desorption of Humic Acids from an Iron Oxide Surface. *Environmental Science & Technology,* 32**,** 2572-2577.

BAILEY, E. H. 1993. Determination of uranium and thorium in basalts and uranium in aqueous solution by inductively coupled plasma mass spectrometry. *J. Anal. Atom. Spectrom. ,* 8**,** 551-556.

BANFIELD, J. F. & HAMERS, R. J. 1998. Processes at minerals and surfaces with relevance to microorganisms and prebiotic synthesis. *In:* BANFIELD, J. F. & NEALSON, K. H. (eds.) *Geomicrobiology - Interactionsbetween Microbes and Minerals, Rev. Mineralogy.*

BARISIC, D., LULIC, S. & MILETIC, P. 1992. Radium and uranium in phosphate fertilizers and their impact on the radioactivity of waters. *Water Res. ,* 26**,** 607-611.

BARNETT, M. O., JARDINE, P. M., BROOKS, S. C. & SELIM, H. M. 2000. Adsorption and Transport of Uranium(VI) in Subsurface Media *Soil Sci. Soc. Am. J.,* 64**,** 908-917.

BAXTER, M. S. 1991. Personal perspectives on radioactivity in the environment. *Science of The Total Environment,* 100**,** 29-42.

BEAUCHEMIN, D., KYSER, K. & CHIPLEY, D. 2002. Inductively coupled plasma mass spectrometry with on-line leaching: A method to assess the mobility and fractionation of elements. *Analytical Chemistry,* 74**,** 3924-3928.

BEDNAR, A. J., MEDINA, V. F., ULMER-SCHOLLE, D. S., FREY, B. A., JOHNSON, B. L., BROSTOFF, W. N. & LARSON, S. L. 2007. Effects of organic matter on the distribution of uranium in soil and plant matrices. *Chemosphere,* 70**,** 237-247.

BELLIS, D. J., MA, R. & MCLEOD, C. W. 2001. Characterisation of airborne uranium and thorium contamination in Northern England through measurement of U, Th and U-235/U-238 in tree bark. *Journal of Environmental Monitoring,* 3**,** 198-201.

BERMOND, A. 2001. Limits of sequential extraction procedures re-examined with emphasis on the role of H+ ion reactivity. *Analytica Chimica Acta,* 445**,** 79-88.

BERNHARD, G., GERHARD, G., REICH, T., BRENDLER, V., AMAYRI, S. & HEINO, N. 2001. Uranyl(VI) carbonate complex formation: Validation of the Ca2UO2(CO3)3(aq.) species. *Radiochimica Acta International journal for chemical aspects of nuclear science and technology,* 89.

BHOGAL, A., YOUNG, S. D., SYLVESTER-BRADLEY, R., O'DONNELL, F. M. & RALPH, R. L. 1997. Cumulative effects of nitrogen application to winter wheat at Ropsley, UK, from 1978 to 1990. *The Journal of Agricultural Science,* 129**,** 1-12.

BLANCO, P., TOMÉ, F. V. & LOZANO, J. C. 2004. Sequential extraction for radionuclide fractionation in soil samples: a comparative study. *Applied Radiation and Isotopes,* 61**,** 345-350.

BLANCO, P., TOMÉ, F. V. & LOZANO, J. C. 2005. Fractionation of natural radionuclides in soils from a uranium mineralized area in the south-west of Spain. *Journal of Environmental Radioactivity,* 79**,** 315-330.

BOND, D. L., DAVIS, J. A. & ZACHARA, J. M. 2007. Chapter 14 Uranium(VI) Release from Contaminated Vadose Zone Sediments: Estimation of Potential Contributions from Dissolution and Desorption. *In:* MARK, O. B. & DOUGLAS, B. K. (eds.) *Developments in Earth and Environmental Sciences.* Elsevier.

BONTEN, L. T. C., GROENENBERG, J. E., WENG, L. & VAN RIEMSDIJK, W. H. 2008. Use of speciation and complexation models to estimate heavy metal sorption in soils. *Geoderma,* 146**,** 303-310.

BOUBY, M., GECKEIS, H., LUETZENKIRCHEN, J., MIHAI, S. & SCHAEFER, T. 2011. Interaction of bentonite colloids with Cs, Eu, Th and U in presence of humic acid: A flow field-flow fractionation study. *Geochimica Et Cosmochimica Acta,* 75**,** 3866-3880.

BRAUN, J.-J., VIERS, J., DUPRÉ, B., POLVE, M., NDAM, J. & MULLER, J.-P. 1998. Solid/Liquid REE Fractionation in the Lateritic System of Goyoum, East Cameroon: The Implication for the Present Dynamics of the Soil Covers of the Humid Tropical Regions. *Geochimica et Cosmochimica Acta,* 62**,** 273-299.

BROOKS, S. C., FREDRICKSON, J. K., CARROLL, S. L., KENNEDY, D. W., ZACHARA, J. M., PLYMALE, A. E., KELLY, S. D., KEMNER, K. M. & FENDORF, S. 2003. Inhibition of Bacterial U(VI) Reduction by Calcium. *Environmental Science & Technology,* 37**,** 1850-1858.

BUANUAM, J., SHIOWATANA, J. & PONGSAKUL, P. 2005. Fractionation and elemental association of Zn, Cd and Pb in soils contaminated by Zn minings using a continuous-flow sequential extraction. *Journal of Environmental Monitoring,* 7**,** 778-784.

BUANUAM, J., TIPTANASUP, K., SHIOWATANA, J., MIRO, M. & HANSEN, E. H. 2006. Development of a simple extraction cell with bi-directional continuous flow coupled on-line to ICP-MS for assessment of elemental associations in solid samples. *Journal of Environmental Monitoring,* 8**,** 1248-1254.

BUEKERS, J., DEGRYSE, F., MAES, A. & SMOLDERS, E. 2008. Modelling the effects of ageing on Cd, Zn, Ni and Cu solubility in soils using an assemblage model. *European Journal of Soil Science,* 59**,** 1160-1170.

BUEKERS, J., VAN LAER, L., AMERY, F., VAN BUGGENHOUT, S., MAES, A. & SMOLDERS, E. 2007. Role of soil constituents in fixation of soluble Zn, Cu, Ni and Cd added to soils. *European Journal of Soil Science,* 58**,** 1514-1524.

BUNKER, D. J., SMITH, J. T., LIVENS, F. R. & HILTON, J. 2000. Determination of radionuclide exchangeability in freshwater systems. *Science of The Total Environment,* 263**,** 171-183.

BUNZL, K., KRETNER, R., SCHRAMEL, P., SZELES, M. & WINKLER, R. 1995. Speciation of ^{238}U, ^{226}Ra, ^{210}Pb, ^{228}Ra and stable Pb in the soil near an exhaust ventilating shaft of uranium mine. *Geoderma,* 67**,** 45-53.

CANCÈS, B., PONTHIEU, M., CASTREC-ROUELLE, M., AUBRY, E. & BENEDETTI, M. F. 2003. Metal ions speciation in a soil and its solution: experimental data and model results. *Geoderma,* 113**,** 341-355.

CARTWRIGHT, A. J., MAY, C. C., WORSFOLD, P. J. & KEITH-ROACH, M. J. 2007. Characterisation of thorium-ethylenediaminetetraacetic acid and thorium-nitrilotriacetic acid species by electrospray ionisation-mass spectrometry. *Analytica Chimica Acta,* 590**,** 125-131.

CASARTELLI, E. A. & MIEKELEY, N. 2003. Determination of thorium and light rare-earth elements in soil water and its high molecular mass organic fractions by inductively coupled plasma mass spectrometry and on-line-coupled size-exclusion chromatography. *Analytical and Bioanalytical Chemistry,* 377**,** 58-64.

CHEN, C. L. & WANG, X. K. 2007. Influence of pH, soil humic/fulvic acid, ionic strength and foreign ions on sorption of thorium(IV) onto γ-Al_2O_3. *Applied Geochemistry,* 22**,** 436-445.

CHEN, W., CHANG, A. C. & WU, L. 2007. Assessing long-term environmental risks of trace elements in phosphate fertilizers. *Ecotoxicology and Environmental Safety,* 67**,** 48-58.

CHENG, T., BARNETT, M. O., RODEN, E. E. & ZHUANG, J. 2004. Effects of Phosphate on Uranium(VI) Adsorption to Goethite-Coated Sand. *Environmental Science & Technology,* 38**,** 6059-6065.

CHENG, T., SCHAMPHELAERE, K. D., LOFTS, S., JANSSEN, C. & ALLEN, H. E. 2005. Measurement and computation of zinc binding to natural dissolved organic matter in European surface waters. *Analytica Chimica Acta,* 542**,** 230-239.

CHIN, Y.-P. & GSCHWEND, P. M. 1991. The abundance, distribution, and configuration of porewater organic colloids in recent sediments. *Geochimica et Cosmochimica Acta,* 55**,** 1309-1317.

CLARK, M. W., HARRISON, J. J. & PAYNE, T. E. 2011. The pH-dependence and reversibility of uranium and thorium binding on a modified bauxite refinery residue using isotopic exchange techniques. *Journal of Colloid and Interface Science,* 356**,** 699-705.

CLEMENTE, R., DICKINSON, N. M. & LEPP, N. W. 2008. Mobility of metals and metalloids in a multi-element contaminated soil 20 years after cessation of the pollution source activity. *Environmental Pollution,* 155**,** 254-261.

COLLINS, R. N. 2004. Separation of low-molecular mass organic acid–metal complexes by high-performance liquid chromatography. *Journal of Chromatography A,* 1059**,** 1-12.

CORNU, J. Y., DENAIX, L., SCHNEIDER, A. & PELLERIN, S. 2007. Temporal evolution of redox processes and free Cd dynamics in a metal-contaminated soil after rewetting. *Chemosphere,* 70**,** 306-314.

CORNU, J. Y., DENAIX, L., SCHNEIDER, A. & PELLERIN, S. 2008. Temporal variability of solution Cd^{2+} concentration in metal-contaminated soils as affected by soil temperature: consequences on lettuce (Lactuca sativa L.) exposure. *Plant and Soil,* 307**,** 51-65.

CORNU, J. Y., SCHNEIDER, A., JEZEQUEL, K. & DENAIX, L. 2011. Modelling the complexation of Cd in soil solution at different temperatures using the UV-absorbance of dissolved organic matter. *Geoderma,* 162**,** 65-70.

CURTIS, G. P., DAVIS, J. A. & NAFTZ, D. L. 2006. Simulation of reactive transport of uranium(VI) in groundwater with variable chemical conditions. *Water Resources Research,* 42**,** W04404.

CURTIS, G. P., FOX, P., KOHLER, M. & DAVIS, J. A. 2004. Comparison of in situ uranium KD values with a laboratory determined surface complexation model. *Applied Geochemistry,* 19**,** 1643-1653.

DAVIS, J. A., COSTON, J. A., KENT, D. B. & FULLER, C. C. 1998. Application of the Surface Complexation Concept to Complex Mineral Assemblages. *Environmental Science & Technology,* 32**,** 2820-2828.

DAVIS, J. A., CURTIS, G. P., WILKINS, M. J., KOHLER, M., FOX, P., NAFTZ, D. L. & LLOYD, J. R. 2006. Processes affecting transport of uranium in a suboxic aquifer. *Physics and Chemistry of the Earth, Parts A/B/C,* 31**,** 548-555.

DAVIS, J. A., MEECE, D. E., KOHLER, M. & CURTIS, G. P. 2004. Approaches to surface complexation modeling of Uranium(VI) adsorption on aquifer sediments. *Geochimica et Cosmochimica Acta,* 68**,** 3621-3641.

DEER, W. A., HOWIE, R. A. & ZUSSMAN, J. 1992. *An introduction to the rock-forming minerals*, Longman Scientific & Technical.

DEGRYSE, F., BROOS, K., SMOLDERS, E. & MERCKX, R. 2003. Soil solution concentration of Cd and Zn canbe predicted with a $CaCl_2$ soil extract. *European Journal of Soil Science,* 54**,** 149-158.

DEGRYSE, F., SMOLDERS, E. & PARKER, D. R. 2009. Partitioning of metals (Cd, Co, Cu, Ni, Pb, Zn) in soils: concepts, methodologies, prediction and applications - a review. *European Journal of Soil Science,* 60**,** 590-612.

DEGRYSE, F., VOEGELIN, A., JACQUAT, O., KRETZSCHMAR, R. & SMOLDERS, E. 2011. Characterization of zinc in contaminated soils: complementary insights from isotopic exchange, batch extractions and XAFS spectroscopy. *European Journal of Soil Science,* 62**,** 318-330.

DEGUELDRE, C. & KLINE, A. 2007. Study of thorium association and surface precipitation on colloids. *Earth and Planetary Science Letters,* 264**,** 104–113.

DEL CARMEN RIVAS, M. 2005. *Interactions Between Soil Uranium Contamination and Fertilization with N, P and S on the Uranium Content and Uptake of*

Corn, Sunflower and Beans, and Soil Microbiological Parameters., FAL Agriculture Research, Special issue 287, Braunschweig, Germany.

DHOUM, R. T. & EVANS, G. J. 1998. Evaluation of uranium and arsenic retention by soil from a low level radioactive waste management site using sequential extraction. *Applied Geochemistry,* 13**,** 415-420.

DIJKSTRA, J. J., MEEUSSEN, J. C. L. & COMANS, R. N. J. 2004. Leaching of Heavy Metals from Contaminated Soils: An Experimental and Modeling Study. *Environmental Science & Technology,* 38**,** 4390-4395.

DONG, W. & BROOKS, S. C. 2006. Determination of the Formation Constants of Ternary Complexes of Uranyl and Carbonate with Alkaline Earth Metals (Mg^{2+}, Ca^{2+}, Sr^{2+}, and Ba^{2+}) Using Anion Exchange Method. *Environmental Science & Technology,* 40**,** 4689-4695.

DU, X., RATE, A. W. & GEE, M. A. M. 2012. Redistribution and mobilization of titanium, zirconium and thorium in an intensely weathered lateritic profile in Western Australia. *Chemical Geology,* 330–331**,** 101-115.

DUFF, M. C. & AMRHEIN, C. 1996a. U (VI) sorption on goethite and soil in carbonate solutions. *Soil Science Society of America Journal* 60**,** 1393-1400.

DUFF, M. C. & AMRHEIN, C. 1996b. Uranium(VI) Adsorption on Goethite and Soil in Carbonate Solutions. *Soil Sci. Soc. Am. J.,* 60**,** 1393-1400.

DUFF, M. C., COUGHLIN, J. U. & HUNTER, D. B. 2002. Uranium co-precipitation with iron oxide minerals. *Geochimica et Cosmochimica Acta,* 66**,** 3533-3547.

DUQUÈNE, L., VANDENHOVE, H., TACK, F., VAN DER AVOORT, E., VAN HEES, M. & WANNIJN, J. 2006. Plant-induced changes in soil chemistry do not explain differences in uranium transfer. *Journal of Environmental Radioactivity,* 90**,** 1-14.

DUQUÈNE, L., VANDENHOVE, H., TACK, F., VAN HEES, M. & WANNIJN, J. 2010. Diffusive gradient in thin FILMS (DGT) compared with soil solution and labile uranium fraction for predicting uranium bioavailability to ryegrass. *Journal of Environmental Radioactivity,* 101**,** 140-147.

EBBS, S. D., BRADY, D. J. & KOCHIAN, L. V. 1998. Role of uranium speciation in the uptake and translocation of uranium by plants. *Journal of Experimental Botany,* 49**,** 1183-1190.

ECHEVARRIA, G., SHEPPARD, M. & MOREL, J. 2001. Effect of pH on the sorption of uranium in soil. *J. Environ Radioact,* 53**,** 257–264.

EGEBERG, P. K. & ALBERTS, J. J. 2003. HPSEC as a prepative fractionation technique for studies of natural organic matter (NOM). *Environmental Technology,* 24**,** 309-318.

EPA, E. E. P. A. 1999. Understanding Variation in Partitioning Coefficients, Kd, Values: Volume II: Review of Geochemistry and Available K_d Values for Cadmium, Caesium, Chromium, Lead, Plutonium, Radon, Strontium, Thorium, Tritium and Uranium. *US-EPA, Office of Air and Radiation, Washington, USA EPA 402-R-99-004B.*

EUSTERHUES, K., RUMPEL, C. & KÖGEL-KNABNER, I. 2005. Organo-mineral associations in sandy acid forest soils: importance of specific surface area, iron oxides and micropores. *European Journal of Soil Science,* 56**,** 753-763.

FEDOTOV, P. S., ZAVARZINA, A. G., SPIVAKOV, B. Y., WENNRICH, R., MATTUSCH, J., TITZE, K. D. P. C. & DEMIN, V. V. 2002. Accelerated fractionation of heavy metals in contaminated soils and sediments using rotating coiled columns. *Journal of Environmental Monitoring,* 4**,** 318-324.

FELMY, A., RAI, D., STERNER, S. M., MASON, M., HESS, N. & CONRADSON, S. 1997. Thermodynamic models for highly charged aqueous species: Solubility of Th(IV) hydrous oxide in concentrated $NaHCO_3$ and Na_2CO_3 solutions. *Journal of Solution Chemistry,* 26**,** 233-248.

FOX, P. M., DAVIS, J. A. & ZACHARA, J. M. 2006. The effect of calcium on aqueous uranium(VI) speciation and adsorption to ferrihydrite and quartz. *Geochimica et Cosmochimica Acta,* 70**,** 1379-1387.

FRANCIS, A. J., DODGE, C. J., GILLOW, J. B. & PAPENGUTH, H. W. 2000. Biotransformation of Uranium Compounds in High Ionic Strength Brine by a Halophilic Bacterium under Denitrifying Conditions. *Environmental Science & Technology,* 34**,** 2311-2317.

FREDRICKSON, J. K., ZACHARA, J. M., KENNEDY, D. W., LIU, C., DUFF, M. C., HUNTER, D. B. & DOHNALKOVA, A. 2002. Influence of Mn oxides on the reduction of uranium(VI) by the metal-reducing bacterium Shewanella putrefaciens. *Geochimica et Cosmochimica Acta,* 66**,** 3247-3262.

FULLER, C. C., BARGAR, J. R., DAVIS, J. A. & PIANA, M. J. 2001. Mechanisms of Uranium Interactions with Hydroxyapatite: Implications for Groundwater Remediation. *Environmental Science & Technology,* 36**,** 158-165.

GÄBLER, H. E., BAHR, A., HEIDKAMP, A. & UTERMANN, J. 2007. Enriched stable isotopes for determining the isotopically exchangeable element content in soils. *European Journal of Soil Science,* 58**,** 746-757.

GADELLE, F., WAN, J. & TOKUNAGA, T. K. 2001. Removal of Uranium(VI) from Contaminated Sediments by Surfactants. *Journal of Environmental Quality,* 30**,** 470-478.

GAVRILESCU, M., PAVEL, L. V. & CRETESCU, I. 2009. Characterization and remediation of soils contaminated with uranium. *Journal of Hazardous Materials,* 163**,** 475-510.

GIAMMAR, D. E. & HERING, J. G. 2001. Time Scales for Sorption−Desorption and Surface Precipitation of Uranyl on Goethite. *Environmental Science & Technology,* 35**,** 3332-3337.

GLAUS, M. A., HUMMEL, W., VAN LOON, L. R., INSTITUT, P. S. & ENTSORGUNG, P. S. I. L. F. 1997. *Experimental Determination and Modelling of Trace Metal-humate Interactions: A Pragmatic Approach for Applications in Groundwater*, Paul Scherrer Institut, Labor für Entsorgung.

GLEYZES, C., TELLIER, S. & ASTRUC, M. 2002. Fractionation studies of trace elements in contaminated soils and sediments: a review of sequential extraction procedures. *TrAC Trends in Analytical Chemistry,* 21**,** 451-467.

GLOOR, R., LEIDNER, H., WUHRMANN, K. & FLEISCHMANN, T. 1981. Exclusion chromatography with carbon detection. A tool for further characterization of dissolved organic carbon. *Water Research,* 15**,** 457-462.

GÓMEZ-ARIZA, J. L., GIRÁLDEZ, I., SÁNCHEZ-RODAS, D. & MORALES, E. 1999. Metal readsorption and redistribution during the analytical fractionation

of trace elements in oxic estuarine sediments. *Analytica Chimica Acta,* 399**,** 295-307.

GOODDY, D. C., SHAND, P., KINNIBURGH, D. G. & VAN RIEMSDIJK, W. H. 1995. Field-based partition coefficients for trace elements in soil solutions. *European Journal of Soil Science,* 46**,** 265-285.

GROENENBERG, J. E., DIJKSTRA, J. J., BONTEN, L. T. C., DE VRIES, W. & COMANS, R. N. J. 2012. Evaluation of the performance and limitations of empirical partition-relations and process based multisurface models to predict trace element solubility in soils. *Environmental Pollution,* 166**,** 98-107.

GRYBOS, M., DAVRANCHE, M., GRUAU, G. & PETITJEAN, P. 2007. Is trace metal release in wetland soils controlled by organic matter mobility or Fe-oxyhydroxides reduction? *Journal of Colloid and Interface Science,* 314**,** 490-501.

GU, B. & CHEN, J. 2003. Enhanced microbial reduction of Cr(VI) and U(VI) by different natural organic matter fractions. *Geochimica et Cosmochimica Acta,* 67**,** 3575-3582.

GU, B. H., YAN, H., ZHOU, P., WATSON, D. B., PARK, M. & ISTOK, J. 2005. Natural humics impact uranium bioreduction and oxidation. *Environmental Science & Technology,* 39**,** 5268-5275.

GUO, P., DUAN, T., SONG, X. & CHEN, H. 2007. Evaluation of a sequential extraction for the speciation of thorium in soils from Baotou area, Inner Mongolia. *Talanta,* 71**,** 778-783.

GUO, P., DUAN, T., SONG, X., XU, J. & CHEN, H. 2008. Effects of soil pH and organic matter on distribution of thorium fractions in soil contaminated by rare-earth industries. *Talanta,* 77**,** 624-627.

GUO, P., JIA, X., DUAN, T., XU, J. & CHEN, H. 2010. Influence of plant activity and phosphates on thorium bioavailability in soils from Baotou area, Inner Mongolia. *Journal of Environmental Radioactivity,* 101**,** 767-772.

GUO, Z.-J., YU, X.-M., GUO, F.-H. & TAO, Z.-Y. 2005. Th(IV) adsorption on alumina: Effects of contact time, pH, ionic strength and phosphate. *Journal of Colloid and Interface Science,* 288**,** 14-20.

GUSTAFSSON, J. P. 2001. Modeling the Acid–Base Properties and Metal Complexation of Humic Substances with the Stockholm Humic Model. *Journal of Colloid and Interface Science,* 244**,** 102-112.

GUSTAFSSON, J. P., DASSMAN, E. & BACKSTROM, M. 2009. Towards a consistent geochemical model for prediction of uranium(VI) removal from groundwater by ferrihydrite. *Applied Geochemistry,* 24**,** 454-462.

HAMON, R. E., MCLAUGHLIN, M. J. & COZENS, G. 2002. Mechanisms of Attenuation of Metal Availability in In Situ Remediation Treatments. *Environmental Science & Technology,* 36**,** 3991-3996.

HAMON, R. E., PARKER, D. R. & LOMBI, E. 2008. Chapter - 6 Advances in Isotopic Dilution Techniques in Trace Element Research: A Review of Methodologies, Benefits, and Limitations. *In:* DONALD, L. S. (ed.) *Advances in Agronomy.* Academic Press.

HINSIN, D., PDUNGSAP, L. & SHIOWATANA, J. 2002. Continuous-flow extraction system for elemental association study: a case of synthetic metal-doped iron hydroxide. *Talanta,* 58**,** 1365-1373.

HOLMES, L. 2001. Determination of thorium by ICP-MS and ICP-OES. *Radiation Protection Dosimetry,* 97**,** 117-122.

HOLMES, L. & PILVIO, R. 2000. Determination of thorium in environmental and workplace materials by ICP–MS. *Applied Radiation and Isotopes,* 53**,** 63-68.

HSI, C.-K. D. & LANGMUIR, D. 1985. Adsorption of uranyl onto ferric oxyhydroxides: Application of the surface complexation site-binding model. *Geochimica et Cosmochimica Acta,* 49**,** 1931-1941.

IAEA 2003. Extent of environmental contamination by naturally occurring radioactive material (NORM) and technological options for mitigation. *Technical Reports SeriesVienna: International Atomic Energy Agency 87 pp.*

ISTOK, J. D., SENKO, J. M., KRUMHOLZ, L. R., WATSON, D., BOGLE, M. A., PEACOCK, A., CHANG, Y. J. & WHITE, D. C. 2003. In Situ Bioreduction of Technetium and Uranium in a Nitrate-Contaminated Aquifer. *Environmental Science & Technology,* 38**,** 468-475.

JACKSON, B. P., RANVILLE, J. F., BERTSCH, P. M. & SOWDER, A. G. 2005. Characterization of Colloidal and Humic-Bound Ni and U in the "Dissolved" Fraction of Contaminated Sediment Extracts. *Environmental Science & Technology,* 39**,** 2478-2485.

JERDEN JR, J. L. & SINHA, A. K. 2003. Phosphate based immobilization of uranium in an oxidizing bedrock aquifer. *Applied Geochemistry,* 18**,** 823-843.

JERDEN JR, J. L., SINHA, A. K. & ZELAZNY, L. 2003. Natural immobilization of uranium by phosphate mineralization in an oxidizing saprolite–soil profile: chemical weathering of the Coles Hill uranium deposit, Virginia. *Chemical Geology,* 199**,** 129-157.

JIMOH, M., FRENZEL, W., MÜLLER, V., STEPHANOWITZ, H. & HOFFMANN, E. 2004. Development of a Hyphenated Microanalytical System for the Investigation of Leaching Kinetics of Heavy Metals in Environmental Samples. *Analytical Chemistry,* 76**,** 1197-1203.

KABATA-PENDIAS, A. 2011. *Trace Elements in Soils and Plants,* CRC Press.

KAPLAN, D. I. & KNOX, A. S. 2003. Role of naturally occurring organic matter on thorium transport in a wetland. *In:* FINCH, R. J. & BULLEN, D. B. (eds.) *Scientific Basis for Nuclear Waste Management Xxvi.* Warrendale: Materials Research Society.

KAPLAN, D. I. & SERKIZ, S. M. 2001. Quantification of thorium and uranium sorption to contaminated sediments. *Journal of Radioanalytical and Nuclear Chemistry,* 248**,** 529-535.

KAPLAN, D. I., SUMNER, M. E., BERTSCH, P. M. & ADRIANO, D. C. 1996. Chemical Conditions Conducive to the Release of Mobile Colloids from Ultisol Profiles. *Soil Sci. Soc. Am. J.,* 60**,** 269-274.

KELLY, S. D., KEMNER, K. M. & BROOKS, S. C. 2007. X-ray absorption spectroscopy identifies calcium-uranyl-carbonate complexes at environmental concentrations. *Geochimica et Cosmochimica Acta,* 71**,** 821-834.

KIRK, G. J. D. 2004. The Biogeochemistry of Submerged Soils. John Wiley & Sons, Chichester, England.

KISS, J. J., DE JONG, E. & BETTANY, J. R. 1988. The distribution of natural radionuclides in native soils of southern Saskatchewan, Canada. *J. Environ. Qual.,* 17**,** 437–445.

KOCH-STEINDL, H. & PRÖHL, G. 2001. Considerations on the behaviour of long-lived radionuclides in the soil. *Radiation and Environmental Biophysics,* 40**,** 93-104.

KOHLER, M., CURTIS, G. P., KENT, D. B. & DAVIS, J. A. 1996. Experimental Investigation and Modeling of Uranium (VI) Transport Under Variable Chemical Conditions. *Water Resources Research,* 32**,** 3539-3551.

KOHLER, M., CURTIS, G. P., MEECE, D. E. & DAVIS, J. A. 2003. Methods for Estimating Adsorbed Uranium(VI) and Distribution Coefficients of Contaminated Sediments. *Environmental Science & Technology,* 38**,** 240-247.

KOHLER, M., CURTIS, G. P., MEECE, D. E. & DAVIS, J. A. 2004. Methods for estimating adsorbed uranium(VI) and distribution coefficients of contaminated sediments. *Environmental Science & Technology,* 38**,** 240-247.

KOSTKA, J. E. & LUTHER III, G. W. 1994. Partitioning and speciation of solid phase iron in saltmarsh sediments. *Geochimica et Cosmochimica Acta,* 58**,** 1701-1710.

KOZAI, N., OHNUKI, T. & IWATSUKI, T. 2013. Characterization of saline groundwater at Horonobe, Hokkaido, Japan by SEC-UV-ICP-MS: Speciation of uranium and iodine. *Water Research,* 47**,** 1570-1584.

KUROSAKI, H., LOYLAND ASBURY, S. M., NAVRATIL, J. D. & CLARK, S. B. 2002. Flow-through Sequential Extraction Approach Developed from a Batch Extraction Method. *Environmental Science & Technology,* 36**,** 4880-4885.

LAFLAMME, B. D. & MURRAY, J. W. 1987. Solid solution interaction: The effect of carbonate alkalinity on adsorbed thorium. *Geochimica et Cosmochimica Acta,* 51**,** 243-250.

LAING, G. D. 2010a. Chapter - 4 Analysis and Fractionation of Trace Elements in Soils. *In:* HOODA, P. S. (ed.) *Trace elements in soils.* Wiley, Chichester, pp. xix, 596 p.

LAING, G. D. 2010b. Chapter - 5 Fractionation and Speciation of Trace Elements in Soil Solution. *In:* HOODA, P. S. (ed.) *Trace elements in soils.* Wiley, Chichester, pp. xix, 596 p.

LAKE, D. L., KIRK, P. W. W. & LESTER, J. N. 1984. Fractionation, characterization, and speciation of heavy metals in sewage sludge and sludge-amended soils: a review. *J. Environ. Qual,* 13**,** 175–183.

LANGMUIR, D. 1978. Uranium solution-mineral equilibria at low temperatures with applications to sedimentary ore deposits. *Geochimica et Cosmochimica Acta,* 42**,** 547-569.

LANGMUIR, D. 1997. *Aqueous Environmental Geochemistry,* Prentice-Hall, Inc., Upper Saddle River, New Jersey.

LANGMUIR, D. & HERMAN, J. S. 1980. The mobility of thorium in natural waters at low temperatures. *Geochimica et Cosmochimica Acta,* 44**,** 1753-1766.

LEBOURG, A., STERCKEMAN, T., CIESIELSKI, H. & PROIX, N. 1996. Suitability of chemical extraction to assess risks of toxicity induced by soil trace metal bioavailability. *Agronomie,* 16**,** 201-215.

LENHART, J. J. & HONEYMAN, B. D. 1999. Uranium(VI) sorption to hematite in the presence of humic acid. *Geochimica et Cosmochimica Acta,* 63**,** 2891-2901.

LEVESQUE, M. & MATHUR, S. P. 1988. Soil Tests for Copper, Iron, Manganese, and Zinc in Histosols: 3. A Comparison of Eight Extractants for Measuring Active and Reserve Forms of the Elements1. *Soil Science* 145.

LI, X. & THORNTON, I. 2001. Chemical partitioning of trace and major elements in soils contaminated by mining and smelting activities. *Applied Geochemistry,* 16**,** 1693-1706.

LOFTS, S. & TIPPING, E. 1998. An assemblage model for cation binding by natural particulate matter. *Geochimica et Cosmochimica Acta,* 62**,** 2609-2625.

LOFTS, S. & TIPPING, E. 2011. Assessing WHAM/Model VII against field measurements of free metal ion concentrations: model performance and the role of uncertainty in parameters and inputs. *Environmental Chemistry,* 8**,** 501-516.

LOFTS, S., WOOF, C., TIPPING, E., CLARKE, N. & MULDER, J. 2001. Modelling pH buffering and aluminium solubility in European forest soils. *European Journal of Soil Science,* 52**,** 189-204.

LOMBI, E. & GERZABEK, M. H. 1998. Determination of mobile heavy metal fraction in soil: Results of a pot experiment with sewage sludge. *Communications in Soil Science and Plant Analysis,* 29**,** 2545-2556.

LOMBI, E., HAMON, R. E., MCGRATH, S. P. & MCLAUGHLIN, M. J. 2003. Lability of Cd, Cu, and Zn in Polluted Soils Treated with Lime, Beringite, and Red Mud and Identification of a Non-Labile Colloidal Fraction of Metals Using Isotopic Techniques. *Environmental Science & Technology,* 37**,** 979-984.

LOVLEY, D. R. 1996. Humic substances as electron acceptors for microbial respiration. *Nature,* 382**,** 445−448.

LYONS, J. B. 1964. Distribution of thorium and uranium in three early Paleozoic plutonic series of New Hampshire. *Geological Survey Bulletin.*

MA, Y. & HOODA, P. S. 2010. Characteristics and behaviour of individual elements, Chromium, Nickel and Cobalt. *In:* HOODA, P. S. (ed.) *Trace element in the soils.* John Wiley and Sons, Ltd. London pp. 461-475.

MA, Y. B., LOMBI, E., NOLAN, A. L. & MCLAUGHLIN, M. J. 2006. Determination of labile Cu in soils and isotopic exchangeability of colloidal Cu complexes. *European journal of soil science.,* 57**,** 147-153.

MARIN, S. R., CORNEJO, S. G. & ARRIAGADA, L. 1994. Spectral line selection for determination of zirconium, cerium, thorium and titanium by inductively coupled plasma atomic emission spectrometry in zirconia-based ceramic materials. *Journal of Analytical Atomic Spectrometry,* 9**,** 93-97.

MARINUSSEN, M. P. J. C., VAN DER ZEE, S. E. A. T. M. & DE HAAN, F. A. M. 1997. Cu Accumulation inLumbricus rubellusunder Laboratory Conditions

Compared with Accumulation under Field Conditions. *Ecotoxicology and Environmental Safety,* 36**,** 17-26.

MARINUSSEN, M. P. J. C., VAN DER ZEE, S. E. A. T. M., DE HAAN, F. A. M., BOUWMAN, L. M. & HEFTING, M. M. 1997b. Heavy Metal (Copper, Lead, and Zinc) Accumulation and Excretion by the Earthworm, Dendrobaena veneta. *J. Environ. Qual.,* 26**,** 278-284.

MARSCHNER, B. & BREDOW, A. 2002. Temperature effects on release and ecologically relevant properties of dissolved organic carbon in sterilised and biologically active soil samples. *Soil Biology and Biochemistry,* 34**,** 459-466.

MARSHALL, S. J., YOUNG, S. D. & GREGSON, K. 1995. Humic acid–proton equilibria: A comparison of two models and assessment of titration error. *European Journal of Soil Science,* 46**,** 471-480.

MARTÍNEZ-AGUIRRE, A. & PERIÁÑEZ, R. 2001. Sedimentary speciation of U and Th isotopes in a marsh area at the southwest of Spain. *Journal of Radioanalytical and Nuclear Chemistry,* 247**,** 45-52.

MARZOUK, E. R., CHENERY, S. R. & YOUNG, S. D. 2013a. Measuring reactive metal in soil: a comparison of multi-element isotopic dilution and chemical extraction. *European Journal of Soil Science,* 64**,** 526-536.

MARZOUK, E. R., CHENERY, S. R. & YOUNG, S. D. 2013b. Predicting the solubility and lability of Zn, Cd, and Pb in soils from a minespoil-contaminated catchment by stable isotopic exchange. *Geochimica et Cosmochimica Acta,* 123**,** 1-16.

MASON, C. F. V., TURNEY, W. R. J. R., THOMSON, B. M., LU, N., LONGMIRE, P. A. & CHISHOLM-BRAUSE, C. J. 1997. Carbonate Leaching of Uranium from Contaminated Soils. *Environmental Science & Technology,* 31**,** 2707-2711.

MCCARTHY, J. F., ROBERSON, L. E. & BURRUS, L. W. 1989. Association of benzo(a)pyrene with dissolved organic matter: Prediction of Kdom from structural and chemical properties of the organic matter. *Chemosphere,* 19**,** 1911-1920.

MCKENZIE, R. M. 1980. The Adsorption of Lead and Other Heavy Metals on Oxides of Manganese and Iron. *Australian Journal of Soil Research,* 18**,** 61-73.

MCKINLEY, J. P., ZACHARA, J. M., WAN, J., MCCREADY, D. E. & HEALD, S. M. 2007. Geochemical Controls on Contaminant Uranium in Vadose Hanford Formation Sediments at the 200 Area and 300 Area, Hanford Site, Washington. *Vadose Zone J.,* 6**,** 1004-1017.

MCLAREN, R. G., LAWSON, D. M. & SWIFT, S. 1986. The forms of cobalt in some Scottish soils as determined by extraction and isotopic exchange. *Journal of Soil Science,* 37**,** 223-234.

MCLAUGHLIN, M. J., ZARCINAS, B. A., STEVENS, D. P. & COOK, N. 2000. Soil testing for heavy metals. *Communications in Soil Science and Plant Analysis,* 31**,** 1661-1700.

MEERS, E., DU LAING, G., UNAMUNO, V., RUTTENS, A., VANGRONSVELD, J., TACK, F. M. G. & VERLOO, M. G. 2007. Comparison of cadmium

extractability from soils by commonly used single extraction protocols. *Geoderma,* 141**,** 247-259.

MEERS, E., UNAMUNO, V. R., DU LAING, G., VANGRONSVELD, J., VANBROEKHOVEN, K., SAMSON, R., DIELS, L., GEEBELEN, W., RUTTENS, A., VANDEGEHUCHTE, M. & TACK, F. M. G. 2006. Zn in the soil solution of unpolluted and polluted soils as affected by soil characteristics. *Geoderma,* 136**,** 107-119.

MEEUSSEN, J. C. L. 2003. ORCHESTRA: An Object-Oriented Framework for Implementing Chemical Equilibrium Models. *Environmental Science & Technology,* 37**,** 1175-1182.

MELSON, N. H., HALIENA, B. P., KAPLAN, D. I. & BARNETT, M. O. 2012. Adsorption of tetravalent thorium by geomedia. *Radiochimica Acta,* 100**,** 827-832.

MIEKELEY, N., DOTTO, R. M., KUCHLER, I. L. & LINSALATA, P. 1984. The Importance of Organic Compounds on the Modbilization and Bioassimilation of Thorium in the Morro do Ferro Environment. *MRS Online Proceedings Library,* 44.

MIRÓ, M., HANSEN, E. H., CHOMCHOEI, R. & FRENZEL, W. 2005. Dynamic flow-through approaches for metal fractionation in environmentally relevant solid samples. *TrAC Trends in Analytical Chemistry,* 24**,** 759-771.

MURAKAMI, T., OHNUKI, T., ISOBE, H. & SATO, T. 1997. Mobility of uranium during weathering. *Am. Mineral,* 82.

MURAKAMI, T., SATO, T., OHNUKI, T. & ISOBE, H. 2005. Field evidence for uranium nanocrystallization and its implications for uranium transport. *Chemical Geology,* 221.

MURPHY, R. J., LENHART, J. J. & HONEYMAN, B. D. 1999. The sorption of thorium (IV) and uranium (VI) to hematite in the presence of natural organic matter. *Colloids and Surfaces A: Physicochemical and Engineering Aspects,* 157**,** 47-62.

NAKHONE, L. N. & YOUNG, S. D. 1993. The significance of (radio-) labile cadmium pools in soil. *Environmental Pollution,* 82**,** 73-77.

NANZYO, M., DAHLGREN, R. & SHOJI, S. 1993. Chemical characteristics of volcanic ash soils. In: Shoji S, Nanzyo M, Dahlgren RA, editors. Volcanic ash soils: genesis, properties, and utilization *Amsterdam: Elsevier, 145–187.*

NASH, K. L. & CHOPPIN, G. R. 1980. Interaction of humic and fulvic acids with Th(IV). *Journal of Inorganic and Nuclear Chemistry,* 42**,** 1045-1050.

NAVAS, A., MACHIN, J. & SOTO, J. 2005. Mobility of natural radionuclides and selected major and trace elements along a soil toposequence in the Central Spanish Pyrenees. *Soil Science,* 170**,** 743-757.

NILSSON, N., LÖVGREN, L. & SJÖBERG, S. 1992. Phosphate complexation at the surface of goethite. *Chem. Speciation Bioavailability,* 4**,** 121-130.

NOLAN, A. L., MA, Y. B., LOMBI, E. & MCLAUGHLIN, M. J. 2009. Speciation and Isotopic Exchangeability of Nickel in Soil Solution. *Journal of Environmental Quality,* 38**,** 485-492.

NOLAN, A. L., MCLAUGHLIN, M. J. & MASON, S. D. 2003. Chemical speciation of Zn, Cd, Cu, and Pb in pore waters of agricultural and contaminated soils using Donnan dialysis. *Environmental Science & Technology,* 37**,** 90-98.

NOVOZAMSKY, I., LEXMOND, T. M. & HOUBA, V. J. G. 1993. A single extraction procedure of soil for evaluation of uptake of some heavy-metals by plants. *International Journal of Environmental Analytical Chemistry,* 51**,** 47-58.

OLIVER, I. W., MACKENZIE, A. B., ELLAM, R. M., GRAHAM, M. C. & FARMER, J. G. 2006. Determining the extent of depleted uranium contamination in soils at a weapons test site: An isotopic investigation. *Geochimica Et Cosmochimica Acta,* 70**,** A457-A457.

OSTE, L. A., TEMMINGHOFF, E. J. M. & RIEMSDIJK, W. H. V. 2001. Solid-solution Partitioning of Organic Matter in Soils as Influenced by an Increase in pH or Ca Concentration. *Environmental Science & Technology,* 36**,** 208-214.

ÖSTHOLS, E., BRUNO, J. & GRENTHE, I. 1994. On the influence of carbonate on mineral dissolution: III. The solubility of microcrystalline ThO_2 in CO_2-H_2O media. *Geochimica et Cosmochimica Acta,* 58**,** 613-623.

PABALAN, R. T., TURNER, D. R., PAUL BERTETTI, F. & PRIKRYL, J. D. 1998. Chapter 3 - UraniumVI Sorption onto Selected Mineral Surfaces: Key Geochemical Parameters. *In:* JENNE, E. A. (ed.) *Adsorption of Metals by Geomedia.* San Diego: Academic Press.

PARAT, C., CORNU, J. Y., SCHNEIDER, A., AUTHIER, L., SAPIN-DIDIER, V., DENAIX, L. & POTIN-GAUTIER, M. 2009. Comparison of two experimental speciation methods with a theoretical approach to monitor free and labile Cd fractions in soil solutions. *Analytica Chimica Acta,* 648**,** 157-161.

PAYNE, T. E., DAVIS, J. A. & WAITE, T. D. 1996. Uranium adsorption on ferrihydrite - Effects of phosphate and humic acid. *Radiochimica Acta,* 74**,** 239-243.

PAYNE, T. E., EDIS, R., FENTON, B. R. & WAITE, T. D. 2001. Comparison of laboratory uranium sorption data with 'in situ distribution coefficients' at the Koongarra uranium deposit, Northern Australia. *Journal of Environmental Radioactivity,* 57**,** 35-55.

PAYNE, T. E., HATJE, V., ITAKURA, T., MCORIST, G. D. & RUSSELL, R. 2004. Radionuclide applications in laboratory studies of environmental surface reactions. *Journal of Environmental Radioactivity,* 76**,** 237-251.

PAYNE, T. E., LUMPKIN, G. R. & WAITE, T. D. 1998. Chapter 2 - UraniumVI Adsorption on Model Minerals: Controlling Factors and Surface Complexation Modeling. *In:* JENNE, E. A. (ed.) *Adsorption of Metals by Geomedia.* San Diego: Academic Press.

PAYNE, T. E. & WAITE, T. D. 1991. Surface complexation modeling of uranium sorption data obtained by isotope exchange techniques. *Radiochimica Acta,* 52-3**,** 487-493.

PELEKANI, C., NEWCOMBE, G., SNOEYINK, V. L., HEPPLEWHITE, C., ASSEMI, S. & BECKETT, R. 1999. Characterization of Natural Organic

Matter Using High Performance Size Exclusion Chromatography. *Environmental Science & Technology,* 33**,** 2807-2813.

PERMINOVA, I. V., FRIMMEL, F. H., KUDRYAVTSEV, A. V., KULIKOVA, N. A., ABBT-BRAUN, G., HESSE, S. & PETROSYAN, V. S. 2003. Molecular Weight Characteristics of Humic Substances from Different Environments As Determined by Size Exclusion Chromatography and Their Statistical Evaluation. *Environmental Science & Technology,* 37**,** 2477-2485.

PETT-RIDGE, J. C., MONASTRA, V. M., DERRY, L. A. & CHADWICK, O. A. 2007. Importance of atmospheric inputs and Fe-oxides in controlling soil uranium budgets and behavior along a Hawaiian chronosequence. *Chemical Geology,* 244**,** 691-707.

PHILLIPS, D. H., WATSON, D. B. & ROH, Y. 2007. Uranium Deposition in a Weathered Fractured Saprolite/Shale. *Environmental Science & Technology,* 41**,** 7653-7660.

PUNSHON, T., GAINES, K. F., BERTSCH, P. M. & BURGER, J. 2003. Bioavailability of uranium and nickel to vegetation in a contaminated riparian ecosystem. *Environmental Toxicology and Chemistry,* 22**,** 1146-1154.

QIU, S., MCCOMB, A., BELL, R. & DAVIS, J. 2005. Response of soil microbial activity to temperature, moisture, and litter leaching on a wetland transect during seasonal refilling. *Wetlands Ecology and Management,* 13**,** 43-54.

QUEVAUVILLER, P. 1998. Operationally defined extraction procedures for soil and sediment analysis I. Standardization. *Trends in Analytical Chemistry,* 17**,** 289-298.

QUEVAUVILLER, P., LACHICA, M., BARAHONA, E., RAURET, G., URE, A., GOMEZ, A. & MUNTAU, H. 1996. Interlaboratory comparison of EDTA and DTPA procedures prior to certification of extractable trace elements in calcareous soil. *Science of The Total Environment,* 178**,** 127-132.

RAI, D., FELMY, A. R., MOORE, D. A. & MASON, M. J. 1994. The Solubility of Th(IV) and U(IV) Hydrous Oxides in Concentrated $NaHCO_3$ and Na_2CO_3 Solutions. *MRS Online Proceedings Library,* 353**,** null-null.

RAND, H., MOMPEAN, F. J., PERRONE, J. & ILLEMASSÈNE, M. 2008. Chemical Thermodynamics of Thorium, OECD Publishing.

RANVILLE, J. F., HENDRY, M. J., RESZAT, T. N., XIE, Q. & HONEYMAN, B. D. 2007. Quantifying uranium complexation by groundwater dissolved organic carbon using asymmetrical flow field-flow fractionation. *Journal of Contaminant Hydrology,* 91**,** 233-246.

RAO, C. R. M., SAHUQUILLO, A. & SANCHEZ, J. F. L. 2008. A review of the different methods applied in environmental geochemistry for single and sequential extraction of trace elements in soils and related materials. *Water Air and Soil Pollution,* 189**,** 291-333.

RAO, V. N. & RAO, G. G. 1957. Volumetric determination of thorium with disodium EDTA — Using Fe(II)-cacotheline as indicator. *Fresenius' Zeitschrift für analytische Chemie,* 155**,** 334-336.

RAURET, G. 1998. Extraction procedures for the determination of heavy metals in contaminated soil and sediment. *Talanta,* 46**,** 449-455.

RECOUS, S., FRESNEAU, C., FAURIE, G. & MARY, B. 1988. The fate of labelled15N urea and ammonium nitrate applied to a winter wheat crop. *Plant and Soil,* 112**,** 205-214.

REILLER, P., CASANOVA, F. & MOULIN, V. 2005. Influence of Addition Order and Contact Time on Thorium(IV) Retention by Hematite in the Presence of Humic Acids. *Environmental Science & Technology,* 39**,** 1641-1648.

REILLER, P., MOULIN, V., CASANOVA, F. & DAUTEL, C. 2002. Retention behaviour of humic substances onto mineral surfaces and consequences upon thorium (IV) mobility: case of iron oxides. *Applied Geochemistry,* 17**,** 1551-1562.

REILLER, P., MOULIN, V., CASANOVA, F. & DAUTEL, C. 2003. On the study of Th(IV)-humic acid interactions by competition sorption studies with silica and determination of global interaction constants. *Radiochimica Acta,* 91**,** 513-524.

RENDELL, P. S., BATLEY, G. E. & CAMERON, A. J. 1980. Adsorption as a control of metal concentrations in sediment extracts. *Environmental Science & Technology,* 14**,** 314-318.

RESZAT, T. N. & HENDRY, M. J. 2007. Complexation of Aqueous Elements by DOC in a Clay Aquitard. *Ground Water,* 45**,** 542-553.

RODRIGUES, S. M., HENRIQUES, B., DA SILVA, E. F., PEREIRA, M. E., DUARTE, A. C., GROENENBERG, J. E. & RÖMKENS, P. F. A. M. 2010. Evaluation of an approach for the characterization of reactive and available pools of 20 potentially toxic elements in soils: Part II – Solid-solution partition relationships and ion activity in soil solutions. *Chemosphere,* 81**,** 1560-1570.

RÖMKENS, P. F., BRIL, J. & SALOMONS, W. 1996. Interaction between Ca^{2+} and dissolved organic carbon: implications for metal mobilization. *Applied Geochemistry,* 11**,** 109-115.

ROTHBAUM, H. P., MCGAVESTON, D. A., WALL, T., JOHNSTON, A. E. & MATTINGLY, G. E. G. 1979. Uranium accumulation in soils from long-continued applications of superphosphate. *Eur J Soil Sci,* 30**,** 147-153.

ROWELL, D. L. 1994. *Soil science: methods and applications*, Longman Scientific & Technical.

ROYER, R. A., BURGOS, W. D., FISHER, A. S., JEON, B.-H., UNZ, R. F. & DEMPSEY, B. A. 2002. Enhancement of Hematite Bioreduction by Natural Organic Matter. *Environmental Science & Technology,* 36**,** 2897-2904.

SADI, B. B. M., WROBEL, K., KANNAMKUMARATH, S. S., CASTILLO, J. R. & CARUSO, J. A. 2002. SEC-ICP-MS studies for elements binding to different molecular weight fractions of humic substances in compost extract obtained from urban solid waste. *Journal of Environmental Monitoring,* 4**,** 1010-1016.

SAITO, T., NAGASAKI, S., TANAKA, S. & KOOPAL, L. K. 2004. Application of the NICA-Donnan model for proton, copper and uranyl binding to humic acid. *Radiochimica Acta,* 92**,** 567-574.

SATO, T., MURAKAMI, T., YANASE, N., ISOBE, H., PAYNE, T. E. & AIREY, P. L. 1997. Iron Nodules Scavenging Uranium from Groundwater. *Environmental Science & Technology,* 31**,** 2854-2858.

SAUERBECK, D. 1993. Conditions controlling the bioavailability of trace elements and heavy metals derived from phosphate fertilizers in soils. Proceedings of

the International IMPHOS Conference on Phosphorus, Life and Environment, Casablanca, Morocco. Institute Mondial du Phosphate, 419-448.

SAUVÉ, S., HENDERSHOT, W. & ALLEN, H. E. 2000. Solid-Solution Partitioning of Metals in Contaminated Soils: Dependence on pH, Total Metal Burden, and Organic Matter. *Environmental Science & Technology,* 34**,** 1125-1131.

SCHMITT, D., MÜLLER, M. B. & FRIMMEL, F. H. 2001. Metal Distribution in Different Size Fractions of Natural Organic Matter. *Acta hydrochimica et hydrobiologica,* 28**,** 400-410.

SCHRAMEL, P., WENDLER, I., ROTH, P. & WERNER, E. 1997. Method for the determination of thorium and uranium in urine by ICP-MS. *Microchimica Acta,* 126**,** 263-266.

SCHULTZ, M. K., BURNETT, W. C. & INN, K. G. W. 1998. Evaluation of a sequential extraction method for determining actinide fractionation in soils and sediments. *Journal of Environmental Radioactivity,* 40**,** 155-174.

SECO, F., HENNIG, C., DE PABLO, J., ROVIRA, M., ROJO, I., MARTI, V., GIMENEZ, J., DURO, L., GRIVE, M. & BRUNO, J. 2009. Sorption of Th(IV) onto Iron Corrosion Products: EXAFS Study. *Environmental Science & Technology,* 43**,** 2825-2830.

SENKO, J. M., ISTOK, J. D., SUFLITA, J. M. & KRUMHOLZ, L. R. 2002. In-Situ Evidence for Uranium Immobilization and Remobilization. *Environmental Science & Technology,* 36**,** 1491-1496.

SHAHANDEH, H. & HOSSNER, L. R. 2002a. Enhancement of uranium phytoaccumulation from contaminated soils. *Soil Science,* 167**,** 269-280.

SHEPPARD, M. I. & HAWKINS, J. L. 1991. A linear sorption/dynamic water flow model applied to the results of a four-year soil core study. *Ecological Modelling,* 55**,** 175-201.

SHEPPARD, M. I., SHEPPARD, S. C. & GRANT, C. A. 2007. Solid/liquid partition coefficients to model trace element critical loads for agricultural soils in Canada. *Canadian Journal of Soil Science,* 87**,** 189-201.

SHEPPARD, S. C., Long, J. & SANIPELLI, B. L. 2009. Solid/liquid partition coefficients (Kd) for selected soils and sediments at Forsmark and Laxemar-Simpevarp. *Geological Survey of Sweden (SGU).*

SHEPPARD, S. C. & EVENDEN, W. G. 1992. BIOAVAILABILITY INDEXES FOR URANIUM - EFFECT OF CONCENTRATION IN 11 SOILS. *Archives of Environmental Contamination and Toxicology,* 23**,** 117-124.

SHEPPARD, S. C., SHEPPARD, M. I., TAIT, J. C. & SANIPELLI, B. L. 2006. Revision and meta-analysis of selected biosphere parameter values for chlorine, iodine, neptunium, radium, radon and uranium. *Journal of Environmental Radioactivity,* 89**,** 115-137.

SHIOWATANA, J., MCLAREN, R. G., CHANMEKHA, N. & SAMPHAO, A. 2001a. Fractionation of arsenic in soil by a continuous-flow sequential extraction method. *Journal of Environmental Quality,* 30**,** 1940-1949.

SHIOWATANA, J., TANTIDANAI, N., NOOKABKAEW, S. & NACAPRICHA, D. 2001b. A novel continuous-flow sequential extraction procedure for metal speciation in solids. *Journal of Environmental Quality,* 30**,** 1195-1205.

SINGH, A., ULRICH, K.-U. & GIAMMAR, D. E. 2010. Impact of phosphate on U(VI) immobilization in the presence of goethite. *Geochimica et Cosmochimica Acta,* 74**,** 6324-6343.

SINGH, B. R. 2007. Natural attenuation of trace element availability assessed by chemical extraction. *In:* HAMON, R., MCLAUGHLIN, J. & LOMBI, E. (eds.) *Natural Attenuation of Trace Element Availability in Soils.* Pensacola; Boca Raton [et al.]: The Society of Environmental Toxicology and Chemistry (SETAC) ; CRC Taylor & Francis, pp 1-18.

SINGHAL, R. K. 2005. Association of uranium with colloids of natural organic matter in subsurface aquatic environment. *Journal of Radioanalytical and Nuclear Chemistry,* 265**,** 405-408.

SMOLDERS, E., BRANS, K., FÖLDI, A. & MERCKX, R. 1999. Cadmium Fixation in Soils Measured by Isotopic Dilution. *Soil Sci. Soc. Am. J.,* 63**,** 78-85.

SOWDER, A. G., BERTSCH, P. M. & MORRIS, P. J. 2003. Partitioning and availability of uranium and nickel in contaminated riparian sediments. *Journal of Environmental Quality,* 32**,** 885-898.

SPALDING, R. F. & SACKETT, W. M. 1972. Uranium in runoff from the Gulf of Mexico distributive province: anomalous concentrations. *Science* 175**,** 629-31.

STACEY, S. P., MCLAUGHLIN, M. J. & HETTIARACHCHI, G. M. 2010. Chapter - 7 Fertilizer-Borne Trace Element Contaminants in Soils. *In:* HOODA, P. S. (ed.) *Trace Elements in Soils.* John Wiley & Sons, Ltd. pp 135-154.

STERCKEMAN, T., CARIGNAN, J., SRAYEDDIN, I., BAIZE, D. & CLOQUET, C. 2009. Availability of soil cadmium using stable and radioactive isotope dilution. *Geoderma,* 153**,** 372-378.

STOCKDALE, A. & BRYAN, N. D. 2012. Uranyl binding to humic acid under conditions relevant to cementitious geological disposal of radioactive wastes. *Mineralogical Magazine,* 76**,** 3391-3399.

STOCKDALE, A. & BRYAN, N. D. 2013. The influence of natural organic matter on radionuclide mobility under conditions relevant to cementitious disposal of radioactive wastes: A review of direct evidence. *Earth-Science Reviews,* 121**,** 1-17.

STOCKDALE, A., BRYAN, N. D., LOFTS, S. & TIPPING, E. 2013. Investigating humic substances interactions with Th4+, , and at high pH: Relevance to cementitious disposal of radioactive wastes. *Geochimica et Cosmochimica Acta,* 121**,** 214-228.

STROK, M. & SMODIS, B. 2010a. Comparison of two sequential extraction protocols for fractionation of natural radionuclides in soil samples. *Radiochimica Acta,* 98**,** 221-229.

STROK, M. & SMODIS, B. 2010b. Comparison of two sequential extraction protocols for fractionation of natural radionuclides in soil samples. *Radiochimica Acta* 98**,** 221.

STUBBS, J. E., ELBERT, D. C., VEBLEN, D. R. & ZHU, C. 2006. Electron Microbeam Investigation of Uranium-Contaminated Soils from Oak Ridge, TN, USA. *Environmental Science & Technology,* 40**,** 2108-2113.

SUZUKI, Y., KELLY, S. D., KEMNER, K. M. & BANFIELD, J. F. 2002. Radionuclide contamination: Nanometre-size products of uranium bioreduction. *Nature,* 419**,** 134.

SWIFT, R. & POSNER, A. 1971. Gel chromatography of humic acid. *Soil Sci.,* 22**,** 237–249.

TABOADA, T., CORTIZAS, A. M., GARCÍA, C. & RODEJA, E. G. 2006. Uranium and thorium in weathering and pedogenetic profiles developed on granitic rocks from NW Spain. *Science of The Total Environment,* 356**,** 192-206.

TACK, F. M. G. 2010. Trace Elements: General Soil Chemistry, Principles and Processes. *Trace Elements in Soils.* John Wiley & Sons, Ltd.

TAKEDA, A., KIMURA, K. & YAMASAKI, S. I. 2004. Analysis of 57 elements in Japanese soils, with special reference to soil group and agricultural use. *Geoderma,* 119**,** 291-307.

TAKEDA, A., TSUKADA, H., NANZYO, M., TAKAKU, Y., UEMURA, T., HISAMATSU, S. I. & INABA, J. 2005. Effect of Long-term Fertilizer Application on the Concentration and Solubility of Major and Trace Elements in a Cultivated Andisol. *Soil Science & Plant Nutrition,* 51**,** 251-260.

TAKEDA, A., TSUKADA, H., TAKAKU, Y. & HISAMATSU, S. I. 2009. Fractionation of metal complexes with dissolved organic matter in a rhizosphere soil solution of a humus-rich Andosol using size exclusion chromatography with inductively coupled plasma-mass spectrometry. *Soil Science & Plant Nutrition,* 55**,** 349-357.

TAKEDA, A., TSUKADA, H., TAKAKU, Y., HISAMATSU, S. I., INABA, J. & NANZYO, M. 2006b. Extractability of major and trace elements from agricultural soils using chemical extraction methods: Application for phytoavailability assessment. *Soil Science and Plant Nutrition,* 52**,** 406-417.

TAKEDA, A., TSUKADA, H., TAKAKU, Y., HISAMATSU, S. I. & NANZYO, M. 2006a. Accumulation of uranium derived from long-term fertilizer applications in a cultivated Andisol. *Science of The Total Environment,* 367**,** 924-931.

TAYLOR, M. D. 2007. Accumulation of uranium in soils from impurities in phosphate fertilisers. *Landbauforschung Volkenrode,* 57**,** 133-139.

TESSIER, A. & CAMPBELL, P. G. C. 1988. Comments on the testing of the accuracy of an extraction procedure for determining the partitioning of trace metals in sediments. *Analytical Chemistry,* 60**,** 1475-1476.

TESSIER, A., CAMPBELL, P. G. C. & BISSON, M. 1979. Sequential extraction procedure for the speciation of particulate trace metals. *Analytical Chemistry,* 51**,** 844-851.

TESTA, C., DESIDERI, D., GUERRA, F., MELI, M. A., ROSELLI, C. & DEGETTO, S. 1999. Concentration and speciation of plutonium, americium, uranium, thorium, potassium and Cs-137 in a Venice canal sediment sample. *Czechoslovak Journal of Physics,* 49**,** 649-656.

THIBAULT, D. H., SHEPPARD, M. I. & SMITH, P. A. 1990. A critical compilation and review of default soil solid/liquid partition coefficients, Kd, for use in environmental assessments. *Atomic Energy of Canada Limited, AECL ‑10125*.

TIENSING, T., PRESTON, S., STRACHAN, N. & PATON, G. I. 2001. Soil solution extraction techniques for microbial ecotoxicity testing: a comparative evaluation. *Journal of Environmental Monitoring,* 3**,** 91-96.

TIPPING, E. 1994. WHAM - a chemical-equilibrium model and computer code for waters, sediments, and soils incorporating a discrete site electrostatic model of ion-binding by humic substances. *Computers & Geosciences,* 20**,** 973-1023.

TIPPING, E. 1998. Humic ion-binding model VI: An improved description of the interactions of protons and metal ions with humic substances. *Aquatic Geochemistry,* 4**,** 3-48.

TIPPING, E., LOFTS, S. & SONKE, J. E. 2011. Humic Ion-Binding Model VII: a revised parameterisation of cation-binding by humic substances. *Environmental Chemistry,* 8**,** 225-235.

TIPPING, E., RIEUWERTS, J., PAN, G., ASHMORE, M. R., LOFTS, S., HILL, M. T. R., FARAGO, M. E. & THORNTON, I. 2003. The solid–solution partitioning of heavy metals (Cu, Zn, Cd, Pb) in upland soils of England and Wales. *Environmental Pollution,* 125**,** 213-225.

TIPPING, E., WOOF, C., KELLY, M., BRADSHAW, K. & ROWE, J. E. 1995. Solid-Solution Distributions of Radionuclides in Acid Soils: Application of the WHAM Chemical Speciation Model. *Environmental Science & Technology,* 29**,** 1365-1372.

TONGTAVEE, N., SHIOWATANA, J. & MCLAREN, R. G. 2005b. Fractionation of lead in soils affected by smelter activities using a continuous-flow sequential extraction system. *International Journal of Environmental Analytical Chemistry,* 85**,** 567-583.

TONGTAVEE, N., SHIOWATANA, J., MCLAREN, R. G. & GRAY, C. W. 2005a. Assessment of lead availability in contaminated soil using isotope dilution techniques. *Science of The Total Environment,* 348**,** 244-256.

TRIPATHI, V. S. 1984. *Uranium(VI) transport modeling: geochemical data and submodels.* Ph.D. Dissertation, Stanford University, Stanford, CA.

TSUMURA, A. & YAMASAKI, S. 1993. Behavior of uranium, thorium, and lanthanoids in paddy fields. *Radioisotopes,* 42**,** 265-272.

TU, C. & MA, L. Q. 2003. Effects of arsenate and phosphate on their accumulation by an arsenic-hyperaccumulator Pteris vittata L. *Plant and Soil,* 249**,** 373-382.

TUNNEY, H., STOJANOVIĆ, M., MRDAKOVIĆ POPIĆ, J., MCGRATH, D. & ZHANG, C. 2009. Relationship of soil phosphorus with uranium in grassland mineral soils in Ireland using soils from a long-term phosphorus experiment and a National Soil Database. *Journal of Plant Nutrition and Soil Science,* 172**,** 346-352.

UM, W., ICENHOWER, J. P., BROWN, C. F., SERNE, R. J., WANG, Z., DODGE, C. J. & FRANCIS, A. J. 2010. Characterization of uranium-contaminated sediments from beneath a nuclear waste storage tank from Hanford, Washington: Implications for contaminant transport and fate. *Geochimica et Cosmochimica Acta,* 74**,** 1363-1380.

UNSCEAR 1988. Report to the general assembly, with scientific annexes. *New York: United Nations.*

URE, A. & DAVIDSON, C. 2002. Chemical Speciation in the Environment, 2nd Edition.

URE, A. M. 1996. Single extraction schemes for soil analysis and related applications. *Science of The Total Environment,* 178**,** 3-10.

URE, A. M., QUEVAUVILLER, P., MUNTAU, H. & GRIEPINK, B. 1993. Speciation of heavy metals in soils and sediments. An account of the improvement and harmonization of extraction techniques undertaken under the auspices of the BCR of the Commission of the European Communities. *Environmental Analytical Chemistry,* 51**,** 135-151.

VANDENHOVE, H., ANTUNES, K., WANNIJN, J., DUQUÈNE, L. & VAN HEES, M. 2007c. Method of diffusive gradients in thin films (DGT) compared with other soil testing methods to predict uranium phytoavailability. *Science of The Total Environment,* 373**,** 542-555.

VANDENHOVE, H., OLYSLAEGERS, G., SANZHAROVA, N., SHUBINA, O., REED, E., SHANG, Z. & VELASCO, H. 2009. Proposal for new best estimates of the soil-to-plant transfer factor of U, Th, Ra, Pb and Po. *Journal of Environmental Radioactivity,* 100**,** 721-732.

VANDENHOVE, H., VAN HEES, M., WANNIJN, J., WOUTERS, K. & WANG, L. 2007b. Can we predict uranium bioavailability based on soil parameters? Part 2: Soil solution uranium concentration is not a good bioavailability index. *Environmental Pollution,* 145**,** 577-586.

VANDENHOVE, H., VAN HEES, M., WOUTERS, K. & WANNIJN, J. 2007a. Can we predict uranium bioavailability based on soil parameters? Part 1: Effect of soil parameters on soil solution uranium concentration. *Environmental Pollution,,* 145**,** 587-595.

WAITE, T. D., DAVIS, J. A., PAYNE, T. E., WAYCHUNAS, G. A. & XU, N. 1994a. Uranium(VI) adsorption to ferrihydrite: Application of a surface complexation model. *Geochimica et Cosmochimica Acta,* 58**,** 5465-5478.

WAITE, T. D., DAVIS, J. A., PAYNE, T. E. & WAYCHUNAS, G. A., XU, N. 1994b. U (VI) sorption to ferrihydrite: application of the surface complexation model. *Geochimica et Cosmochimica Acta.,* 58**,** 5465-5478.

WAN, J., TOKUNAGA, T. K., BRODIE, E., WANG, Z., ZHENG, Z., HERMAN, D., HAZEN, T. C., FIRESTONE, M. K. & SUTTON, S. R. 2005. Reoxidation of Bioreduced Uranium under Reducing Conditions. *Environmental Science & Technology,* 39**,** 6162-6169.

WANG, X.-P., SHAN, X.-Q., ZHANG, S.-Z. & WEN, B. 2004. A model for evaluation of the phytoavailability of trace elements to vegetables under the field conditions. *Chemosphere,* 55**,** 811-822.

WATTS, M. J. 2002. Determination of iodine in geological and biological samples by ICP-MS. *Paper presented at the 11th Biannual National Atomic Spectroscopy Symposium, Loughborough University, UK.*

WAZNE, M., KORFIATIS, G. P. & MENG, X. 2003. Carbonate Effects on Hexavalent Uranium Adsorption by Iron Oxyhydroxide. *Environmental Science & Technology,* 37**,** 3619-3624.

WENG, L. P., TEMMINGHOFF, E. J. M., LOFTS, S., TIPPING, E. & VAN RIEMSDIJK, W. H. 2002. Complexation with dissolved organic matter and

solubility control of heavy metals in a sandy soil. *Environmental Science & Technology,* 36**,** 4804-4810.

WENG, L. P., TEMMINGHOFF, E. J. M. & VAN RIEMSDIJK, W. H. 2001. Contribution of individual sorhents to the control of heavy metal activity in sandy soil. *Environmental Science & Technology,* 35**,** 4436-4443.

WHALLEY, C. & GRANT, A. 1994. Assessment of the phase selectivity of the European Community Bureau of Reference (BCR) sequential extraction procedure for metals in sediment. *Analytica Chimica Acta,* 291**,** 287-295.

WIELINGA, B., BOSTICK, B., HANSEL, C. M., ROSENZWEIG, R. F. & FENDORF, S. 2000. Inhibition of Bacterially Promoted Uranium Reduction: Ferric (Hydr)oxides as Competitive Electron Acceptors. *Environmental Science & Technology,* 34**,** 2190-2195.

WISOTZKY, F. & CREMER, N. 2003. Sequential extraction procedure in columns. Part 1: Development and description of a new method. *Environmental Geology,* 44**,** 799-804.

WU, F., EVANS, D., DILLON, P. & SCHIFF, S. 2004. Molecular size distribution characteristics of the metal-DOM complexes in stream waters by high-performance size-exclusion chromatography (HPSEC) and high-resolution inductively coupled plasma mass spectrometry (ICP-MS). *Journal of Analytical Atomic Spectrometry,* 19**,** 979-983.

WU, J. & NOFZIGER, D. L. 1999. Incorporating temperature effects on pesticide degradation into a management model. *J. Env. Qual.,* 28**,** 92–100.

YAMAGUCHI, N., KAWASAKI, A. & IIYAMA, I. 2009. Distribution of uranium in soil components of agricultural fields after long-term application of phosphate fertilizers. *Science of The Total Environment,* 407**,** 1383-1390.

YAMASAKI, S.-I., TAKEDA, A., NANZYO, M., TANIYAMA, I. & NAKAI, M. 2001. Background levels of trace and ultra-trace elements in soils of Japan. *Soil Science and Plant Nutrition,* 47**,** 755-765.

YANG, Y., SAIERS, J. E. & BARNETT, M. O. 2013. Impact of Interactions between Natural Organic Matter and Metal Oxides on the Desorption Kinetics of Uranium from Heterogeneous Colloidal Suspensions. *Environmental Science & Technology,* 47**,** 2661-2669.

YIN, Y., IMPELLITTERI, C. A., YOU, S.-J. & ALLEN, H. E. 2002. The importance of organic matter distribution and extract soil:solution ratio on the desorption of heavy metals from soils. *Science of The Total Environment,* 287**,** 107-119.

YOSHIDA, S., MURAMATSU, Y., TAGAMI, K. & UCHIDA, S. 1998. Concentrations of lanthanide elements, Th, and U in 77 Japanese surface soils. *Environment International,* 24**,** 275-286.

YOUNG, S., CROUT, N., HUTCHINSON, J., TYE, A., TANDY, S. & NAKHONE, L. N. 2007. Techniques for measuring attenuation: Isotopic dilution methods. *In:* HAMON, R., MCLAUGHLIN, J. & LOMBI, E. (eds.) *Natural Attenuation of Trace Element Availability in Soils.* Pensacola; Boca Raton [et al.]: The Society of Environmental Toxicology and Chemistry (SETAC) ; CRC Taylor & Francis, pp 19-40.

YOUNG, S. D., TYE, A., CARSTENSEN, A., RESENDE, L. & CROUT, N. 2000. Methods for determining labile cadmium and zinc in soil. *European Journal of Soil Science,* 51**,** 129-136.

YOUNG, S. D., ZHANG, H., TYE, A. M., MAXTED, A., THUMS, C. THORNTON, I. 2005. Characterizing the availability of metals in contaminated soils. I. The solid phase: sequential extraction and isotopic dilution. *Soil Use and Management,* 21**,** 450-458.

YUHENG, W., MANON, F., ELENA, S., VANNAPHA, P., MICHAEL, D., ALFATIH, A. A. O., GERHARD, G. & RIZLAN, B.-L. 2013. Mobile uranium(IV)-bearing colloids in a mining-impacted wetland. *Nature Communications,* 4.

ZHANG, H., DONG, Z. & TAO, Z. 2006. Sorption of thorium(IV) ions on gibbsite: Effects of contact time, pH, ionic strength, concentration, phosphate and fulvic acid. *Colloids and Surfaces A: Physicochemical and Engineering Aspects,* 278**,** 46-52.

ZHANG, H., YUAN, J. & TAO, Z. 2007. Effects of phosphate and Cr^{3+} on the sorption and transport of Th(IV) on a silica column. *Journal of Radioanalytical and Nuclear Chemistry,* 273**,** 465-471.

ZHANG, H., ZHAO, F.-J., SUN, B., DAVISON, W. & MCGRATH, S. P. 2001. A New Method to Measure Effective Soil Solution Concentration Predicts Copper Availability to Plants. *Environmental Science & Technology,* 35**,** 2602-2607.

ZHANG, Y. J., BRYAN, N. D., LIVENS, F. R. & JONES, M. N. 1997. Selectivity in the complexation of actinides by humic substances. *Environmental Pollution,* 96**,** 361-367.

ZHENG, Z., TOKUNAGA, T. K. & WAN, J. 2003. Influence of Calcium Carbonate on U(VI) Sorption to Soils. *Environmental Science & Technology,* 37**,** 5603-5608.

Appendix 1: ICP-MS instrumental settings

Fast uptake wash = 45 seconds, fast uptake sample = 60 seconds, Quadrupole sweeps = 200

Analytes and (dwell times, milli-seconds): ^{193}Ir(10), ^{206,207,208}Pb(10), ^{209}Bi(10), ^{232}Th(20), ^{238}U(20)

Instrumental settings and operating conditions

	Extraction (V)	Lens 1 (V)	Lens 2 (V)	Lens 3 (V)	Pole Bias (V)	Sampling Depth	Horizontal	Vertical	Cool
Acquisition Settings	-905.88	-1513.73	-84.71	-185.1	-6.00	150.00	81.00	30.00	3.02
Description	Auxiliary	Nebuliser	Forward Power (Watts)	Analogue Detector	PC Detector	DI (V)	Focus (V)	CT Gas 1 (rpm)	CT Gas 2 (rpm)
Acquisition Settings	0.65	0.90	1403.92	1627.45	1270.00	-36.08	11.96	0.00	0.00
Description	D 2 (V)	DA	Hexapole Bias (V)	Standard resolution	High resolution	Peri-pump (rpm)			
Acquisition Settings	-130.20	-35.29	-10.00	125.00	125.00	17.00			